SEDIMENTOLOGY, FACIES ASSOCIATIONS AND SEQUENCE STRATIGRAPHY OF FALHER DIVISIONS C AND D, LOWER CRETACEOUS SPIRIT RIVER FORMATION, WEST-CENTRAL ALBERTA, CANADA

BY

JHONNY EDGAR CASAS

A Thesis submitted to the School of Graduate
Studies in partial fulfillment of the
requirements for the degree
Master of Science

McMaster University
January 1996

MASTER OF SCIENCE (1996)
(Geology)

McMASTER UNIVERSITY
Hamilton, Ontario,
Canada

TITLE: Sedimentology, Facies Associations and Sequence Stratigraphy of Falher Divisions C and D of the Lower Cretaceous Spirit River Formation, West-Central Alberta, Canada

AUTHOR: Jhonny Edgar Casas (Geologist, Universidad Central de Venezuela)

SUPERVISOR: Dr. Roger G. Walker

NUMBER OF PAGES: xvii, 231

ABSTRACT

The Lower Cretaceous Falher Member (Spirit River Formation) in the Deep Basin of Alberta is composed of 5 coarsening-upward successions (A-E). Using an allostratigraphic approach, Falher D and C were each split into four shoreface units, deposited as a strandplain system trending east-west, with the open sea to the north.

The shoreface units of Falher D are characterized by very fine-to-fine-grained sandstones with swaley cross-stratification. Conglomerates and conglomeratic sandstones with cross-bedding are present in limited bodies trending east-west across the study area. The presence of swaley cross-stratification in the sandstones, combined with a *Skolithos-Cruziana* trace fauna assemblage, suggest that this facies represents wave- to storm-dominated deposition in a high-energy, upper to middle shoreface environment, above fair-weather wave base. Seaward, sandier-upward successions with hummocky cross-stratified very fine-grained sandstones interbedded with marine mudstones represent lower shoreface to offshore deposits.

The basal surface of Falher D overlies nonmarine deposits (Falher E) and is defined by a marine flooding surface (transgressive surface of erosion). Southward, all the facies become more continental and the marine flooding surface passes into a lagoon-on-nonmarine contact. Falher D contains a series of shingled marine sandstone lenses (units D1, D2, D3 and D4) separated by erosional surfaces interpreted as seaward-dipping ravinement surfaces. These

indicate different phases of marine transgression and regression. In each unit the transgressive system tract can be preserved as barrier sands, transgressive lagoonal deposits, transgressive marine mudstones or coarse transgressive lag deposits. The highstand systems tract comprises a shoreface succession which prograded as a strandplain composed of sandy and conglomeratic shoreface deposits. In most of the units, upper shoreface conglomerates trend east-west parallel to the paleoshoreline. The top of Falher D is represented by aggradational coastal plain deposits.

The shoreface units of Falher C are characterized by very-fine to fine-grained sandstones with swaley cross-stratification. The presence of swaley cross-stratification in the sandstones, combined with a *Skolithos-Cruziana* ichnofossil assemblage, suggest that this facies represents wave- to storm-dominated deposition in a high-energy, upper to middle shoreface environment. Upper shoreface conglomerates and conglomeratic sandstones with cross-bedding are present in limited bodies trending east-west.

The basal surface of Falher C across the study area is a composite of different marine flooding surfaces which overlie the aggradational coastal plain deposits of Falher D.

Falher C contains a series of shoreface units (C1, C2 and C3) separated by erosional surfaces. The transgressive systems tract in each unit can be preserved as transgressive marine mudstones and/or coarse transgressive lag deposits. The highstand systems tract comprises a succession of sandy and conglomeratic shoreface deposits, prograded as a strandplain system.

A major relative sea level fall ended the progradation of unit C3 producing a sequence boundary and a seaward shift of the shoreface facies beyond the northern edge of the study area. A relative sea level rise caused shoreface migration southward (landward) and the transgressive system tract is preserved as 4-7 m thick marine mudstones. Progradational shoreface deposits of unit C4 took place during highstand.

In Falher C, a north-south trending channel (C5) cuts into shoreface deposits of unit C4. This channel was probably feeding shoreface C4 during its progradation. The uppermost part of Falher C was filled by aggradational coastal plain deposits and the top of Falher C is defined by a marine flooding surface with erosional truncation during the shoreface retreat that defines the base of Falher B.

The duration of the transgressive-regressive event in each shoreface unit within Falher D and C has been estimated to be approximately 42,968 years, corresponding with fifth-order cyclic sea level changes. The changes in relative sea level during deposition of Falher D and C may be controlled by combined autocyclic and allocyclic processes.

ACKNOWLEDGEMENTS

I would like to thank Dr. Roger G. Walker for allowing me the opportunity to study at McMaster University under his supervision. His teaching during the courses and his guidance during the research are greatly appreciated.

I would also like to thank MARAVEN (Venezuelan Oil Company) for giving me the opportunity to study in Canada, providing me with a scholarship and the funding for the research. Partial funding for the Core Lab was provided by N.S.E.R.C. grants to Dr. Walker.

I am indebted to Mike Ranger who kindly permited the use of AppleCore to draft all the core data.

Esso Imperial Oil is thanked for providing support for this study permitting access to well log information, and especially Dr. Charle Gamba for his comments and recommendations.

Finally I would like to express with these words all my gratitude and love to my wife, who was a constant support during this two unforgettable years.

To my daughter Joanna and son Jonathan because they are the light of my eyes.

God sort all! Now I am here,
It is useless to grieve and sigh.
No din shall make me fear,
Even if I have to die.

Sir Gawain and the Green Knight

Medieval Arthurian Romance

TABLE OF CONTENTS

LIST OF FIGURES

LIST OF APPENDIX

1. INTRODUCTION

1.1. THE GEOLOGICAL PROBLEM

The Falher Member (Spirit River Formation) provides an excellent opportunity to study well-cored successions and systems tracts in nonmarine to marine settings and how relative sea level changes affected the facies distribution. The study will be concentrated in Falher units C and D where the core control will allow the correlation of these systems tracts and the identification of facies changes within the systems tracts. The study area (Figure 1) was selected where Falher units C and D change from nonmarine facies in the south to shore-zone and basin facies to the north (Cant, 1984; 1995), because it is in the transition zone where the sea level changes are best documented. This makes this study area an ideal location for a detailed stratigraphic study of the lateral and vertical relationships of facies.

The Spirit River Formation (Upper Mannville Group) is a 350 m thick clastic wedge which prograded into an epeiric Boreal Sea in Alberta and British Columbia during the Early Cretaceous as a result of tectonic events in the Cordilleran orogenic belt of western Canada.

The Spirit River Formation is divided into three lithostratigraphic members (Figure 2): the Wilrich, Falher and Notikewin. Within the Falher, five units (Falher A through Falher E) are recognized, each of them composed of a coarsening-upward sandbody capped by regionally extensive coals or coaly mudstones. Previous authors have based the subdivision of the Falher Member on the occurrence of these capping coals (Jackson, 1984; Smith, *et al.*, 1984; Cant, 1984) but recent papers demonstrate the presence of new stratigraphic units and associated bounding discontinuities within the existing Falher A and B units (Rouble and Walker, 1994; Cant, 1995) and Falher D (Arnott, 1994).

The main purpose of this study of Falher C and D is to examine a number of geological problems related to changes in relative sea level and to test or extend some ideas proposed by previous authors for Falher A, B and D. Some of these problems are:

i) Did units C and D of the Falher Member respond to similar mechanisms that controlled the sedimentation of units A and B ?

ii) Can units C and D be subdivided using high resolution sequence stratigraphic techniques?

iii) How do shoreline depositional systems respond to sea level changes?

iv) How does the coastal plain respond to sea level changes?

v) Were the conglomerates within Falher units C and D deposited in a marine or fluvial setting?

vi) Were the marine conglomerates deposited in a transgressive, highstand or lowstand system tract?

vii) What is the relationship between the main sandstone body and a shaly succession in the middle of the study area in unit C?

viii) What is the temporal scale of the sea level fluctuations?

These problems are addressed in the thesis using detailed core descriptions and well log correlations across the study area.

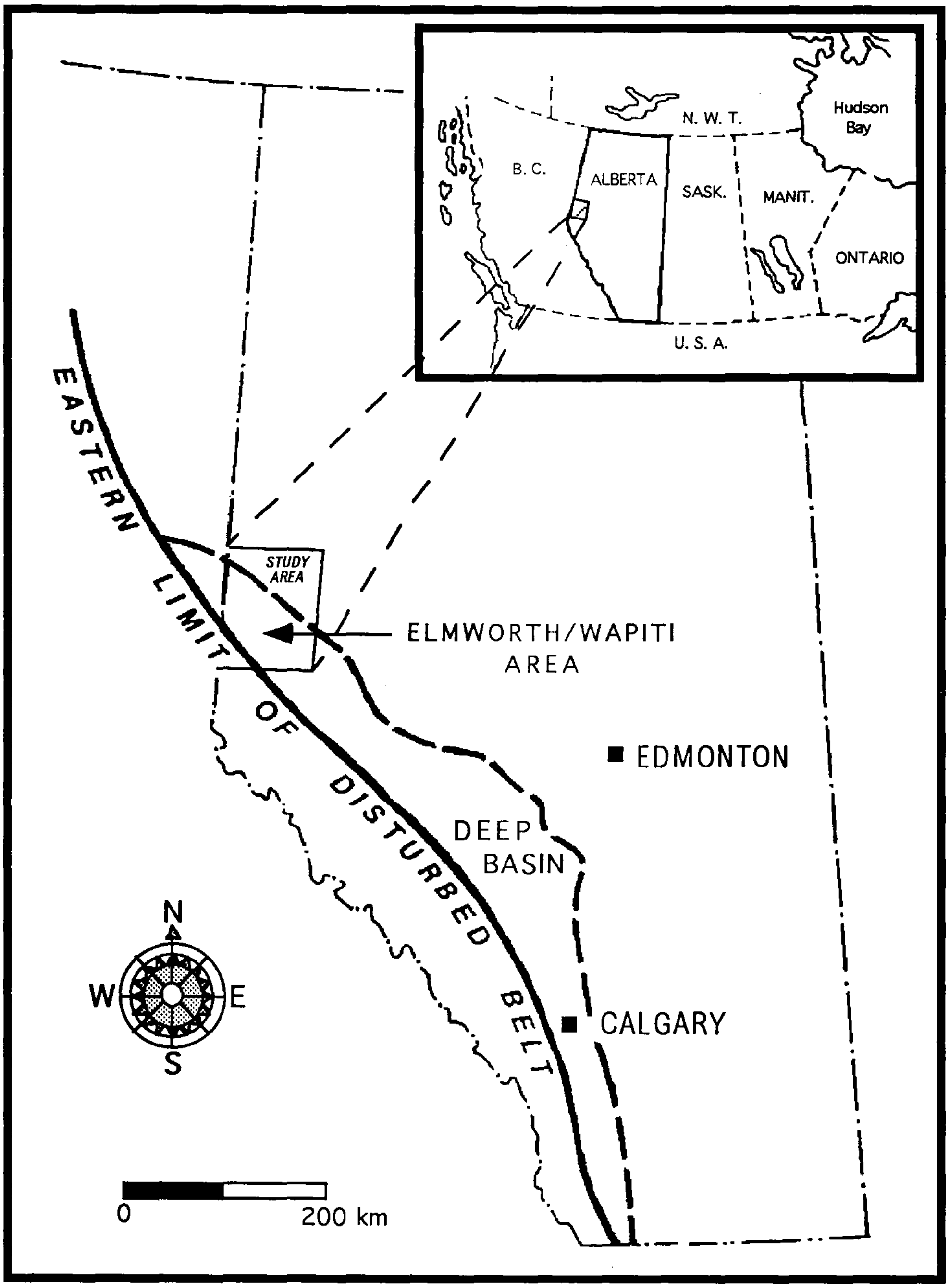

Fig. 1. Location map showing the position of the study area relative to the Deep Basin of Alberta. The segment of the Deep Basin which occurs within the study area is essentially the Elmworth gas field.

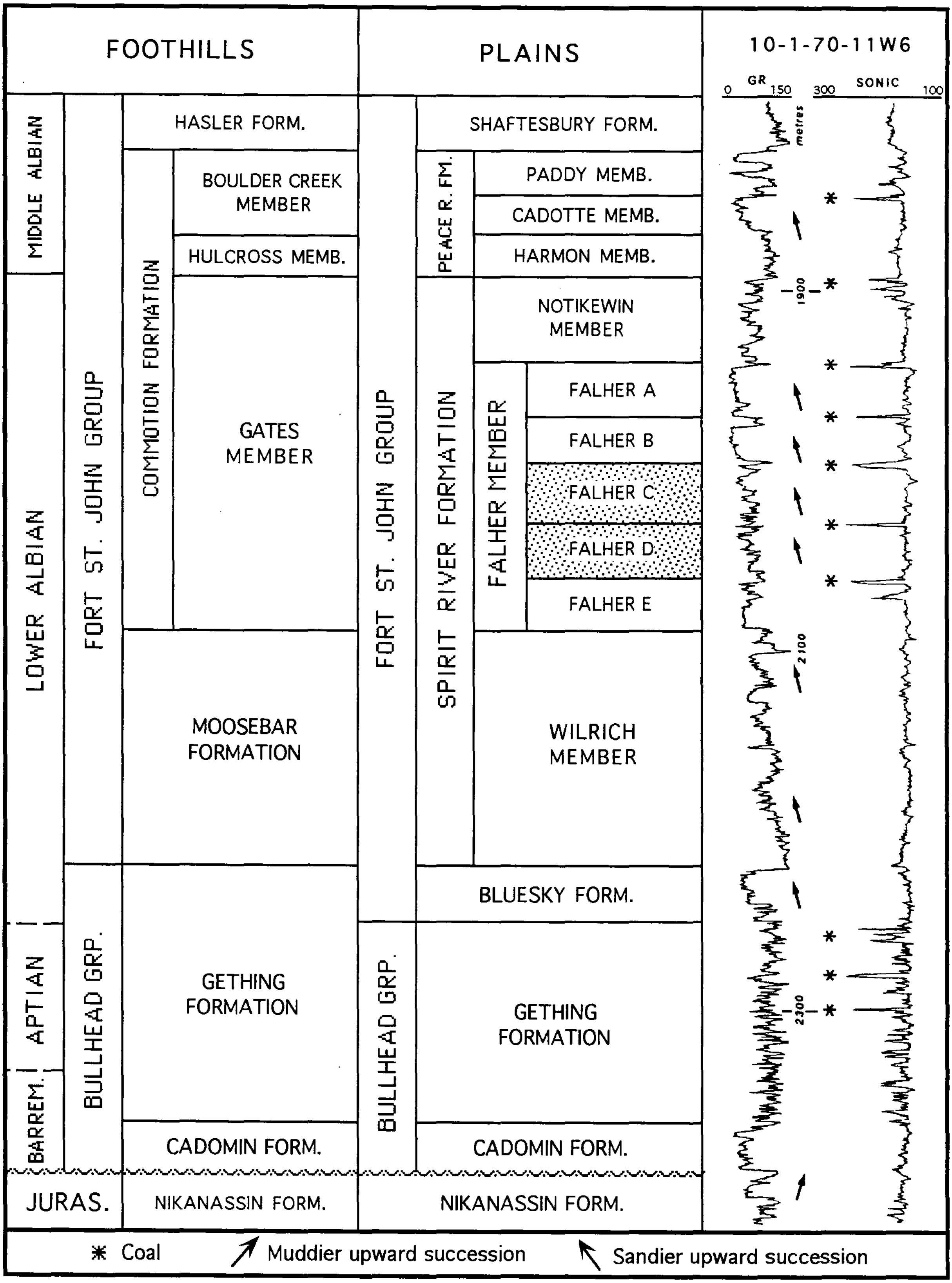

Figure 2. Lower Cretaceous correlation chart for the Foothills outcrop belt and the adjacent Plains of Alberta. After Smith *et al.* (1984). Studied units of Falher C and D are stippled.

1.2. THE STUDY AREA

The study area is located in west-central Alberta (Figure 1). In this area a thick wedge of sedimentary rocks is part of the filling of the Alberta Foreland Basin, which was created as a response to lithospheric loading by an arc during the Middle Jurassic. This caused subsidence from the Upper Jurassic to the Eocene.

The rocks of the Alberta foreland basin are now contained in four major structural elements, (1) the eastern part of the Rocky Mountain belt, (2) the folded and thrusted Foothills belt, (3) the area of maximum subsidence (foredeep) and (4) the broad, undeformed platform of sediments to the east that comprises the Plains of the Alberta Foreland Basin (Jackson, 1984; Cant, 1989).

Within the Plains, the area adjacent to the Foothills in western Alberta and eastern British Columbia is termed the "Deep Basin" (Figure 1), not because of its original water depths but because of the depths of present oil and gas drilling targets. The northwestern part of the Deep Basin within the study area is also referred as the Elmworth/Wapiti area (Smith *et al.*,1984).

The study area covers about 5200 km^2 and extends from Township 66 to 73 and Ranges 7-13, west of sixth meridian. The database consists of 333 well logs; 71 of them with cores in Falher C and or D (Figure 3).

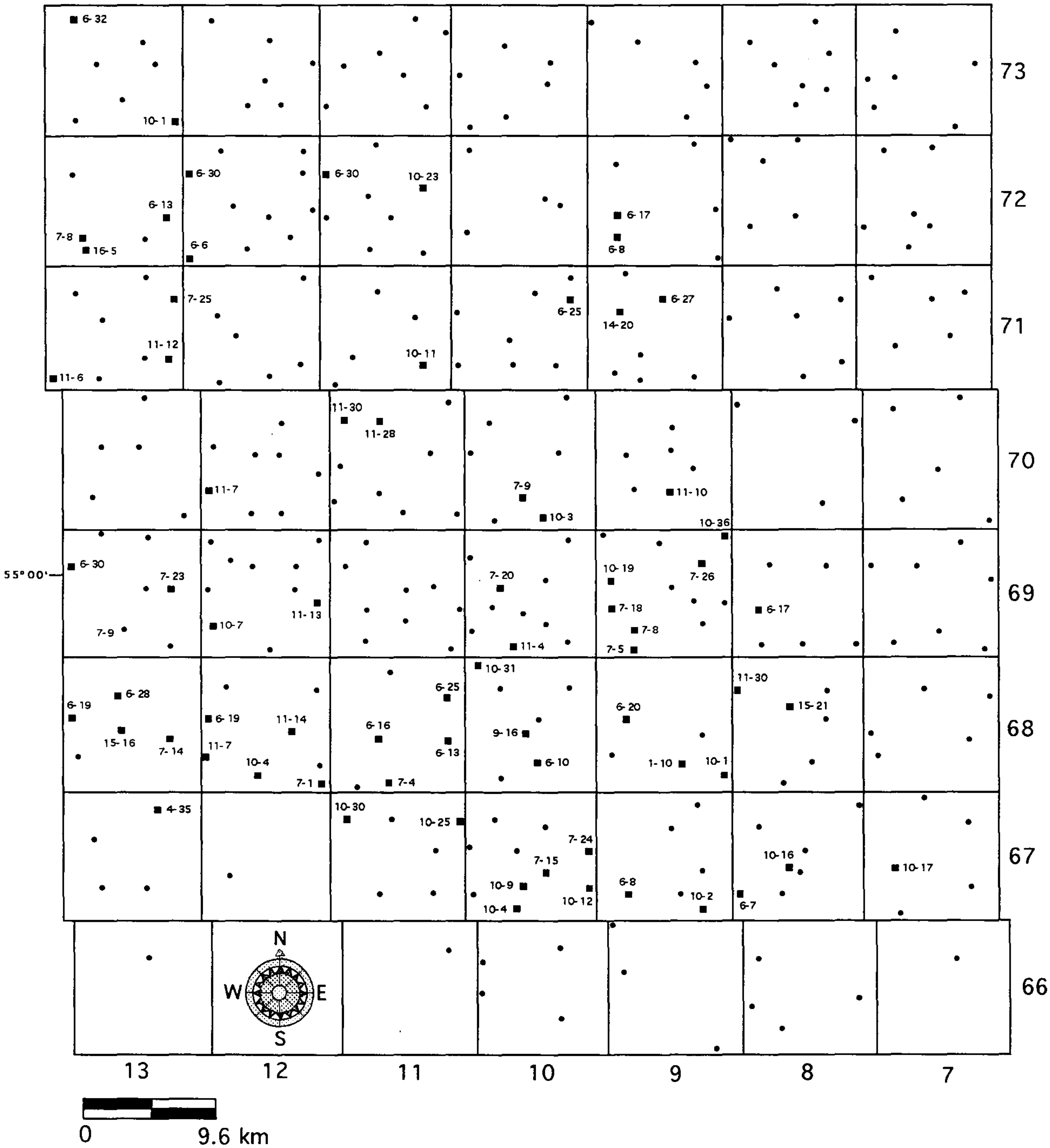

Fig. 3. Index map of the study area showing the location of wells (●) and cores (■). The study area encompasses Townships 66-73, Ranges 7-13W6. Each township in the Township-Range geographical system of Alberta is 9.6 km (6 miles) on each side.

2. REGIONAL SETTING AND STRATIGRAPHY

2.1. REGIONAL STRUCTURAL SETTING

The Western Canadian Sedimentary Basin has the form of a southwest-dipping asymmetrical trough (Monger, 1989). It was created toward the end of the Jurassic in response to arc accretion and lithospheric loading. During the Paleozoic, western Canada was characterized by an extensional passive margin setting; this changed to a highly compressional region when the overthrusted terranes of the early Cordillera loaded the western margin of the continent, creating a foreland basin to the east (Jackson, 1984).

Monger (1989) defined the Western Canadian Cordillera as a "collage" of terranes. The Cordillera appears to have been built by mainly Mesozoic accretion of terranes to the ancestral North America. These relationships were used by Monger (1989) to construct a time-space diagram of this Cordilleran collage, where three morphogeological belts (Insular, Coast, Intermontane; Figure 4) collided with part of the North America plate (Omineca and Rocky Mountain). The belts reflect the sum of the processes which occurred from Proterozoic to recent times, but are dominated by features formed during Middle Jurassic to Early Tertiary convergence (Monger, 1989).

In recent years, van der Heyden (1992) proposed a rather different scenario from the one conceived by Monger (1989). New stratigraphic, paleontologic and geochronologic data presented by van der Heyden (1992) suggest that the tectonic features of the Western Canadian Cordillera can be

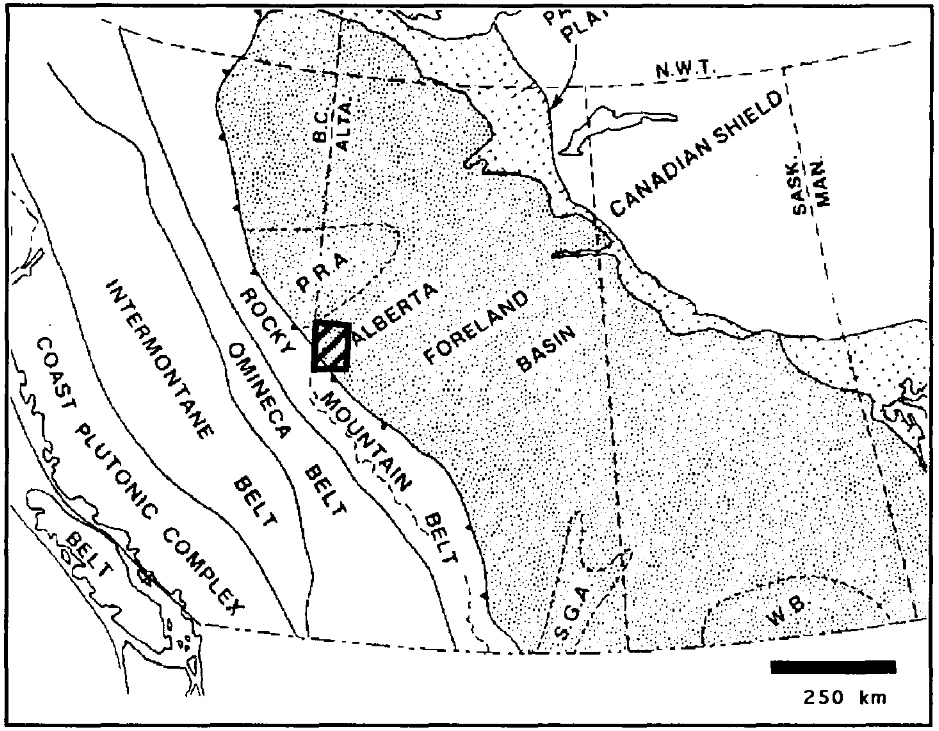

Fig. 4. Map of the Canadian portion of the foreland basin showing the tectonic elements; the Canadian Shield, the Williston Basin (WB), the structural belts in the orogen, the Peace River Arch (PRA), and the Sweetgrass Arch (SGA). Modified from Cant (1984). The study area is shown with a ruled rectangle in the west-central part of Alberta.

interpreted in terms of Middle Jurassic accretion of a single composite superterrane (Stikinia/Wrangellia/Alexander) to ancestral North America in a single arc collision event. The Coastal belt is interpreted primarily as the result of successive intraterrane, magmatic, metamorphic, structural and stratigraphic overprints related to prolonged subduction of Pacific Ocean lithosphere beneath the North American margin. The Insular and Intramontane superterranes, previously viewed as widely separate entities prior to mid-Cretaceous time, were already amalgamated to the Coastal belt before Middle Jurassic.

The tectonic evolution of all these areas was the result of prolonged east-dipping subduction in a primary subduction-related Andean magmatic arc, which created a complex succession of magmatic arcs and related intraterrane compressive and extensional structures (van der Heyden, 1992).

During the Middle Jurassic, a foreland basin was created by lithospheric loading of the arc. The basin was affected by two large basement structures which originated in the Paleozoic, but which also affected sedimentation in the Cretaceous, the Peace River Arch and the Sweetgrass Arch (Figure 4). They moved upward and downward, probably in response to thrust loading in the Cordillera, affecting the stratigraphy, facies distribution and thicknesses of the units overlying them (Cant, 1989; O'Connell *et al.*, 1990). The foreland basin continued subsiding and receiving sediments until the Eocene when the basin was filled.

2.2. REGIONAL DEPOSITIONAL HISTORY OF THE LOWER CRETACEOUS IN ALBERTA

Following a period of Early Cretaceous (Hauterivian) uplift and erosion, the area began to subside and receive sediments from the rising Cordillera to the west. During the Barremian, alluvial fan and braid-plain conglomerates of the Cadomin Formation were deposited, followed by Aptian fluvial and delta plain sediments of the Gething Formation (Smith *et al.*, 1984). In early Albian time, continued subsidence of the trough resulted in a major transgression from the north by the Boreal sea. This event is represented by the coastal and shallow marine sandstones of the Bluesky Formation. The Bluesky was capped by the marine shales of the Moosebar Formation and the Wilrich Member (Spirit River Formation) as the Boreal sea continued to deepen and advance southward (Smith *et al.*, 1984).

During middle-to-late early Albian time, a major flood of sediment restored the continental conditions. The regressive, coastal/deltaic sandstones and conglomerates of the Falher and Notikewin members (Spirit River Formation) represent the northward advance of the coastline during this period of marine retreat (Smith *et al.*, 1984).

Another major marine transgression occurred during the early part of the middle Albian. This event is represented by the marine shales of the Harmon Member which cap the Notikewin Member. A well-developed regressive cycle, represented by the coastal plain to shallow marine sediments of the Paddy and

Cadotte members occurs within this transgressive pulse, which continued until at least the end of Albian time (Smith *et al.*, 1984).

2.3. LITHO- AND BIOSTRATIGRAPHY OF THE SPIRIT RIVER FORMATION AND EQUIVALENTS

The Spirit River Formation comprises the upper portion of the Mannville Group in western Alberta (Figure 5) and eastern British Columbia and occurs entirely in the subsurface. It consists of a sandstone-dominated, unconformity-bounded, Aptian to lower Albian clastic wedge that was deposited in the foreland basin. This prograding clastic wedge built northward into an embayment of the Arctic Ocean created earlier by a transgression of the Boreal sea.

The Spirit River Formation has been divided into three members (Wilrich, Falher and Notikewin) on a lithologic basis. Within the Falher, Cant (1984) defined five units named A to E and within the Wilrich, he recognized two more units named A and B. Some of these units are coarsening-upward or fining-upward, while others are defined only by lithologic breaks such as coals or coaly mudstones (Figure 2).

Most of the units in the Falher Member consists of major bodies of sandstone and conglomerate which are separated by mudstones, coaly mudstones and/or coals. South of township 67 the successions are dominantly nonmarine, and units A to E cannot be easily recognized (Cant, 1984). A number of these sandier upward sedimentary units were interpreted by Cant

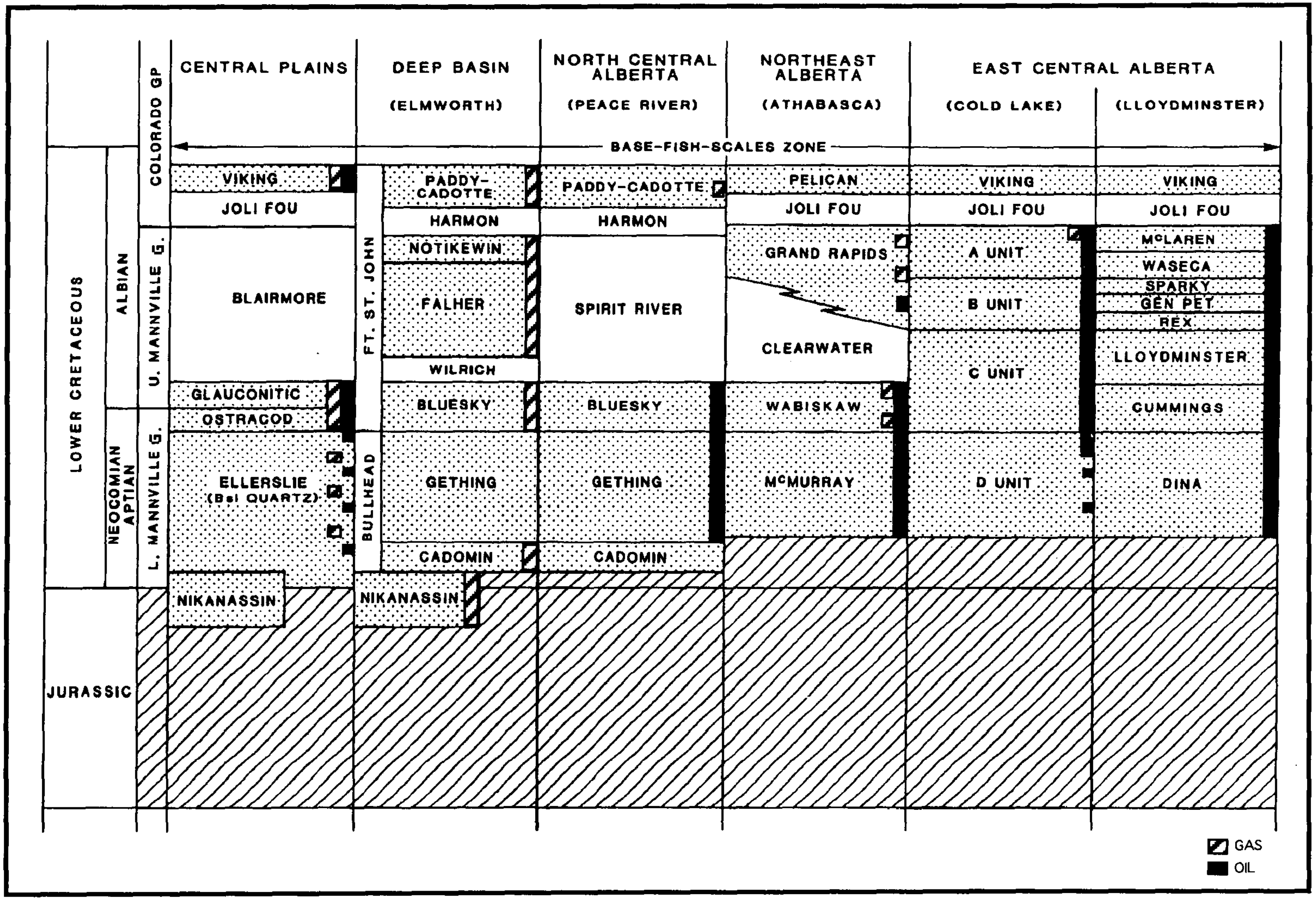

Fig. 5. Correlation chart of Jurassic-Lower Cretaceous formations across Alberta, showing principal oil and gas zones. Resevoir beds stippled. After Masters (1984).

(1984) to be the result of fluctuation in sediment supply, possibly related to episodic Cordilleran thrusting events. Despite a rising relative sea level, the abundance of sediment supply overwhelmed the sea level rise and caused rapid progradation. Cant (1988, 1995) and Cant and Stockmal (1993) suggested that the subsidence of the Peace River Arch (a large basement structure originated in the Paleozoic) also affected the sedimentation of the transgressive-regressive successions of the entire Spirit River Formation and proposed that the transgressive-regressive limits were partly constrained by the subsidence of this arch. Near the southwestern margin of the arch, several shoreface sandstones are stacked vertically in the Falher Member as a result of this high rate of subsidence.

The members of the Spirit River Formation thicken very little in the seaward direction over 140 km. This near parallelism of the upper and lower boundaries is a consequence of the very low slopes in the epeiric seaway (Cant, 1984).

The Spirit River Formation pinches out northward and passes into the marine shales of the Clearwater (Buckinghorse) Formation (Smith *et al.*, 1984). To the south in the central plains of Alberta, the nonmarine equivalent to the Spirit River Formation is the Blairmore group (Jackson, 1984).

The stratigraphic equivalents of the Spirit River Formation in British Columbia are the Moosebar Formation and the Gates Member of the Commotion Formation (Figure 5). These units are exposed in outcrops within the Foothills belt. Leckie and Walker (1982) recognized a series of coarsening-upward, marine to nonmarine successions in the Moosebar-Gates interval. Flow directions indicated a north-dipping paleoslope.

Caldwell *et al.* (1978) identified the *Rectobolivina* sp. Subzone (early Albian) in the Moosebar Formation and the *Marginulinopsis collinsi-Verneulinoides cummingensis* Subzone (early middle Albian) in the middle-upper part of the same formation and in the Clearwater Formation, both equivalents of Falher-Wilrich Members. For the transition between the Moosebar Formation and Notikewin Member, the same authors identified the *Gaudryna nanushukensis* Zone (middle Albian).

2.4. OIL AND GAS

Great volumes of oil and gas have been generated, migrated and trapped in the clastic sediments of the lower Cretaceous Mannville Group of Alberta Basin (Figure 4). Within the Spirit River Formation, specifically in Falher units A, B and D, major reserves have been discovered. Each of these units contains lenticular bodies of conglomerate that are the main conventional reservoir (Cant and Either, 1989) in the Deep Basin.

The sandstone reservoirs in the Deep Basin have average porosities of 8.0 % and average permeabilities from 0.001 to 0.5 millidarcys, reflecting the "tight sand" nature of the Deep Basin. Massive hydraulic fracturing may allow high flows from these "tight sands" but economic production is a function of technology and gas prices (Masters, 1979). However, the coarse-grained sandstone and conglomerate reservoirs have much higher average permeabilities, ranging from 20 to 80 millidarcys. As a result, in areas of the Deep Basin containing such reservoir rock, gas productivity is quite high (Smith *et al.* 1984).

Well performance in the Deep Basin is variable. High-productivity wells can be capable of producing as much as 100 mmcf/d from a high-permeability conglomeratic sandstone. Low-permeability tight sandstones, although gas charged, are incapable of producing at commercial rates into conventional gathering systems (Smith, 1984). The total gas reserves in the Elmworth/Wapiti area alone have been estimated to be approximately 9.8 Tcf or 2.8 x 10^{11} m^3 (Masters, 1984; Smith, 1984).

3. PREVIOUS WORK IN THE FALHER MEMBER AND EQUIVALENTS

In the early 1980s many studies were published involving the description and sedimentological interpretation of Lower Cretaceous sandstone reservoirs in the Deep Basin of Alberta and British Columbia.

In 1984 Smith, Zorn and Sneider published a study of the depositional history and paleogeography of the Lower Cretaceous sediments in the Deep Basin. They recognized five distinct units (A to E) in the Falher Member where each unit represents a rapid transgression followed by a slow regression as the coastline moved back and forth across the area. Using paleographic maps these authors showed the landward limits of transgression in each unit and the extension of various log facies across the study area.

To compare with the subsurface units, Leckie and Walker (1982) studied the Moosebar Formation and Gates Member that crop out in the deformed Foothills belt south of Fort St. John, British Columbia. These formations are equivalent to the Wilrich-Falher interval of the Deep Basin in Alberta and British Columbia. The Moosebar-Gates interval contains a series of coarsening upward, marine to nonmarine units. The units begin with turbidites deposited below storm wave base, followed by sharp-based sandstones with hummocky cross-stratification above storm wave base. As the units prograde, nearshore deposits are preserved with some swaley cross-stratification. The nonmarine environments include vertical accretion deposits of mud and silt in both lagoonal and floodplain areas.

Cant (1984) defined eight major transgressive and regressive units of sedimentation, 30-50 m thick, within the Spirit River Formation. Each unit was interpreted to consist of shoreface and beach deposits with nonmarine deposits to the south, all of them overlain by backswamp-lagoon sediments. On a large scale, the shoreline successions were correlated northward to marine successions which grade from shale at the base to fine sandstone at the top. Each coarsening-upward succession is bounded by marine shale laid down during a transgression, when coarser sediment was trapped in nonmarine or marginal areas.

Because of the importance of the Falher Member as a gas reservoir in the Deep Basin, Cant and Ethier (1984) discussed the reservoir properties of conglomerates in units A and B, relating the type of conglomerate (unimodal, bimodal grain supported, and bimodal sand supported) and the diagenetic processes suffered by these rocks. They concluded that bimodal conglomerates (sand and pebble supported) have lost a significant amount of porosity because of cementation of the quartz-rich matrix. Unimodal conglomerates have not experienced major reduction of porosity and permeability because the original low content of quartz.

One interesting modification of Cant's (1984) core cross-sections and his ideas about Falher A was made by Demarest and Kraft (1987). In the modified section (Figure 6), Demarest and Kraft (1987) interpreted the lower dashed line as the ravinement surface produced by a beach migrating through the area prior to deposition of the transgressive nearshore sandstones. They did not interpret the ravinement surface at 0 m as a sequence boundary. Instead, they

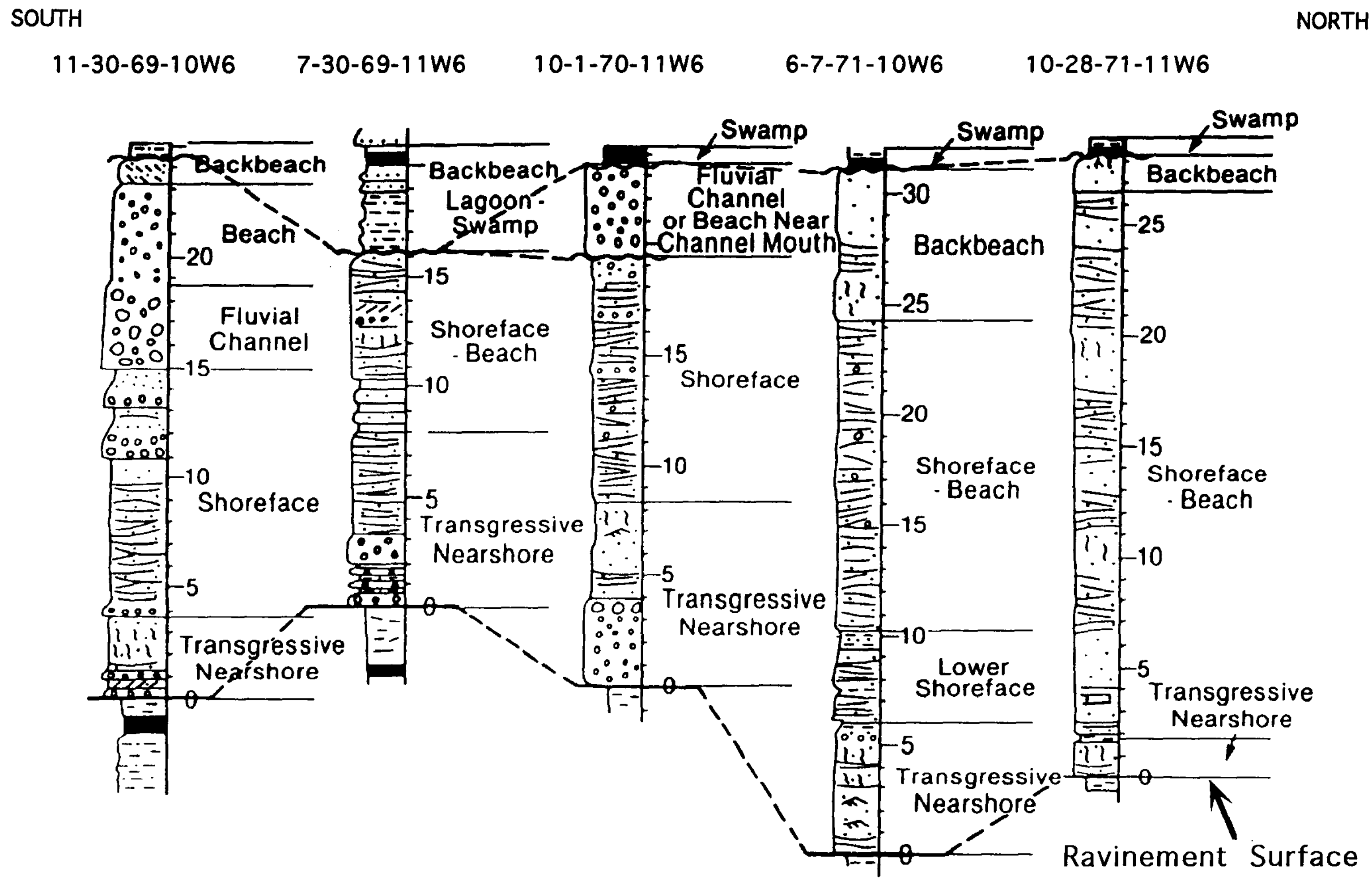

Figure 6. Measured sections of the Falher A by Cant (1984) and modified by Demarest and Kraft (1987). The dashed horizon at 0 m represents the ravinement surface below the transgressive sequence and the dashed line near the top represents the basal unconformity over which the next transgression occurred.

suggested that the section from the base of the paralic deposits (below 0 m, Figure 6) to the top of the transgressive sandstones (5-7 m above 0 m) represents the entire transgressive section and the section from the top of the transgressive deposits to the top of the beach and the fluvial section represents the regressive section. The only change introduced by Demarest and Kraft (1987) to Cant's (1984) interpretation is the inclusion of the lagoonal deposits in the base of the transgressive part of the section rather than at the top of the regressive section (Fig 6). This change results in a somewhat different view of the depositional history, correlations and interpretations. The implication is that the base of Falher A is the sequence boundary over which the transgression occurred (at the base of the lagoonal deposits) instead of the ravinement surface (0 m in Figure 6), so that Falher A now only includes genetically related strata.

In a more specific study of diagenesis, Tilley and Longstaffe (1989) analyzed the porewater evolution of the Falher Member, combining results from petrologic, stable isotope and fluid inclusion analysis of diagenetic minerals. Four stages of diagenesis and porewater evolution were identified by these authors. Stage 1 (deposition and burial) is marked by early precipitation of hematite, siderite and the dissolution of unstable detrital grains. Stage 2 (maximum burial and relief) is dominated by precipitation of quartz druse in conglomerates and horizontal fractures. Stage 3 (uplift and erosion) is dominated by precipitation of dickite. Finally during stage 4 (maximum generation of methane from coals) methane saturation of the porespaces marked the end of diagenesis in the down-dip part of the Deep Basin.

Following the "boom" of papers describing many of the Alberta Basin formations in terms of sequence stratigraphy, Arnott (1993) studied the Falher D pool in northwestern Alberta-northeastern British Columbia and identified four depositional units within Falher D (D1, D2, LS1 and D3). He suggested that not only were changes of relative sea level important in controlling the distribution of reservoir strata within the study area but also temporal changes in the nature of sediment being supplied to the Falher shoreline.

In his paper Arnott (1993) showed a diagrammatic cross-section of the eastern portion of his study area. In this section (Figure 7) he suggested that the D2 shoreline prograded northward, followed by a relative sea level fall of several meters, with the creation of a regressive surface of erosion (sequence boundary in Figure 7a). In Figure 7b, Arnott (1993) suggested that the deposition of LS1 took place after a relative sea level rise, the re-establishment of stillstand, and the progradation. Another rise, followed by sediment input and progradation during a slow rise, gave D3. Finally, a regional flooding event terminated the Falher D deposition.

One year later, Rouble and Walker (1994) studied units A and B of the Falher Member in northwestern Alberta. They suggested that the 10-30 m thick coarsening-upward sandbodies of Falher A and B are split by mudstone tongues that represent marine flooding surfaces. These tongues split each existing Falher unit into two separate allostratigraphic units. Each of these four allomembers (A1, A2, B1 and B2) was deposited as a barrier/strandplain system formed of shoreface deposits, and sandy and gravely beach ridges.

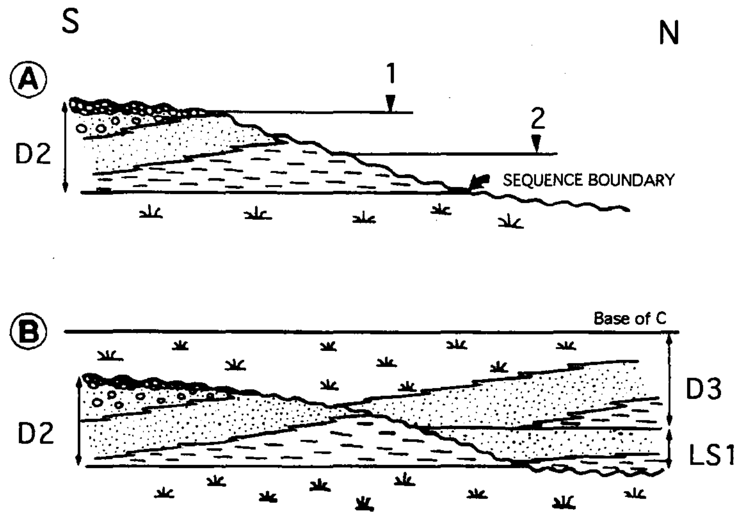

Fig. 7. Diagrammatic cross-section illustrating the development of the sequence boundary and subsequent deposition interpreted by Arnott (1993). In A, after the progradation of D2, a relative sea level fall (1 to 2) shifted the shoreline northward and a regressive surface of erosion was created (sequence boundary). In B, following a RSL rise and progradation, LS1 strata were deposited. A new RSL rise brought the shoreline southward, followed by the progradation of D3. Finally, a regional flooding surface event terminated the deposition of Falher D. After Arnott (1993).

Rouble and Walker (1994) described the preserved transgressive system tract as barrier sands, transgressive lag deposits, some lagoonal deposits, an estuary fill and onlapping transgressive offshore storm deposits. The highstand system tract comprises the prograding shoreface succession.

In a different study, Cant (1995) suggested that unit B of the Falher Member contained a basal sheet-like shoreface unit of hummocky cross-stratified sandstone that thins seaward and terminates about 30 km seaward of the landward limit of the transgression. These sandstones are interpreted by the author to be sandy wave-dominated, regressive shoreface deposits. In some areas Cant (1995) described the basal prograding shoreface sandstone as being overlain by a transgressive sand sheet, in places conglomeratic. He described this transgressive succession as a fine- to medium-grained sandstone-dominated zone with layers of pebbles, cross-bedding and numerous zones of *Palaeophycus* burrows. In other parts of the shore zone, conglomeratic bodies are placed by Cant (1995) at the top of these transgressive sandstones, suggesting that the base of these conglomerates is a ravinement surface developed after the transgressive event. Cant (1995) seems to contradict himself when he suggested that the conglomerates can be the product of migrating tidal channels, but drew these conglomerates within an incised shoreface rather than in tidal channels (Figure 8).

Basinward, the succession shows a thick sandstone (detached from the previous prograding shoreface) interpreted as a different shoreface deposit, and an overlying coarsening-upward shoreface succession with thin muds and coals interpreted as back-barrier deposits. These basinward facies are

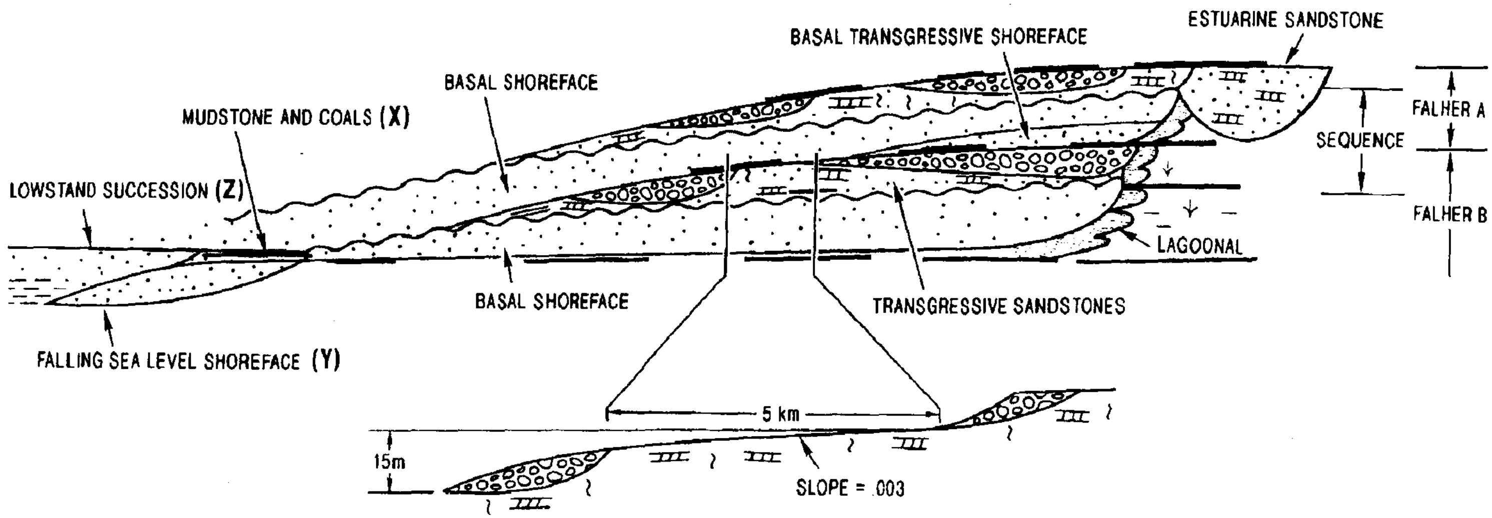

Figure 8. Diagram summarizing Cant's (1995) interpretation for Falher A and B. Notice that the sequence boundary within each succession underlies the transgressive sandstones, and the conglomerates are separated from the transgressive sandstones by a ravinement surface in the shore complex. After Cant (1995).

interpreted by Cant (1995) to be the result of a relative sea level fall and subsequent relative sea level rise. The Falher A unit is described by Cant (1995) as similar in most respects to B, with A regressive shoreface sheet sandstone overlain by ridges of transgressive barrier conglomerate.

One of the most important differences between the interpretations of Cant (1995) and Rouble and Walker (1994) concerns the position and significance of the conglomerates.

In Figure 8 Cant (1995) summarized the stratigraphy of the Falher A and B. Here, the sequence boundary within each succession underlies the transgressive sandstone and conglomerates in the shore-zone complex and Cant (1995) states that "In this case, the conglomerates are separated from the sandstones by a ravinement surface and sit in scoop-shaped transgressive erosional scours cut on the flatter surface". Thus, Cant (1995) favored a hypothesis where a sandy coastal transgressive deposit was laid down before the final barrier transgression implying the existence of a ravinement surface formed after the transgressive sand sheet.

By comparison, Rouble and Walker (1994) suggested that these conglomerates formed part of the prograding sandy to gravely upper shoreface. If so, the bounding discontinuity occurs above the conglomerates and not below as Cant (1995) proposed. Rouble and Walker (1994) also described a poorly-sorted conglomeratic facies, massive or crudely stratified, commonly containing abundant wood and coal fragments. These conglomerates occur abruptly on top of a coal and are normally overlain by sharp-based swaley cross-stratified sandstones. Rouble and Walker (1994) interpreted these conglomerates (based upon their stratigraphic position and sedimentology) as a transgressive lag. These conglomeratic facies were not mentioned or interpreted by Cant (1995).

4. FACIES DEFINITION AND INTERPRETATION

4.1. ALLOMEMBER FALHER D

4.1.1. BOUNDING SURFACES

4.1.1.1. Basal Surface

The basal surface of Falher D is defined by a **marine flooding surface,** interpreted as a **transgressive surface of erosion** (TSE) in places modified by a **regressive surface of erosion** (RSE). This surface overlies mostly nonmarine deposits (coals, mudstones and sandstones) of Falher E. Southward, in T66 and T67, the marine flooding surface probably changes in character and the logs suggest that the marine flooding surface passes into a **flooding surface** (FS) characterized by a contact of lagoonal-on-nonmarine deposits.

4.1.1.2. Top Surface

The top surface of Falher D will be defined below and it is represented by the basal transgressive bounding surface of Falher C.

4.1.2. FACIES DEFINED BY WELL LOG PATTERNS - D

The correlation of 331 well logs allowed the identification of four well log facies characterized by (1) Blocky to sandier-upward gamma-ray log signal, (2) Variable gamma ray log signal, (3) Spiky-sonic log signal and (4) Blocky to muddier-upward gamma ray log signal. These log facies are described and interpreted here and they will be placed in a stratigraphic context using maps, log and core sections in following chapters.

4.1.2.1. Blocky to sandier upward log facies (Allomember D)

Blocky to sandier-upward signals in the gamma ray log are found from T68 northward. Commonly, two blocky to sandier upward successions are superimposed (e.g. well 6-28-68-13W6, Appendix A35).

The density-porosity logs also show a blocky to an upwardly-increasing log response.

The resistivity logs always show a resistivity increase upwards. Good examples of this signature are in wells 7-4-68-11W6, 1-10-68-9W6 and 11-6-71-13W6.

This blocky to sandier-upward log signal changes in character southward (T67) and is replaced by variable log responses suggesting mudstones, coals and some sandstones.

The thickness is very variable (5-25 m) and the reasons for that will be discussed later.

4.1.2.2. Variable log facies (Allomember D)

Northward from T70, the basal part of Falher D shows variable responses in the gamma ray log, in places with a sandier-upward trend. The density-porosity and neutron logs show also very variable responses.

The logs also suggest alternation of sandstones and mudstones in equal proportions. The thickness of this facies ranges from 5 to 15 m. Good examples of this facies are present in cores 6-6-72-12W6 (Appendix A40) and 10-23-72-11W6 (Appendix A9).

4.1.2.3. Spiky-sonic log facies (Allomember D)

The spiky-sonic log signal is characterized by big low-velocity spikes in the sonic log that always correlate with coals or coaly mudstones in core. The density-porosity log shows low values without any dominant trend. The gamma ray log also shows no dominat trend.

These log signals occur across the entire study area and characterize the top of Falher D. The thickness of this log response is very variable. It is about 15 m in the area of townships 68 and 69, but thins northward to T73 where it almost disappears. To the south (townships 66 and 67) the entire succession of Falher D is composed of this log pattern with a thickness about 20-30 m.

Good examples of this type of signal are in wells 15-16-68-13W6 (Appendix A22), 11-7-68-12W6 (Appendix A20), 6-10-68-10W6 (Appendix A26), and 6-20-68-9W6 (Appendix A31), where the log response can be calibrated with cores. The cores always show coals, mudstones and siltstones. Sandstones with roots traces and fining-upward trends are commonly present.

4.1.2.4. Blocky to muddier-upward log facies (Allomember D)

This facies is characterized by a blocky or muddier-upward trend in the gamma ray log. The density-porosity and sonic logs show low responses and the resistivity logs show a flat profile without any trend. Nevertheless, in some cases it is absolutely impossible without core control (e.g. 6-17-72-9W6, Appendix A29) to distinguish between this facies and the blocky facies previously described. The thickness is very variable ranging from 5 to 15 m.

4.1.3. FACIES DESCRIPTION AND INTERPRETATION

4.1.3.1. Blocky to sandier-upward log facies (D)

- Description

This facies is characterized by a blocky to sandier upward well log response, as described previously. Twenty one cores were taken in this succession because is the main pool in Falher D, and three of the best examples are 11-7-68-12W6, 6-16-68-11W6 and 6-8-67-9W6 (Appendix A20, A28 and A42).

This succession is mainly composed of very-fine to fine-grained sandstones with **swaley cross-stratification** (SCS) (Figure 9) and low angle parallel stratification (Figure 10). Cross-stratification occurs in fine- to medium-grained sandstone beds, in sets 10 to 15 cm thick. In many places, the main sandstone body has some conglomeratic beds interbedded with the sandstones.

In situ root traces are present at the top of the main sandstone body over the entire study area.

Trace fossils include *Macaronichnus* (6-8-72-9W6, Figure 11), 4-35-67-13W6, 11-7-68-12W6, 15-16-68-13W6, 6-28-68-13W6, 10-1-73-13W6, 6-30-72-11W6, 6-20-68-9W6, 6-25-71-10W6 and 7-25-71-13W6), *Palaeophycus* (4-35-67-13W6, 6-28-68-13W6, 16-5-72-13W6, 7-4-68-11W6, 6-30-72-11W6, 6-30-72-12W6, 9-16-68-10W6 and 7-5-69-9W6), *Teichichnus* (6-8-72-9W6 and 10-31-68-10W6), *Planolites* (6-30-69-13W6 and 10-1-73-13W6) and *Terebellina* (9-16-68-10W6).

In many cores (e.g. 10-1-73-13W6 and 6-17-72-9W6) the sandstones appear structureless (Figure 12) probably because of the action of interstitial meiofauna (Bromley, 1990). In some cores (e.g. 7-25-71-13W6, Figure 13) the disappearance of the sedimentary structures because of this kind of bioturbation can be seen in few centimeters.

Figure 9. Fine-grained sandstone containing low angle cross-lamination interpreted as swaley cross-stratification (Well 10-1-73-13W6 depth 1867.8 m)

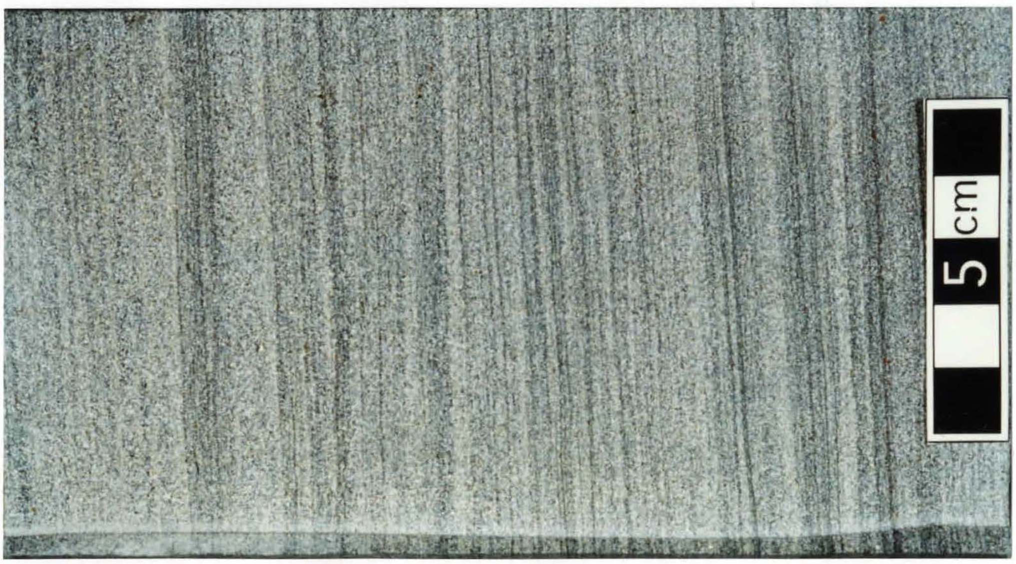

Figure 10. Fine-grained sandstone with very low angle parallel lamination (Well 7-5-69-9W6 depth 2074.5 m)

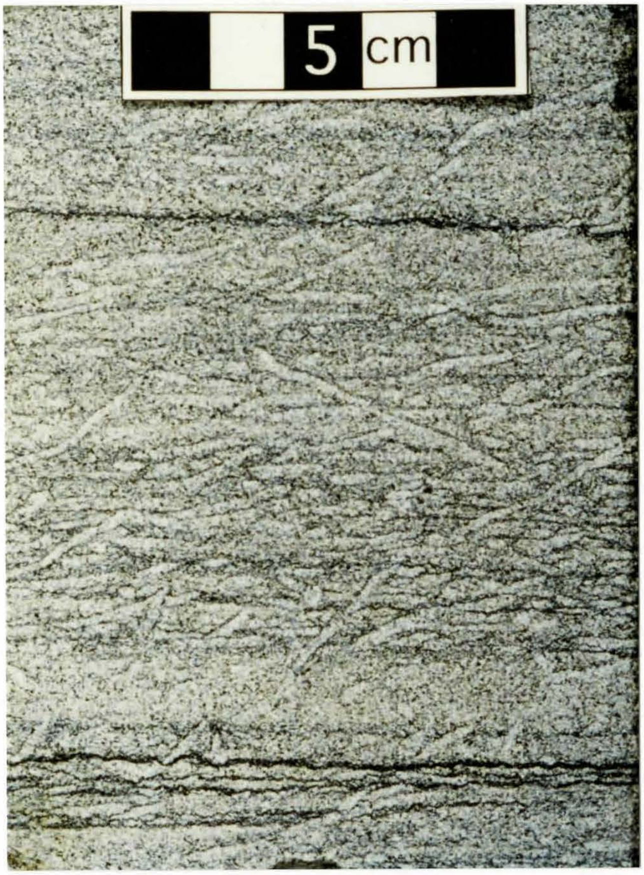

Figure 11. Fine- to medium-grained sandstone containing abundant traces of *Macaronichnus* (Well 6-8-72-9W6 depth 1747.3 m)

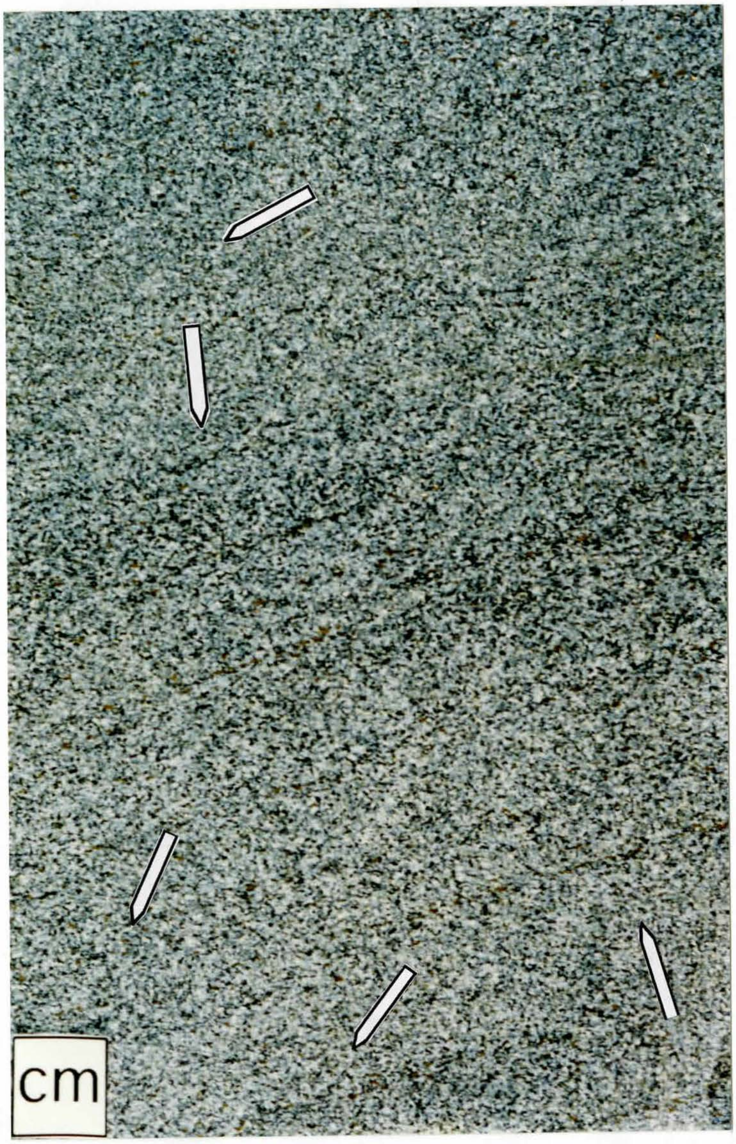

Figure 12. Almost structureless fine-grained sandstone, probably the result of an intense bioturbation by meiofaunal organisms (white arrows). Well 6-17-72-9W6 depth 1730.6 m.

Figure 13. Medium-grained sandstone completely bioturbated (lower half of core) by small *Macaronichnus* and interstitial meiofauna. The sandstone gradually shows cross-bedding upwards with a decrease in the intensity of the bioturbation (Well 7-25-71-13W6 depth 1998.6 m). Dark curved marks in centre of core are saw cuts.

Macaronichnus (Figure 14) and *Palaeophycus* (Figure 15) are normally present together in high concentrations. Along with the meiofaunal bioturbation, they are present in almost every core.

In township 67 and 68, conglomerates and conglomeratic sandstones are commonly interbedded. The conglomerates normally range from a few centimeters to 2 m thick; they are variably sorted (Figure 16), and either clast supported (Figure 17) or sand-matrix supported. Conglomeratic sandstones are moderately sorted with only a few scattered large pebbles. Cross-stratification (Figure 18) is the most common sedimentary structure in both the conglomerates and the conglomeratic sandstones.

In cores 6-19-68-12W6 (Appendix 30), 7-14-68-13W6 (Appendix A45), 15-16-68-13W6 (Appendix A22), 7-4-68-11W6 (Appendix A51), 7-1-68-12W6 (Appendix A44), and 11-7-68-12W6 (Appendix A20), a well developed succession up to 2 m thick of well sorted granule- to very coarse-grained sandstone, is present overlaying the fine-grained sandstones and/or poorly-sorted conglomerates.

4.1.3.2. Blocky to sandier upward log facies (D)
- Interpretation

The presence of cross-stratification and swaley cross-stratification in the sandstones, combined with a *Skolithos-Cruziana* trace fauna assemblage (Pemberton *et al.*, 1992a), suggest that this facies represents wave- to storm-

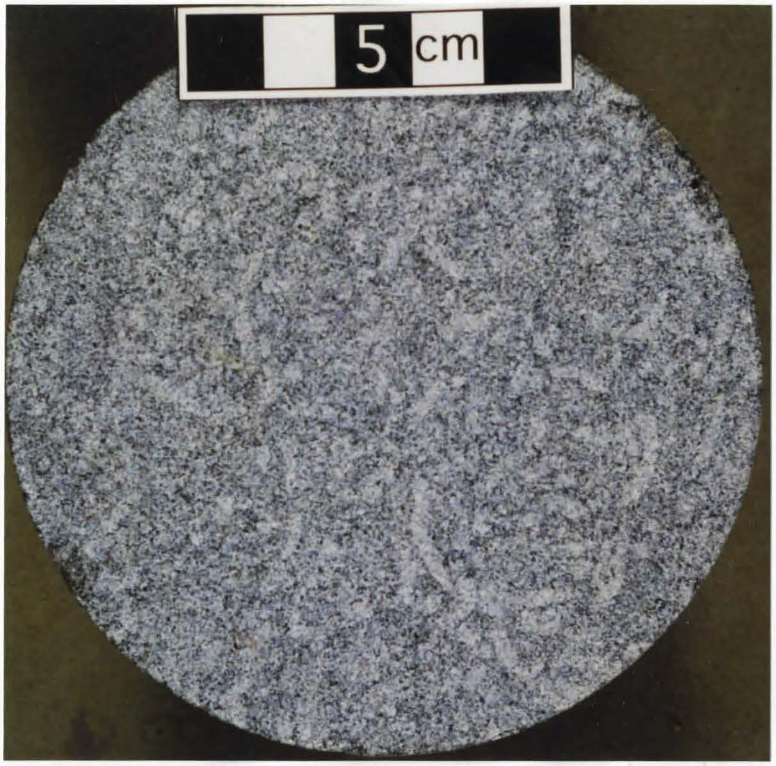

Figure 14. Plain view of a fine-grained sandstone completely bioturbated by traces of *Macaronichnus* (Well 6-30-72-11W6 depth 1788.3 m)

Figure 15. Plain view of a very fine-grained sandstone completely bioturbated by traces of *Palaeophycus* (Well 6-13-72-11W6 depth 2280.6 m)

Figure 16. Stratified granule-conglomerate succession showing different grain size and sorting (Well 7-1-68-12W6 depth 2424 m)

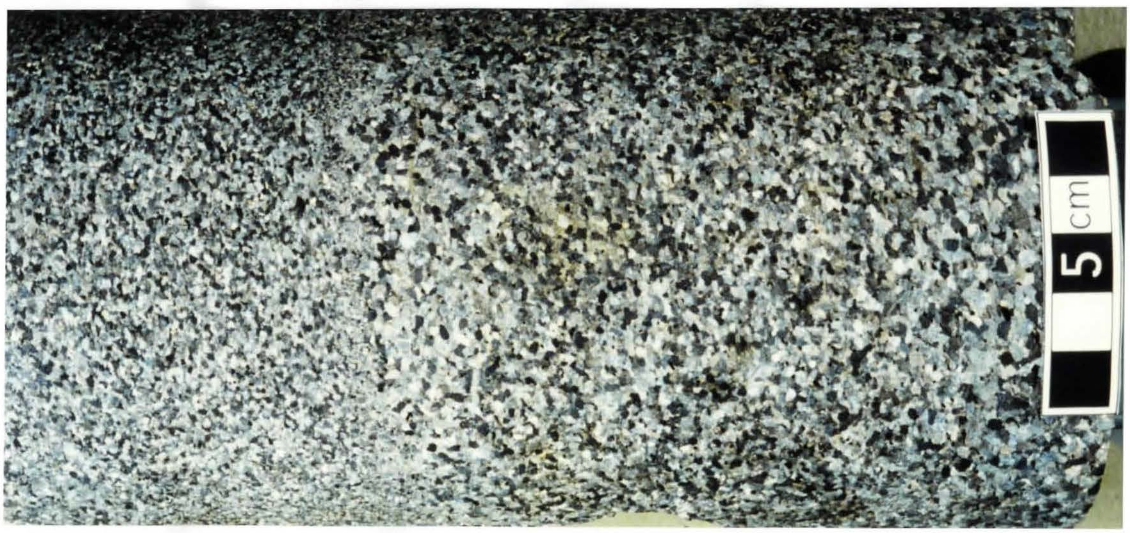

Figure 17. A clast-supported granule conglomerate (Well 7-1-68-12W6 depth 2433.7 m)

dominated deposition in a high-energy, upper to middle shoreface environment, above fair-weather wave base (Leckie and Walker, 1982).

The presence of SCS is a reliable indicator of a shoreface environment particularly if is overlain by beach and rooted coastal plain deposits and underlain by sandier-upward successions with hummocky cross-stratified sandstones interbedded with mudstones, which represent lower shoreface to offshore deposits (Leckie and Walker, 1982; Plint and Walker, 1987).

4.1.3.3. Variable log facies (Allomember D)

- Description

This facies is typical of the lower part of Falher D, from T71 northward. It is defined by a variable response in the gamma ray log, suggesting an interbedded succession of sandstones and mudstones.

In core this facies consists of very fine-grained sandstones interbedded with dark mudstones and siltstones. The sandstones vary from a few centimeters to 2 m thick and show predominantly swaley (Figure 19) to **hummocky cross-stratification** (HCS). The basal contacts of the sandstones with the mudstones are always sharp.

The commonest traces are *Planolites*, (6-17-72-9W6, 10-23-72-11W6 and 6-6-72-12W6), *Teichichnus* (6-8-72-9W6 and 10-23-72-11W6) *Helminthopsis* (10-23-72-11W6) and *Rosselia* (6-6-72-12W6, Figure 20). A few *Terebellina* were also recognized in core 10-23-72-11W6.

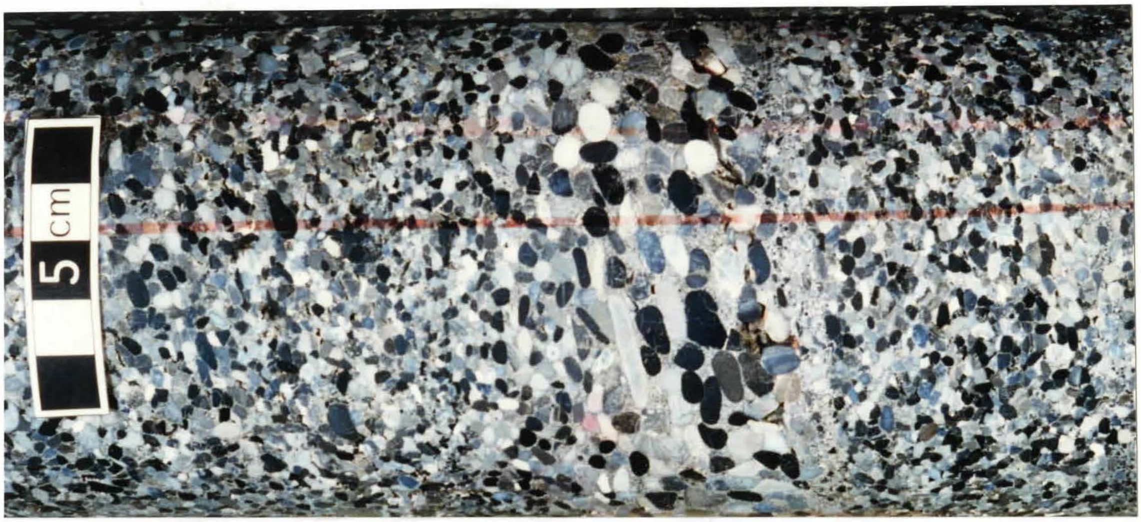

Figure 18. A stratified granule-pebble conglomerate containing low angle cross-bedding (Well 6-19-68-13W6 depth 2675.8 m)

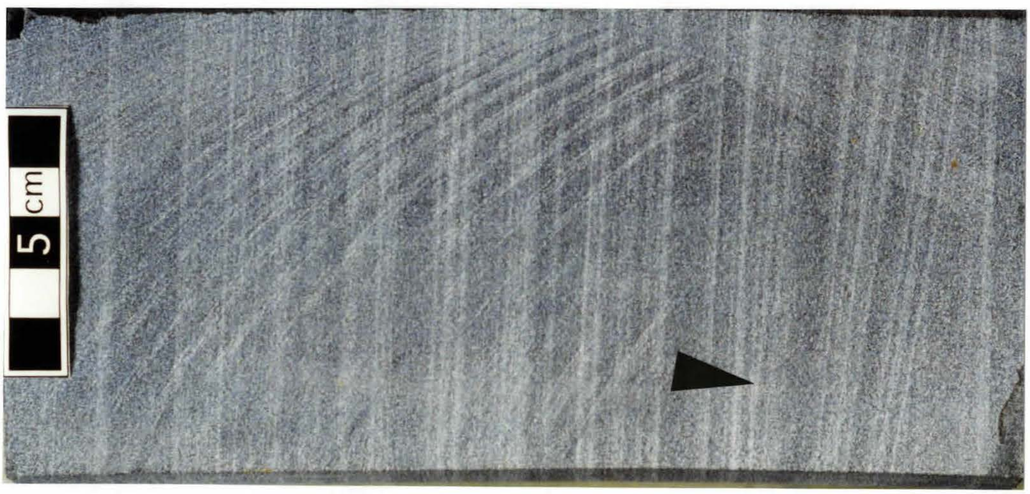

Figure 19. Very fine-grained sandstone with swaley cross-stratification. Note low angle divergences of stratification (Well 10-23-72-11W6 depth 1788 m)

4.1.3.4. Variable log facies (D) - Interpretation

The presence of very fine-grained sandstone beds with SCS and HCS suggest deposition during storm conditions. The interbedding with marine mudstones, combined with the *Cruziana* trace fossil assemblage, suggest deposition in a lower shoreface to offshore environment. The interbedded mudstones represent fair weather sedimentation by deposition from suspension. The HCS sandstones beds are interpreted as sand rapidly emplaced and reworked by storms in the lower shoreface, below fair weather wave base, but above storm wave base (Walker and Plint, 1992).

4.1.3.5. Spiky-sonic log facies (Allomember D) - Description

This facies is defined by a irregular response in the gamma ray log, prominent low-velocity spikes in the sonic log and low values in the density logs.

In the south (T66 and 67) this facies overlies sediments corresponding to Falher E. Northward, this facies overlies the blocky to sandier-upward facies (D) described previously.

In cores this facies consists of dark mudstones and siltstones interbedded with coals up to 1 m thick, coaly mudstones and very fine to fine-grained sandstones. The sandstones range from a few centimeters to 5 m thick and mostly display fining-upward trends.

The sedimentary structures include ripple cross-lamination (Figure 21) and convolute lamination. Horizontal lamination and cross-bedding are less commonly present.

Most of the sections have *in situ* root traces. Plant fragments and sideritized patches are commonly present.

Trace fossils include a very low diversity assemblage dominated almost exclusively by small *Planolites* (15-16-68-13W6, 6-10-68-10W6), but many parts of these successions appear to be undisturbed by organisms. Cores 15-16-68-13W6 and 11-14-68-12W6 show very few examples of *Terebellina*.

Some horizons containing bivalves are concentrated in the south-western part of the study area (T68, R12-13). Among them, *Corbiculia* sp. and *Unio* sp. (Figure 22) were identified (Plint, pers. com., 1994).

4.1.3.6. Spiky-sonic log facies (D)

- Interpretation

The presence of thick coal beds, well preserved plant fragments, *in situ* roots and organic-rich mudstones suggest a coastal plain environment. In T68 R12-13 the presence of *Corbiculia* sp. suggests brackish water conditions meanwhile *Unio* sp. is a freshwater to very low salinity indicator (Plint, pers. com., 1994).

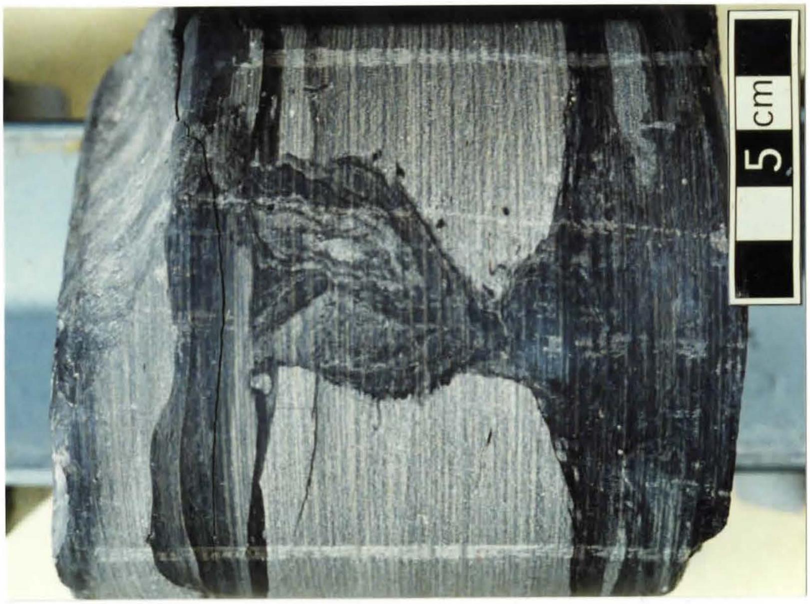

Figure 20. Very fine-grained sandstone interbedded with black mudstones, containing one trace of *Rosselia* (Well 6-6-72-12W6 depth 2002.2 m)

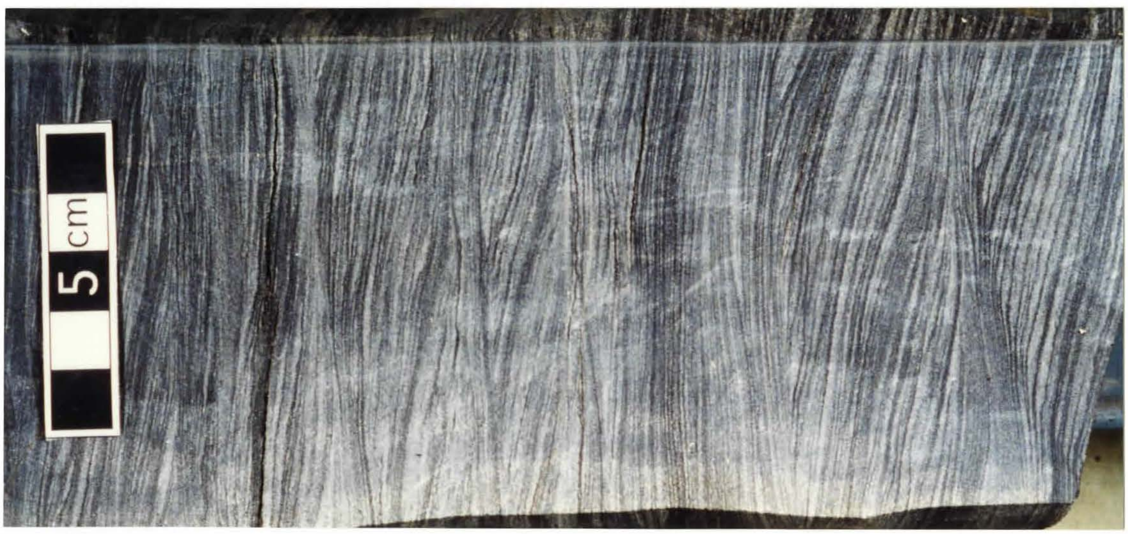

Figure 21. Ripple cross-lamination in very fine-grained sandstone (Well 6-10-68-10W6 depth 2243 m)

4.1.3.7. Blocky to muddier-upward facies (Allomember D) - Description.

Blocky to muddier-upward gamma ray log facies occur across the entire study area.

Few cores are available in this facies (e.g. 6-7-67-8W6, 6-10-68-10W6 and 6-17-72-9W6, Appendix A41, A26 and A29). Three of the best examples in well logs are 10-31-69-12W6, 11-7-70-12W6 and 10-11-71-11W6.

In core this facies is composed of coarse to medium-grained sandstones, always with a fining-upward trend. The sandstones ranges from 1 m to 6 m thick.

The sedimentary structures include trough cross-bedding, parallel lamination and ripple cross lamination.

In core 6-17-72-9W6 (Appendix A29) the coarse grained sandstones contain large angular pieces of mudstone (Figure 23).

Trace fossils in this facies are conspicuously absent.

4.1.3.8. Blocky to muddier-upward facies (D) - Interpretation.

The predominance of cross-bedding and current ripples, together with the absence of bioturbation in the sandstones suggest deposition as channel fills. Also, the presence of large angular mud clasts within the sandstones is

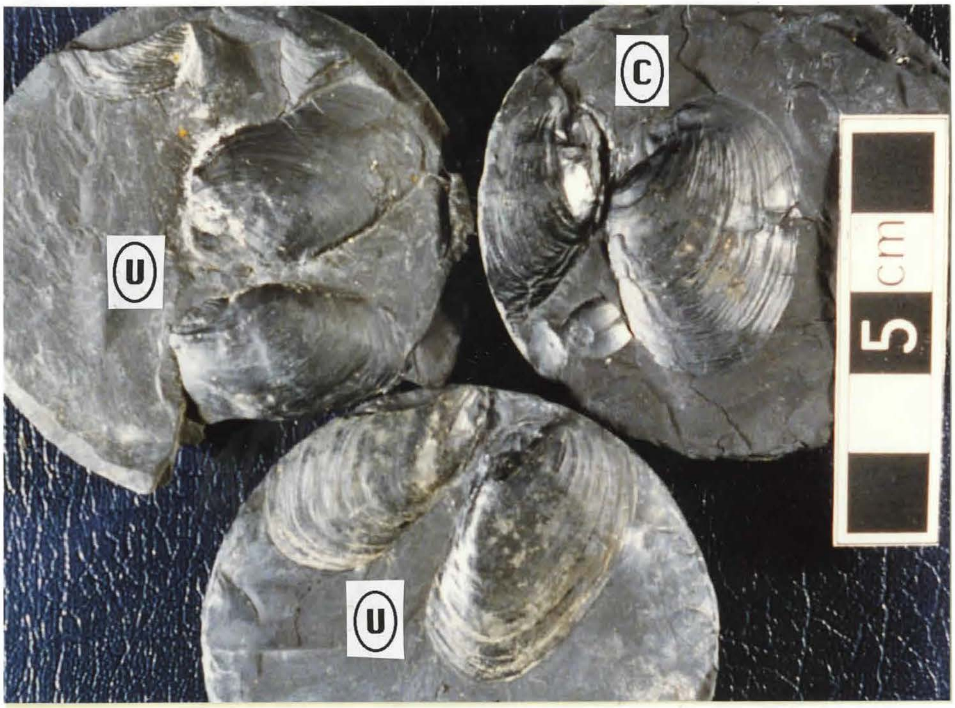

Figure 22. Mudstones containing *Corbiculia* sp. (C) and *Unio* sp. (U). Well 15-16-68-13W6 depth 2588.8 m

Figure 23. Coarse-grained sandstone with angular mud ripped-up clasts (Well 6-17-72-9W6 depth 1724 m)

interpreted to be the result of the collapse of channel walls or channel cut bank erosion during channel lateral migration.

4.2. ALLOMEMBER FALHER C

4.2.1. BOUNDING SURFACES

4.2.1.1. Basal Surface

The basal surface of Falher C is defined by marine flooding surfaces (Transgressive Surfaces of Erosion or TSEs) in places modified by subsequent regressive surfaces of erosion (RSEs). These surfaces overlie nonmarine deposits (coals and mudstones) of Falher D. Southward, in T66, the marine flooding surface probably changes in character. There is no core control in this area, but the logs suggest that the marine flooding surface passes into a flooding surface characterized by a lagoonal-on-coal contact.

Alternations of conglomerates, sandstones and mudstones suggest that three TSEs (TSE C1, TSE C2 and TSE C4) can be correlated across T69-73. Their identification and interpretation would not be possible without core control. An additional TSE (TSE C3) is only recognized south of T69, acting as the basal surface of Falher C. Normally in T69-73, TSE C1 is identified as the basal bounding surface of allomember C but in places TSE C1 was modified by subsequent TSE C2 and/or TSE C4. The relationships between all the TSEs defined in the study area will be disccussed in detail in Chapters 5 and 6.

4.2.1.2. Top Surface

The top surface of Falher C (base of Falher B) is defined by a marine flooding surface interpreted as a TSE, in places modified by a subsequent RSE. This surface overlies coastal plain deposits (coals, mudstones and sandstones) typical of the upper part of Falher C. From the northern part of T69 to T66, the marine flooding surface changes its character. There is little core control in this area, but the logs suggest again that the marine flooding surface passes into a FS characterized by lagoonal deposits overlying coastal plain deposits.

From the northern part of T69 to T72, Falher C is capped by a marine flooding surface. This surface is placed at the abrupt contact between a coal deposit and an overlying fine grained sandstone with SCS, HCS and conglomerate. The contact is well displayed in cores 10-19-69-9W6 (Appendix A8), 7-9-70-10W6 (Appendix A55), 10-30-70-11W6 (Appendix A12), 10-3-70-10W6, 11-10-70-9W6, 11-7-70-12W6, 11-12-71-13W6 and 11-28-70-11W6.

Rouble (1994) termed this marine flooding surface MFS B1 and interpreted it as a discontinuity surface which represents an abrupt increase in water depth and erosional truncation during shoreface retreat.

From T69 to T68, the coal is overlain by lagoonal mudstones. Rouble (1994) termed this a FS (rather than a marine flooding surface) and correlated it with marine flooding surface B1. The surface has been mapped southward into T66 in this study.

The presence of additional coal beds overlying and underlying Coal 1 (Rouble 1994) makes the contact between Falher C and B difficult to define in some parts of T66 to T69.

In T73, Rouble (1994) defined the base of Falher B as a marine flooding surface overlain by a series of interbedded fine grained sandstones with hummocky cross-stratification and mudstones, interpreted as storm and offshore deposits. In some wells across T73 (e.g. 11-10-73-13W6, 6-32-73-12W6, 6-2-73-7W6) this marine flooding surface overlies a coal deposit defining the stratigraphic break between Falher B and C.

4.2.2. FACIES DEFINED BY WELL LOG PATTERNS - C

Within the study area, 333 well logs were correlated allowing the identification of five log facies characterized by (1) a blocky gamma-ray log signal, (2) a ratty gamma-ray log signal, (3) a sandier-upward gamma-ray log signal, (4) a spiky-sonic log signal and (5) a blocky to muddier-upward gamma-ray log signal. These log facies represent approximately 90% of the log responses in the study area. The rest will be discussed in next chapters when the facies are placed in context.

All the log facies described and interpreted here will be placed in stratigraphic context in chapter 5 and 6, using log, core cross-sections, and maps.

4.2.2.1. Blocky Sandstone log signal (Allomember C)

The blocky log signals are found mostly in the southern part of the study area (T67 and T68). The gamma ray log shows a blocky or slightly sandier-upward pattern. The resistivity log shows variable trends. Some wells have an increase in resistivity upwards (e.g. 10-12-67-10W6) but most of them show no trend (e.g. 6-8-67-9W6).

The blocky log signal changes southward (T66) and is replaced abruptly by log responses suggesting mudstones and coals.

The best example of this blocky log pattern is in well 15-16-68-13W6. The pattern is also well developed in 11-7-68-12W6 (Appendix A20), where it can be calibrated with thick sandstones in core.

In ranges 13 and 12 the thickness of the blocky signal is about 15 m. In ranges 11, 10 and 9, the thickness decreases to 10-15 m, decreasing in ranges 8 and 7 to about 10 m. Thus there is a progressive thinning eastward.

4.2.2.2. Ratty log signal (Allomember C)

In the middle of the area, Falher C shows very variable responses in the gamma ray log, without any dominant trend. Adjacent wells are difficult to correlate in detail. Some well logs suggest a muddy section, others show a interbedded succession and few of them show a sandy section.

The thickness of the ratty signal is more or less constant at about 16-20 m

Some good examples of this type of variable signal are wells 10-11-71-11W6, 7-20-69-10W6 and 11-30-68-8W6 (Appendix A5, A47 and A17), where the well log response can be calibrated with cores.

4.2.2.3. Sandier-upward log signal (Allomember C)

Most of the northern half of the study area is characterized by a sandier-upward response in the gamma ray log. The thickness of this sandier-upward log response varies from 14 to 20 m but the most common values are about 18 m.

This well log response suggests a basal muddy interval, 1-5 m thick, with an increase in the amount and thickness of sandstones upward.

Good examples of this type of response are wells 6-29-72-13W6, 6-6-72-12W6 (Appendix A40), 6-30-72-11W6 (Appendix A37), 6-25-71-10W6 (Appendix A33) and 14-2-73-9W6.

4.2.2.4. Spiky-sonic log signal (Allomember C)

The spiky-sonic log signal is variable, somewhat like the ratty signature discussed above. However, it is characterized by big low-velocity spikes in the sonic log that always correlate with coals in core. The density-porosity and sonic logs also show low values.

This log signal occurs over all the study area and represents the top of Falher C. The thickness of this log response varies between 5 and 20 m. Good examples of this type of signal are in wells 10-11-71-11W6 (Appendix A5), 7-20-69-10W6 (Appendix A47) and 10-3-70-10W6, where the log response can be calibrated with cores. The cores always show coals and mudstones. Sandstones with root traces are commonly present.

4.2.2.5. Blocky to muddier-upward log signal (Allomember C)

This type of log signature can be found mostly in T66-68 R8-10. The density log shows low and variable responses, which allow it to be distinguished from the blocky log signal previously defined where there is no core control.

The thickness of this log response is very variable in cores, ranging between 1 and 20 m. Good examples of this type of signal are in wells 7-29-67-8W6, 6-22-67-8W6, 10-26-66-11W6 and in wells 10-1-68-9W6 (Appendix A3) and 11-4-69-10W6 (Appendix A18) where the log response can be calibrated with a core.

4.2.3. FACIES DESCRIPTION AND INTERPRETATION

4.2.3.1. Blocky facies (C) - Description

This facies is characterized by a blocky well log response, as described above. Fifteen cores were taken in this succession because is the main pool in Falher C, and three of the best are 11-7-68-12W6 (Appendix A20), 6-16-68-11W6 (Appendix A28) and 6-8-67-9W6 (Appendix A42).

This succession is composed mainly of very-fine to fine-grained sandstones with very low angle stratification and SCS. Cross-bedding occurs in medium grained sandstone beds (Figure 24). In places, the main sandstone body has many conglomeratic beds interbedded with the sandstones.

In situ root traces are present at the top of the main sandstone body (e.g. 10-17-67-7W6, Appendix A7).

Trace fossils include *Teichichnus* (11-7-68-12W6, 10-12-67-10W6, 7-24-67-10W6), *Macaronichnus* (10-9-67-10W6, 6-25-68-11W6, 6-7-67-8W6, 6-16-68-11W6, 11-7-68-12W6, 10-12-67-10W6, 7-15-67-10W6), *Palaeophycus* (7-24-67-10W6 (Figure 25), 6-8-67-9W6, 10-25-67-11W6), *Rosselia* (7-24-67-10W6, 10-30-67-11W6), *Planolites* (11-7-68-12W6, 10-30-67-11W6) and *Terebellina* (11-14-68-12W6).

Where *Macaronichnus* is present, *Palaeophycus* is also normally present in high concentrations.

In several cores (6-16-68-11W6, 11-7-68-12W6, 10-30-67-11W6, 7-24-67-10W6 and 10-16-67-8W6) the sandstones have no sedimentary structures and appear structureless. The loss of structure is interpreted to be due to

Figure 24. Pebbly fine-to-medium-grained sandstone with cross-bedding (Well 10-17-67-7W6 depth 2168.1 m)

Figure 25. Bioturbated horizon with the trace *Palaeophycus tubularis* (Well 7-24-67-10W6 depth 2325.4 m)

bioturbation by interstitial meiofauna such as copepods, ostracodes and nematodes (Cullen, 1973; Bromley, 1990).

In township 67, ranges 7-10, conglomerates and conglomeratic sandstones are commonly present. The conglomerates are commonly massive, poorly sorted (Figure 26) and can be either clast-supported or sand-matrix supported. In cores 10-17-67-7W6, 6-7-67-8W6 and 6-8-67-9W6 a well developed succession of clast supported pebble to granule conglomerate is present, overlaying interbedded sandstones and poorly sorted conglomerates. In places, this pebble to granule conglomerate also fines upward into a well-sorted very coarse- to coarse-grained sandstone (e.g. 10-17-67-7W6, Appendix A7) Conglomeratic sandstones are normally well to moderately sorted with only a few scattered large pebbles. Cross-bedding is the most common sedimentary structure in both the conglomerates and the conglomeratic sandstones.

4.2.3.2. Blocky facies (C) - Interpretation

The combination of swaley cross-stratification in the sandstones and the *Skolithos-Cruziana* trace fauna assemblage (Pemberton *et al.*, 1992a) suggest that this facies represents wave to storm dominated deposition in a high-energy, fully marine shoreface environment in which storm processes have overprinted all record of fairweather sedimentation (Leckie and Walker, 1982).

The conglomeratic deposits described previously are similar to other ancient conglomeratic upper shoreface deposits (Bourgeois and Leithold, 1984;

Massari and Parea, 1988). The sharp-based, poorly sorted conglomerate beds in the upper part of the SCS bodies are interpreted as deposits emplaced and transported by storm-intensified seaward-trending flows (Massari and Parea, 1988). Walker and Plint (1992) suggest that sand and gravel can be moved seaward by rip currents. This transport would be enhanced during storm events.

The presence of well sorted granule conglomerates overlaying truly shoreface sandstones and overlain by rooted nonmarine deposits indicate deposition along beachface at the swash and backwash zone (Bourgeois and Leithold, 1984). The massive, poorly-sorted pebble conglomerates associated with the granule conglomerate beds represent deposition at the plunge step of breaking waves at the top of the beachface (Massari and Parea, 1988).

The absence of beach conglomerates in some examples (e.g. 10-25-67-11W6, Appendix A10) may suggests two possibilities, one in which much of the gravel and pebbles were mainly transported out of the inmediate area by longshore drift (Massari and Parea, 1988) or a second one where there was not a close source to supply this size of material.

Finally the medium-grained sandstones with cross-bedding indicate deposition by fairweather wave process and probably represent a complex mixture of bedforms associated with the shoaling wave zone, ridge and runnel (breaking zone) and rip currents (Walker and Plint, 1992)

4.2.3.3. Ratty facies (C) - Description

This facies is typical of the central part of the study area. The succession is well represented by different cores but is very difficult to correlate in detail because of variability from well to well. In some cores (e.g. 7-20-69-10W6, Appendix A47), the facies consists of silty mudstones and some thin, very-fine to medium-grained sandstones. In cores 11-30-68-8W6 (Appendix A17) and 10-11-71-11W6 (Appendix A5), the entire succession is composed of black mudstones interbedded with very-fine to fine-grained, thin sandstones. Ripple cross-lamination (Figure 27), convolute lamination (Figure 28) and sideritized patches are commonly present.

In core 11-4-69-10W6 (Appendix A18) the succession is dominantly sandy. In places there are thin layers of conglomerate or conglomeratic sandstones (Figure 29). Cross-bedding, sideritized mud clasts and small clasts of coal are commonly present.

Trace fossils are common in these successions but there are few ichnospecies. The most common association is *Teichichnus* (Figure 30) and *Planolites* (11-30-68-8W6, 11-30-70-11W6, 7-20-69-10W6).

In situ root traces are commonly found at the top of the ratty facies succession.

4.2.3.4. Ratty facies (C) - Interpretation

The interbedding of mudstones and sandstones with a restricted trace fauna (*Teichichnus* / *Planolites*), suggests a stressed environment such a lagoon

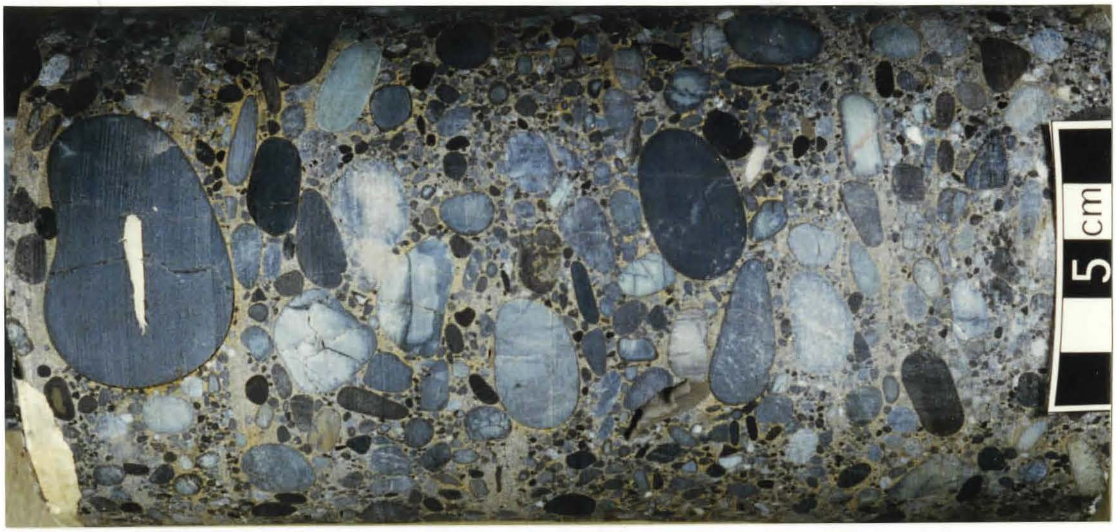

Figure 26. Poorly-sorted, matrix-supported conglomerate. Matrix is very fine-grained sand. Note the wide variability of clast size and the poorly developed clast fabric (Well 6-16-68-11W6 depth 2281.9 m)

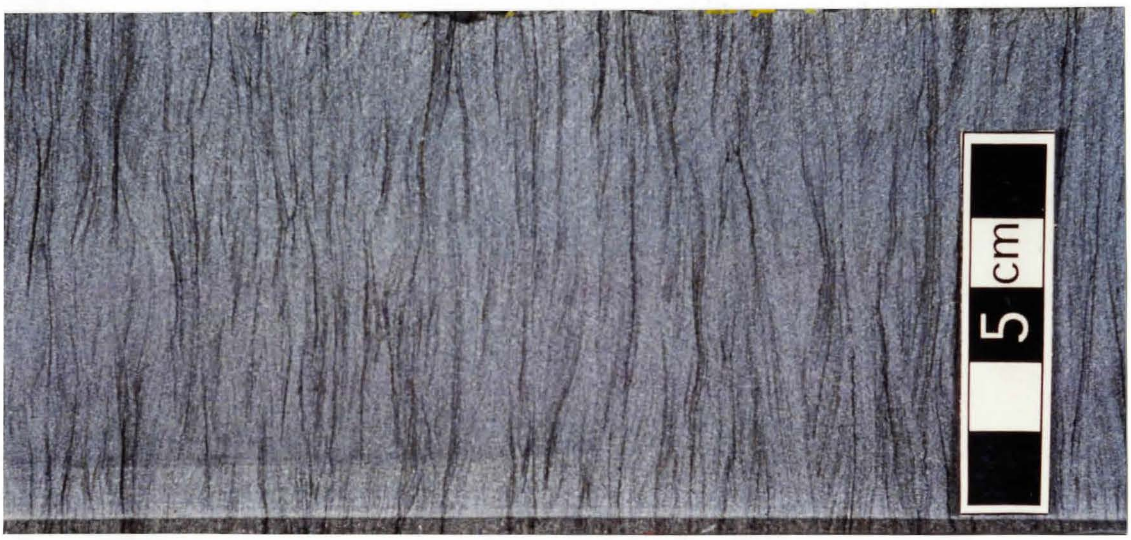

Figure 27. Very fine-grained sandstone with ripple cross-lamination (Well 7-9-70-10W6 depth 1930.9 m)

Figure 28. Very fine-grained sandstone showing soft sediment deformation (Well 10-11-71-11W6 depth 1869 m)

Figure 29. Conglomeratic sandstone showing cross-bedding and coal clasts (well 11-4-69-10W6 depth 2072.3 m)

or estuary. This interpretation will be expanded later when the facies are placed in context.

4.2.3.5. Sandier-upward facies (Allomember C)
- Description

This facies is typical of part of township 69 and townships 70-73. The logs show a smooth sandier-upward succession starting with black mudstone (2-5 m thick) well exposed in cores 6-27-71-9W6 (Appendix A34) and 6-25-71-10W6 (Appendix A33). This black mudstone commonly contains interbedded siltstones or very fine grained sandstones. Trace fossils include *Helminthopsis* (Figure 31), *Planolites*, *Teichichnus* and *Rosselia.* These mudstones grade up into fine-grained sandstones, apparently structureless, sometimes with parallel stratification and with very low angle stratification interpreted as SCS. This section is well exposed in cores 7-8-69-9W6 (Appendix A53), 10-19-69-9W6 (Appendix A8) and 6-32-73-13W6 (Appendix A39). *In situ* root traces are present at the top of the main sandstone body (e.g. 10-19-69-9W6, Appendix A8 and 7-8-69-9W6, Appendix A53).

4.2.3.6. Sandier-upward facies (C)
- Interpretation

The combination of very low angle stratification and SCS in the sandstones, and the *Skolithos-Cruziana* trace fauna assemblage suggests that

Figure 30. Bioturbated very fine-grained sandstone containing traces of *Teichichnus* (Well 10-11-71-11W6 depth 1879.5 m)

Figure 31. Bioturbated very fine-grained sandstones and mudstones containing dominant traces of *Helminthopsis* (Well 6-25-71-10W6 depth 1721.3 m)

these facies represent wave to storm dominated deposition in a shoreface environment, above fair-weather wave base (Leckie and Walker, 1982). The black mudstones and siltstones at the base are interpreted as offshore deposits, indicating deposition below storm wave base. The overall muddy character at the base of the succession probably implies sedimentation during relative sea level rise (transgressive mudstones).

4.2.3.7. Spiky-sonic facies (Allomember C)

- Description

This facies extends across the entire study area overlying the three previous facies and occupying the entire Township 66. It is defined by a variable response in the gamma ray log and prominent low-velocity spikes in the sonic log, and low response in density logs.

In cores these facies consist of dark mudstones and siltstones interbedded with coals, coaly mudstones and very-fine to fine grained sandstones. The sandstones range from few centimeters to 2 m and either show no trend, or display a fining-upward trend.

The sedimentary structures include ripple cross-lamination and soft sediment deformation (Figure 32). Less commonly present are horizontal lamination and cross-bedding.

Most of the succession contains *in situ* root traces (Figure 33). In places, plant fragments, mud clasts and sideritized patches are present.

Figure 32. Fine-grained sandstone interbedded with thin dark mudstones showing small faulting and soft sediment deformation. (Well 10-3-70-10W6 depth 1908.4 m)

Figure 33. Very fine-grained sandstone with *in situ* roots (arrows) overlain by a coal bed (Well 11-30-68-8W6 depth 2003.2 m)

Trace fossils include a low diversity assemblage dominated by the association *Chondrites / Planolites* (e.g. 7-20-69-10W6, 11-30-70-11W6).

The spiky-sonic facies are capped abruptly by shoreface sandstones and conglomerates corresponding to Falher B. The contact is well displayed in many cores (e.g. 11-28-70-11W6 (Figure 34), 10-3-70-10W6, 7-9-70-10W6, 11-10-70-9W6, 11-7-70-12W6 and 11-12-71-13W6).

4.2.3.8. Spiky-sonic facies (C) Interpretation

The presence of coal beds, *in situ* roots and organic-rich mudstones with plant fragments, suggests deposition in a coastal plain setting. The predominance of cross-bedding and current ripples within the sandstones in an overall coastal plain setting suggests deposition in small channel fills. The association *Chondrites/ Planolites* is common across the entire succession, but the traces are small and in low concentrations. Vossler and Pemberton (1988) suggest that the presence of *Chondrites* indicates a response to local anoxic conditions.

4.2.3.9. Blocky to muddier-upward facies (Allomember C) - Description

This facies occurs in the area dominated by the ratty, the blocky and the spiky-sonic log signals (R66-R69) and is defined as a blocky to muddier-upward response in the gamma ray log.

Few cores were taken in this type of facies but include wells 1-10-68-9W6 (Appendix A2), 10-1-68-9W6 (Appendix A3), 14-20-71-9W6 (Appendix A21), 10-30-67-11W6 (Appendix A11) and 6-32-73-13W6 (Appendix A39). Two of the best examples defined only by well logs are 15-27-66-10W6 and 10-26-66-11W6.

In core, the sandstones are mostly medium-grained with a fining-upward trend. The thickness of these sandstones ranges from 1 to 20 m.

The sedimentary structures include trough cross-bedding (Figure 35), parallel lamination and ripple cross-lamination.

In cores such as 6-32-73-13W6 and 7-20-69-10W6, the medium-grained sandstones include large clasts of mudstones (up to the diameter of the core).

No traces fossils were recognized in this facies.

4.2.3.10. Blocky to fining-upward facies (C)
- Interpretation

The fining-upward character of these medium- to coarse-grained sandstones, the predominance of cross-bedding and current ripples and the absence of trace fossils suggest deposition as channel fills. This interpretation will be expanded later when the facies are placed in context.

Figure 34. Contact between Falher B and C (arrow) in this case is defined by a black coaly mudstone of Falher C (below) overlain by a transgressive conglomerate of Falher B. (Well 11-28-70-11W6 depth 1923.6 m).

Figure 35. Medium- to coarse-grained sandstone with cross-bedding (Well 1-10-68-9W6 depth 2242.6 m).

5. WELL LOG CORRELATIONS

Seven south to north well log cross-sections (A-G) were constructed (Figure 36), to show the stratigraphic relationship in each range (Figures 37-43). These were then condensed into four cross-sections (Figure 44) to show the lateral and vertical log facies relationships within Falher D and C in the study area, using as many cored wells as possible (Appendix C1, C2, C5 and C6). Also four core cross-sections were constructed, two for Falher D (Appendix C3 and C4) and two more for Falher C (Appendix C7 and C8).

Coal beds are present in the cores of Falher D and C. Where there is no core control, log criteria used to identify the coals included (1) gamma-ray values indicating shale volumes equal to or less than 30%, (2) density values lower than 2.1 gm/cm^3, (3) resistivity values greater than 60 ohm-m and (4) interval transit time greater than 300 µs/m (modified from Wyman, 1984).

To identify conglomerate intervals in wells without core control, the criteria used were (1) low gamma-ray values, (2) high resistivity values, (3) bore hole diameter (caliper), (4) low acoustic traveltime (5) high density porosity values and (6) positive microlog separation (Sneider *et al.*, 1984).

5.1. FALHER D

Four well-log facies have been recognized in Falher D, and have been calibrated with cores. The **spiky-sonic facies** represents nonmarine

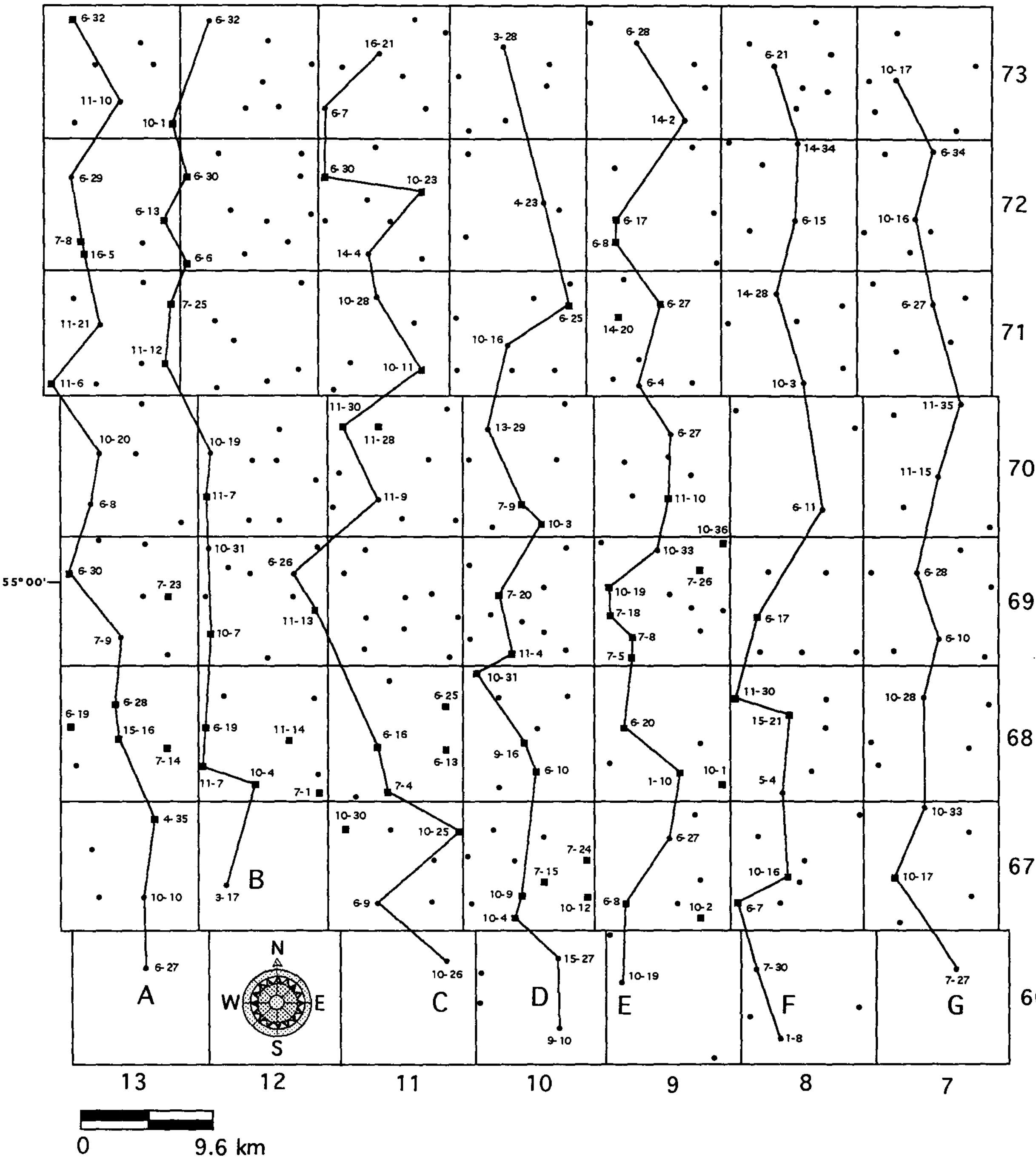

Fig. 36. Index map of the study area showing the location of wells (●), cores (■) and log sections.

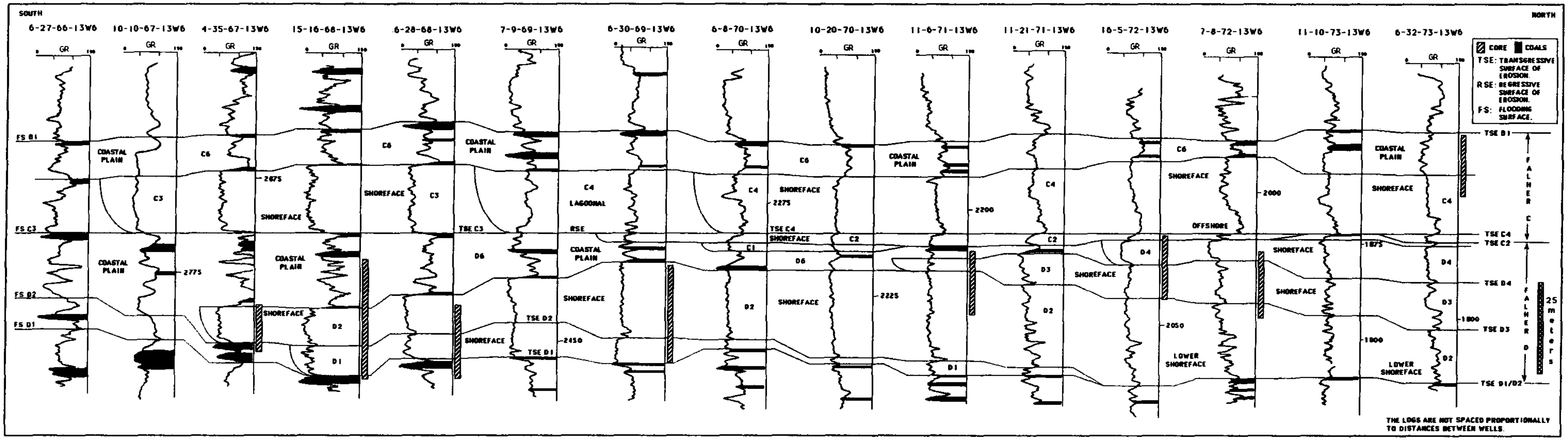

Figure 37. Gamma-ray log cross-section (A) mainly across Range 13W6.
See Figure 36 for location.

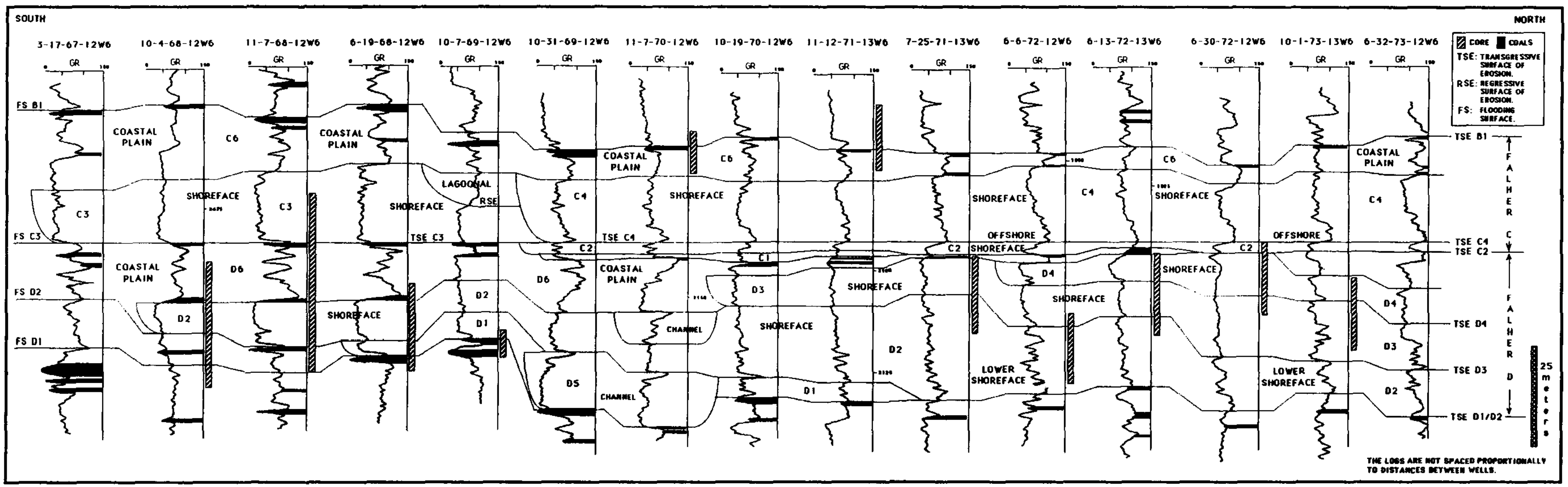

Figure 38. Gamma-ray log cross-section (B) mainly across Range 12W6.
See Figure 36 for location.

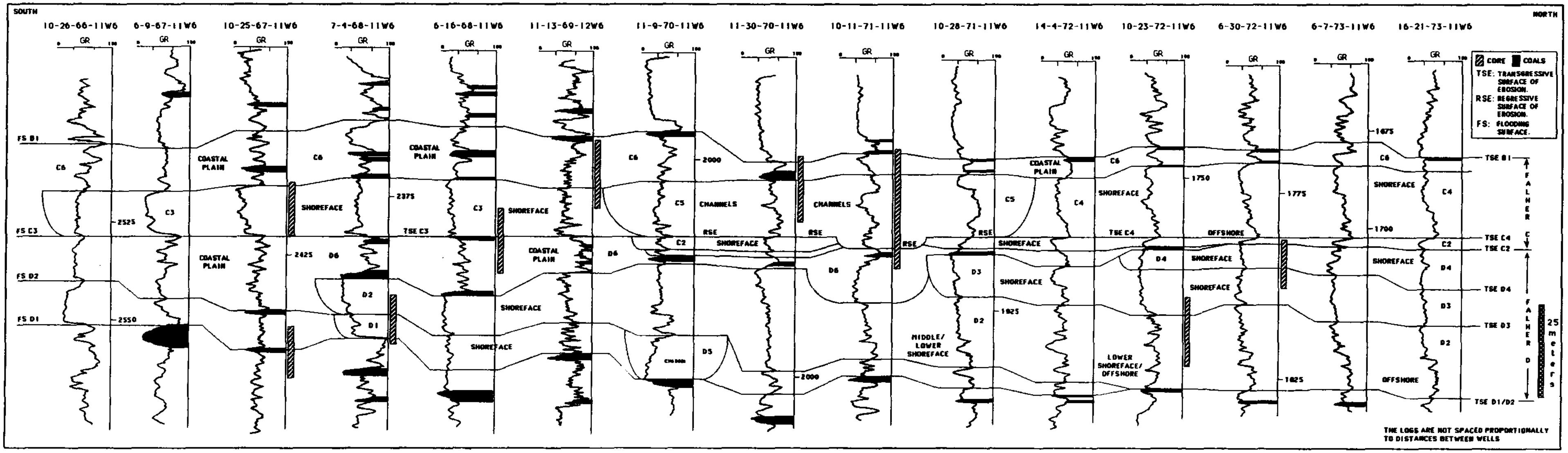

Figure 39. Gamma-ray log cross-section (C) mainly across Range 11W6.
See Figure 36 for location.

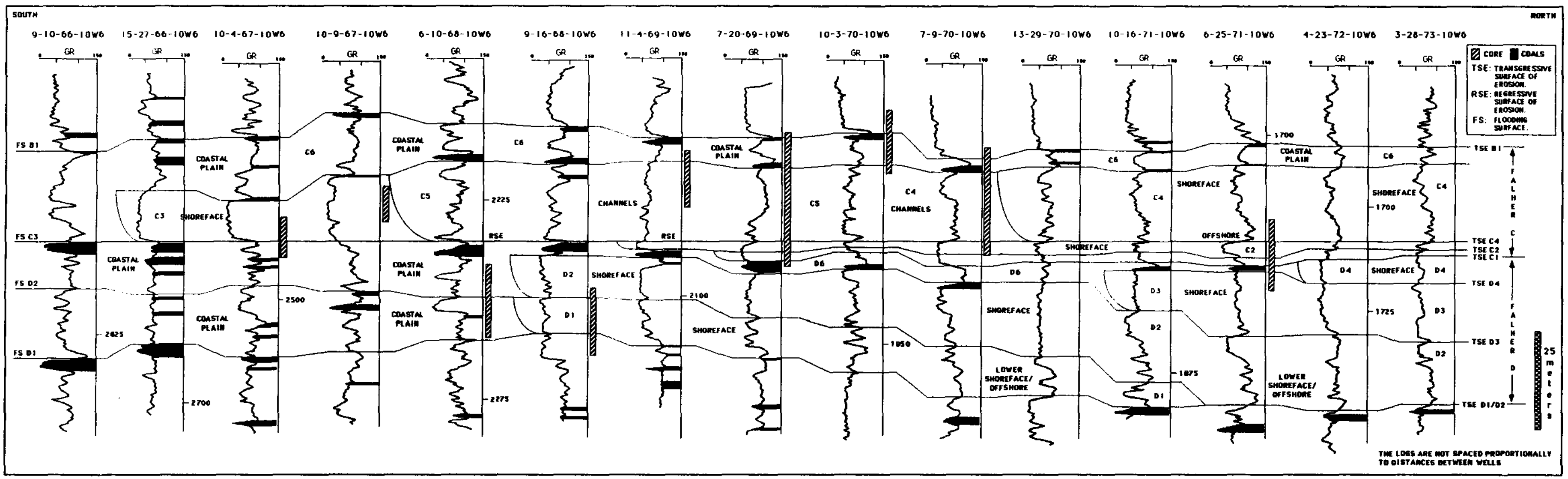

Figure 40. Gamma-ray log cross-section (D) mainly across Range 10W6.
See Figure 36 for location.

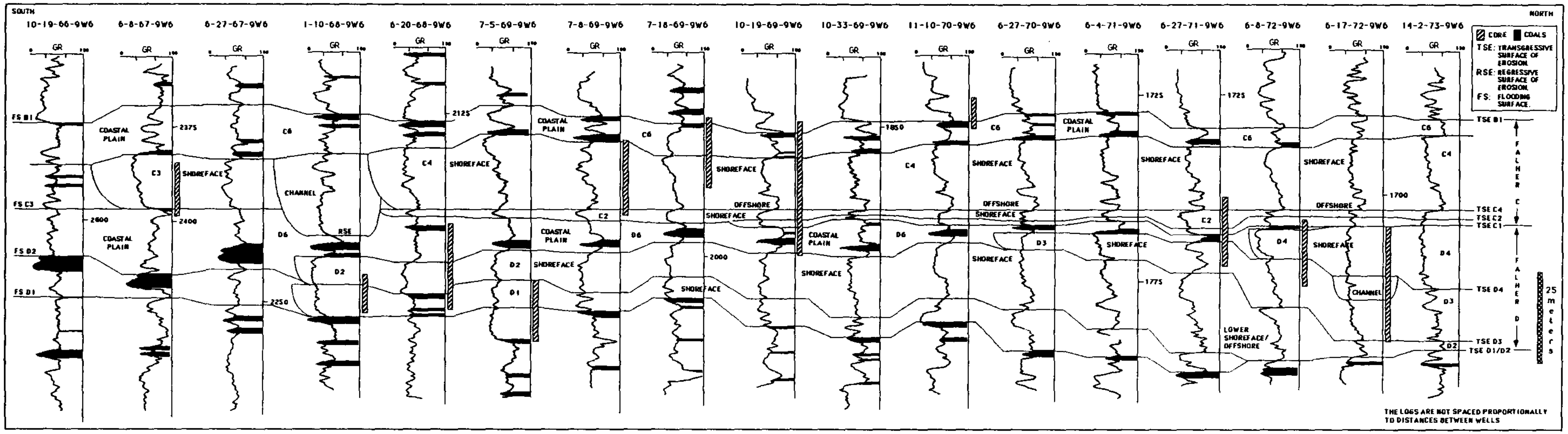

Figure 41. Gamma-ray log cross-section (E) mainly across Range 9W6. See Figure 36 for location.

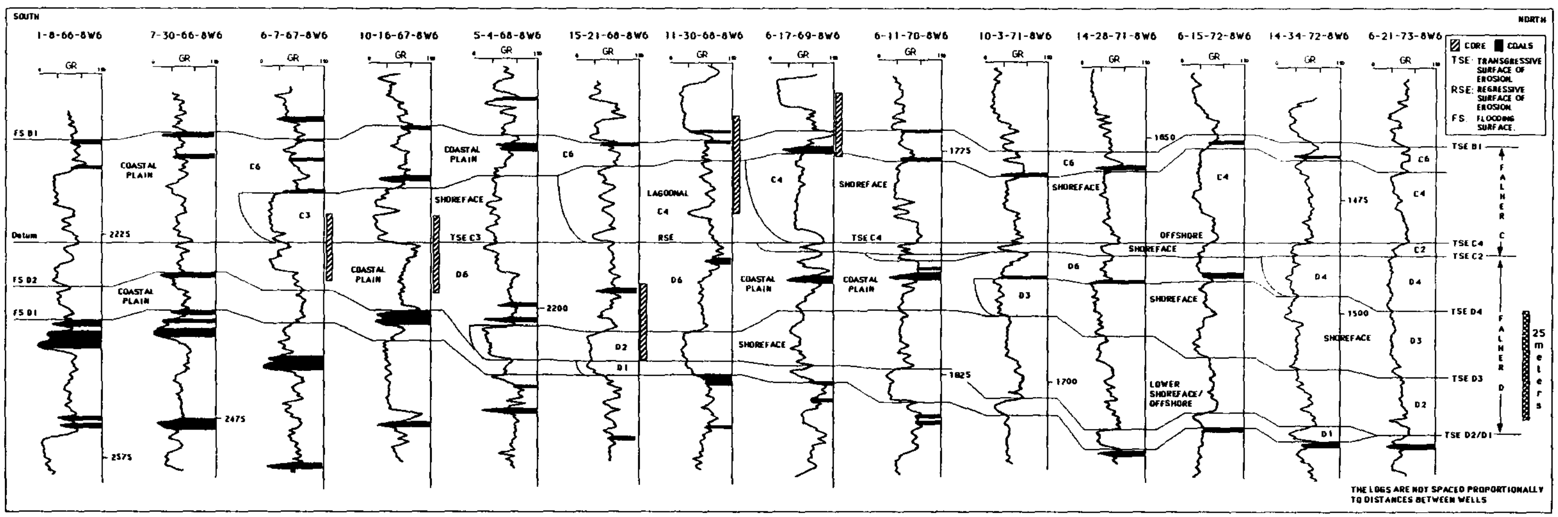

Figure 42. Gamma-ray log cross-section (F) mainly across Range 8W6. See Figure 36 for location.

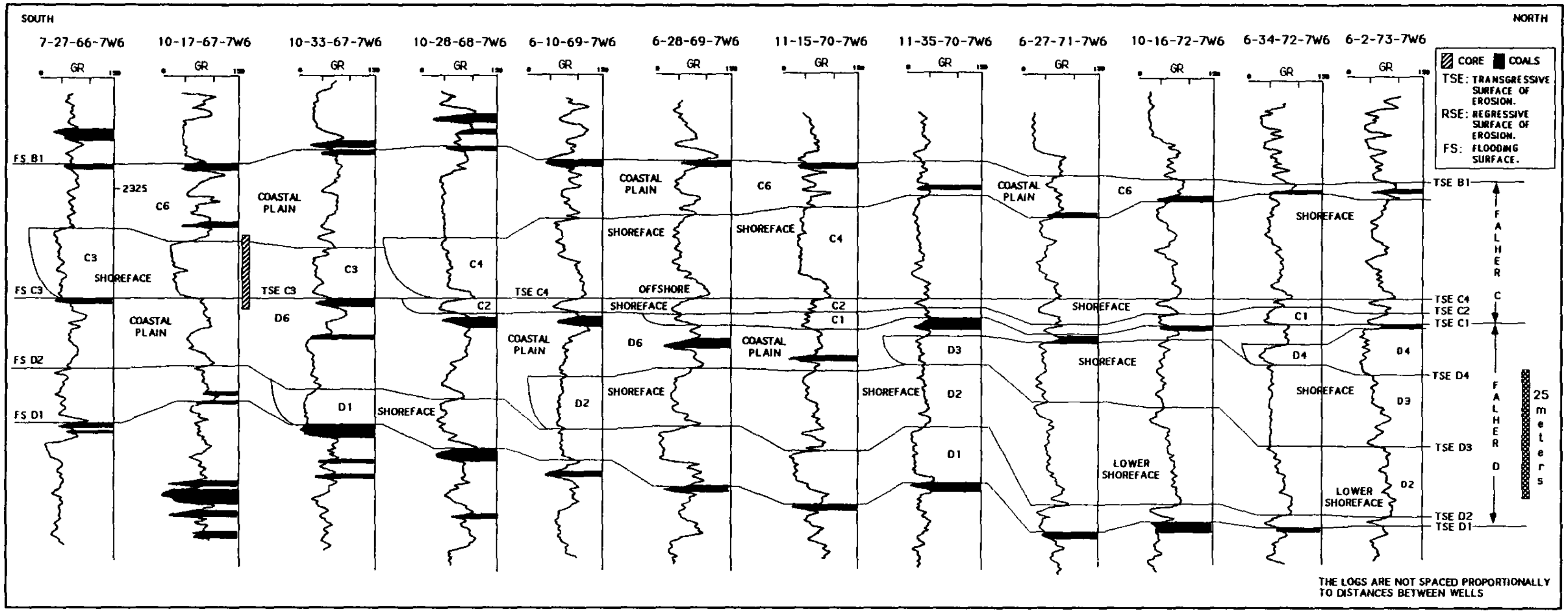

Figure 43. Gamma-ray log cross-section (G), mainly across Range 7W6. See Figure 36 for location.

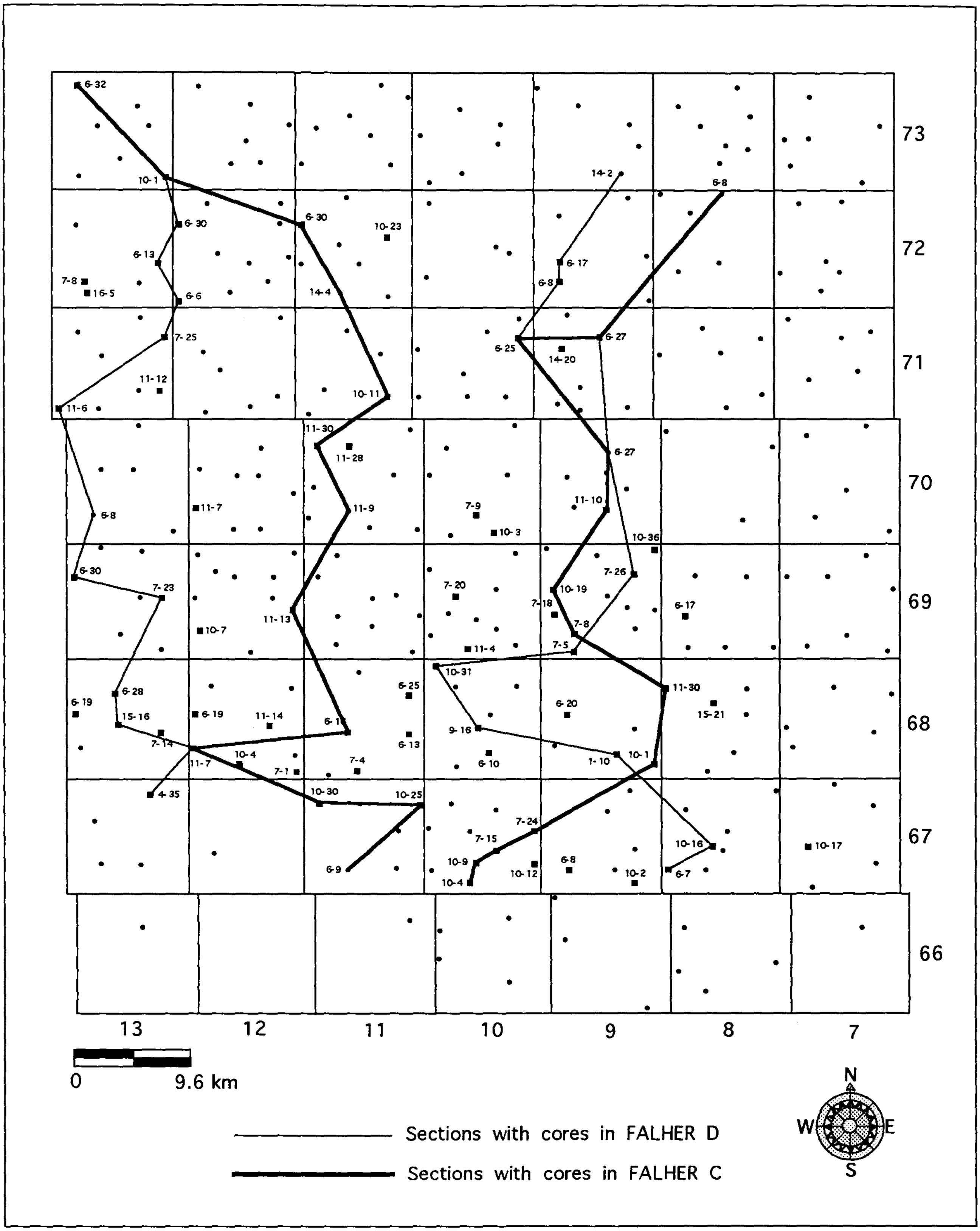

Figure 44. Location of the four condensed log and core cross-sections across the study area.

floodplain deposition, the **blocky** and **sandier-upward facies** represents prograding shoreface deposits and the **variable facies** represents shoreface to offshore storm deposits (Chapter 4).

Preliminary analysis of the distribution of the facies (Figure 45) showed that the spiky-sonic facies occurs (1) from bottom to top of Falher D in the south, and (2) across the entire study area in the upper part of Falher D. The blocky to sandier-upward facies occurs as a relative thin unit (4-35-67-13W6, Figure 45) that increases in thickness northward (15-16-68-13W6, Figure 45), and passes into a much thicker blocky log response (11-6-71-13W6, Figure 45). This blocky response can be subdivided into three stacked sandier-upward responses in the north of the area (7-8-71-13W6, Figure 45). Also in the north, the variable log facies occurs at the base of these sandier-upward units (7-8-71-13W6, Figure 45).

These observations have been used to guide the detailed correlations presented below.

In general all the cross-sections show the same horizontal facies distributions from south to north. The vertical successions are also similar. In the southern area, very irregular responses were identified on the logs, corresponding to the spiky-sonic log facies previously defined and interpreted as coastal plain deposits (facies association of coals, mudstones). The response of this log signal is so variable that detailed correlations are very difficult in the southern portion of the area (T66-67).

In T68 the blocky to sandier upward log facies is interpreted to represent shoreface sandbodies. The change between the blocky-to-sandier-

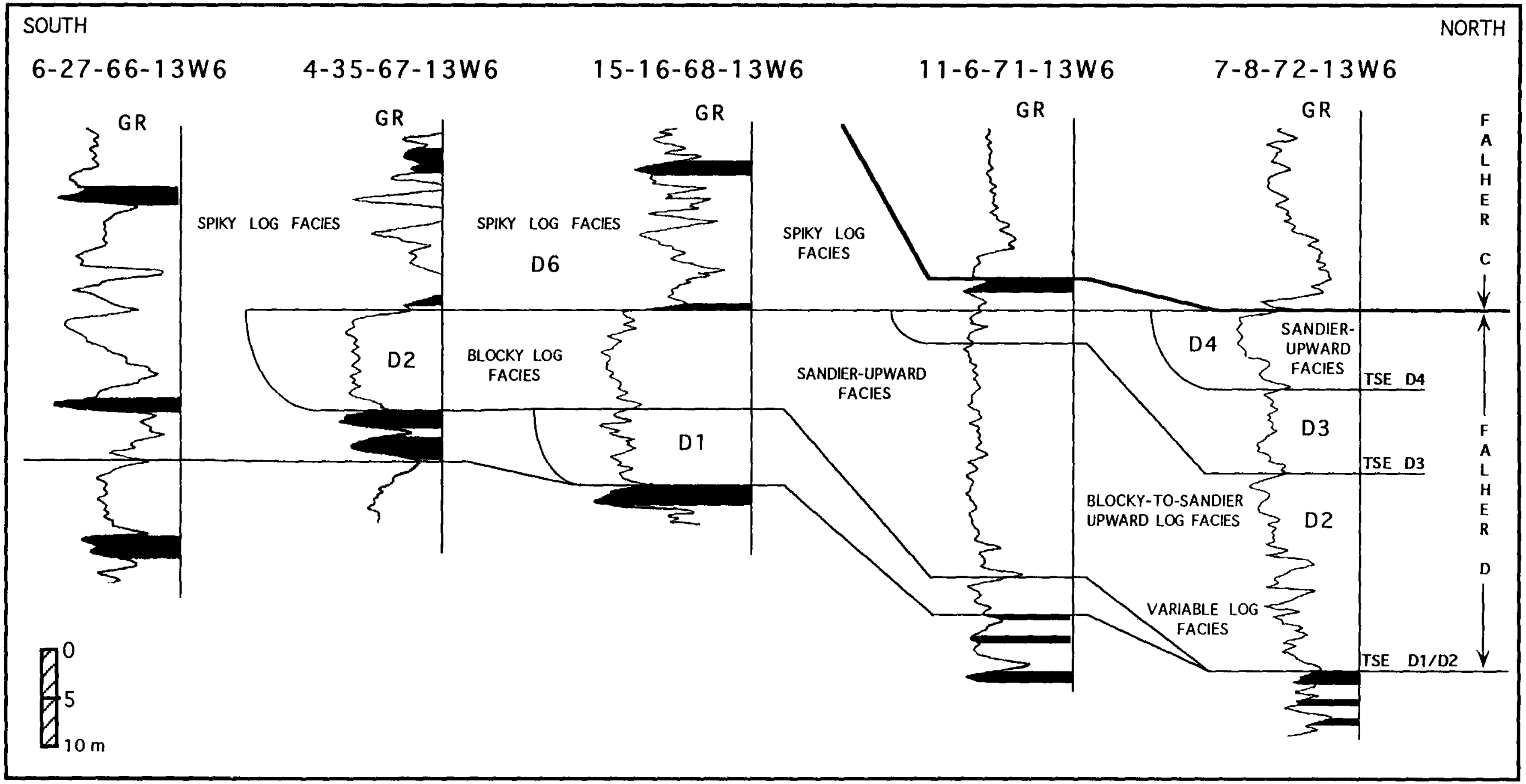

Figure 45. Geographic distribution of Falher D well log responses, showing spiky-sonic log responses in the south and across the study area in the upper part of Falher D. Blocky-to-sandier-upward responses occur north of the spiky-sonic responses, and variable responses occur in the lower part of Falher D in the north. For this diagram only, the datum is taken at the top of the blocky-to-sandier-upward log responses.

upward and the spiky-sonic log facies to the south is very abrupt and can be easily traced from east to west across the area. Sections C and D show this change in a short distance (e.g. between wells 10-25-67-11W6 and 7-4-68-11W6 in section C, Figure 39 or between 6-10-68-10W6 and 9-16-68-10W6 in cross-section D, Figure 40). Here, brackish and coastal plain deposits (spiky-sonic log facies) are laterally equivalent to thick shoreface sandbodies (blocky-to-sandier-upward log facies) to the north. The lateral facies change from brackish deposits (adjacent to a barrier formed transgressively) to truly coastal plain deposits to the south is extremely difficult to distinguish using well logs, and there is no core control. An attempt to trace the marine flooding surfaces (TSEs) into equivalent nonmarine surfaces was made and is shown in all the cross-sections.

Some wells show a single blocky-to-sandier-upward pattern averaging 9 m in thickness (e.g. 4-35-67-13W6, Appendix C1 and 10-4-68-12W6, Appendix A14) while adjacent wells have a blocky response twice this thickness (18 m). This suggests that the thicker response might represent two stacked single blocky-to-sandier-upward patterns representing two stacked shoreface bodies (designated D1 and D2). Good examples of these relationships are shown in (1) Appendix C1, between wells 4-35-67-13W6 and 15-16-68-13W6; and (2) in cross-section G, between 10-28-68-7W6 and 6-10-69-7W6, Figure 43)

In T68 and 69 most of the wells show this pattern of two superimposed blocky-to-sandier-upward log responses. The break between these two patterns is represented in cores by muddy horizons and is interpreted as a TSE. Its significance will be discussed in next chapters. In places, many gamma-ray logs show the possible location of this break as a shaly kick (e.g. 6-28-68-13W6, Appendix A35; 10-31-68-10W6, Appendix A13; 7-5-69-9W6, Appendix A52 and 6-28-69-7W6). In some well logs there is no gamma-ray kick, and the exact position of the break can only be determined in core (e.g. 7-4-68-11W6, Appendix A51; 1-10-68-9W6, Appendix A2, and 15-16-68-13W6, Appendix A22).

Typical gamma-ray values of this blocky to sandier upward pattern are in the order of 40 API units. The density-porosity and resistivity logs also show a similar blocky profile or a slight increase of the response upwards.

The conglomerates and conglomeratic sandstone facies present within this log pattern are concentrated mainly in T68. In places these facies have slightly lower API values compared with the adjacent sandstones, but normally the well log criteria (already described) should be applied to identify them.

In T69 and 70 the blocky-to-sandier-upward log pattern is thicker (e.g. 10-20-70-13W6, 10-30-70-11W6, Appendix C5, and 10-33-69-9W6, section E, Figure 41), corresponding mainly to D2. In cores, D2 consists mostly of sandstones with hummocky to swaley cross-stratification.

From the northern part of T71 to T73, Falher D is characterized by sandier-upward log responses, with two or three sandier-upward log patterns stacked (e.g. 6-27-71-9W6 and 6-25-71-10W6, Appendix C2). The breaks between sandier-upward responses were calibrated with cores, and TSEs were defined (Chapter 7). Some of these breaks are easily identified only with well logs (e.g. 6-13-72-13W6 and 10-1-73-13W6 in section A, Figure 37; 10-16-71-10W6 and 6-25-71-10W6 in section D, Figure 40; 6-8-72-9W6 and 6-27-71-9W6 in section E, Figure 41, and 6-27-71-7W6 and 10-16-72-7W6 in section G, Figure 43). These TSEs strongly suggest stacked shoreface deposits in the study area. Sections A and B are good examples in the T71-73 area of the correlation and development of these units, here termed D3 and D4.

The TSEs are represented in cores by a distinct grain size change, commonly associated with an abrupt facies change from swaley cross-stratified fined-grained sandstone (below) to a conglomeratic upper shoreface deposit (above). In other places the TSE appears as a very thin (few cm) dark mudstone (with or without pebbles) separating two units each composed of fined-grained sandstones with swaley cross-stratification (e.g. TSE D4 in 10-1-73-13W6, Appendix C5 and TSE D4 in 6-8-72-9W6, section E, Figure 41). In some places the TSE appears as an erosive surface, sandstone over sandstone, sometimes with a 1 cm horizon of mud clasts (e.g. the TSE D3 in core 7-8-72-13W6, section A, Figure 37). Such thin horizons are not expressed in well logs. On gamma-ray logs, the expression of this TSE separating two distinct sandbodies can be subtle (e.g. TSE D4 in 6-30-72-11W6, section C, Figure 39 and TSE D3 in 6-5-72-13W6, section A, Figure 37) and the TSE can only be defined in cores. In other cases the TSE separating the shoreface sandstone bodies is marked by a kick in the gamma-ray log or a change in the trend of the API values. Good examples of this change for TSE D4 are in (1) 7-8-72-13W6 and 16-5-72-13W6, section A, Figure 37; (2) 6-8-72-9W6, section E, Figure 41; (3) 10-1-73-13W6 and 6-13-72-13W6, Appendix C1; (4) 6-8-72-9W6, Appendix C2). Good examples for TSE D3 are in (1) 7-8-72-13W in section

A, Figure 37; (2) 6-13-72-13W6 in section B, Figure 38 (3) 6-8-72-9W6 and 6-4-71-9W6 in section E, Figure 41).

Shorefaces D3 and D4 also contain conglomerates within the upper shoreface succession. These occur mainly toward the southern limit of the transgression as east-west trending bodies. In places with very close wells it is possible to correlate these conglomerate bodies. A good example of this relationship is shown in Appendix C1 between wells 15-16-68-13W6 and 6-28-68-13W6.

In cross-section B (Figure 38) at 10-31-69-12W6 and 11-7-70-12W6, a log response interpreted as a channel fill locally incises into shoreface deposits D2. Few channels have core control in the study area, but all of them display a muddier-upward signature on the gamma-ray log (e.g. 6-10-68-10W6, cross-section D, Figure 40). Without core control, it is possible that some channels have not been detected (e.g. the channel incising D2 in well 6-17-72-9W6, Appendix C2).

In T71-73, the lower part of Falher D was defined by a variable gamma-ray log response, corresponding in cores to a facies association of hummocky cross-stratified sandstones interbedded with mudstones and interpreted as the transition between lower shoreface to offshore deposits. Good examples of these log responses and their correlation are shown in cross-sections C, D and E (Figures 39-41).

The upper part of Falher D across the entire study area is characterized by spiky-sonic log patterns corresponding mainly to coaly mudstones and coal beds. These are interpreted as coastal sediments deposited on top of the shoreface units previously discussed. These coastal plain units thin from south (20 m) to north (less than 1 m, and in places are completely eroded by the first marine TSE of Falher C) as seen particularly well in cross-sections A, E and F (Figures 37, 41 and 42). Finally, all the spiky-sonic log patterns of the upper part of Falher D are capped by a bounding discontinuity corresponding to the beginning of Falher C sedimentation.

5.2. FALHER C

Four well log facies have been recognized for most of Falher C and have been calibrated with cores. As in Falher D, a **spiky-sonic facies** represents nonmarine coastal plain deposits and the **blocky** and **sandier-upward facies** represent prograding shoreface deposits. A **ratty log facies** was defined for Falher C, representing deposits in a stressed environment such a lagoon or a estuary (Chapter 4).

Preliminary analysis of the distribution of these facies across the study area (Figure 46) showed that the spiky-sonic facies occurs (1) from bottom to top of the Falher C in the south and (2) across the study area in the upper part of Falher C. The blocky facies occurs as a thick unit across townships 67-68 and abruptly passes into a ratty facies. Northward, the ratty facies also passes abruptly into a sandier-upward facies which can be traced up to the northern limit of the study area.

These relationships (Figure 46) have been used to guide the detailed correlations presented below.

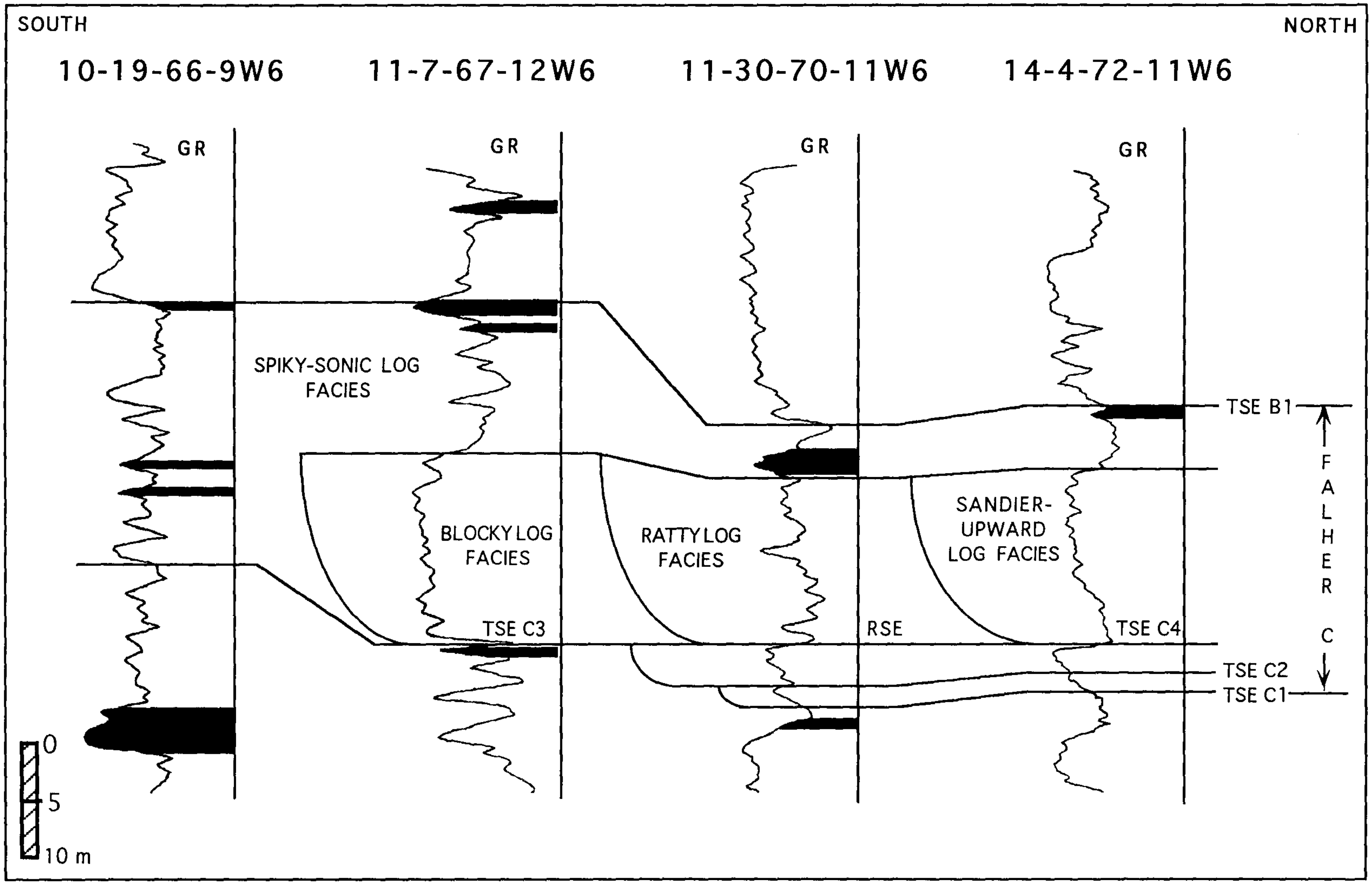

Figure 46. Geographic distribution of Falher C well log responses showing spiky-sonic log facies in the south and across the study area in the upper part of Falher C. Blocky log facies occur north of the spiky-sonic log facies and ratty log facies occurs between the blocky log facies and a sandier-upward log facies to the north. Very thin log facies defined by TSEs C1-C2 occur at the base of Falher C and show a patchy distribution across the study area.

In the southern area, very irregular responses were identified on the logs, corresponding to the spiky-sonic log facies previously defined (Chapter 4) and interpreted as coastal plain deposits (facies association of coals and mudstones). Because of the lack of good well control and the variability of this log signal, detailed correlations are very difficult in this part of the study area. In T67, all sections show a blocky log facies interpreted to represent shoreface sandbodies. The change from the spiky-sonic log facies to the blocky log facies is very abrupt and can be traced from east to west across the study area. Cross-sections A, D, E and F show this change (e.g. between wells 10-19-69-9W6 and 6-8-67-9W6 in section E, Figure 41). In this area the lagoonal and coastal plain deposits (spiky-sonic log facies) are laterally equivalent to thick shoreface sandbodies (blocky facies) to the north. The lateral facies change from lagoonal deposits (adjacent to the barrier associated with the shoreface) to truly coastal plain deposits is extremely difficult to distinguish using the logs from the few wells drilled in the southern portion (T66).

In T67 and part of T68, the wells show the blocky log facies (composed mainly of fine-grained sandstones with SCS) resting directly over the coastal plain deposits of the upper part of Falher D. Thus, the contact between Falher C and D in this area is interpreted as a TSE (TSE C3) which can be traced with logs across this area.

Typical gamma-ray values of the blocky log facies are in the order of 10-20 API units. The density-porosity and resistivity logs also show a similar blocky profile or a slight increase of the response upwards. Conglomerates and conglomeratic sandstones are also present within this log pattern and are concentrated mainly in T67, but can be traced only in very closely spaced wells (e.g. between 7-15-67-10W6 and 7-24-67-10W6, Appendix C6).

Northward of the blocky facies, other facies changes occur abruptly and very from place to place. For example, in cross-sections A, F and G (Figures 37, 42 and 43) the blocky log facies passes northward into a ratty log facies characterized by a very irregular response. Calibration with cores shows the presence of interbedded sandstones and mudstones without coals (Chapter 4). The trace fauna suggests deposition in a stressed environment. Some examples of this log facies are in well 11-30-68-8W6, Appendix C6; 15-21-68-8W6, section F, Figure 42 and 7-9-69-13W6, section A, Figure 37. The extremely variable nature of this facies makes it difficult to correlate in detail from well to well.

The presence of these stressed deposits north of a prograding shoreface where open marine conditions would be predicted is a problem. The cores and correlations strongly suggest that an RSE was formed before the deposition of these ratty log facies. The change from blocky facies to ratty facies can be also traced in a roughly east-west direction.

The same sections (A, F and G, Figures 37, 42 and 43) show that northwards, the ratty log facies is replaced abruptly by a sandier-upward log facies. In some areas (R11 and R12) the sections show that the ratty log facies may be absent, and the change occurs directly from blocky facies to sandier-upward facies (cross-section B, Figure 38). From T70 (and some portions of T69) to the northern part of the study area, Falher C is mostly characterized by the sandier-upward facies designated as C4 (Cross-sections A, B, E, F and G, Figures 37, 38, 41, 42 and 43). The sandier-upward log facies is characterized in this area by a succession grading from marine shales to fine-grained sandstones with SCS and cross stratification interpreted as prograding shoreface sandbodies (Chapter 4). The cross-sections show the gamma-ray logs decreasing from values of about 100-110 API to values of about 50 API upward. This sandier-upward pattern is also expressed in the resistivity and neutron-porosity logs. Conglomerates can be found within this facies, mainly in the upper part, and normally associated with the southern limit of C4 (e.g. 10-31-68-10W6 and 7-5-69-9W6, Appendix C2). The lateral and geographical relationship between the sandier-upward facies (prograding shoreface) and the ratty facies in T69 R13 and in T68 R7-8 suggests that the ratty facies represents lagoonal deposits behind a barrier formed at the southern limit of shoreface C4.

Muddier-upward log facies calibrated with cores have been interpreted in some wells as a north-south trending channel system cutting into the blocky facies C3 (e.g. 10-1-68-9W6, Appendix C6; 1-10-68-9W6 and 9-16-68-10W6, Appendix C2). Cross-section D (Figure 40) shows that this channel system passes northward into ratty log facies where muddier sections are present (e.g. from 11-4-69-10W6 to 7-20-69-10W6). In this case the ratty log facies are oriented (as the channel system) in a north-south direction, apparently cutting also the C4, C2 and C1 shoreface unit (Figure 47). The facies association described for the ratty log facies (a stressed environment, Chapter 4) and the north-south orientation perpendicular to the shoreline, strongly suggests an estuarine environment of deposition. This association of muddier-

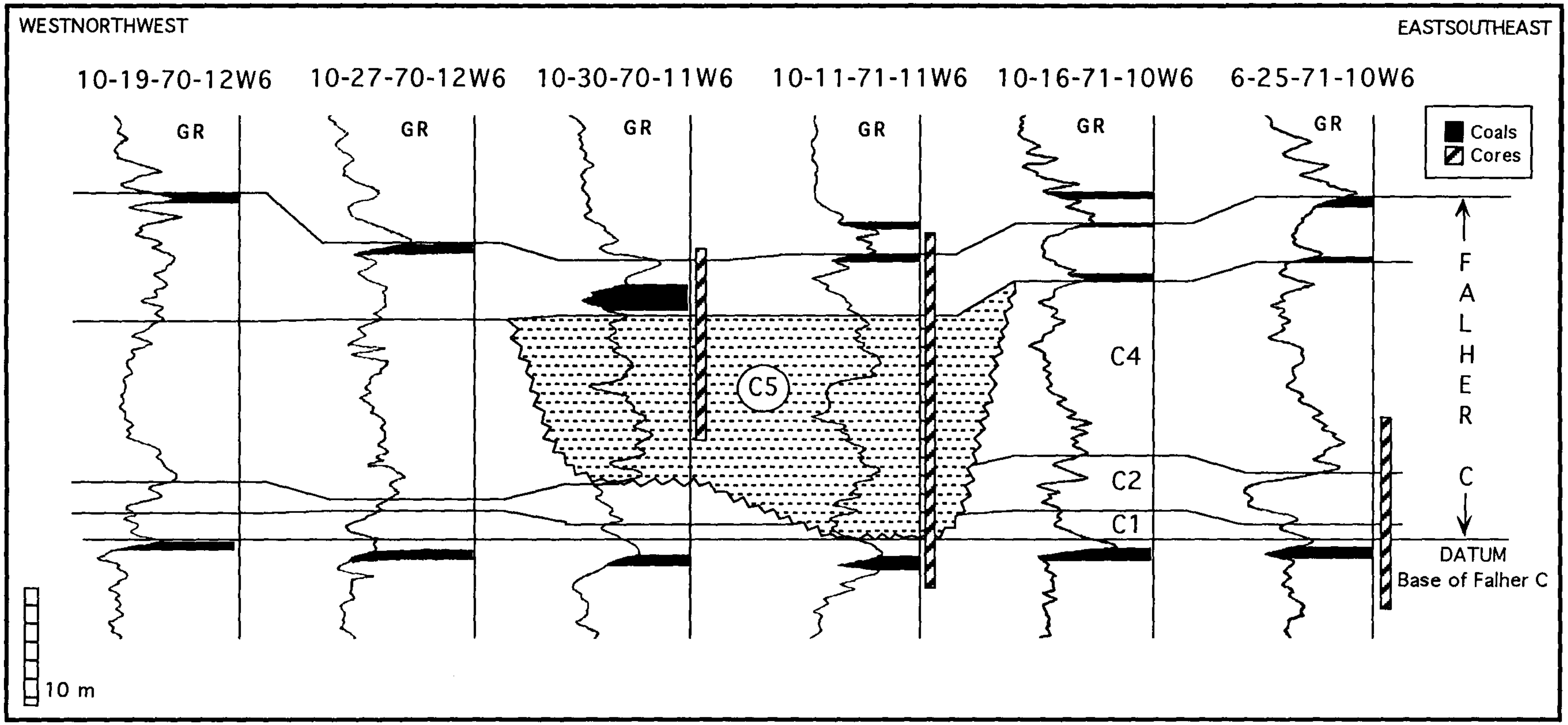

Figure 47. Cross-section westnorthwest-eastsoutheast showing a channel system (shaded area) cutting into units C1, C2 and C4. In this part of the area, the channel was filled by a brackish succession of sediments interpreted as channel fill. Wells 10-30-70-11W6 and 10-11-71-11W6 show a ratty gamma-ray response which contrast with the sandier-upward response of wells 10-16-71-10W6 and 10-27-70-12W6.

upward facies and ratty facies, both with a north-south orientation is designated here as the unit C5.

Underlying C4 and C5 there are two thin successions with patchy distribution across the study area. Calibration of logs with cores in some wells show that two distinctive "spikes" in the gamma-ray log (each averaging 1.5-2 m thick) correspond to remnants of shoreface deposits. In well 6-25-71-10W6, Appendix C2 and A33) these two spikes are well developed and are termed units C1 at the base and C2 at the top (the stratigraphic relationship shows that here C1 and C2 were the first events in the Falher C sedimentation). However, well 6-27-71-9W6 (Appendix C2) shows that without core control is difficult to establish the break between these two units. The bases of C1 and C2 are interpreted as TSEs (TSE C1 and TSE C2) and because the units are so thin, it is easy to understand why C1 is not present in some wells, due to erosion by TSE C2 (e.g. wells 10-23-72-11W6, 6-30-72-11W6, 6-7-73-11W6 and 16-21-73-11W6 in cross-section D, Figure 40). C1 and C2 can also be absent in some wells because of erosion at the base of TSE C4 (e.g. 6-13-72-13W6, Appendix C1 and 11-10-73-13W6 in cross-section A, Figure 37). In all sections, TSE C4 affected mainly unit C2 but because it is so thin, several wells show unit C1 partially or totally eroded by TSE C4. Other bounding discontinuities affecting the presence of C1 and C2 are the preserved RSE landward of shoreface C4, associated to the RSL fall after C3 deposition and the RSE associated with the erosive action of the channel system in unit C5. In both cases the RSEs affected mainly C2 (Appendix C1 and C5).

6. GEOMETRY AND EXTENSION OF THE UNITS WITHIN FALHER C AND D

6.1 FALHER D

6.1.1. Unit D1

The prograded width of shoreface D1 is approximately 38 km, and its thickness decreases from 10 to 2 m northward across the study area. The landward limit of D1 trends roughly east-west (Figure 45). The barrier associated with this shoreface sandbody is longer than 67 km, and the well spacing suggests that the width is less than 1 km. In T68 R9W6 the barrier forms a point protruding to the northwest, documented by the coastal plain/lagoonal deposits in the core 6-20-68-9W6 (Figure 48).

Upper shoreface and beach conglomerates and conglomeratic sandstones occur mainly in T68 R9-13 as discontinuous and linear bodies with an east-west trend. They pinch out eastward, suggesting a source for these conglomerates somewhere west of the study area, close to the British Columbia border. In cores, the thickness of individual beds of conglomerates within these linear bodies varies from 5 cm to 1 m (core 6-28-68-13W6, Appendix A35).

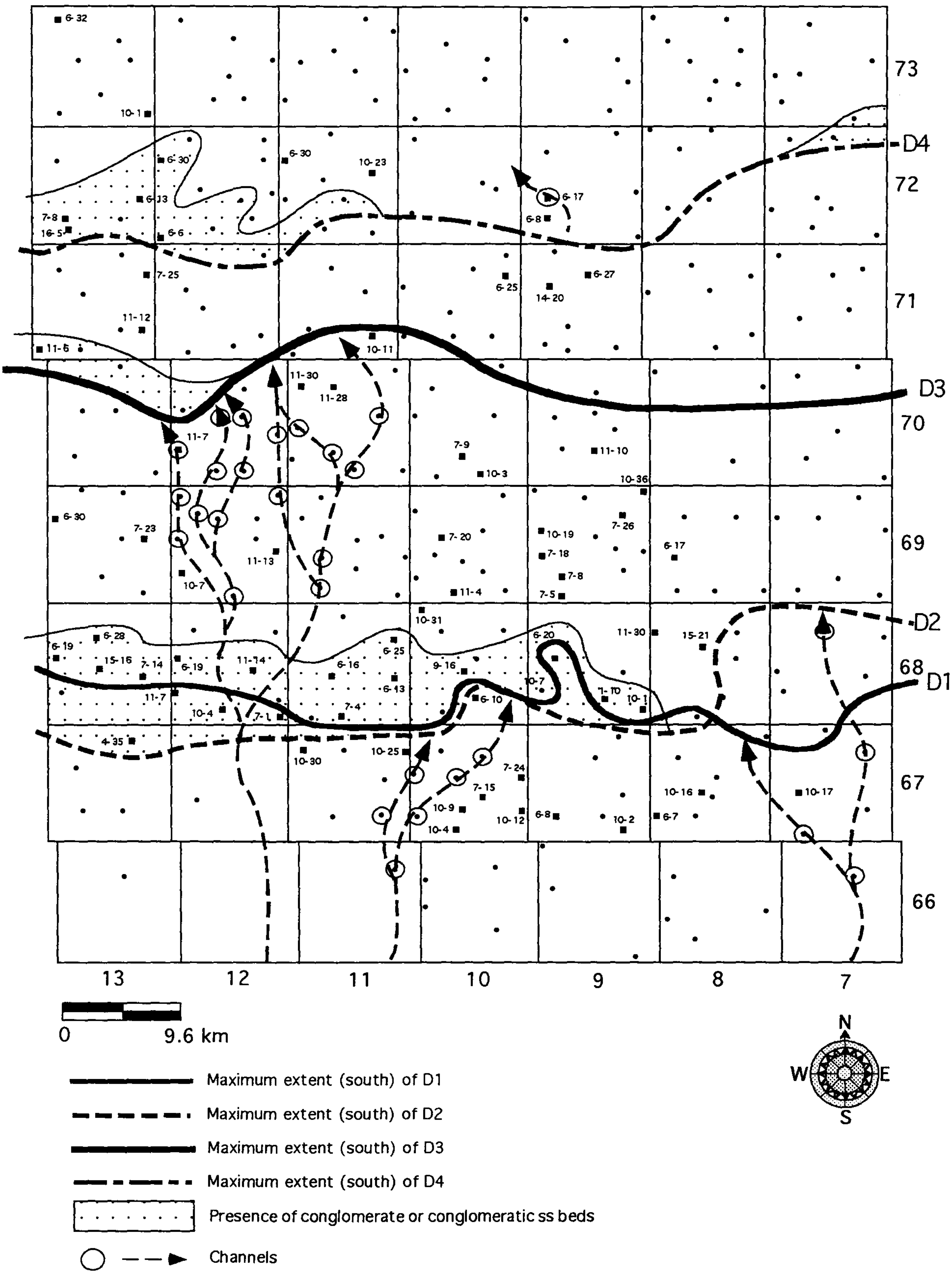

Figure 48. Map of shoreface units D1-D4 (Falher D)

6.1.2. Unit D2

The shoreface succession of Unit D2 thickens northward from about 5 m to 30 m in T70; it then pinches out even farther northward. Its landward limit trends east-west in a very similar position to the D1 limit (Figure 48). The prograded width of this shoreface deposit is greater than 60 km and the morphology of the barrier at the southern edge is similar to unit D1; longer than 67 km but narrower than 1 km. Upper shoreface and beach conglomerates occur essentially in the same geographic area as D1 conglomerates. In cores, the thickness of individual beds of the conglomerate within this unit varies from 5 cm to a maximum of 2 m in core 7-4-68-11W6.

6.1.3. Unit D3

The shoreface sandbody in D3 varies from 5-20 m in thickness, and its southern limit is in T70 (Figure 48). Its prograded width is at least 30 km and it extends even farther northward beyond the study area. The inferred barrier in the south is similar to those in unit 1 and 2. Upper shoreface and beach conglomerates and conglomeratic sandstones are concentrated in a linear body close to the southern limit of the shoreline, in the western part of the study area (T70-71). In cores, the thickness of individual beds of conglomerate within this linear body varies from a few centimeters to a maximum of 1 m in core 11-6-71-13W6 (Appendix A19).

6.1.4. Unit D4

The shoreface sandbody of Unit D4 has a prograded width of approximately 20 km, and it probably extends northward beyond the study area. Its thickness varies from 5 to 10 m. The landward limit of D4 trends generally east-west (Figure 48). The inferred barrier associated with this shoreface is similar to those in units 1, 2 and 3.

Upper shoreface and beach conglomerates are concentrated mainly in the western part of the study area in T72 R11-13W6 (Figure 48), suggesting again that the main source of these conglomerates was located west of the study area, somewhere close to the British Columbia border. The thickness of the individual beds of conglomerate in cores within this unit varies from 5 cm to a maximum of 3.5 m in core 16-5-72-13W6 (Appendix A24).

6.1.5. Unit D5

A series of muddier-upward log responses within D1 and D2 define linear bodies that trend south-north, mainly across R11 and 12 (Figure 48). These are interpreted as channel fills, some up to 15 m thick. Others small channels can be identified in T66 and 67, cutting into units D1 and D2.

6.1.6. Unit D6

Unit D6 is characterized by coastal plain successions that within the study area capped stratigraphically all the units described previously and thinnes northwards due to the first TSE of Falher C .

6.2. FALHER C

6.2.1. Unit C1

This unit represents the remnant of a transgressive-regressive unit at least 40 km wide (north to south) within the study area. The thickness varies between 1 m and 4 m, but the top of C1 was eroded by a TSE and RSE. In Figure 49 the shaded areas show the zero isopach where all of C1 has been eroded.

The landward limit of the C1 shoreface sandbody trends approximately east-west in T69.

6.2.2. Unit C2

This unit is similar to C1. The landward limit of the C2 shoreface sandbody trends in a roughly westnorthwest-eastsoutheast direction across T68-69 with many irregularities (Figure 50). The preserved thickness varies from 1 to 5 m and is strongly influenced by the overlying TSE and RSE. The

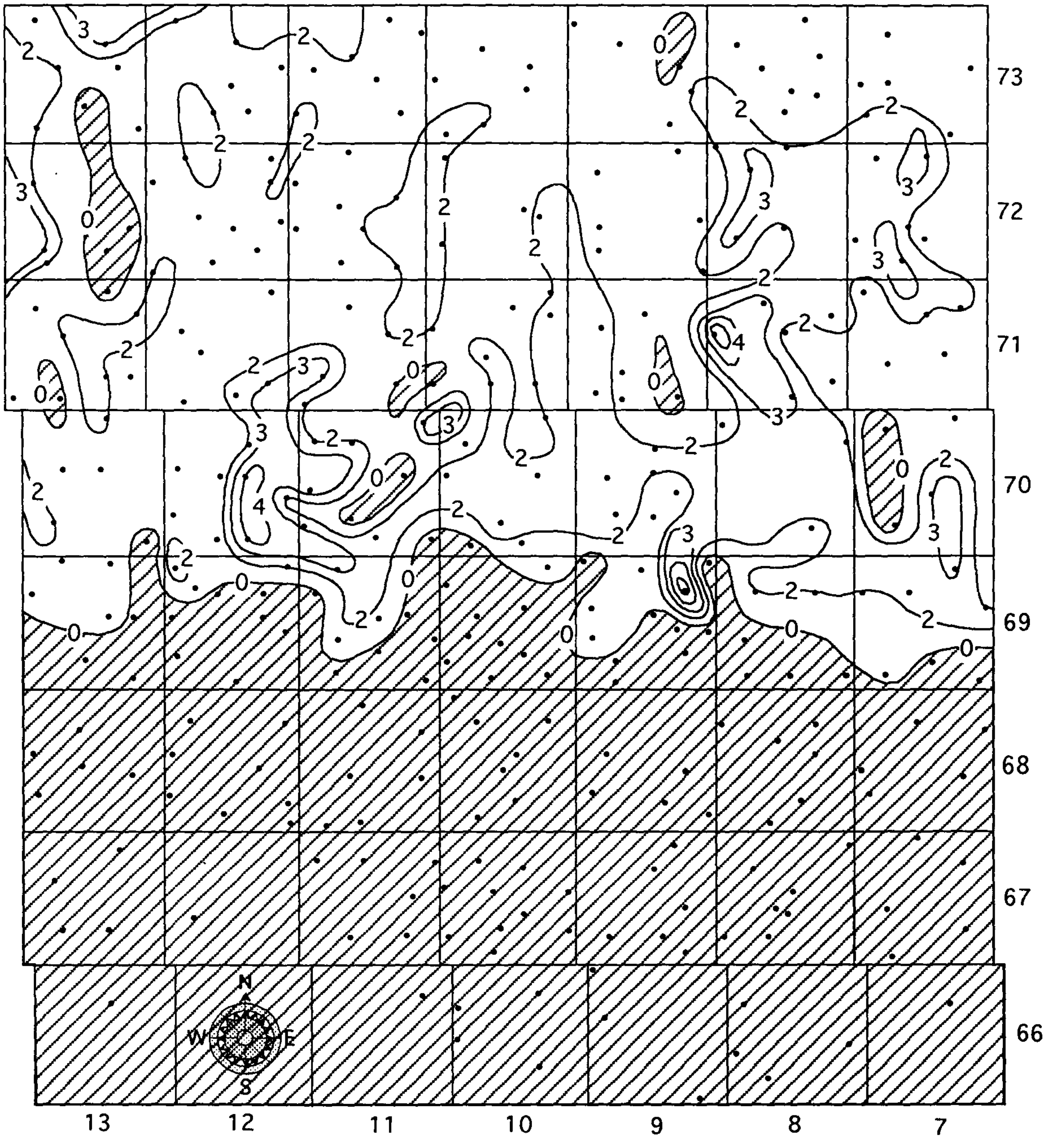

Figure 49. Isopach map of Unit C1. Thickness based on wells logs and cores, and contoured in meters.

isopach map shows a very patchy preserved distribution of this unit, with most of the northwestern portion eroded (Figure 50).

6.2.3. Unit C3

The shoreface sandbody of unit C3 has a maximum width (north to south) of 26 km in the western part of the study area, decreasing to about 15 km eastwards (Figure 51). The thickness varies from 25 m in the west to 7 m in the east (Figure 51), suggesting that the main source of sediments was located west of the study area.

The landward limit of C3 has a east-west trend (Figure 52). The inferred barrier associated with this shoreface sandbody is longer than 67 km and narrower than 1 km wide (based on well spacing) and separates the C3 shoreface sandbodies from lagoonal and coastal plain deposits farther south (non shaded area in Figure 52). These lagoonal and coastal plain sediments are included within the unit C3.

Upper shoreface and beach conglomerates within the shoreface sandbodies are concentrated as linear bodies in an east-west trend (Figure 53) and form the main producing reservoir in T67 R7-10W6 (C. Gamba, pers. com., 1994). In cores, the thickness of individual beds of conglomerates within these linear bodies varies from 5 cm to a maximum of 3 m in core 6-7-67-8W6 (Appendix A41).

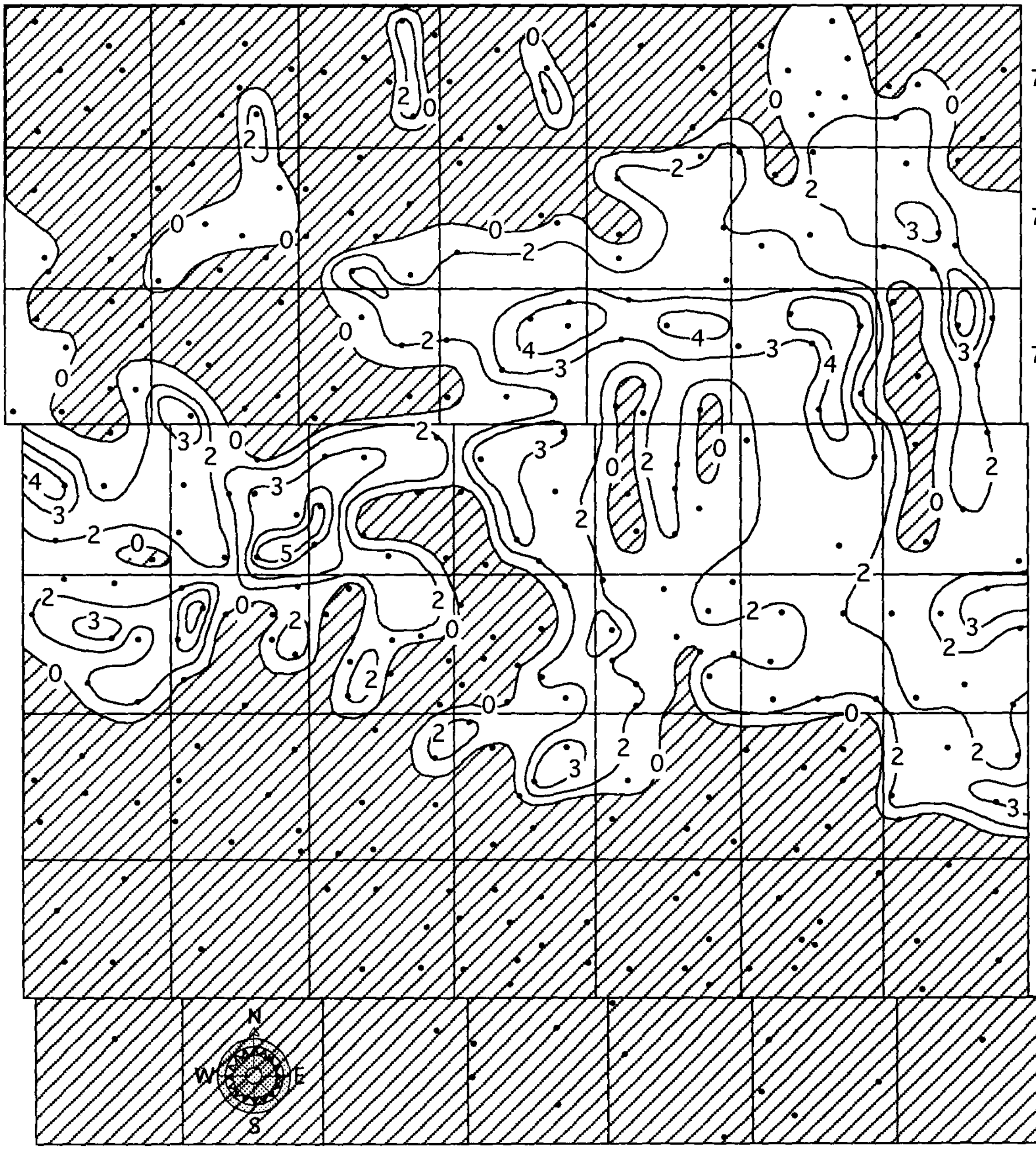

Figure 50. Isopach map of Unit C2. Thickness based on well logs and cores, and contoured in meters.

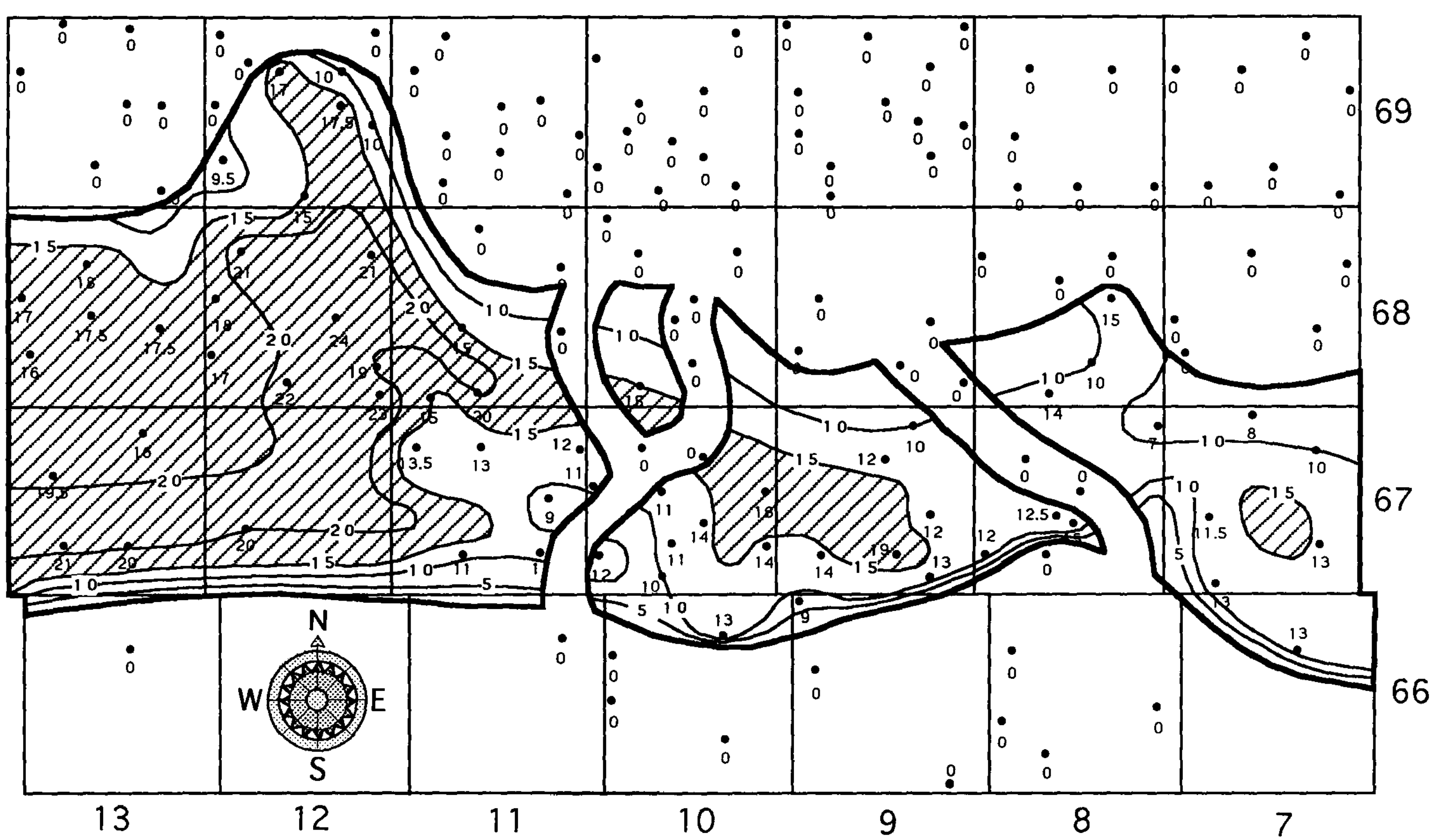

Figure 51. Net sand map of the C3 unit, Falher C. Contour interval is 5 meters.

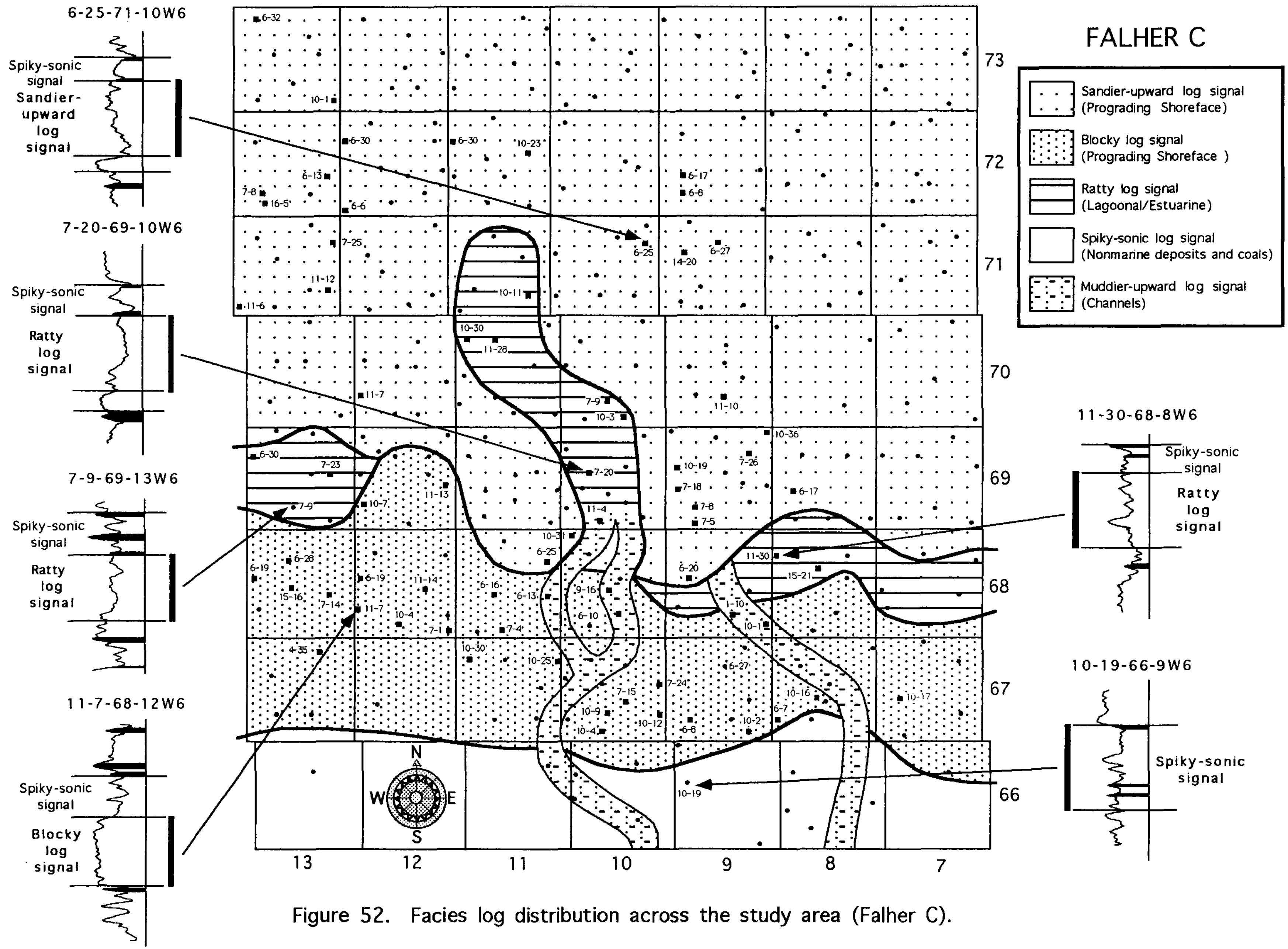

Figure 52. Facies log distribution across the study area (Falher C).

6.2.4. Unit C4

The landward limit of the shoreface sandbody of unit C4 trends approximately in a east-west direction, parallel to shoreface C3 (Figure 52). The width (north to south) of this sandbody is at least 50 km, and it probably continues northward of the study area. The thickness is fairly constant at about 18 m.

The inferred barrier associated with this unit is longer than 67 km and narrower than 1 km wide (based on well spacing). This barrier separates shoreface deposits (lightly stippled, Figure 53) from lagoonal deposits (horizontal ruling, Figure 53) to the south. The lagoonal deposits associated with shoreface deposits C4 were preserved mainly in T68 R7-8 and T69 R13 in a east-west trend.

Upper shoreface and beach conglomerates occur in a linear eastnortheast-westsouthwest trend within the shoreface sandbodies of unit C4, but as discontinuous bodies (Figure 53). Some of them are gas producers (e.g. wells 10-31-68-11W6 and 7-5-69-9W6) but others are wet, like 6-30-69-7W6 (C. Gamba, pers. com., 1994).

6.2.5. Unit C5

Unit C5 contains a brackish succession of facies and trends north-south, perpendicular to the orientation of shoreface C4. Its width is approximately 8 km and its length about 30 km (diagonal ruling in Figure 53). This brackish

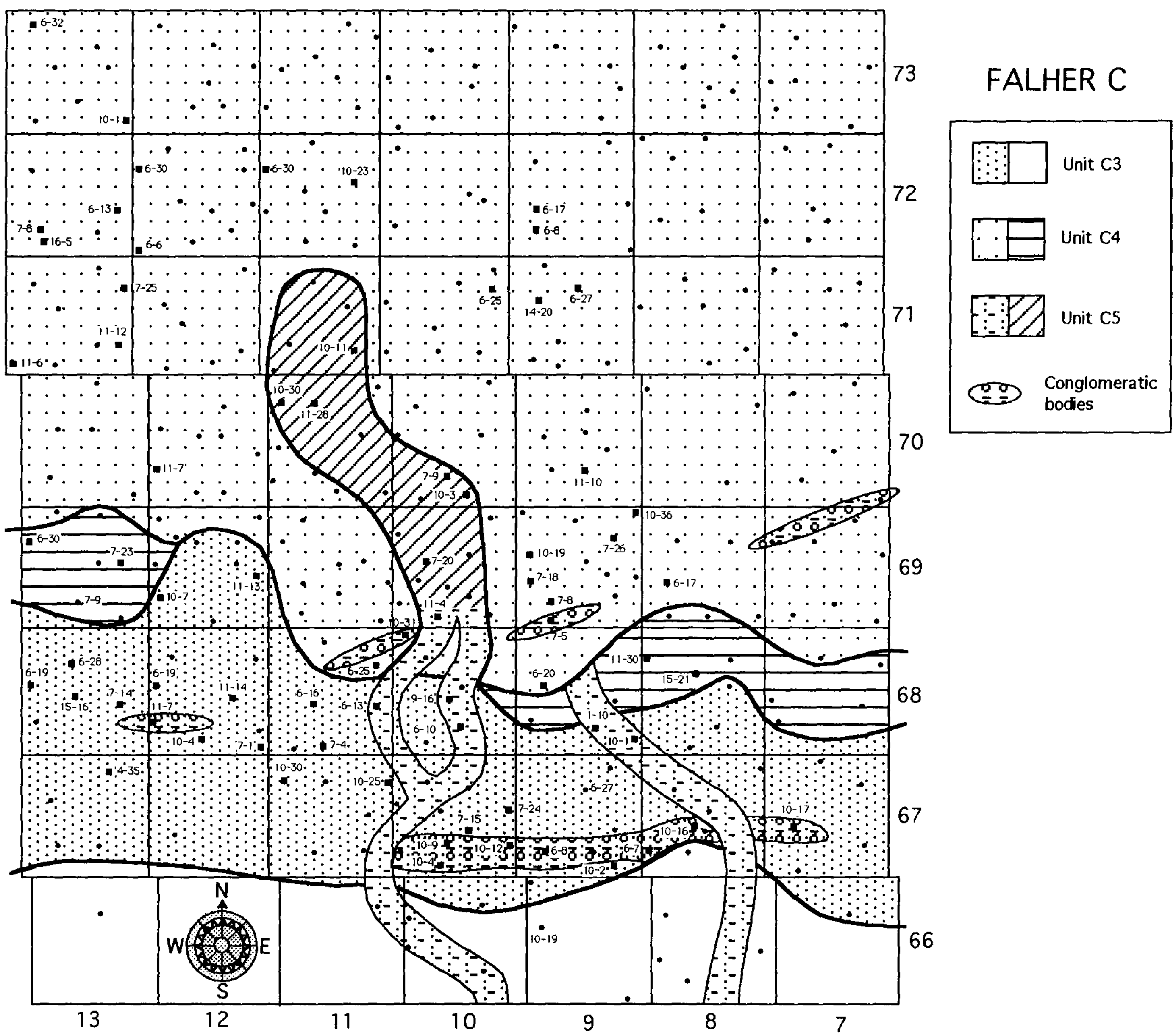

Figure 53. Areal distribution of units C3, C4 and C5 (Falher C), showing also the position of the conglomeratic bodies.

succession is interpreted as estuarine deposits filling a channel cut into units C3 and C4 (also locally in C2 and C1). The estuarine deposits can be traced as far north as T71 R11. A sandy fill occurs in the southern part of the channel (horizontal dashed line and dots, Figure 53) and can be traced in T67/68 R10 with core and log control. The channels are 2-3 km wide and the fill is up to 16-18 m thick. The southern extension of these channel deposits in T66 is poorly known because of sparse well control. Another incision within unit C3 and C4 that trends roughly north-south (T66 to 68 R8/9, Figure 52 and 53) is possibly contemporaneous with the channel system in R10-11 and is included here within unit C-5.

6.2.6. Unit C6

Unit C6 is characterized by a coastal plain succession that within the study area capped stratigraphically all the units described previously.

7. DEPOSITIONAL HISTORY OF FALHER D AND C

The subdivision of Falher D and C into smaller units was made on the basis of their bounding discontinuities. In the North American Stratigraphic Code (NACSN, 1983) bounding discontinuities are defined as laterally traceable surface that represent a hiatus or break in deposition. Bounding discontinuities include unconformities, ravinement surfaces, onlap or downlap surfaces and condensed horizons or hardgrounds.

Each unit within allomembers D and C is bounded at the top by a **marine flooding surface** that extends southward as far as the landward limit of the shoreface, and by a correlative **flooding surface** (FS) within the brackish and coastal plain deposits south of the limit of the shoreface successions. The marine flooding surface is interpreted as a major bounding discontinuity in allomembers D and C. This surface represents an abrupt increase in water depth with evidence of erosion - it is therefore designated as a **transgressive surface of erosion** (Walker, 1992).

The deposition of the units is discussed in this chapter in terms of **systems tracts** which are defined as contemporaneous linked depositional systems (Posamentier *et al.*, 1988; Van Wagoner, *et al.*, 1990; Walker, 1992).

Summarized diagrams of the depositional evolution of allomembers D and C are shown in Figures 54, 55, 56 and 57.

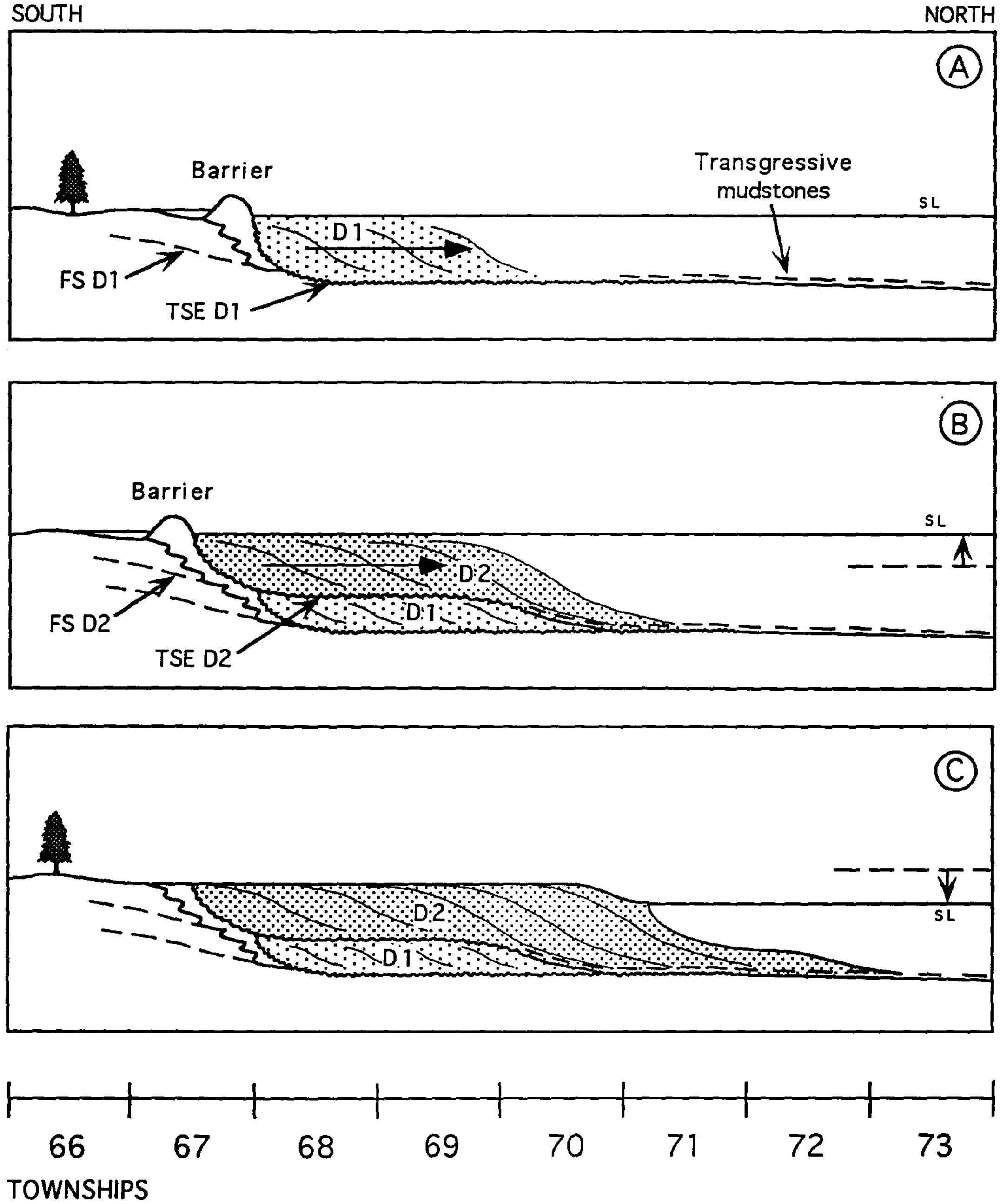

Figure 54. A) Evolution of Falher D. With a relative sea-level rise, the shoreline moved southward by erosional shoreface retreat forming a transgressive surface of erosion (TSE D1). When the rate of RSL rise slowed and the rate of fluvial input to the shoreface became greater than the rate of shoreface erosion, then the migration of the barrier-lagoon system stopped. With renewed sediment supply, a wave-dominated shoreface succession prograded northwards to form an extensive strandplain system. B) After a RSL rise, a new shoreline moved to T67 and an erosion surface (TSE D2) overlies D1. After RSL stopped rising, a wave-dominated shoreface succession (D2) prograded northwards. C) A relative sea-level fall ended the progradation of unit C2.

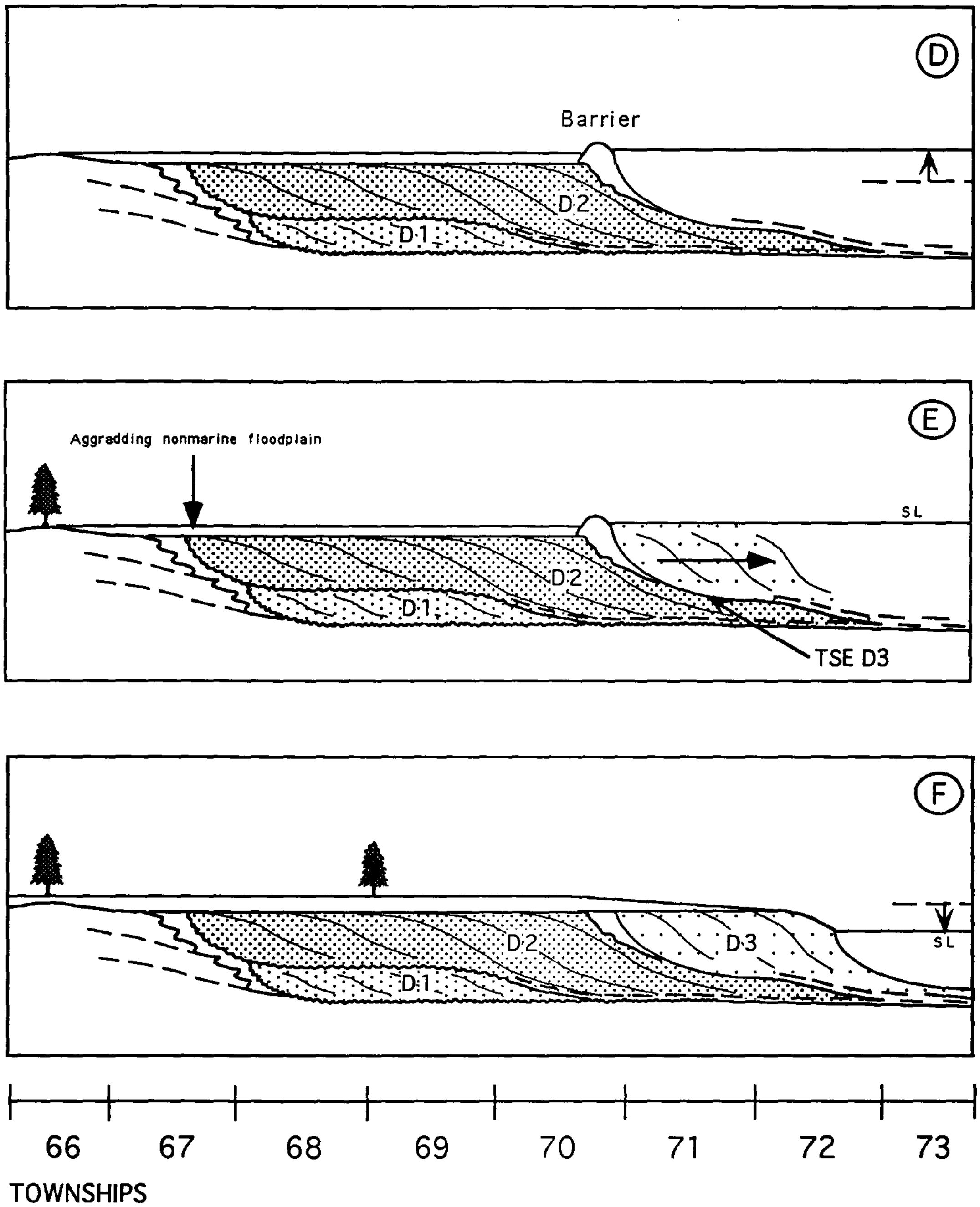

Figure 55. D) After a RSL rise, a new shoreline moved to T70. An erosion surface overlies D2 and some transgressive sediments were deposited. E) After RSL stopped rising, a wave-dominated shoreface succession (D3) prograded northwards. F) A RSL fall ended the progradation of D3.

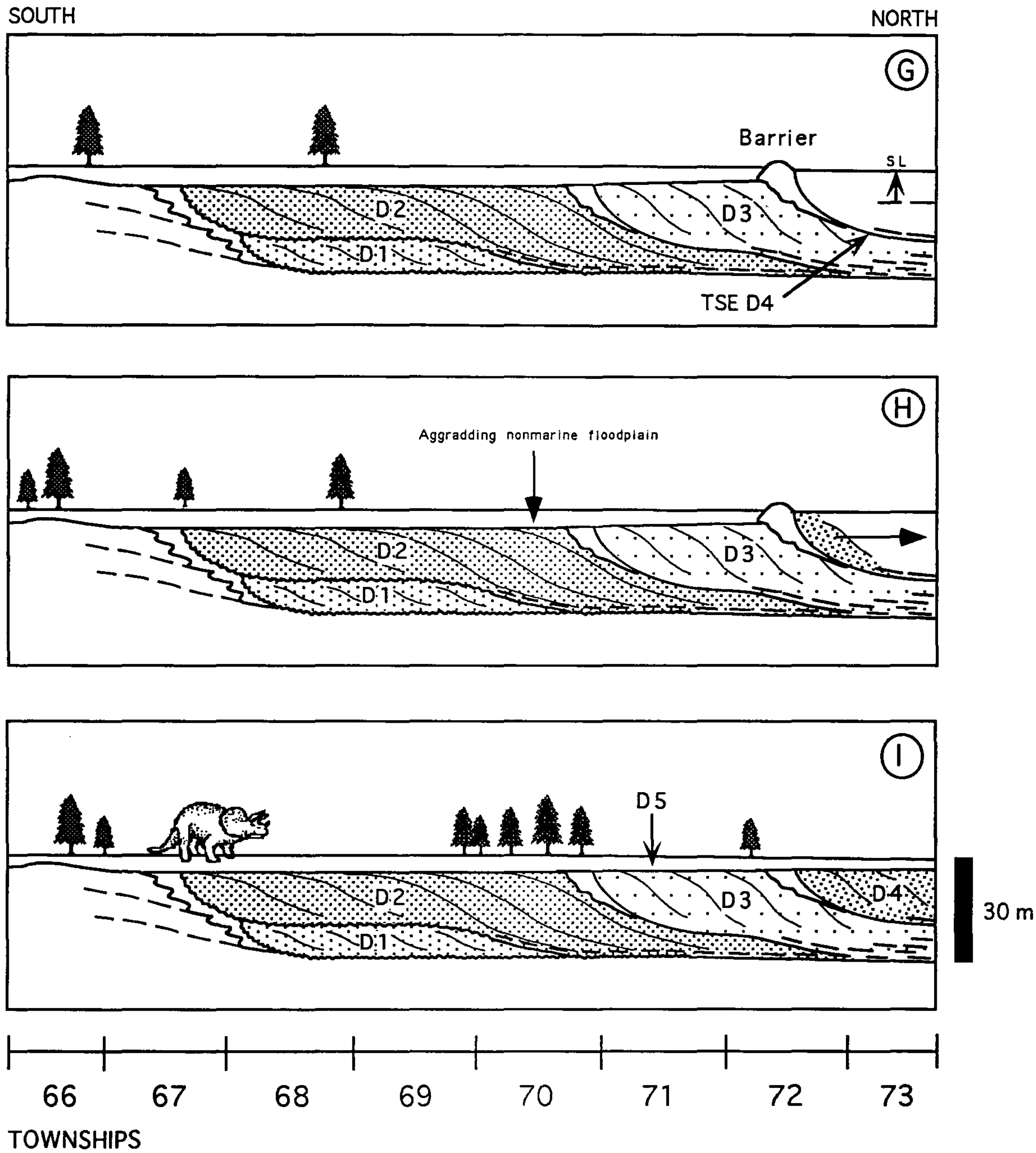

Figure 56. G) After a rise of RSL, a new shoreline moved to T72. An erosion surface overlies D3 and some transgressive sediments were deposited. H) After RSL stopped rising, a wave-dominated shoreface succession (D4) prograded northwards. I) Aggradding coastal plain deposits characterize the top of Falher D.

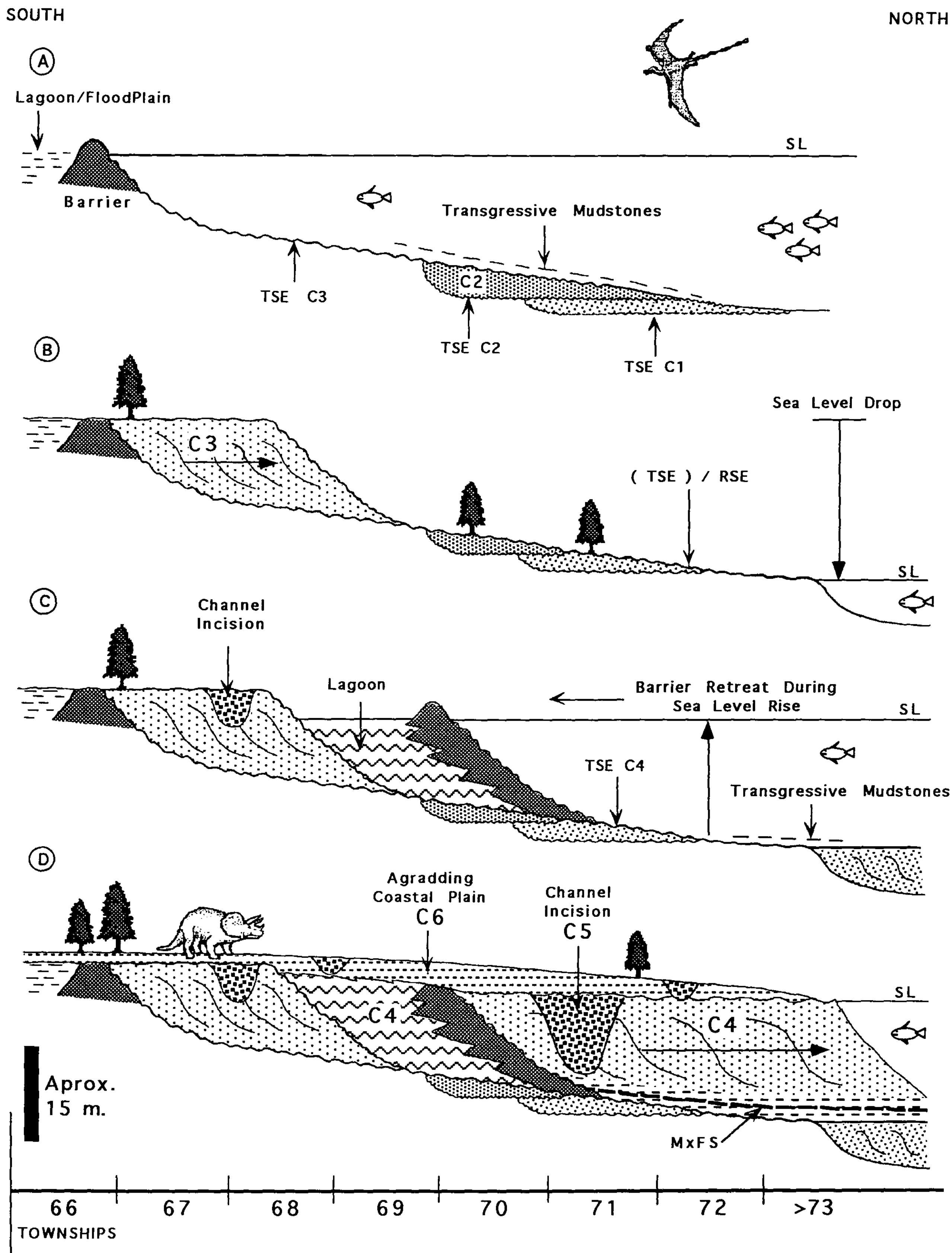

Figure 57. Idealized diagram representing the evolution of the units of Falher C within the study area. A detailed explanation is given in Chapter 7.

7.1. FALHER D

7.1.1 UNIT D1

7.1.1.1 Transgression (Preservation of a Transgressive System Tract)

The deposition of Falher E ended when relative sea-level (RSL) began to rise, flooding the nonmarine deposits of Falher E. The shoreline moved southward by erosional shoreface retreat forming a TSE or ravinement surface (Swift, 1968). Many authors have proposed that a TSE or ravinement process may remove in places up to about 20 m of sediment (Demarest and Kraft, 1987; Plint, 1988; Walker and Eyles, 1991).

Initially wave winnowing probably formed a beach/beach-ridge system attached to the coastal plain. Rapid subsidence resulted in detachment of the beach/beach-ridge and formation of a lagoon (Rampino and Sanders, 1980; Dominguez and Wanless, 1991). Because of a steady and moderate rate of RSL rise, the barrier-lagoon system retreated to the south. Eventually, the rate of RSL rise slowed, and the rate of fluvial input of sediment to the shoreface became greater than the rate of shoreface erosion. The migration of the barrier then stopped in the southern part of T68 (Figure 48).

The preservation of thin brackish deposits overlying coastal plain deposits and underlying shoreface deposits (11-7-68-12W6, Appendix B4, box 11, 10-7-69-12W6 and 6-19-68-12W6, Appendix A30) suggests that a thin veneer of lagoonal to back-barrier deposits was partially preserved during landward barrier migration and erosional shoreface retreat (Rampino and

Sanders, 1980). The position of a inferred barrier at the southern part of T68 represents the landward limit of barrier migration and the position of the shoreline at the time of maximum transgression. Core 11-7-68-12W6 (Appendix A20) is located geographically on the landward side just behind the inferred position of the barrier (Figure 48) and shows coarsening upward successions of very fine to fine-grained sandstones with planar lamination and roots (Appendix B4, boxes 1-9). This association is interpreted as washover fan deposits formed when heavy storms broke through the barrier and deposited sediment on the landward side (Orford, 1977; Reineck and Singh, 1980). These washover fan deposits are characteristic of transgressive barrier settings (Reinson, 1992).

7.1.1.2. Bounding discontinuities

7.1.1.2.1 Marine Flooding surface D1

From T73 to the southern part of T68, the transgressive surface on top of Falher E consists of TSE D1. In the central portion of the study area (T70-71) this surface is normally defined by coastal plain and coal deposits overlain by marine mudstones and sandstones with HCS. In the southern portion (T68-69) it is defined by sandstones with SCS overlying coastal plain deposits (e.g. cores 9-16-68-10W6, Appendix A56; 10-31-68-10W6, Appendix A13; 7-5-69-9W6, Appendix A52; 6-19-68-12W6, Appendix A30; 10-4-68-12W6, Appendix A14; 7-4-68-11W6, Appendix A51 and 6-19-68-13W6, Appendix A30).

7.1.1.2.2. Flooding surface D1

Where present, transgressive lagoonal successions are bounded at the base by a flooding surface (FS D1). This surface represents initial flooding of topographic lows along the inner coastline, landward of the barrier as it moves southward, and indicates the initial development of lagoons during landward barrier migration. No evidence of erosion was observed along this surface. Flooding surface D1 is usually defined in the study area by a thin bioturbated lagoonal mudstone overlying coal deposits, and is correlative with marine flooding surface D1 north of T68. One example of lagoonal mudstones associated with flooding surface D1 can be seen in core 6-19-68-12W6 (Appendix A30). In contrast core 6-20-68-9W6 (Appendix A31) shows that flooding surface D1 correlates with thin coal beds overlying rooted sandstones. These coals might be the first deposit of the transgression if the coastal plain was initially flooded to create broad bays and lagoons (Van Wagoner, 1991; Bhattacharya, 1993), but only coal analysis will indicate if they were deposited in fresh or brackish water.

7.1.1.3. Regression (Preservation of a Highstand system tract)

With renewed sediment supply to the barrier shoreline after RSL stopped rising, a wave-dominated shoreface succession prograded northwards (Figure 54A) to form an extensive strandplain system that extends at least to T71 (a distance of approximately 40 km). This strandplain system consisted of sand and gravel shoreface deposits, probably with beach ridges. Upper shoreface conglomerates prograded at least 6 km but this width probably represents a composite of more than one shoreface conglomeratic body.

Channel fills with north-south trends were interpreted from well logs (e.g. 11-9-70-11W6, 11-7-70-12W6 and 10-31-69-12W6) mainly in R11-12 (Figure 48). They probably fed the prograding strandplain in this part of the study area. Other channel systems were interpreted from core and logs in R9-10 and R7, as far north as the southern limit of coastline D1 (Figure 48). In prograding strandplain systems, channels supplying sediment commonly switch by avulsion. Once a channel system is abandoned it loses its ability to transport sediment and the channel mouth is quickly reworked by waves and longshore drift (Dominguez *et al.*, 1987). This may explain why these two channel systems could not be correlated to the north within the shoreface succession of unit D1.

In T68 R7-8 a mudstone is present in well 14-18-68-7W6, and is surrounded by shoreface deposits. The mudstone is interpreted as having been deposited in a back-spit lagoon during shoreface progradation. The thickness of this back-spit lagoon deposit in 14-18-68-7W6 is apparently equal to the total thickness of the shoreface succession (about 7 m). Back-spit lagoons have been documented in modern strandplains of the eastern coast of Brazil (Dominguez *et al.*, 1987) and in Falher A and B (Rouble, 1994). It was suggested that they are initially formed by high rates of fluvial discharge at a channel mouth with subsequent rapid progradation of the shoreface

(Dominguez *et al.*, 1987), isolating a small lagoonal area behind a new, alongshore-lengthening spit.

Few cores are available in the area landward of the D1 shoreface incision which makes it difficult to differentiate the gradational change from transgressive to regressive deposits. Core 6-10-68-10W6 (Appendix A26) contains very thin sandstones with ripple cross-lamination interbedded with mudstones containing root traces, interpreted as swamp deposits. In contrast, core 10-25-67-11W6 (Appendix A10) is composed almost entirely of a thick succession of black mudstones, completely massive and without bioturbation, reflecting a very restricted environment.

7.1.1.3.1. Bounding discontinuities

Seaward of barrier 1, the shoreface succession is sharp-based and is normally represented by a swaley cross-stratified sandstone which abruptly overlies lagoonal and coastal plain deposits without offshore transitional deposits present at the base of the shoreface succession (e.g. 9-16-68-10W6, Appendix A56; 10-31-68-10W6, Appendix A13, and 7-4-68-11W6, Appendix A51). There are two possible explanations for the sharp (as opposed to gradational) base. Plint (1991) suggested that if offshore transitional sediments were originally deposited during the transgressive event, they can be removed by wave scouring during subsequent progradation as relative sea-level fell (forced regression). In this case the wave scouring creates an erosion surface which is interpreted as an RSE that could modify the original marine flooding surface (TSE).

An alternative explanation can be made assuming that the water depth was never greater than the fairweather wave base during the transgression; in this case, offshore transgressive mudstones would never have been deposited.

Landward of the barrier, the change from transgressive to regressive deposits cannot be defined because the lack of core control.

7.1.1.4. Ichnofacies

The upper shoreface sandstones of Unit D1 are characterized by a *Skolithos* ichnofacies assemblage (Figure 58). The association *Palaeophycus/Macaronichnus* is very typical of these deposits in the study area. The trace makers occur in fine to medium-grained sandstones and normally their activity is so intense that all sedimentary structures are destroyed. *Palaeophycus* is a subcircular burrow in form and has smooth to irregular, distinctly lined walls. It has been interpreted as the dwelling structure created by a suspension feeder or a carnivorous vermiform organism (Pemberton and Frey, 1982). Based on the wall thickness the specimens from allomember Falher D were assigned to the ichnospecies *P. tubularis* (Vossler and Permberton, 1988). *Macaronichnus* appears to be the burrow of highly mobile deposit feeders and it has commonly been recognized as an infaunal burrow in relatively high energy settings and as an excellent indicator of foreshore to upper shoreface environment (Clifton and Thompson, 1978;

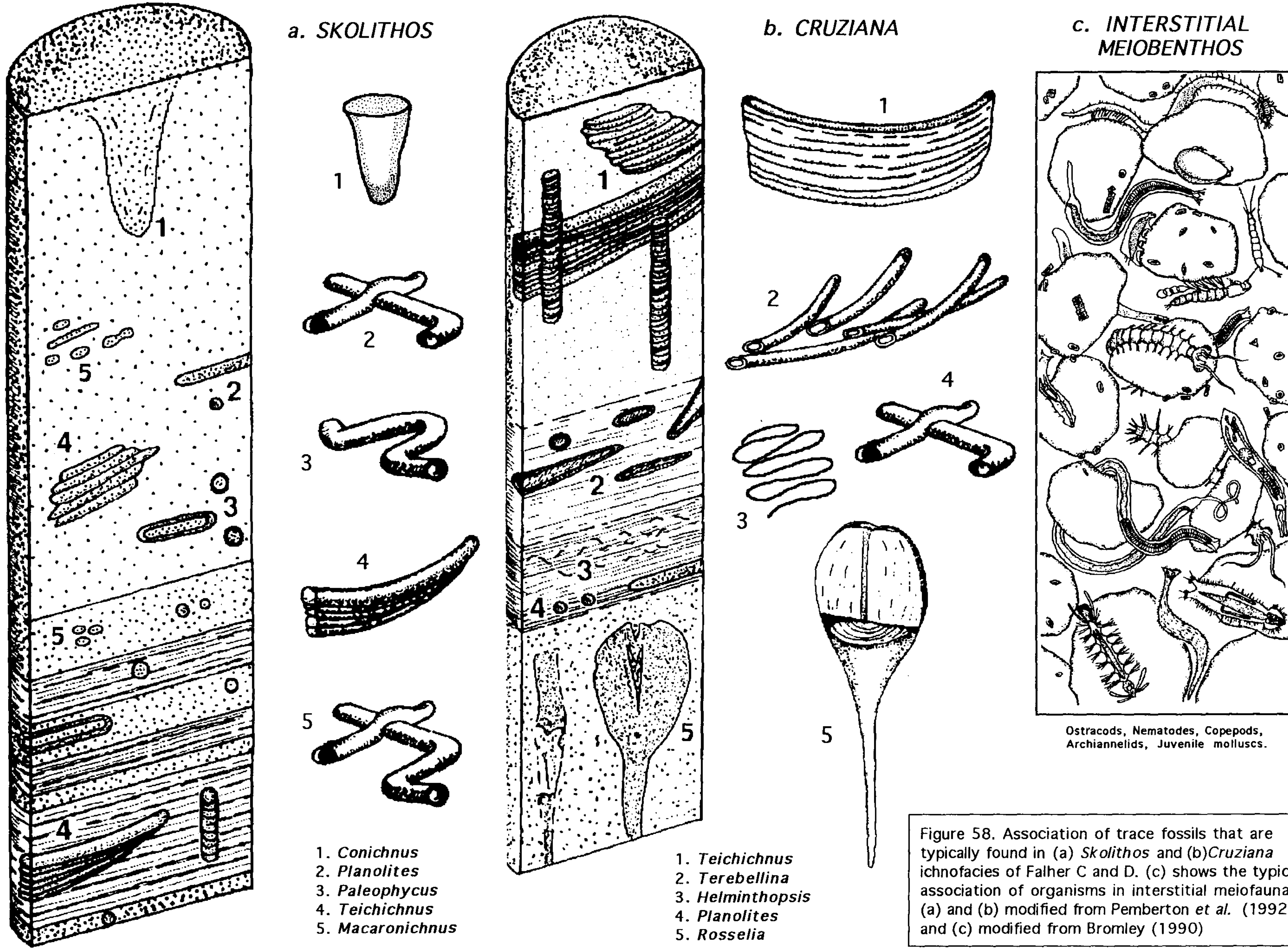

Figure 58. Association of trace fossils that are typically found in (a) *Skolithos* and (b)*Cruziana* ichnofacies of Falher C and D. (c) shows the typical association of organisms in interstitial meiofauna. (a) and (b) modified from Pemberton *et al.* (1992b) and (c) modified from Bromley (1990)

Curran, 1985; Moslow and Pemberton, 1988). The trace makers feed preferentially on micro-organisms colonizing the surfaces of sand grains. *Macaronichnus* appears to have a high preservation potential even under conditions of very active sedimentation (Clifton and Thompson, 1978).

7.1.2. UNIT D2

7.1.2.1 Transgression (Preservation of a Transgressive System Tract)

The progradation of D1 ended because a new RSL rise caused the shoreline to retreat southward to a position close to the maximum southward extent of D1 in T68 (Figure 48). The erosion surface overlying D1 could be interpreted as a seaward dipping ravinement surface indicating a phase of marine transgression.

During landward barrier migration and erosional shoreface retreat, some transgressive marine mudstones were preserved. Cores 9-16-68-10W6 (Appendix A56), 6-28-68-13W6 (Appendix B1, box 13) and 7-26-69-9W6 (Appendix A50) show a 10-20 cm bioturbated marine mudstone separating shoreface D1 from D2. In another example, core 6-20-68-9W6 (Appendix A31) shows an erosive contact and a transgressive deposit characterized by 20 cm of partially sideritized black mudstone, with chert pebbles up to 20 mm, representing a transgressive lag. In core 11-7-68-12W6, the transgressive succession is composed of black mudstones and siltstones interpreted as lagoonal deposits (Appendix B4, box 11).

7.1.2.2. Bounding discontinuities

7.1.2.2.1 Marine Flooding surface D2

From T73 to T68, the transgressive surface on top of unit D1 consists of a TSE (TSE D2). This surface is defined by shoreface sandstone deposits of D1 overlain by thin preserved marine transgressive mudstones (9-16-68-10W6, Appendix A56; 6-30-69-13W6, Appendix A36; 6-28-68-13W6, Appendix B1, and 7-26-69-9W6, Appendix A50) or a pebbly mudstone interpreted as a transgressive lag (6-20-68-9W6, Appendix A31). In core 10-31-68-10W6 (Appendix A13) the bounding discontinuity was interpreted to be at the base of a succession 30 cm thick, composed of very fine-grained sandstones completely bioturbated by *Teichichnus* , which overlie shoreface sandstones of D1.

7.1.2.2.2 Flooding surface D2

Flooding surface D2 is defined by a thin bioturbated lagoonal mudstone overlying coal deposits, and is correlative with marine flooding surface D2 north of T68. One example flooding surface D2 can be seen in core 11-7-68-12W6 (Appendix B4, box 11).

7.1.2.3. Regression (Preservation of a Highstand system tract)

After RSL stopped rising a high energy, wave-dominated shoreface succession rapidly prograded northwards (Figure 54B) to form an extensive shoreface strandplain (Dominguez and Wanless, 1991). The strandplain system of unit D2 extends a distance of approximately 60 km northwards and probably more beyond the study area. The strandplain consists of shoreface sandstones and conglomerates. The upper shoreface conglomerates are up to 5 km wide but probably represent, as in unit D1, a composite of more than one shoreface conglomerate. The shoreface deposits of D2 thicken in the central area (T69-70), and up to 18 m of continuous very fine-grained sandstones with SCS (Figure 59) is present in core 6-30-69-13W6 (Appendix A36). Northward, the unit D2 passes into interbedded successions of fine-grained sandstones with hummocky cross-stratification and marine mudstones, interpreted as lower shoreface to offshore deposits (e.g. 6-6-72-12W6, Appendix B3, and 10-23-72-11W6, Appendix A9)

Some probable channel fills were interpreted from well logs (e.g. 11-7-70-12W6, 11-9-70-11W6, Appendix C5), particularly in R11-12 (Figure 48). They trend north-south and probably fed the prograding strandplain. Other isolated channels were identified, one in core 6-17-72-9W6 (Appendix A29) where a 7 m thick channel incision is encased in D2 shoreface sandstone and overlain by D3 shoreface sandstones. The channel fill is characterized by medium-grained sandstones with angular ripped up mud clasts.

7.1.2.3.1. Bounding discontinuities

The shoreface succession is sharp-based and is normally represented by low angle and cross-stratified sandstones (T67-68) and by swaley cross-stratified sandstones (T69-70) which in places abruptly overlie thin offshore deposits preserved at the base of the shoreface succession. In other places, shoreface unit D2 directly overlies shoreface sandstones of unit D1 or equivalent deposits landward (e.g. 11-7-68-12W6, Appendix C5). In both cases during the progradation, wave scouring can create an erosive surface which is interpreted as an RSE, which in places would have modified the original TSE. Toward the central part of the study area (T69-71), D2 thickens and D1 thins but there is no evidence to suggest that the thickening of D2 is due to erosion of D1.

7.1.2.4. Ichnofacies

The shoreface sandstone bodies of unit D2 are characterized by a *Skolithos* ichnofacies assemblage (Figure 58) in T68-71, which changes northward to a *Skolithos-Cruziana* assemblage in T72-73.

Within the *Skolithos* ichnofacies, the association *Palaeophycus/Macaronichnus* is very common and is interpreted as an upper shoreface indicator. Many sandstones show very small traces that apparently destroyed all the sedimentary structures and give a structureless aspect to the sandstone. These small traces were made by an interstitial meiofauna

(Figure 13). Cullen (1973) reported a series of experiments with marine sediments where trace fossils made by macrobenthic organisms on both sand and mud had been obliterated after few days because of the biogenic activity of small organisms within the sediment. A examination showed a copious interstitial meiofauna composed of ostracods, nematodes, copepods and juvenile molluscs. The movement of sediment particles by interstitial ostracods and nematodes was particularly fast and velocities of 2-3 mm/s were estimated for the movement of the organisms. Such activity, continued over a prolonged period of time by a dense population, obliterated biogenic structures and disrupted the sediment fabric (Cullen, 1973).

In T72-73 unit D2 is characterized by very fine-grained sandstones with hummocky cross-stratification interbedded with mudstones and interpreted as lower shoreface to offshore deposits. In these successions, a characteristic *Cruziana* assemblage (Figure 58) is composed of *Rosselia, Helminthopsis and Planolites. Helminthopsis* is the grazing trail of a vermiform organism characterized by simple meandering smooth trails. It is expressed in these cores as a series of black dots. It is commonly found in deeper marine settings (Vossler and Pemberton, 1988). *Rosselia*, the burrow of a deposit-feeding organism (Vossler and Pemberton, 1988), is characterized in cores by a conical to irregularly bulbous shape structure (Figure 20). Less commonly identified were burrows of *Palaeophycus, Teichichnus*, and meiofaunal traces.

7.1.3 UNIT D3

7.1.3.1 Transgression (Preservation of a Transgressive System Tract)

As in D1, the deposition of D2 ended because of an RSL rise. This moved the new shoreline to the northern part of T70 (Figure 48). An erosion surface overlies D2 and is interpreted as a seaward-dipping ravinement surface produced by the transgressive event (Figure 55D).

Transgressive sediments were deposited during the erosional shoreface retreat. Cores 6-8-72-9W6 (Appendix B2, box 11), 6-27-71-9W6 (Appendix A34) and 10-1-73-13W6 (Appendix A4) show a transgressive succession composed of bioturbated mudstones with some silty layers overlying the shoreface sandstones of D2. Core 11-6-71-13W6 (Appendix A19) shows a 12 cm bed of black mudstone with pebbles up to 10 mm (Figure 60) overlying the shoreface sandstones of D2. This thin pebbly mudstone is interpreted as a transgressive lag. Landward of inferred barrier 3, core 7-26-69-9W6 (Appendix A50) shows a 2.8 m thick succession composed of black mudstones mostly bioturbated by very small *Planolites*, *Teichichnus* and *Arenicolites*. This is interpreted as a transgressive lagoonal succession.

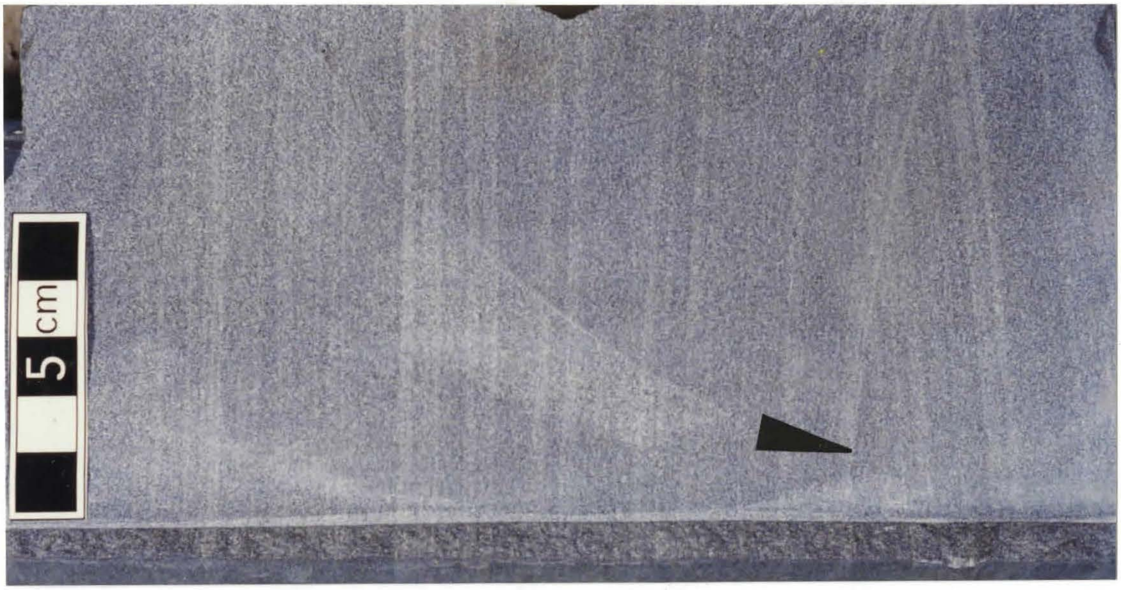

Figure 59. Very fine-grained sandstone with swaley cross-stratification. Note the convex intersection (arrow) of stratification (Well 6-30-69-13W6 depth 2382.5 m).

Figure 60. TSE D3 (arrow) is defined by medium-grained sandstones of unit D2 (below) abruptly overlain by a dark pebbly mudstone, interpreted as a transgressive lag (Well 11-6-71-13W6 depth 2215.4 m).

7.1.3.2. Bounding discontinuities

7.1.3.2.1 Marine Flooding surface D3

From the northern part of T70 to the northern limit of the study area, the basal bounding discontinuity of D3 consists of a TSE (TSE D3). This surface is defined by shoreface sandstone deposits overlain by marine transgressive mudstones or a pebbly mudstone interpreted as a transgressive lag (e.g. 11-6-71-13W6, Figure 61).

7.1.3.2.2 Flooding surface D3

Only one core (7-26-69-9W6, Appendix A50) exists landward of the inferred barrier 3. This core shows a lagoonal succession (2.8 m thick) bioturbated by *Planolites*, *Arenicolites* and *Teichichnus*, overlaying shoreface sandstones of D2 and overlain in turn by coastal plain deposits. The lagoonal succession probably represents the deposits preserved after the initial flooding surface and the coastal plain succession probably represents the deposits associated with the regressive phase.

7.1.3.3. Regression (Preservation of a Highstand system tract)

After RSL stopped rising, a wave-dominated shoreface succession prograded northwards (Figure 55E) to form an extensive strandplain system

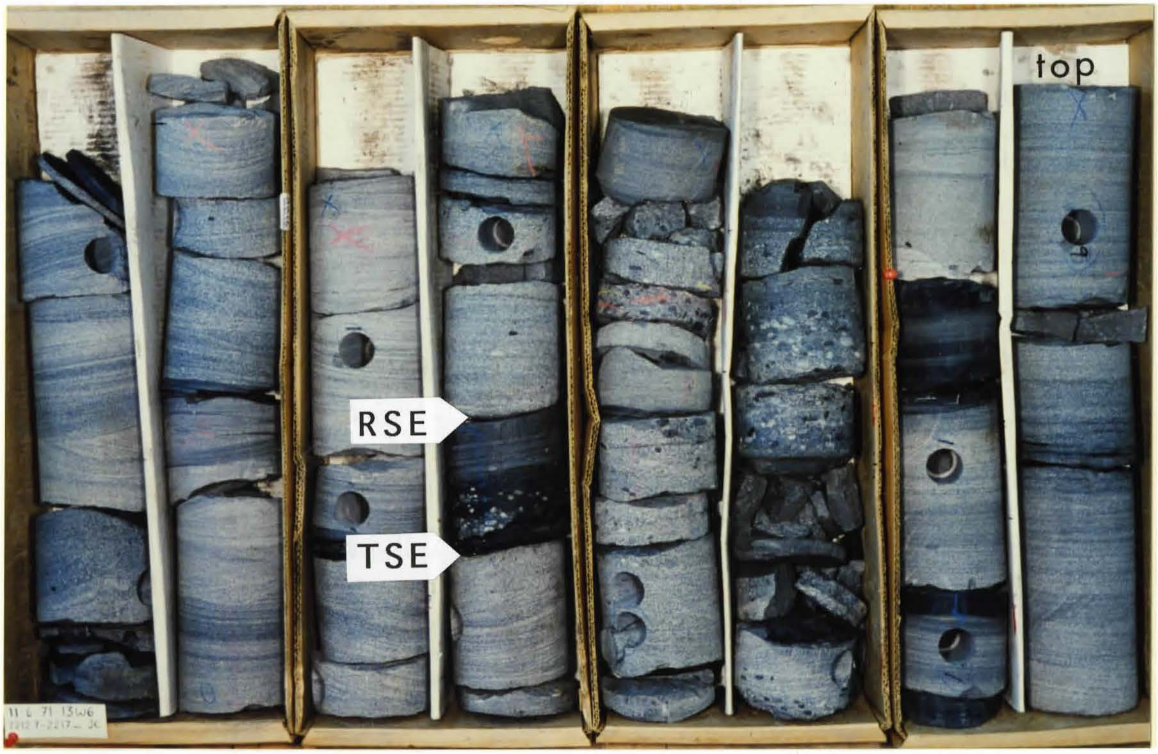

Figure 61. TSE D3 is defined by shoreface sandstone deposits (below the TSE arrow) overlain by a marine transgressive pebbly mudstone (between the TSE and RSE arrows). Well 11-6-71-13W6 depth 2212.7-2217 m.

that extends from the northern part of T70 (Figure 48) to T73, at least 30 km, and probably farther.

The strandplain consists of shoreface sandstones with swaley cross-stratification and conglomeratic deposits exhibiting cross-stratification. The upper shoreface conglomerates are up to 4 km wide, probably composed of more than one body and are localized mainly in the western part of the study area (Figure 48).

7.1.3.3.1. Bounding discontinuities.

Seaward of barrier 3, the shoreface succession is sharp-based and is commonly represented by fine-grained sandstones with swaley cross-stratification that overlie a transgressive succession of marine mudstones.

In places the shoreface sandstones of D3 directly overlie shoreface sandstones of D2. In this case a sharp contact with a change in grain size can be seen (Core 7-25-71-13, Figure 62) or a sharp contact marked by an erosive surface with ripped-up mud clasts (Core 7-8-72-13, Figure 63). In these cases the progradation and wave scouring created an erosive surface interpreted as an RSE that in places modified the original TSE.

7.1.3.4. Ichnofacies

The shoreface deposits of unit D3 are characterized by a *Skolithos* ichnofacies assemblage (Figure 58). This ichnofacies is dominated by the

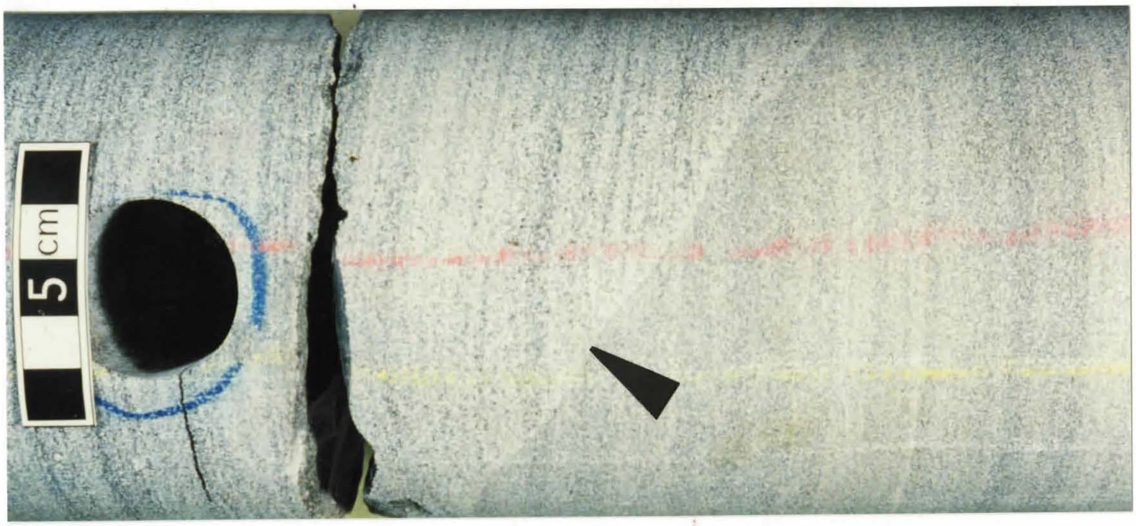

Figure 62. TSE D3 (arrow) is defined by very fine-grained sandstones of unit D2 (below) abruptly overlain (probably with a scoured contact) by fine- to medium-grained sandstones of unit D3 (Well 7-25-71-13W6 depth 2004 m).

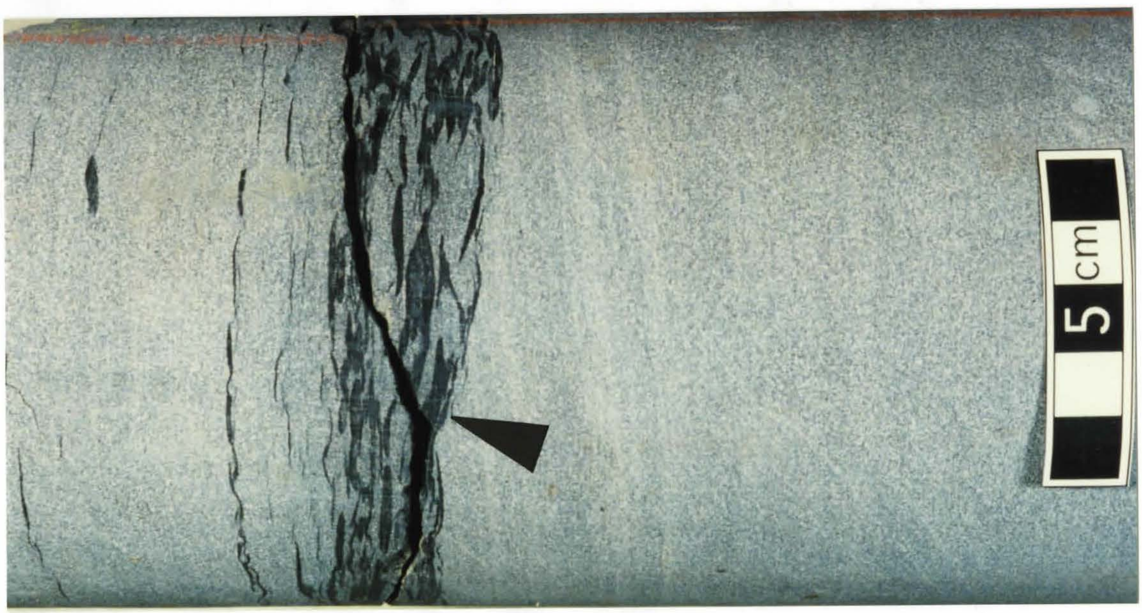

Figure 63. TSE D3 (arrow) is defined by very fine-grained sandstones of unit D2 (below) abruptly overlain by fine-grained sandstones containing ripped-up mud clasts (Well 7-8-72-13W6 depth 2030.6 m).

presence of *Palaeophycus*, *Macaronichnus* and meiofaunal traces (Figure 13), interpreted as an association typical of an upper shoreface environment. The meiofaunal activity is very intense and in cores like 10-1-73-13W6 and 7-8-72-13W6, almost all the sedimentary structures have been destroyed. Other trace fossils present in this assemblage are *Conichnus* and *Planolites*.

7.1.4 UNIT D4

7.1.4.1 Transgression (Preservation of a Transgressive System Tract)

After a rise of RSL, a new shoreline moved to the southern part of T72 (Figure 48). An erosion surface overlies D3, interpreted as a seaward-dipping ravinement surface produced by the last transgressive event (Figure 56G).

During the erosive shoreface retreat, some transgressive sediments were deposited. Cores 10-1-73-13W6 (Figure 64) and 6-13-72-13W6 (Appendix A27) show a 10-20 cm bioturbated mudstone overlying swaley cross-stratified sandstones of D3. Core 6-27-71-9W6 (Figure 65) shows a 4 m thick succession of black bioturbated mudstones interbedded with siltstones, representing the preserved transgressive succession. In contrast cores 6-30-72-12W6 (Appendix A38) and 6-30-72-11W6 (Appendix A37) show a thin layer of sandstone completely bioturbated by *Palaeophycus* and interpreted a transgressive deposit.

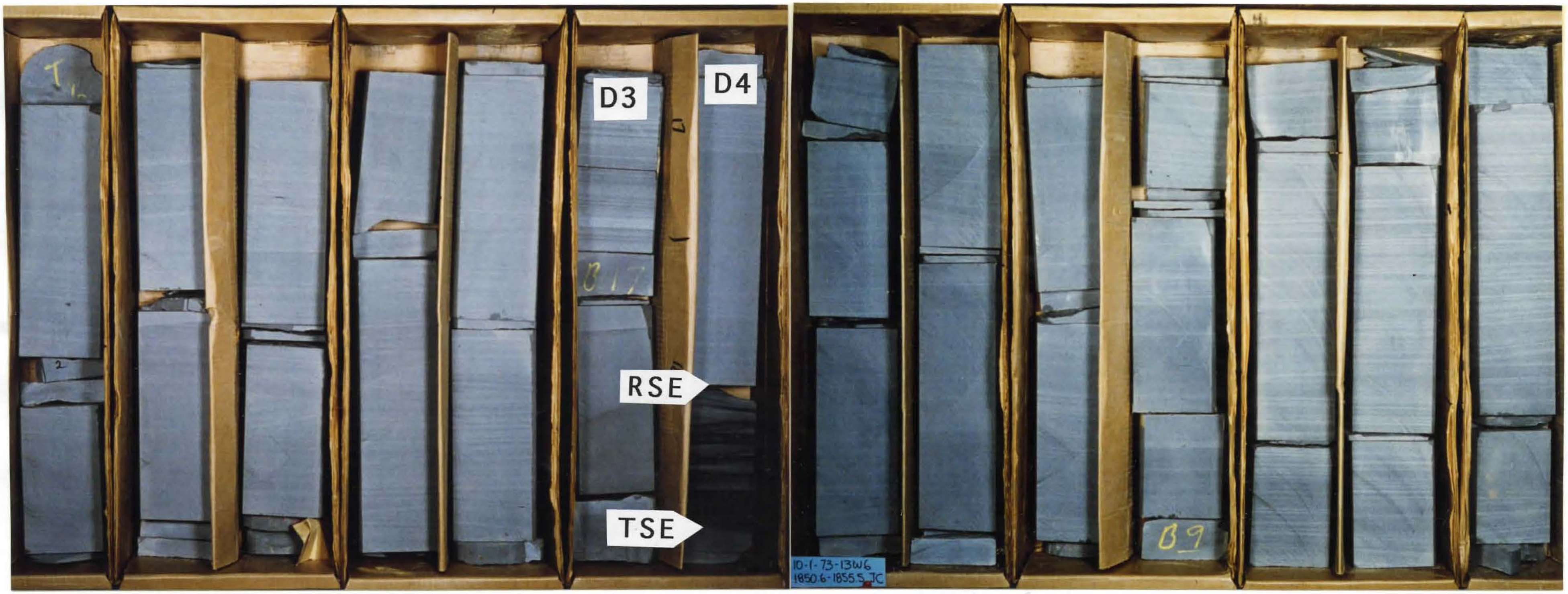

Figure 64. Shoreface sandstones of units D3 and D4 separated by a 20 cm thick succession of bioturbated mudstones and siltstones interpreted as a transgressive marine succession (between the TSE and RSE arrows). Well 10-1-73-13W6 depth 1851.2-1859.6 m.

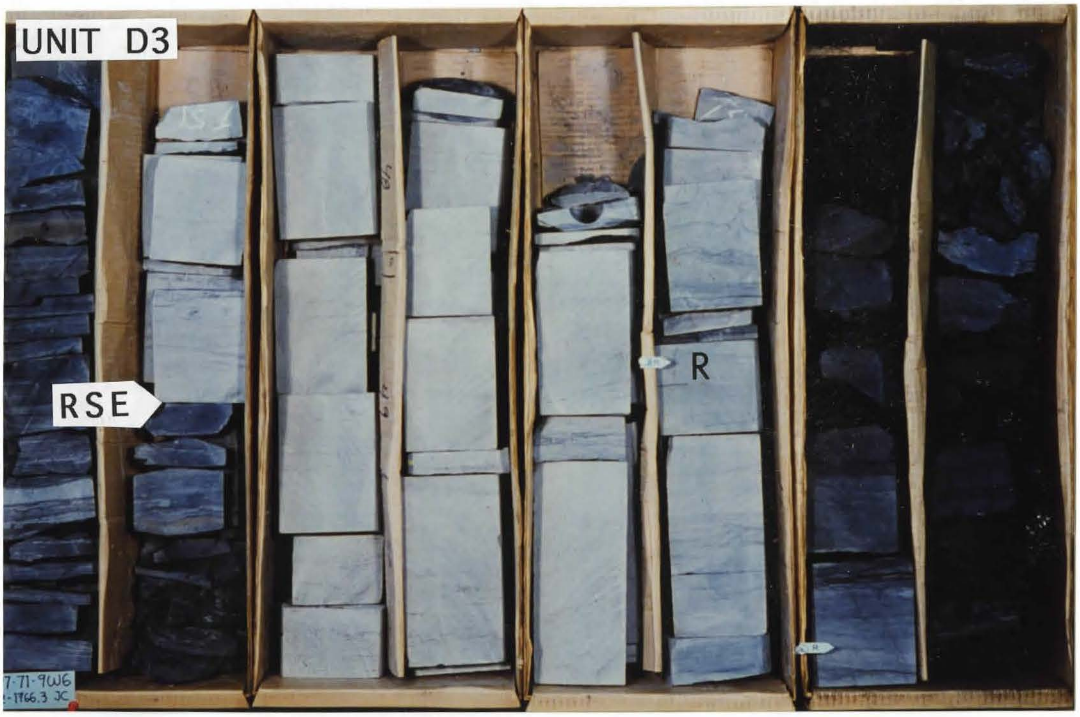

Figure 65. Core 6-27-71-9W6 shows a basal transgressive muddy succession composed of interbedded bioturbated black mudstones and siltstones overlain by a sharp-base shoreface sandstone with roots (R) at the top. The sharp-base is interpreted as an RSE. A coaly succession overlies the rooted sandstones

7.1.4.2. Bounding discontinuities

7.1.4.2.1 Marine Flooding surface D4

From the southern part of T72 to beyond the study area, the marine flooding surface on top of unit D3 consists of a TSE (TSE D4). This surface is defined by shoreface sandstones of D3 overlain by transgressive mudstones (e.g. 10-1-73-13W6, Appendix A4 and 6-13-72-13W6, Appendix A27).

7.1.4.2.2 Flooding surface D4

No core control is available to define the exact nature of flooding surface D4.

7.1.4.3. Regression (Preservation of a Highstand system tract)

After RSL stopped rising, a high-energy wave-dominated shoreface succession prograded northwards to form a strandplain system across T72 and T73 (about 20 km) and probably farther northwards beyond the study area (Figure 56H).

The strandplain consists of very fine- to fine-grained shoreface sandstones with swaley cross-stratification and conglomeratic deposits with cross-stratification. These upper shoreface conglomerates are up to 6 km wide, probably representing a composite of more than one shoreface conglomerate. They are concentrated in the western part of the study area (Figure 48).

At the top of unit D4, the sandstones show roots *in situ* (e.g. 6-8-72-9W6, Appendix B2, box 21).

7.1.4.3.1. Bounding discontinuities

Seaward of barrier 4, the shoreface sandstone deposits are sharp-based and commonly composed of sandstones with swaley cross-stratification overlying a thin transgressive marine succession (e.g. 10-1-73-13W6, Figure 64; 6-27-71-9W6, Figure 65 and 6-13-72-13W6, Appendix A27). In both cases the sharp base is interpreted as an RSE created by wave scouring during progradation.

7.1.4.4. Ichnofacies

The shoreface deposits of unit D4 are characterized by a *Skolithos* ichnofacies assemblage (Figure 58) dominated by the association *Palaeophycus/Macaronichnus* (Figure 11), interpreted as an upper shoreface indicator. Meiofaunal traces were identified in core 10-1-73-13W6 and some *fugichnia* (escape structures) were observed in core 6-30-72-12W6.

7.1.5 UNIT D5

7.1.5.1. Regression (Preservation of a Highstand system tract)

Within units D1 and D2, a series of muddier-upward log responses are oriented in a north-south trend (Figure 48). These responses are interpreted as channel fills that probably fed these prograding shoreface units.

7.1.6 UNIT D6

7.1.6.1. Coastal Plain aggradation

A coastal plain succession (D6) caps shoreface units D1-D4 across the study area (Figure 56I). It is composed mainly of muddy successions interbedded with some very fine-grained sandstones, coals and siltstones (e.g. 7-14-68-13W6, Appendix A45; 15-16-68-13W6, Appendix A22; 6-16-68-11W6, Appendix A28; 11-7-68-12W6, Appendix A20, and 10-16-67-8W6, Appendix A6). The mudstones are black with some graded layers of siltstone and interbedded coal, commonly without bioturbation. Roots and plant fragments are abundant in these successions. When the succession becomes sandier, ripple cross-lamination, some soft sediment deformation, and roots are present. Some fine- to medium-grained sandstones with cross-stratification are interpreted as channel fills in these successions (e.g. 6-7-67-8W6, Appendix A41). Northwards, unit D6 thins due to erosion by TSE C1 and is composed mainly of coal and mudstones (e.g. 6-27-71-9W6, Appendix A34; 6-25-71-

10W6, Appendix A33, and 6-8-72-9W6, Appendix A43, Appendix B2, box 22). Unit D6 is interpreted as coastal plain deposits that aggraded during the regressive event that characterized the upper part of Falher D.

7.2. FALHER C

7.2.1. UNIT C1

7.2.1.1. Transgression (Preservation of a Transgressive System Tract)

The deposition of Falher D ended when RSL began to rise, flooding the coastal plain deposits of the upper part of Falher D. The shoreline moved to the south and wave winnowing formed a beach/beach-ridge system attached to the coastal plain. Rapid subsidence subsequently resulted in detachment of the beach/beach-ridge system and formation of a lagoon (Rampino and Sanders, 1980). Eventually the rate of RSL rise slowed and the fluvial input become greater than the rate of shoreface erosion, stopping the migration of the barrier-lagoon system at T69 (Figure 57A).

The thinness and the patchy distribution of unit C1 is due to partial erosion by subsequent transgressive surfaces. Cores 7-20-69-10W6 (Figure 59 and Appendix B5, box 1), 10-19-69-9W6 (Appendix A8) and 6-25-71-10W6 (Appendix A33) show a 5-8 cm layer of poorly sorted conglomerate that probably represents a transgressive conglomeratic lag. In core 6-25-71-10W6

(Appendix A33 and B6) a 13 cm bed of black mudstone overlies the conglomerate and probably represents transgressive marine mudstones.

7.2.1.2. Bounding discontinuities

7.2.1.2.1. Marine Flooding Surface

From T73 to T69 the surface on top of Falher D consists of a TSE (TSE C1), which in places is defined by a thin transgressive conglomeratic deposit overlying coastal plain deposits (e.g. 7-20-69-9W6, Figure 66, Appendix A47)

7.2.1.3. Regression (Preservation of a Highstand System Tract)

During the HST, a wave-dominated shoreface succession prograded northwards to form an extensive shoreface and strandplain system. The preserved section normally shows a 2-4 m thick fine-grained sandstone, bioturbated in places. In contrast, core 7-26-69-9W6 (Appendix A50) shows a preserved section 7 m thick with the same shoreface sandstone, completely bioturbated with meiofaunal traces. In places the regressive succession contains conglomeratic beds interbedded with the sandstones (e.g. 7-20-69-9W6, Figure 67 and Appendix B5, boxes 7-9).

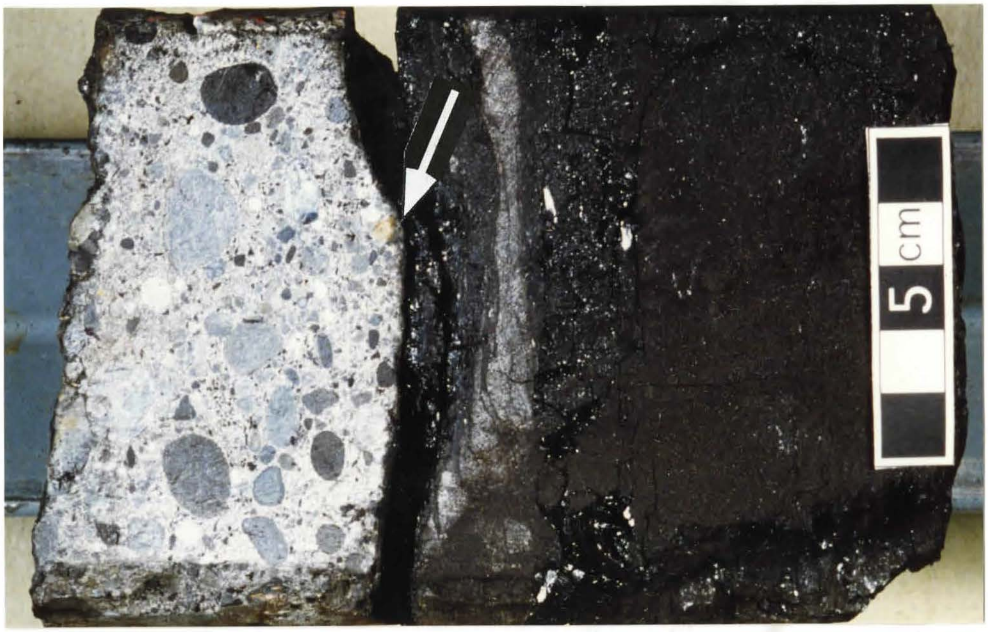

Figure 66. The TSE C1 (arrow) is defined in this case by coals of Falher D (below) abruptly overlain by a conglomerate representing the transgressive lag (Well 7-20-69-10W6 depth 2046.4 m).

Figure 67. Medium-grained sandstone with low angle lamination (below) overlain by a poorly sorted conglomerate (Well 7-20-69-10W6 depth 2045.9 m).

7.2.1.4. Bounding discontinuity

The shoreface succession of unit C1 is sharp-based and is usually represented by fine-grained sandstones with swaley cross-stratification and cross-bedding overlying a thin succession of transgressive conglomerates (e.g. 10-19-69-9W6, Appendix A8 and 7-20-69-10W6, Appendix B5, box 2) or transgressive mudstones (e.g. 6-25-71-10W6, Appendix B6, box 4). In places the transgressive succession apparently was removed by scouring during progradation (e.g. 6-27-71-9W6, Appendix A34) creating an RSE that could modified the original TSE.

7.2.1.5. Ichnofacies

The shoreface sandstones of C1 are characterized by a *Skolithos* ichnofacies assemblage (Figure 58) where examples of *Teichichnus*, *Palaeophycus*, *Macaronichnus* and meiofaunal traces can be identified. The association suggests an upper shoreface setting.

7.2.2. UNIT C2

7.2.2.1. Transgression (Preservation of a Transgressive System Tract)

The deposition of C1 ended when an RSL rise took place in the area and the new transgressive event moved the shoreline southwards to T68. In most aspects unit C2 is similar to unit C1 : the small thickness due to erosion, the patchy distribution and the preservation of a similar transgressive-regressive succession (Figure 57A). Cores 6-27-71-9W6 (Appendix A34), 6-25-71-10W6 (Appendix B6, box 7), 7-26-69-9W6 (Appendix A50), 10-19-69-9W6 (Appendix A8) and 6-30-72-12W6 (Appendix A38) show a conglomeratic layer 3-20 cm thick representing a transgressive lag. The first three cores also show a thin section of transgressive bioturbated mudstones overlying the transgressive conglomeratic lag. In core 7-20-69-10W6 the transgressive succession is represented by marine mudstones and siltstones interbedded (Appendix B5, box 10).

7.2.2.2. Bounding discontinuities

7.2.2.2.1. Marine flooding surface

From T73 to T68 the transgressive surface on top of unit C1 consists of TSE C2 which commonly is defined by a thin transgressive conglomeratic deposit (transgressive lag) overlying shoreface deposits of C1. In core 6-30-72-12W6 (Appendix A38) the TSE is defined by a pebbly mudstone overlying upper shoreface conglomerates of Falher D.

7.2.2.3. Regression (Preservation of a Highstand System Tract)

After RSL stopped rising, a high energy wave-dominated shoreface succession prograded northwards. The preserved section shows 2-3 m thick deposits of fine-grained sandstones mainly with swaley cross-stratification and some bioturbation. Cores 6-25-71-10W6 (Figure 68, Appendix A33, Appendix B6) and 6-27-71-9W6 (Figure 69, Appendix A34) show a very well sorted 1.5-3 m thick granule-conglomerate bed at the top of this succession; it probably represents a regressive beach deposit.

7.2.2.4. Bounding discontinuities

The shoreface succession of unit C2 is sharp-based and is normally represented by fine-grained sandstones overlying a thin transgressive conglomeratic lag or transgressive mudstones. The sharp-base of the sandstone deposits is interpreted as the RSE formed by wave scouring during progradation when RSL fell (forced regression).

7.2.2.5. Ichnofacies

The little core control and thinness of the preserved C2 unit only permitted the identification of few traces; *Teichichnus* (10-19-69-9W6), *Planolites* (7-20-69-10W6), *Palaeophycus* (6-27-71-9W6), *Macaronichnus* (6-8-

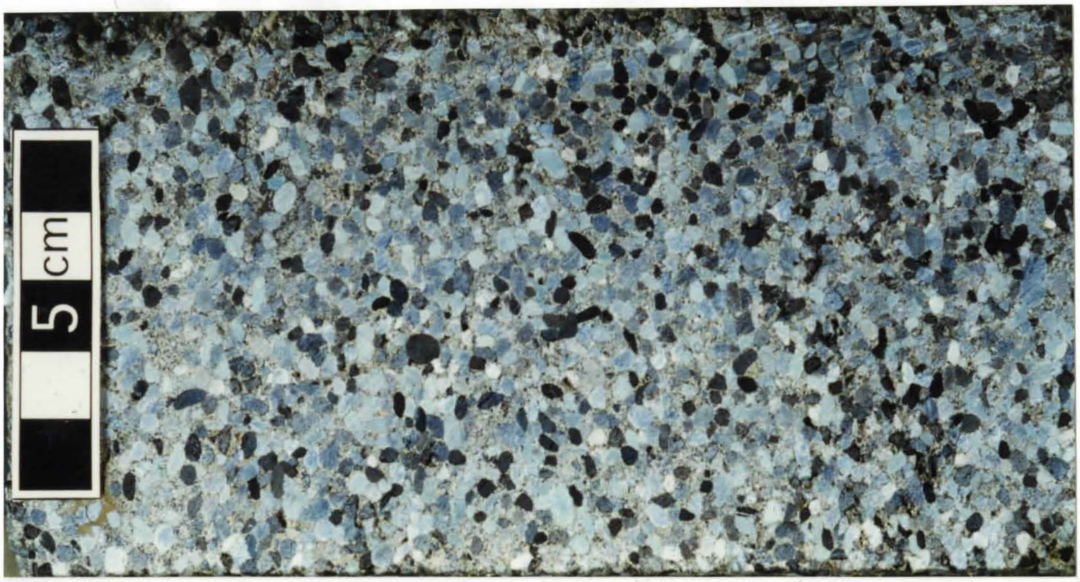

Figure 68. A clast-supported granule conglomerate in unit C2 interpreted as a beach succession (Well 6-25-71-10W6 depth 1727.7 m)

Figure 69. Well sorted, matrix-supported conglomerate in unit C2 (Well 6-27-71-9W6 depth 1756.3 m)

72-9W6) and *Asterosoma* (6-27-71-9W6) were identified. The association of all these traces from different cores suggests a *Skolithos* ichnofacies assemblage (Figure 58) for the unit.

7.2.3. UNIT C3

7.2.3.1. Transgression (Preservation of a Transgressive System Tract)

The deposition of unit C2 ended when RSL began to rise. The shoreline moved southwards by erosional shoreface retreat forming a TSE (TSE C3). Eventually the rate of RSL slowed and the migration of the barrier of unit C3 stopped in the northern part of T66 (Figure 57A). Core 6-8-67-9W6 (Figure 70) shows a 2 cm thick layer of conglomeratic sandstone that can be interpreted as a transgressive lag. In the rest of the area, no preserved transgressive deposits were identified in cores and the lack of core in T66 makes it impossible to describe the nature of the transgressive deposits landward of the barrier.

7.2.3.2. Regression (Preservation of a Highstand System Tract)

With renewed sediment supply to the barrier shoreline after RSL stopped rising, a wave-dominated shoreface succession prograded northwards to form an extensive strandplain system that extends from T67 to at least T69 (about 26 km). The strandplain system consists of sand and gravel shoreface

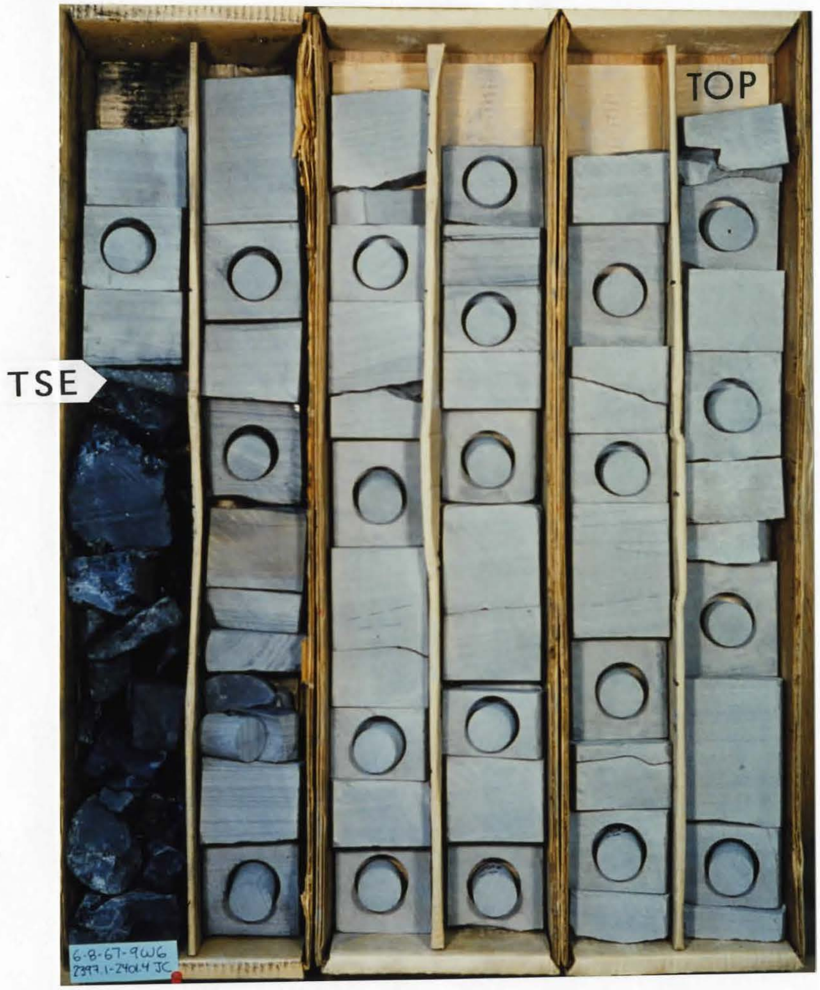

Figure 70. TSE C3 is defined by a succession of coal and coaly mudstones abruptly overlain by a 2 cm thick conglomeratic layer interpreted as a transgressive lag. Overlying the transgressive lag, the shoreface sandbody of C3 is composed of fine-grained sandstones with SCS (Well 6-8-67-9W6 depth 2397.1-2401.4 m).

deposits. The sandstones bodies are up to 17 m thick with roots traces at the top. Upper shoreface conglomerates (Figure 71) are concentrated in T67 R8-10 (Figure 53) and probably represent a composite of more than one shoreface conglomeratic body

7.2.3.3. Bounding discontinuities

The shoreface succession is sharp-based and is normally represented by swaley cross-stratified sandstones which abruptly overlie coastal plain deposits of Falher D. There are no transitional deposits (transgressive mudstones) at the base of the shoreface succession (e.g. 10-4-67-10W6, 7-24-67-10W6, Appendix A48; 7-15-67-10W6, Appendix A46, and 10-12-67-10W6).

Plint (1991) suggested that during a forced regression an erosive surface interpreted as an RSE could modify the original TSE, removing the offshore transitional sediments. Another explanation (section 7.1.1.2.1.) is the fact that if the depth were never greater than fairweather wave base during the transgression, transgressive mudstones would never have been deposited. There is no evidence to suggest which explanation is the more likely.

7.2.3.4. Ichnofacies

The shoreface succession of C3 is characterized by a *Skolithos* ichnofacies assemblage (Figure 58). This assemblage is dominated in C3 by *Macaronichnus tubularis* (Figure 25) which is recognized as an infaunal burrow in a relative high energy foreshore to upper shoreface setting (Moslow and Pemberton, 1988). Other trace fossils commonly present are *Palaeophycus*, *Teichichnus* and meiofaunal traces.

7.2.4. UNIT C4

Seaward of shoreface unit C3 in T68 R7-9 and T69 R13 a lagoonal succession is present that is stratigraphically equivalent to unit C3. This relationship creates a problem because the thick lagoonal succession is oriented east-west and separates shoreface unit C3 (in the south) from shoreface unit C4 (in the north).

One explanation for these relationships is to assume that a major RSL drop occurred and ended the progradation of C3. This sea level fall would have moved the shoreline to a location north of T73 and would have formed an RSE within the study area. This RSE would have partly truncated units C1, C2 and C3 (Figure 57B).

7.2.4.1. Transgression (Preservation of a Transgressive System Tract)

With a new RSL rise, the shoreline returned to the area of T68-69, with erosional shoreface retreat. Initially, a beach/beach ridge system attached to the coastal plain was formed and rapid subsidence resulted in detachment of the beach/beach ridge system to form a lagoon (Rampino and Sanders, 1980) along the inner part of the shoreline coast, as suggested for other units.

The lagoonal to brackish deposits preserved in this area are represented by a thick succession composed of dark mudstones interbedded with some sandstones with parallel stratification and ripple cross-lamination. The succession shows a low diversity and monotypic ichnofossil assemblage, reflecting extremely stressful environmental conditions. Seaward, a thick succession (4-7 m) of transgressive deposits was preserved (e.g. 10-19-69-9W6, (Appendix A8; 6-25-71-10W6, Appendix B6, box 13; 7-8-69-9W6, Appendix A53, and 7-26-69-9W6, Appendix A50) composed mainly by mudstones interbedded with siltstones and few sandstones, representing offshore deposits. Within this succession, a maximum flooding surface separates the TST from the HST, but the exact position of the surface could not be identified.

7.2.4.2. Bounding discontinuities

Within the study area from T73 to the north part of T69, the transgressive offshore succession is bounded by a TSE (TSE C4) which overlies shoreface sandstones of unit C2 or C1 (e.g. 6-25-71-10, Appendix B6 and 6-27-71-9W6, Appendix A34)

7.2.4.3. Regression (Preservation of a Highstand System Tract)

After RSL stopped rising, a regressive barrier built seaward and the associated lagoon filled in (Figure 57C). The barrier developed into a strandplain and a wave-dominated shoreface succession prograded northwards to form an extensive shoreface and strandplain system (Figure 57C) that extends northwards for more than 50 km. The shoreface consists of fine-grained sandstones with low angle and parallel stratification. Upper shoreface conglomeratic bodies are present (Figure 53).

7.2.4.4. Bounding discontinuities

Seaward of the barrier of unit C4, the prograding shoreface succession is sharp-based and is represented by low angle and parallel stratified sandstones which overlie transgressive offshore deposits. The sharp base is interpreted as an RSE created by wave scouring during progradation. Examples of this erosive surface can be seen in cores 7-8-69-9W6 (Appendix A53) and 10-19-69-9W6 (Appendix A8). It is possible that basinward, a preserved maximum flooding surface can be identified within the offshore deposits. This MxFS is the bounding discontinuity that separates the TST from the HST.

7.2.4.5. Ichnofacies

The lagoonal succession behind barrier 4 is characterized by a *Teichichnus/Planolites* association. The overall reduction in size of the traces and the reduction in ichnotaxonomic diversity suggests a somewhat stressful environment such as brackish water conditions (Pemberton and Wightman, 1992).

The transgressive shoreface succession of C4 is characterized by a *Skolithos-Cruziana* ichnofacies assemblage dominated by *Helminthopsis* (Figure 31), *Teichichnus*, *Planolites* and rare *Macanopsis* and *Bergaueria*.

The regressive shoreface succession of C4 is characterized by a *Skolithos* ichnofacies assemblage, with examples of *Teichichnus*, *Ophiomorpha*, *Macaronichnus*, *Conichnus* and interstitial meiofaunal traces. In core 6-32-73-13W6 (Appendix B7, boxes 1-5) the bioturbation by interstitial meiofauna was so intense that the sandstones are completely structureless (Figure 72).

7.2.5. UNIT C5

7.2.5.1. Regression (Preservation of a Highstand System Tract)

During the progradation of the C4 unit a channel systems (C5 unit) were developed with a north-south trend in R10-11 and in R8-9 (Figures 52 and 53). These channel systems are denominated here C5 unit. The channel system in R10-11 is relatively straight (Figure 53), at least 60 km long, up to 9 km wide

Figure 71. Poorly-sorted matrix-supported conglomerate. The matrix is composed of fine-grained sand (Well 6-7-67-8W6 depth 2336.4 m).

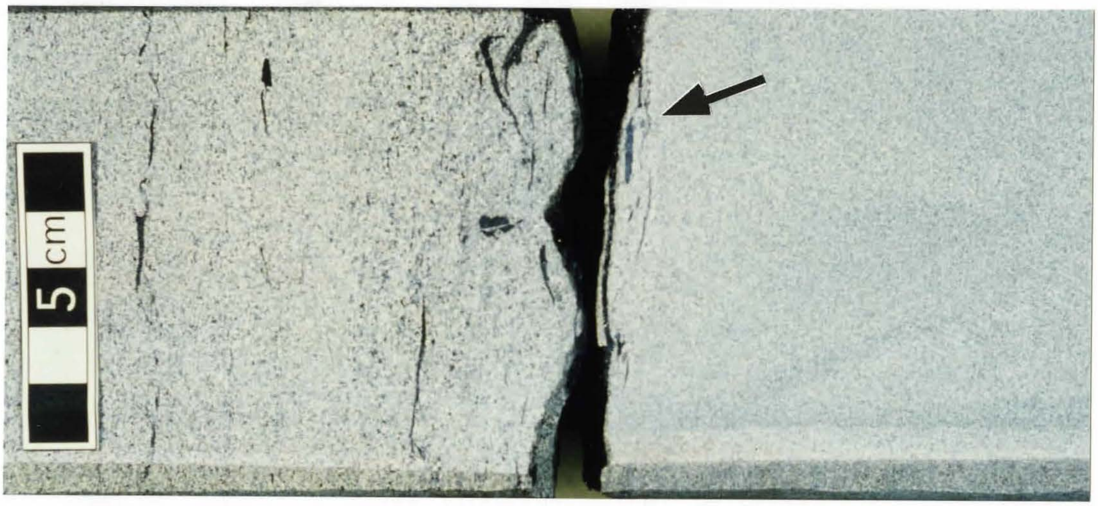

Figure 72. Erosive contact (arrow) between medium-grained sandstones (above) interpreted as a fluvial channel and very fine-grained sandstones (below) interpreted as shoreface sandstones of unit C4. The shoreface sandstone appears structureless and is interpreted to be the result of meiofaunal bioturbation.

and about 16-18 m deep. The RSE at the base of the channel cuts into the prograding storm-dominated shoreface units of C4 (Figure 57D), and in places cuts older deposits like C1, C2 and the top of Falher D (Figure 47). The channel system is characterized by fluvial deposits preserved in the southern part, defined by fining-upward successions ranging from conglomerates to fine-grained sandstones with cross-stratification, sideritized clasts and in places discontinuous layers of coal, and slumps (e.g. 11-4-69-10W6, Appendix A18 and 10-1-68-9W6, Appendix A3).

The central part of the channel system (T69-71, R10-11) is characterized mainly by muddy or silty successions (Figure 73), bioturbated and interbedded with some very fine-grained sandstones with ripple cross-lamination (e.g. 7-20-69-10W6, Appendix B5, and 7-9-70-10W6, Appendix A55). The northern part of the channel system is sandier and is characterized very fine-grained sandstones with slumps, interbedded with mudstones and siltstones. A more marine influence is reflected in the bioturbation.

Both channel systems in unit C5 (Figure 53) end abruptly, and appear to be cut off by shoreface unit C4. Feeder channel systems supplying sediment to the strandplain commonly switch by channel avulsion and once the channel is abandoned and loses its ability to transport sediments, the channel mouth would be reworked by the action of waves and longshore drift (Dominguez, *et al.*, 1987). This may explain why the channel system appears to end abruptly and be truncated by the C4 shoreface.

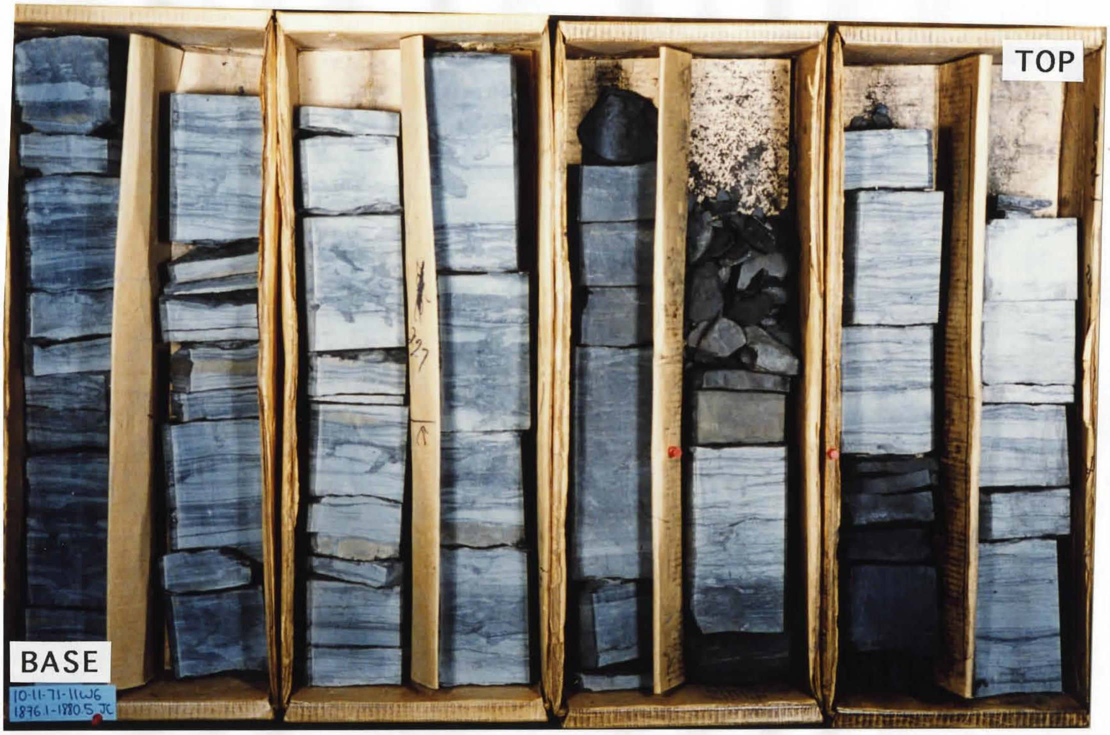

Figure 73. Heterolithic succession of unit C5, characterized by dark mudstones interbedded with siltstones and very fine-grained sandstones. Some sideritized levels and bioturbation are present (Well 10-11-71-11W6 depth 1876.1-1880.5 m).

7.2.5.2. Ichnofacies

The northern and central part of the main channel system is characterized by the presence of the *Teichichnus/Planolites* association. The low diversity and monotypic nature of the ichnofossil assemblage of this association reflect the stressed conditions that typify brackish water environments (Vossler and Pemberton, 1988). Distinctly absent from this association are fully marine ichnofossils, with the exception of some *Helminthopsis* at the northern end of the channel system. Although the presence or absence of these forms is not conclusive evidence for a brackish water interpretation, it is not in conflict with a brackish environment. Beynon *et al.*, (1988) suggest that a brackish water faunal assemblage is more appropriately represented by an impoverished marine assemblage rather than a true mixture of freshwater and marine elements.

In the southern part of the main channel system, very rare and unidentified trace fossils are present.

7.2.6. UNIT C6

7.2.6.1. Regression (Preservation of a Highstand System Tract)

A coastal plain succession (C6) caps shoreface units C3 and C4 across the study area (Figure 57D). It is composed mainly of black mudstones with interbedded silty layers. Coal beds are also present in abundance (e.g. 10-30-

70-11W6, Appendix A12; 10-1-68-9W6, Appendix A3, and 10-11-71-11W6, Appendix A5). The top of this unit is commonly defined by laterally extensive coal or coaly deposits which are overlain by the first TSE of Falher B. Some sandstones are present in the unit, exhibiting fining-upward trends, ripple cross-lamination, ripped up clasts (e.g. 6-32-73-13W6, Appendix B7, box 13) and *in situ* roots (Figure 33). They are interpreted as small channel fills and crevasse splays.

This unit is interpreted as coastal plain deposits that aggraded during the regressive event that characterizes the upper part of Falher C. Some brackish conditions during deposition of this units are suggested by the trace fossil association present.

7.2.6.2. Ichnofacies

The succession of unit C6 is characterized by a *Chondrites/Planolites* association. In cores *Chondrites* is represented by a clustering of small, sharp walled, circular to elliptical burrows arranged in a ramified network. Vossler and Pemberton (1988) suggest that the presence of abundant *Chondrites* may be the response to local anoxic conditions. The low diversity that characterizes this unit may be interpreted as a response to stressful conditions possibly associated with brackish episodic events affecting the coastal plain setting.

8. DEPOSITIONAL CONTROLS OF ALLOMEMBERS D AND C.

8.1. RELATIVE SEA LEVEL FLUCTUATIONS

The systems tracts of Allomembers D and C seem to be controlled by changes of relative sea level (RSL). These RSL fluctuations depend on the interplay of three variables: eustasy, local tectonics and the rates of sedimentation. However, change in relative water depth is the only parameter that can be inferred from facies analysis. Therefore, in order to study the effects of these variables in the geologic record, it is commonly necessary to isolate one of these parameters (eustasy, tectonics or sedimentation) and make assumptions about the magnitude and rate of change of the other two parameters (Plint *et al.*, 1992). The influence of eustasy and tectonics on RSL fluctuations largely depends on the absolute time scale of sea level fluctuation. Therefore, a rough estimate of the absolute time duration of the Falher cycles will be made before the effects of eustasy, tectonics and sedimentation can be considered.

8.2 TEMPORAL SCALE OF RELATIVE SEA-LEVEL CHANGE

The foraminiferal zonation by Caldwell *et al.* (1978) suggests that the relative age of the Lower Cretaceous Spirit River Formation is early Albian to middle middle Albian. This relative age compared with the eustatic sea level curve of Haq *et al.* (1988) gives an absolute duration of approximately 5.5 m.y. for the sedimentation of the Spirit River Formation (Figure 74). If the biochronologic methods of Caldwell *et al.* (1978) and Haq *et al.* (1988) are similar, the temporal scale of sea level change can be estimated for the Falher Member. Because there is no way to determine the precise duration of each member within the Spirit River Formation, an equal time duration will be assumed for each member. The Spirit River Formation consists of eight coarsening-upward successions (Cant, 1984), with two coarsening-upward successions within the Wilrich Member, five within Falher Member and the Notikewin Member (Figure 2). The eight successions are divided into the absolute time span of the Spirit River Formation giving a rough time duration of 687,500 years for each Falher coarsening upward succession (A-E). To estimate the time duration of each unit within Falher D and C, the duration of each Falher succession is further divided by two, assuming equal time for erosion (343,750 years) and for deposition (343,750 years). Because there is no way to determine the absolute time span for each transgressive and regressive event, an equal time is allotted to each. The deposition time is divided by two and an equal time-duration is estimated for progradation (171,875 years) and for aggradation (171,875 years). Because four transgressive-regressive units (four transgression plus four regressions) have been defined in this study for Falher D and for Falher C, the total time is further divided by eight in each Falher succession. This gives a time duration of approximately 21,484 years for each prograding unit within Falher D and C. Although Falher allomembers D and C are composed of additional units (D5 and

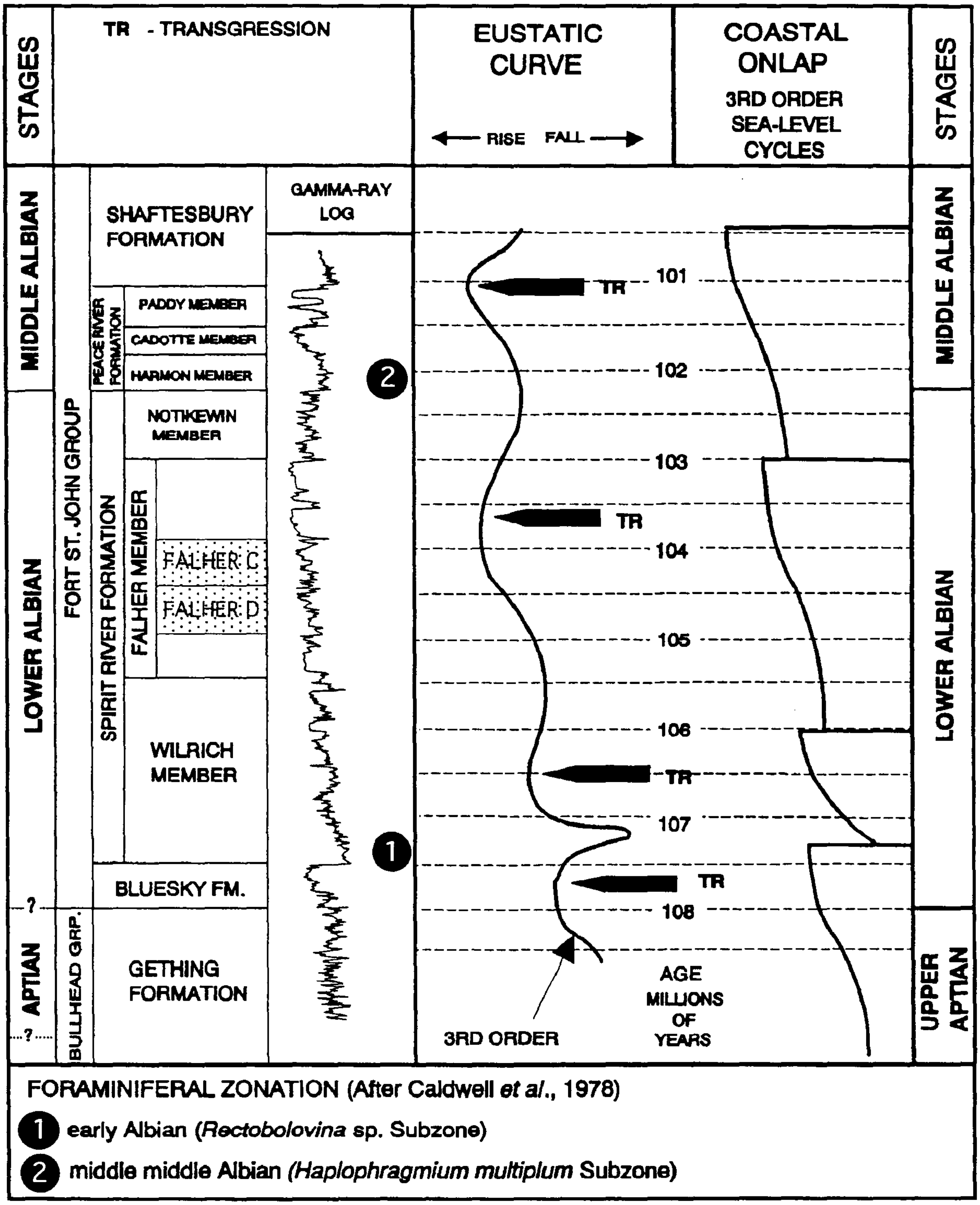

Figure 74. Correlation of Exxon eustatic sea level and coastal onlap curve with the Lower Cretaceous stratigraphy of northwestern Alberta. After Rouble (1994).

C5), it is assumed that they developed during the progradation of the units D1-D2 and C4.

Modern rates of transgression and regression can be used to compare with the rates of Falher D and C units. Only the transgressive and regressive limits of unit D1 (Falher D) occur within the study area. It therefore provides an opportunity to compare estimated rates with present day rates of progradation and transgression. The distance between the transgressive and regressive limits of D1 is about 45 km, giving an estimated rate of regression of 2.09 m/yr. This is much slower than the coast of Nayarit, Mexico, where the strandplain has prograded 15 km during the last 3,600 years (Curray *et al.*, 1967 *fide* Reineck and Singh, 1980) at an average rate of 4.1 m/yr.

Because the regressive limits of the other units in Falher D and C are not known, it is not possible to make the same calculations. However, assuming the northern limit of the study area lies close to the limit of progradation (about 60 km) for the most extensive unit (D2), the rate of progradation in this case (2.79 m/yr.) is still quite reasonable compared with modern rates for the coast of Nayarit.

8.3. EUSTATIC CHANGES IN SEA LEVEL

Five orders of cyclic sea level change have been defined by Vail *et al.* (1977). The first order cycles have a duration of 200-400 m.y. and are widely interpreted to be related to the accretion and break-up of supercontinents (Vail *et al.*, 1977; Plint *et al.*, 1992). This is controlled by the increase and decrease of the volume of oceanic spreading ridges (Plint *et al.* 1992). Second order cycles span 10 to 100 m.y. and consist of a grouping of third-order cycles. It is generally accepted that second order cycles are related to changes in the volume of oceanic ridges, related to changes in spreading rates (Pitman, 1978).

Third order cycles have a duration of 1 to 10 m.y. and their possible controls are reviewed by Plint *et al.* (1992). Some of the controls include (1) variations in spreading rates on ocean ridges, (2) episodic changes in the horizontal stress field within plates; and (3) geoidal eustasy (irregularities in the earth's gravitational field caused by "sags" and "bulges" on the ocean surface).

Fourth and fifth order cyclicity (500,000-200,000 years and 200,000-10,000 years respectively) is widely documented and explained by changes in climate, driven by cyclic perturbations of the Earth's tilt and orbit (Milankovitch cycles, Plint *et al.,* 1992).

To obtain some idea of the eustatic influence on the deposition of the Lower Cretaceous successions in northwestern Alberta, the Exxon coastal onlap curve of Haq *et al.* (1988) was correlated by Rouble (1994) with the biochronology of the Fort St. John Group (Figure 74), based on the foraminiferal zonation of Caldwell *et al.* (1978). This foraminiferal zonation is used to correlate the stratigraphy of the Spirit River Formation (Fort St. John Group) with the coastal onlap and inferred global eustatic sea level curves (Figure 74).

The correlation of the eustatic sea level curve with the Wilrich and Falher Member of the Spirit River Formation is very poor (Figure 74). The eustatic curve of Haq *et al.* (1988) does not show a regionally extensive transgression that correlates with the deposition of the marine shales of the Harmon Member.

This poor correlation suggests that the transgressive events within the Spirit River Formation and the overlying Harmon Member were probably controlled by some other mechanism, assuming that the Exxon coastal onlap curve of Haq *et al.* (1988) is correct and eustatically controlled.

The absolute time duration of each transgressive-regressive unit within Falher D and C was calculated previously as 42,968 years. This duration is characteristic of fifth order (Mitchum and Van Wagoner, 1991; Plint *et al.,* 1992) which is far beyond the resolution of the Exxon eustatic curve. The most commonly cited mechanism to explain this order of cyclicity is the influence of the Milankovitch cycles on the melting of glacial ice sheets (Plint *et al.*, 1992). However, when considering Milankovitch cycles as a possible mechanism controlling the cyclicity observed within Falher D and C, there is one major problem, namely, that there is no strong geological evidence to suggest continental glaciation between the Triassic and the early Tertiary. Plint (1991) reviewed some recent studies that provided tantalizing geological evidence for ice accumulation in the Cretaceous polar areas but the absence of absolute proof of continental ice sheets during the Cretaceous period makes glacio-eustatic controls unlikely (Plint *et al.*, 1992).

8.4. LOCAL TECTONIC CONTROLS

The Peace River Arch of north-central Alberta (Figure 4) is a large-scale structure formed in the Late Precambrian to Early Paleozoic that subsided differentially during deposition of the Upper Mannville Group (Cant, 1989; Cant and Stockmal, 1993).

Cant (1989) suggested that the Peace River Arch moved upward and downward during the Cretaceous, probably in response to thrust loading in the Cordillera, affecting the stratigraphy, facies distribution and thicknesses of the Mannville Group. However the exact relationship between the subsiding arch, the tectonic loading and the sedimentation rate in these formations is not known. Pate (1988) compared isopach maps and total subsidence maps and suggested that the subsidence of the Peace River Arch controlled the position of the shoreline, whereas the relative degree of subsidence controlled the distribution of sand and conglomerate bodies. However, neither tectono-eustacy, nor tectonic movement of the basin floor operate on a sufficiently rapid scale (Plint *et al.*, 1992) to explain the high-frequency sea level changes implied by the bounding discontinuities described for Falher D and C.

8.5. AUTOCYCLIC CONTROLS

A particularly interesting idea discussed by Plint *et al.* (1992) is that many short-period cyclic sedimentary successions can be influenced or controlled by autocyclic mechanisms such as delta-switching.

Following the ideas of Plint *et al.* (1992) and Rouble (1994), and assuming that the sedimentation rates were fairly constant during deposition of the Falher Member, a contributing factor in controlling RSL fluctuations of Falher allomember D could involve autocyclic processes such as delta lobe switching.

There is some evidence for autocyclic controls, for example the rates of transgression-regression that characterize D1, D2, D3 and D4. These cannot be explained by glacio-eustatic cycles because of the lack of continental glaciation during the Cretaceous. This fact makes autocyclic controls a more likely hypothesis.

Evidence supporting an autocyclic process is given by the proposed active subsidence of the Peace River Arch during deposition of the Falher Member (Cant, 1989). Here, Cant (1995) has suggested that several shoreface sandstones are stacked vertically in the Falher Member as a result of high rates of subsidence near the southern margin of the Peace River Arch. This subsidence may have been comparable to the subsidence required for a deltaic switching event like the deltaic lobe switching and transgression of abandoned delta lobes of Mississippi delta (Bhattacharya and Walker, 1992). Swift *et al.* (1991) suggest that the high-frequency shifts in position of the Mississippi Delta lobes during the last 6000 years are of mixed origin, but dominated by the autocyclic component. Although these hypothesis are attractive to apply within the study area, they remain purely speculative and a large regional study to the east and west of the area will be necessary to test the idea.

The only evidence from outside the study area favoring an autocyclic control is a recurring sediment depocenter within the Falher Member which occurs in the northeastern part of British Columbia, about 38 km west of the Alberta-British Columbia border (Leckie, 1986). The abandonment of strandplain deposits that characterize the upper part of Falher D and C within the study area can be related to a switching event of this depocenter in British Columbia. Also the upper shoreface conglomerates in each Falher D unit (D1-D4) show an east-west trend, pinching out eastwards (Figure 48) suggesting a distribution of coarse sediment alongstrike and downdrift from a point source somewhere west of the study area. The alternation between conglomerates and fine- to medium-grained sandstones in the upper shoreface successions of Falher D units suggests that these might be explained by temporal changes in sediment supply related to autocyclic process involving switching of deltaic lobes (Arnott, 1993).

9. CONCLUSIONS

i) Using an allostratigraphic approach, Falher units D and C can be subdivided into 8 shoreface units (4 in Falher D and 4 in Falher C). Each of these newly recognized units (C1, C2, C3, C4, D1, D2, D3 and D4) represents a transgressive-regressive depositional event.

ii) Units C1-C4 and D1-D4 were deposited as a barrier-strandplain system. The transgressive systems tracts are probably preserved as barrier sandstones in the shoreline position at the time of maximum transgression. Lagoonal deposits, coarse transgressive lags and transgressive mudstones were partially preserved seaward of the barrier during each shoreface retreat. The highstand systems tracts are composed of shoreface successions which prograded as strandplain systems.

iii) The marine flooding surface at the base of each shoreface unit correlates landward with a nonmarine flooding surface. This flooding surface represents initial flooding of topographic lows and development of lagoons along the inner coastline, landward of the barrier system as it moves southward.

iv) Upper shoreface conglomerates in Falher D and C are mainly regressive. These conglomerates trend east-west, parallel to the paleoshoreline. Transgressive marine conglomerates occur only as lag deposits at the base of the shoreface units.

v) Some conglomeratic successions are fluvial in origin and represent channel fills that fed the shoreface during the progradation.

vi) During C3 time, a major relative sea level fall occurred, ending the progradation. This interpretation opens the possibility for a lowstand shoreface deposit north of the study area, as a target for oil and gas exploration.

vii) The muddy succession that trends north-south in Falher C (unit C-5) probably represents the fill of a channel system that fed the prograding shoreface unit C4.

viii) The time-duration of the transgressive-regressive events in each shoreface unit within Falher D and C have been estimated to be approximately 43,000 years, corresponding with fourth to fifth-order of cyclic sea level change.

ix) Combinations of allocyclic and autocyclic processes may have controlled the relative sea level fluctuations during deposition of Falher D and C.

x) The depositional evolution of Falher D and C seems to be quite different. Falher D is characterized by four shoreface units (D1-D4) associated with small relative sea level fluctuations that imparted a cyclic aspect to the stratigraphic unit.

In contrast, Falher C is also characterized by four shoreface units but the first two (C1-C2) are poorly preserved with a patchy distribution across the north-central part of the study area. The other two units (C3-C4) are separated by a major relative sea level fluctuation. In places unit C4 contains lagoonal successions trending east-west that separate unit C4 from unit C3 which occurs only in the southern part of the study area.

xi) The complex depositional evolution of Falher D and C also make contrast with a simpler depositional evolution of Falher B and A (Rouble and Walker, 1994). In this case, Falher A and B each contain two vertically stacked shoreface deposits separated by an extensive marine flooding surface. This contrast with the more shingled shoreface sandbody of Falher D, and also contrast with the much muddier facies of Falher C.

10. REFERENCES

Arnott, R.W.C., 1993, Sedimentological and Sequence stratigraphic model of the Falher "D" Pool, Lower Cretaceous, northwestern Alberta: Bulletin of Canadian Petroleum Geology, v. 41, p. 453-464.

Bhattacharya, J.P., 1993, The expression and interpretation of marine flooding surfaces and erosional surfaces in core; examples from the Upper Cretaceous Dunvegan Formation, Alberta foreland basin, Canada, *in* : Posamentier *et al.*, eds., Sequence Stratigraphy and Facies association: International Association of Sedimentologists, Special Publication 18, p. 125-160.

Bhattacharya, J.P. and Walker, R.G., 1992, Deltas, *in* : Walker, R.G. and James, N. P., eds., Facies models: response to sea level change: Geological Association of Canada, p. 157-177.

Beynon, B.M., Pemberton, S.G., Bell, D.D. and Logan, C.A., 1988, Environmental implications of ichnofossils from the lower Cretaceous Grand Rapids Formation, Cold Lake oil sands deposit, *in* : James, D.P. and Leckie, D.A., eds., Sequences, stratigraphy, sedimentology: surface and subsurface: Canadian Society of Petroleum Geologists, Memoir 15, p. 275-290.

Bromley, R.G., 1990, Trace Fossils : Biology and Taphonomy. Unwin Hyman, London, 280 p.

Cant, D.J., 1984, Development of shoreline-shelf sand bodies in a Cretaceous epeiric sea deposit: Journal of Sedimentary Petrology, v. 54, p. 541-556.

Cant, D.J., and Ethier, V.G., 1984, Lithology-dependent diagenetic control of reservoir properties of conglomerates, Falher Member, Elmworth Field, Alberta: American Association of Petroleum Geologists Bulletin, v. 68, p. 1044-1054.

Cant, D.J., 1989, Zuni Sequence : The Foreland Basin, *in* : Ricketts, B.D., ed., Western Canada Sedimentary Basin : A Case History: Canadian Society of Petroleum Geologists, p. 251-267.

Cant, D.J., 1995, Sequence Stratigraphic analysis of individual depositional successions : Effects of marine/nonmarine sediment partitioning and longitudinal sediment transport, Mannville Group, Alberta Foreland basin, Canada: American Association of Petroleum Geologists Bulletin, v. 79, p. 749-762.

Clifton, H.E., and Thompson, J.K., 1978, *Macaronichnus segregatis* : a feeding structure of shallow marine polychaetes: Journal of Sedimentary Petrology, v. 48, p. 1293-1302.

Cullen, D.J., 1973, Bioturbation of superficial marine sediments by Interstitial Meiobenthos: Nature, v. 242, p. 223-324.

Curran, H.A., 1985, The trace fossil assemblage of a Cretaceous nearshore environment: Englishtown Formation of Delaware, U.S.A, *in* : Curran, H.A., ed., Biogenic structures: Their use in interpreting depositional environments: Society of Economic Paleontologists and Mineralogists, Special Publication 35, p. 261-276.

Demarest, J.M. and Kraft, J.C., 1987, Stratigraphic record of Quaternary sea levels: Implications for more ancient strata, *in* : Nummedal, D., Pilkey, O.H. and Howard, J.D. eds., Sea-level fluctuation and coastal evolution: Society of Economic Paleontologists and Mineralogists, Special publication 41, p. 223-239.

Dominguez, JM.C., Martin, L. and Bittencourt, A.C.S.P., 1987, Sea-level history and Quaternary evolution of river mouth-associated beach-ridge plains along the east-southeast Brazilian coast : a summary, *in* : Nummedal, D., Pilkey, O.H. and Howard, J.D. eds., Sea-level fluctuation and coastal evolution: Society of Economic Paleontologists and Mineralogists, Special publication 41, p. 115-127.

Dominguez, JM.L. and Wanless, H.R., 1991, Facies architecture of a falling sea-level strandplain, Doce River coast, Brazil, *in* : Swift, D.P.J. *et al.*, ed., Shelf sands and sandstone bodies: Geometry, facies and sequence stratigraphy, Special Publication 14, p. 259-281.

Haq, B.U., Hardenbol, J. and Vail, P.R., 1988, Mesozoic and Cenozoic chronostratigraphy and cycles of sea level change, *in* : Wilgus, C.K. *et al.*, eds., Sea level changes: an integrated approach: Society of Economic Paleontologists and Mineralogists, Special Publication 42, p. 71-108.

Hart, B.S. and Plint, A.G., 1993, Origin and erosion surface in shoreface sandstone of the Kakwa Member (Upper Cretaceous Cardium Formation, Canada): importance for reconstruction of stratal geometry and depositional history, *in* : Posamentier *et al.*, eds., Sequence Stratigraphy and Facies association: International Association of Sedimentologists, Special Publication 18, p. 451-467.

Howard, J.D. and Frey, R.W., 1973, Characteristic physical and biogenic sedimentary structures in Georgia estuaries: American Association of Petroleum Geologists Bulletin, v. 57, p. 1169-1184.

Jackson, P.C., 1984, Paleogeography of the Lower Cretaceous Mannville Group of western Canada, *in* : Masters, J.A., ed., Elmworth -- Case Study of a Deep Basin Gas Field: American Association of Petroleum Geologists, Memoir 38, p. 49-79.

Leckie, D.A., and Walker, R.G., 1982, Storm- and tide-dominated shorelines in Cretaceous Moosebar-Lower Gates Interval -- outcrop equivalents of Deep Basin gas trap in Western Canada: American Association of Petroleum Geologists Bulletin, v. 66, p. 138-157.

Leckie, D.A., 1986, Rates, controls, and sand-body geometries of transgressive-regressive cycles: Cretaceous Moosebar and Gates Formations, British Columbia: American Association of Petroleum Geologists Bulletin, v. 70, p. 516-535.

Massari, F., and Parea, G.C., 1988, Progradational gravel beach sequences in a moderate- to high-energy, microtidal marine environment: Sedimentology, v.35, p. 881-913.

Masters, J.A., 1984, Lower Cretaceous oil and gas in western Canada, *in* : Masters, J.A., ed., Elmworth - Case Study of a Deep Basin Gas Field, American Association of Petroleum Geologists, Memoir 38, p. 1-35.

Mitchum, R.M. and Van Wagoner, J.C., 1991, High-frequency sequences and their stacking patterns: sequence-stratigraphic evidence of high-frequency eustatic cycles: Sedimentary Geology, v. 70, p. 131-160.

Monger, J.W.H., 1989, Overview of Cordilleran geology, *in* : Ricketts, B.D., ed., Western Canada Sedimentary Basin : A Case History: Canadian Society of Petroleum Geologists, p. 9-32.

Moslow, T.F. and Pemberton, S.G., 1988, An integrated approach to the sedimentological analysis of some lower Cretaceous shoreface and delta front sandstones sequences, *in* : James, D.P. and Leckie, D.A., eds., Sequences, Stratigraphy, Sedimentology: Surface and subsurface: Canadian Society of Petroleum Geologists, Memoir 15, p. 373-386.

North American Commission on Stratigraphic Nomenclature, 1983, North American Stratigraphic Code: American Association of Petroleum Geologists, v. 67, p. 841-875.

Orford, J.D., 1977, A proposed mechanism fro storm beach sedimentation: Earth Surface Processes Landforms, v.2, p. 381-400.

O'Connell, S.C., Dix, G.R., and Barclay, J.E., 1990, The origin, history, and regional structural development of the Peace River Arch, Western Canada: Bulletin of Canadian Petroleum Geology, v. 38A, p. 4-24.

Pate, C., 1988, A Comparison of isopach maps and total subsidence maps: Implications for basin development and sandstone distribution during the Lower Cretaceous in the Deep basin area of Alberta and British Columbia, *in* : James, D.P. and Leckie, D.A., eds., Sequences, Stratigraphy, Sedimentology: Surface and subsurface: Canadian Society of Petroleum Geologists, Memoir 15, p. 553-562.

Pemberton, S.G., MacEachern, J.A. and Frey, R.W., 1992a, Trace fossil facies models : Environmental and allostratigraphic significance, *in* : Walker, R.G. and James, N. P., eds., Facies models: response to sea level change: Geological Association of Canada, p. 47-72.

Pemberton, S.G.; Van Wagoner, J.C. and Wach, G.D., 1992b, Ichnofacies of a wave-dominated shoreline, *in* : Pemberton, G.S., ed., Applications of Ichnology to Petroleum exploration - A Core Workshop: Society of Economic Mineralogists and Paleontologists, Core Workshop, no. 17, p. 339-382.

Pemberton, S.G., and Wightman, D.M., 1992, Ichnological characteristics of brackish deposits, *in* : Pemberton, G.S., ed., Applications of Ichnology to Petroleum exploration - A Core Workshop: Society of Economic Mineralogists and Paleontologists, Core Workshop, no. 17, p. 141-167.

Pitman, W.C., 1978, Relationship between eustacy and stratigraphic sequences of passive margins: Geological Society of America Bulletin, v. 89, p. 1387-1403.

Plint, A.G., 1991, High frequency relative sea-level oscillations in Upper Cretaceous shelf clastics of the Alberta foreland basin: possible evidence for a glacio-eustatic control? *in* : MacDonald, D.I.M., ed., Sedimentation, Tectonics and Eustasy: International Association of Sedimentologists, Special Publication 12, p. 409-428.

Plint, A.G., Eyles, N., Eyles, C.H. and Walker, R.G., 1992, Control of Sea level change, *in* : Walker, R.G. and James, N. P., eds., Facies models: response to sea level change: Geological Association of Canada, p. 15-25.

Plint, A.G. and Walker, R.G., 1987, Cardium Formation 8. Facies and environments of the Cardium shoreline in the Kakwa field and adjacent areas, northwestern Alberta: Bulletin of Canadian Petroleum Geology, v. 35, p. 48-64.

Posamentier, H.W., Jervey, M.T. and Vail, P.R., 1988, Eustatic controls on clastic deposition I - conceptual framework, *in* : Wilgus, C. K., *et al.*, eds., Sea-level changes: an integrated approach: Society of Economic Paleontologists and Mineralogists, Special Publication 42, p. 104-124.

Reineck, H.E. and Singh, I.P., 1980, Depositional sedimentary environments. Springer-Verlag, Berlin Heidelberg, 549 p.

Reinson, G.E., 1992, Transgressive barrier island and estuarine systems, *in* : Walker, R.G. and James, N. P., eds., Facies models: response to sea level change: Geological Association of Canada, p. 179-194.

Rouble, R.G., 1994, Sedimentology and allostratigraphy of Falher Members A and B of the Lower Cretaceous Spirit River Formation, Northwestern Alberta, Canada, MSc thesis, McMaster University, Hamilton, Ontario, 192 p.

Rouble, R.G. and Walker, R.G., 1994, High resolution sequence stratigraphy and depositional environments of Falher Members A and B, Lower Cretaceous Spirit River Formation of Northwestern Alberta: Canadian Society of Petroleum Geologists, Mannville Core Conference, Alberta, p. 1-12.

Smith, D.G., 1984, Gas reserves and production performance of the Elmworth/Wapiti area of the Deep Basin, *in* : Masters, J.A., ed., Elmworth -- Case Study of a Deep Basin Gas Field: American Association of Petroleum Geologists, Memoir 38, p. 153-172.

Smith, D.G., Zorn, C.E., and Sneider, R.M., 1984, The paleogeography of the Lower Cretaceous of western Alberta and northeastern British Columbia in and adjacent to the deep basin of the Elmworth area, *in* : Masters, J.A., ed., Elmworth -- Case Study of a Deep Basin Gas Field,: American Association of Petroleum Geologists, Memoir 38, p. 79-115.

Swift, D.J.P., 1968, Coastal erosion and transgressive stratigraphy: Journal of Geology, v. 76, p. 444-456.

Swift, D.J.P., Phillips, S. and Thorne, J.A., 1991, Sedimentation on continental margins, V: Parasequences, , *in* : Swift, D.P.J. *et al.*, ed., Shelf sands and sandstone bodies: Geometry, facies and sequence stratigraphy, Special Publication 14, p. 153-187.

Tilley, B.J. and Longstaffe, F.J., 1989, Diagenesis and isotopic evolution of porewaters in the Alberta Deep Basin: The Falher Member and Cadomin Formation: Geochimica *et* Cosmochimica Acta, V. 53, p. 2529-2546.

Vail, P.R., Mitchum, R.M., Todd, R.G., Widmier, J.M., Thompson, S., Sangree, J.B., Bubb, J.N. and Hatlelid, W.G., 1977, Seismic stratigraphy and global changes of sea level, *in* Payton, C.E., ed., Seismic stratigraphy - applications to hydrocarbon exploration: American Association of Petroleum Geologists, Memoir 26, p. 49-212

Van Wagoner, J.C., Michum, R.M., Campion, K.M. and Rahmanian, V.D., 1990, Siliciclastic sequence stratigraphy in well logs, cores and outcrops: American Association of Petroleum Geologists, Methods in Exploration Series, N. 7, 55 p.

Van Wagoner, J.C., 1991, Sequence stratigraphy and facies architecture of the Desert Member of the Blackhawk Formation and the Castlegate Formation in the Book Cliffs of eastern Utah and western Colorado, *in* : Van Wagoner *et al.*, eds., Sequence Stratigraphy applications to shelf sandstone reservoirs: American Association of Petroleum Geologists Field Conference, p. 4.1-4.7

Vossler, S.M. and Pemberton, S.G., 1988, Ichnology of the Cardium Formation (Pembina oilfield): Implications for depositional and sequence stratigraphic interpretations, *in* : James, D.P. and Leckie, D.A., eds., Sequences, Stratigraphy, Sedimentology: Surface and subsurface: Canadian Society of Petroleum Geologists, Memoir 15, p. 237-254.

Walker, R.G., 1992, Facies, facies models and modern stratigraphic concepts, *in* : Walker, R.G. and James, N. P., eds., Facies models: response to sea level change: Geological Association of Canada, p. 1-14.

Walker, R.G., and Eyles, C.H., 1991, Topography and significance of a basinwide sequence-bounding erosion surface in the Cretaceous Cardium Formation, Alberta, Canada: Journal of Sedimentary Petrology, V. 61, p. 473-496.

Walker, R.G. and Plint, A.G., 1992, Wave- and storm-dominated shallow marine systems, *in* : Walker, R.G. and James, N. P., eds., Facies models: response to sea level change: Geological Association of Canada, p. 219-238.

Wyman, R. E., 1984, Gas resources in Elmworth coal seams, *in* : Masters, J.A., ed., Elmworth -- Case Study of a Deep Basin Gas Field: American Association of Petroleum Geologists, Memoir 38, p. 173-187.

APPENDIX A

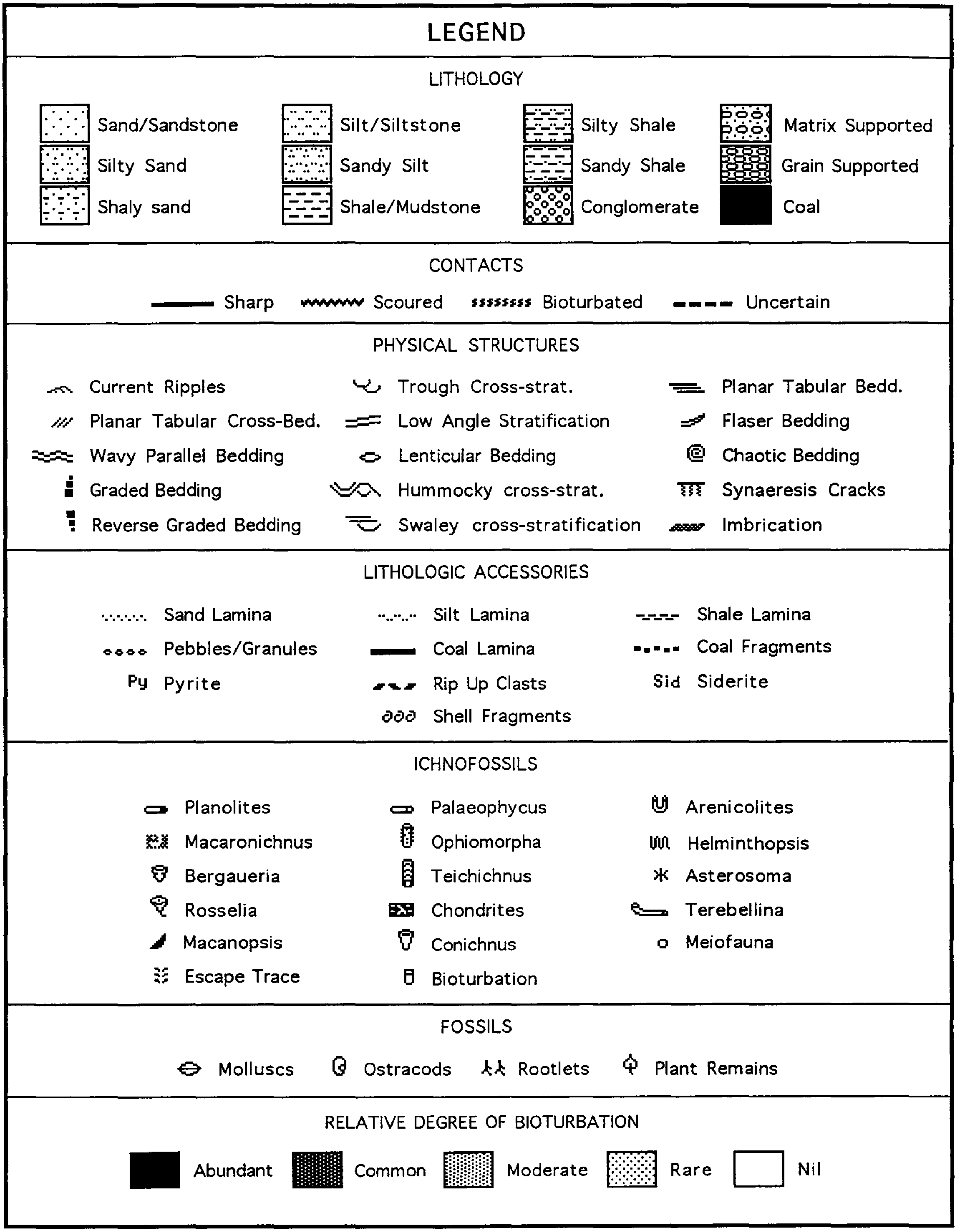

Appendix A1. Legend for the sedimentary core logs and core cross-sections.

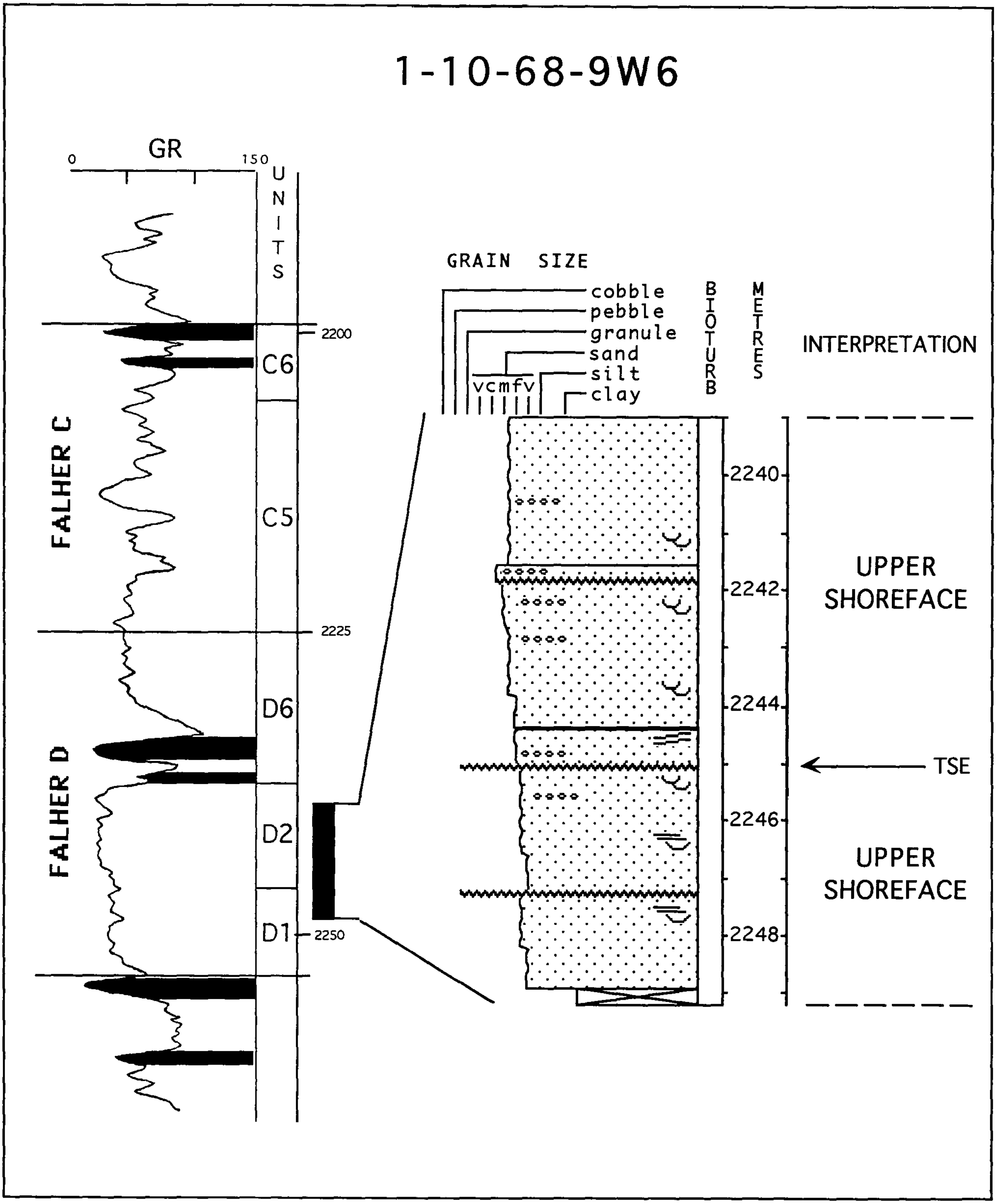

Appendix A2. Detailed sedimentary core log of 1-10-68-9W6. See Appendix A1 for legend and Figure 36 for location.

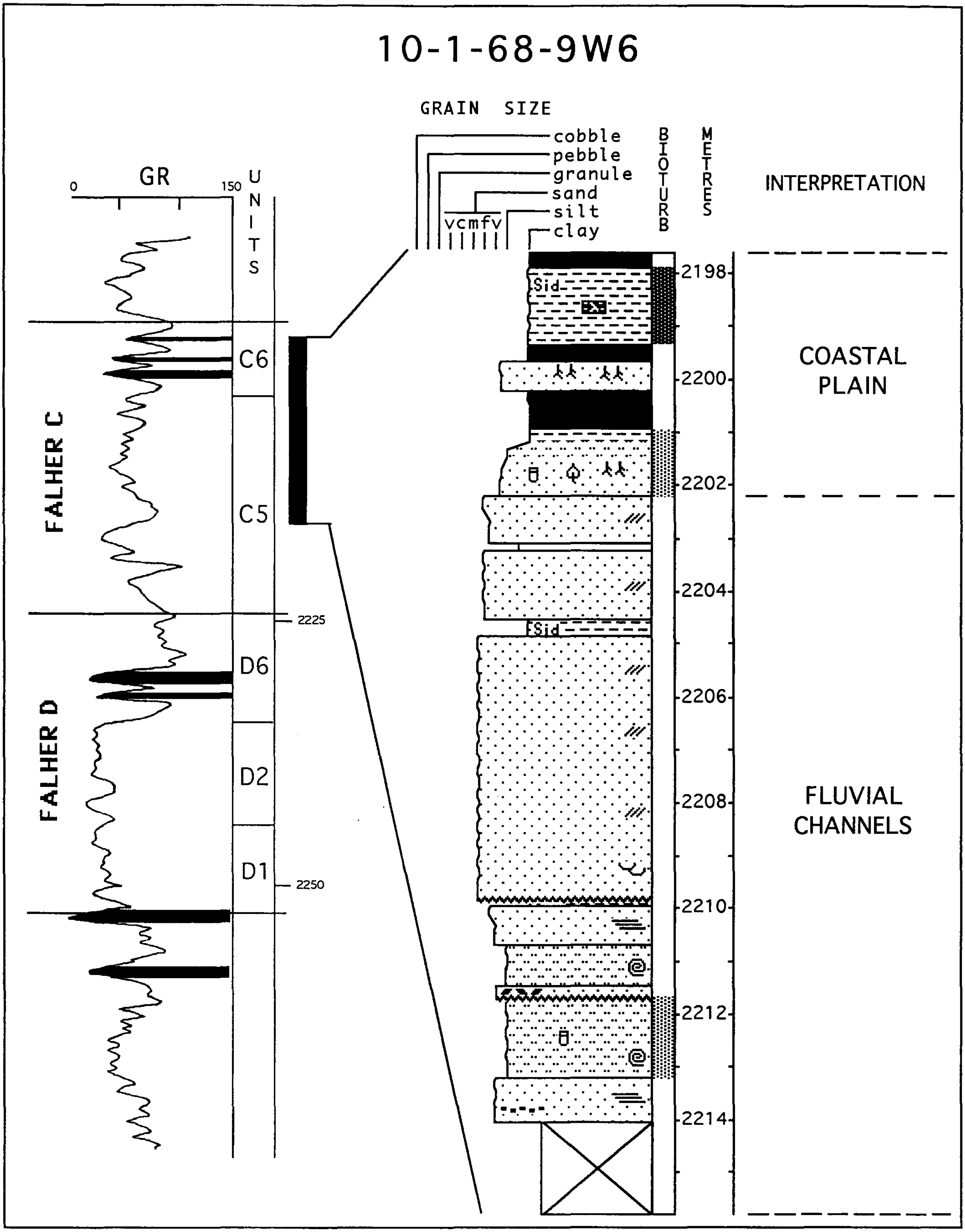

Appendix A3. Detailed sedimentary core log of 10-1-68-9W6. See Appendix A1 for legend and Figure 36 for location.

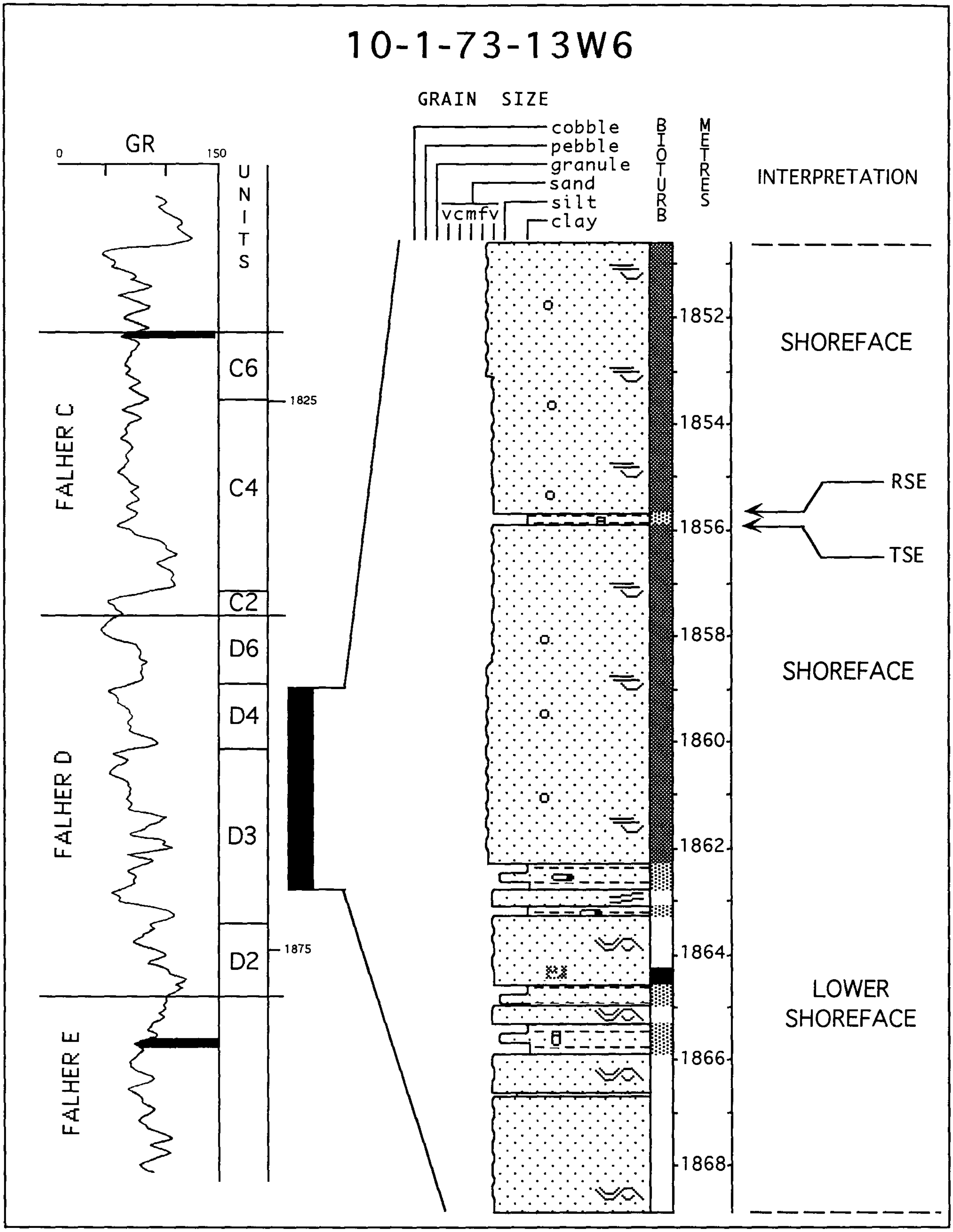

Appendix A4. Detailed sedimentary core log of 10-1-73-13W6. See Appendix A1 for legend and Figure 36 for location.

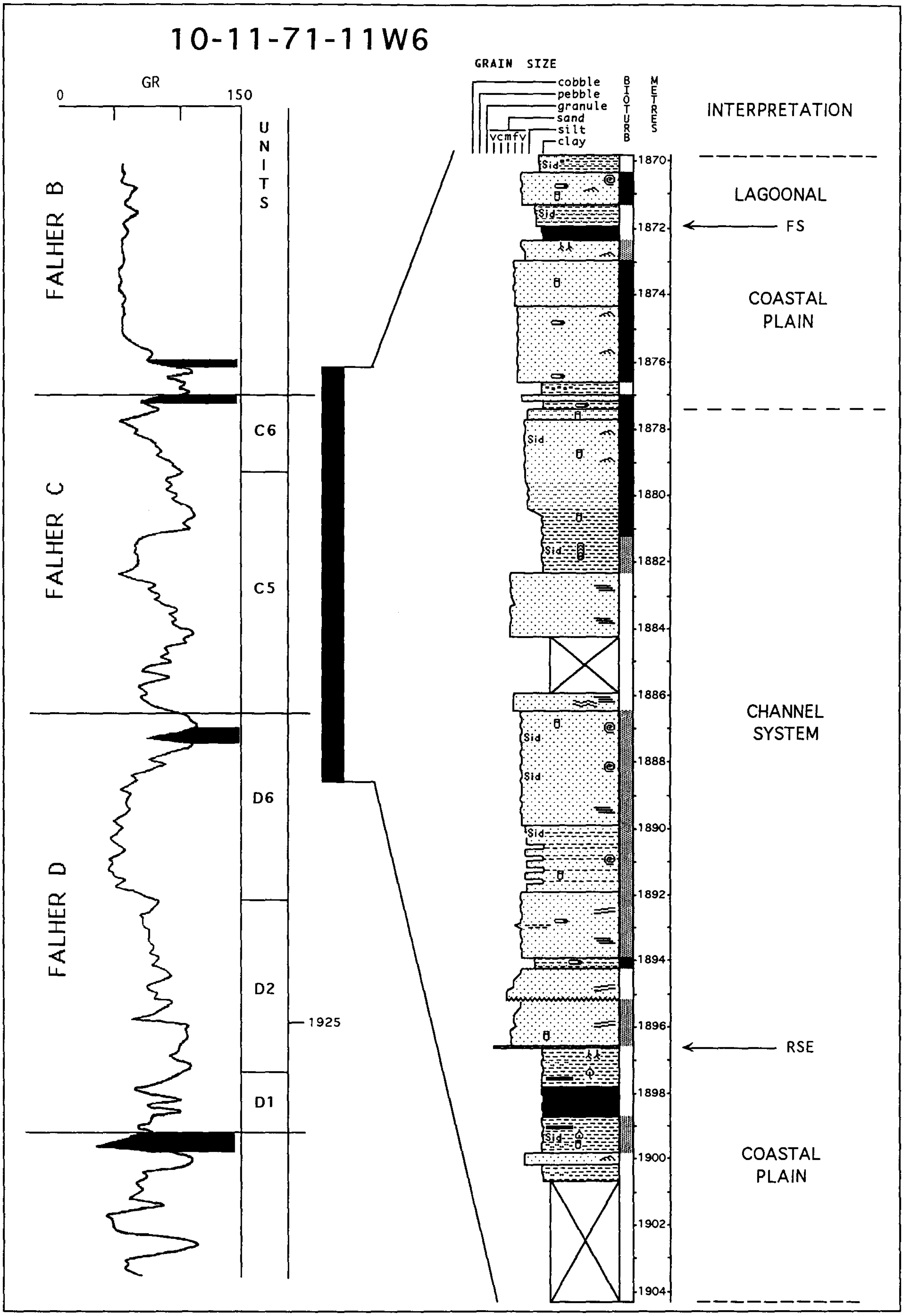

Appendix A5. Detailed sedimentary core log of 10-15-71-11W6.
See Appendix A1 for legend and Figure 36 for location.

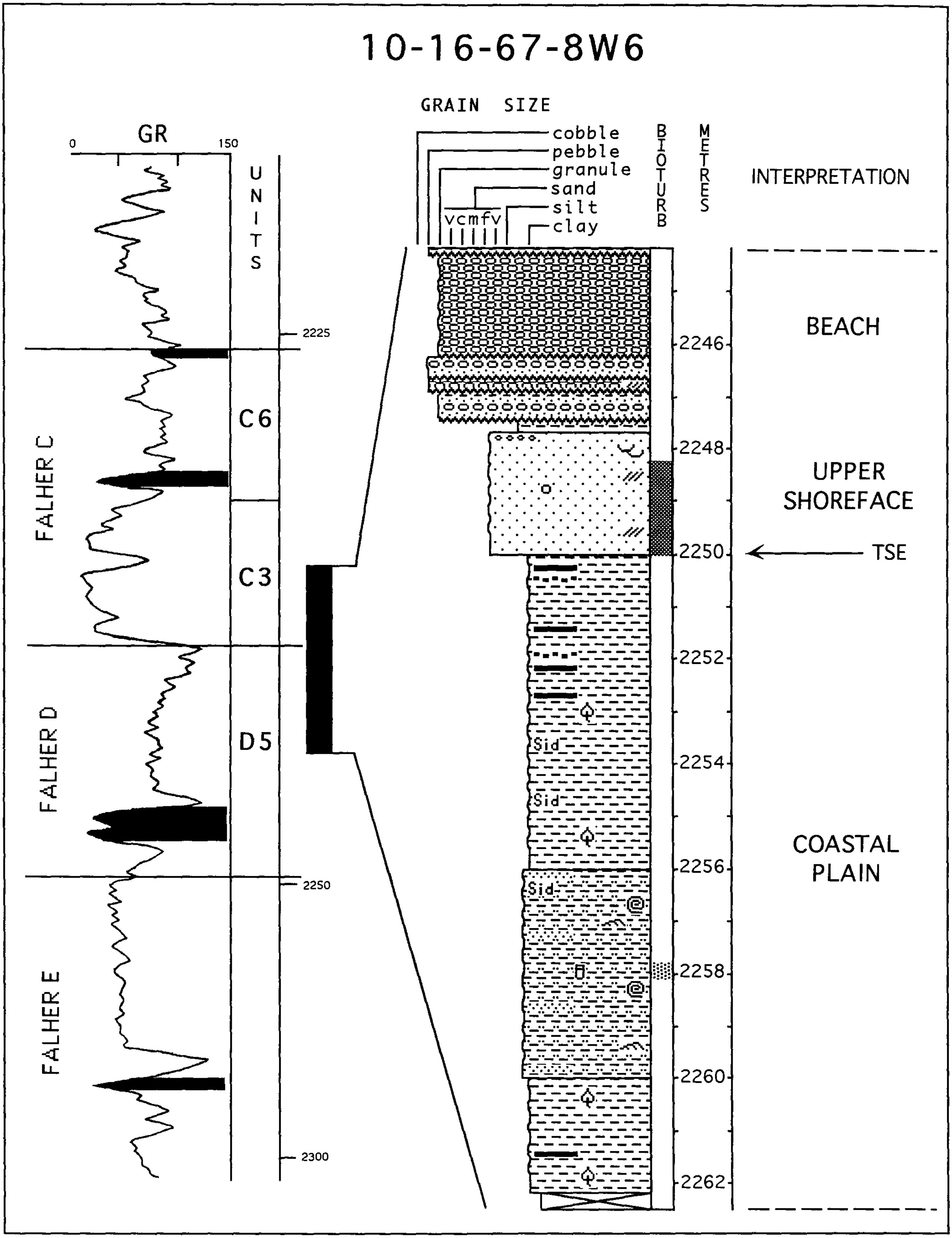

Appendix A6. Detailed sedimentary core log of 10-16-67-8W6.
See Appendix A1 for legend and Figure 36 for location.

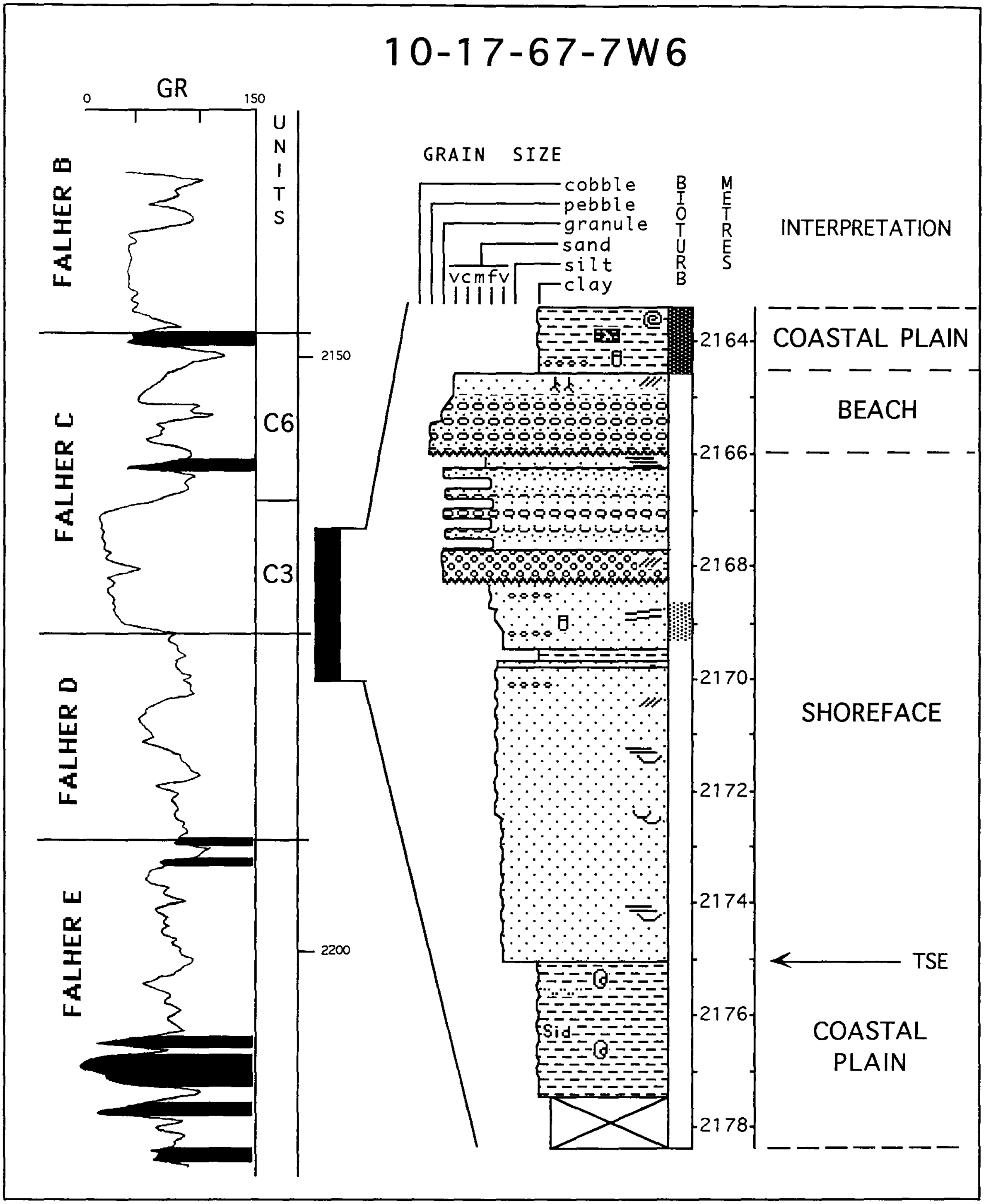

Appendix A7. Detailed sedimentary core log of 10-17-67-7W6. See Appendix A1 for legend and Figure 36 for location.

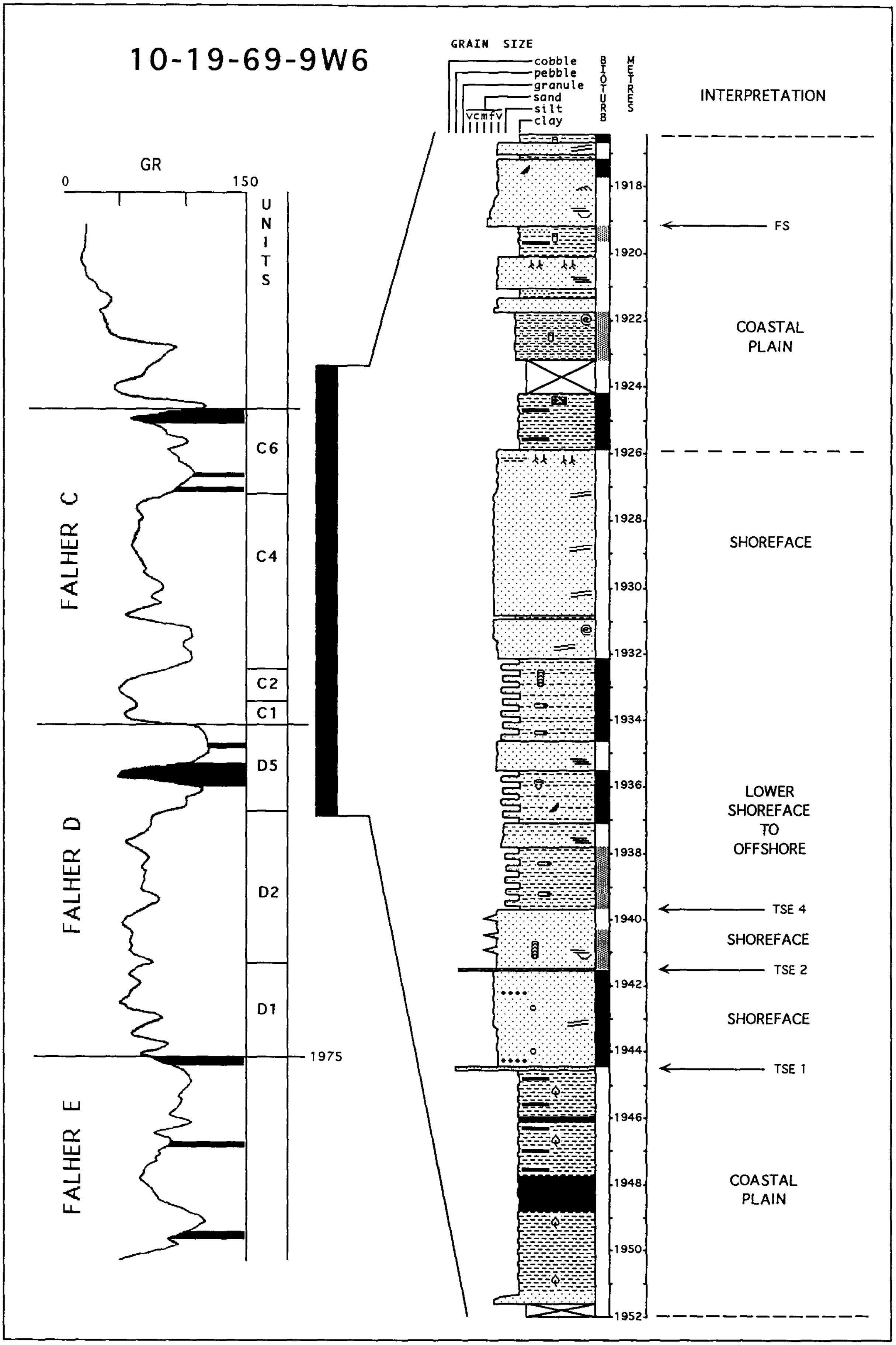

Appendix A8. Detailed sedimentary core log of 10-19-69-9W6.
See Appendix A1 for legend and Figure 36 for location.

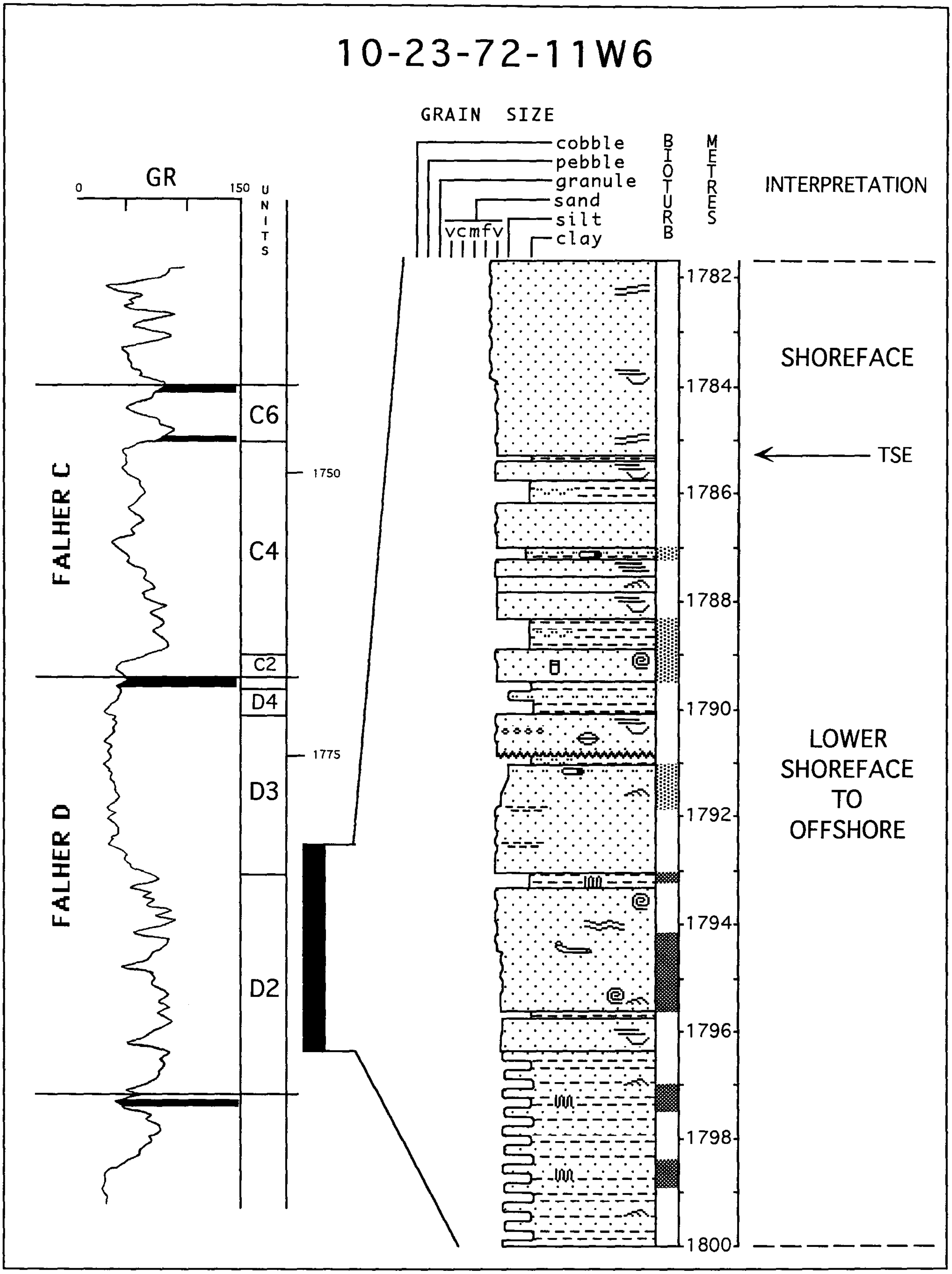

Appendix A9. Detailed sedimentary core log of 10-23-72-11W6.
See Appendix A1 for legend and Figure 36 for location.

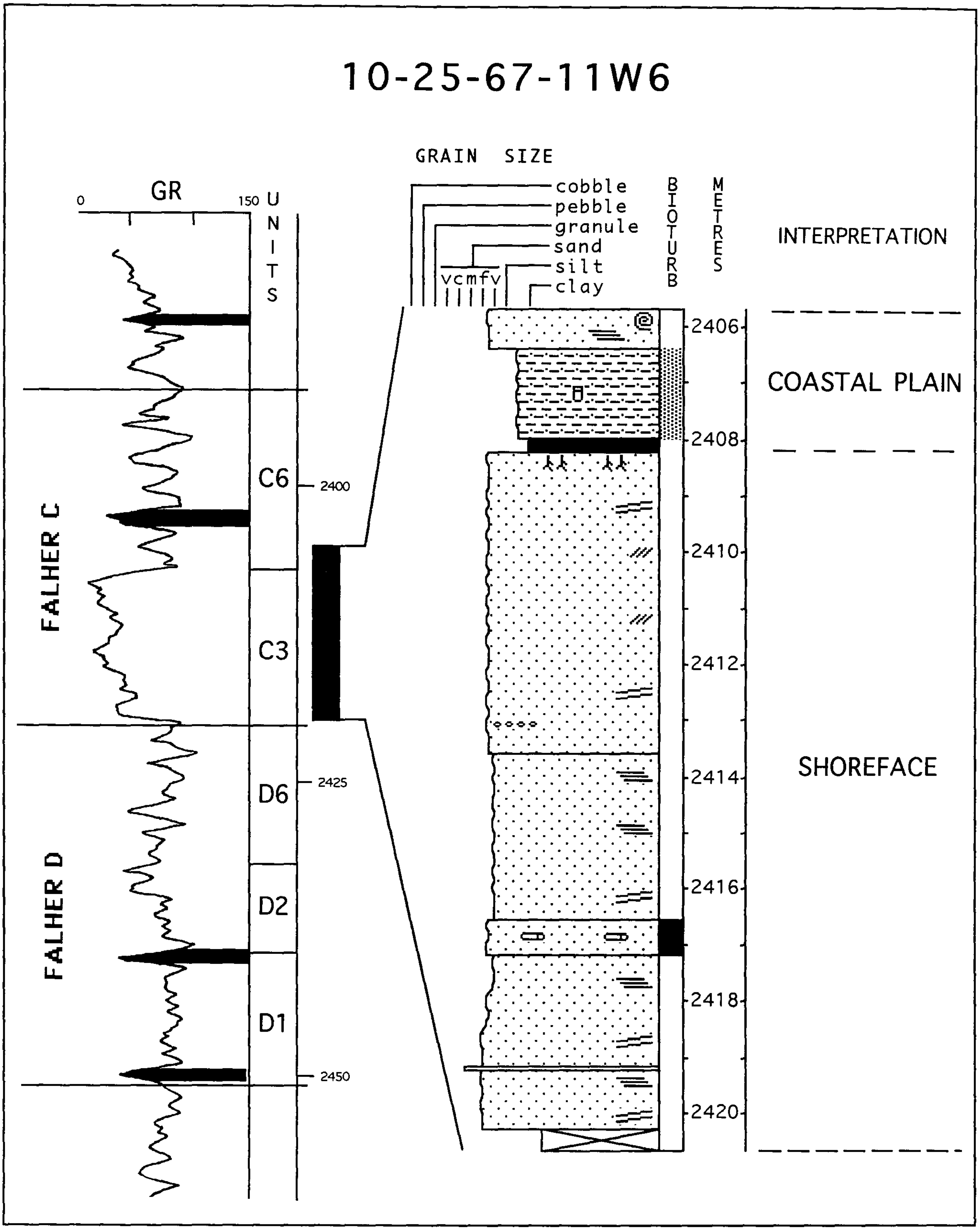

Appendix A10. Detailed sedimentary core log of 10-25-67-11W6. See Appendix A1 for legend and Figure 36 for location.

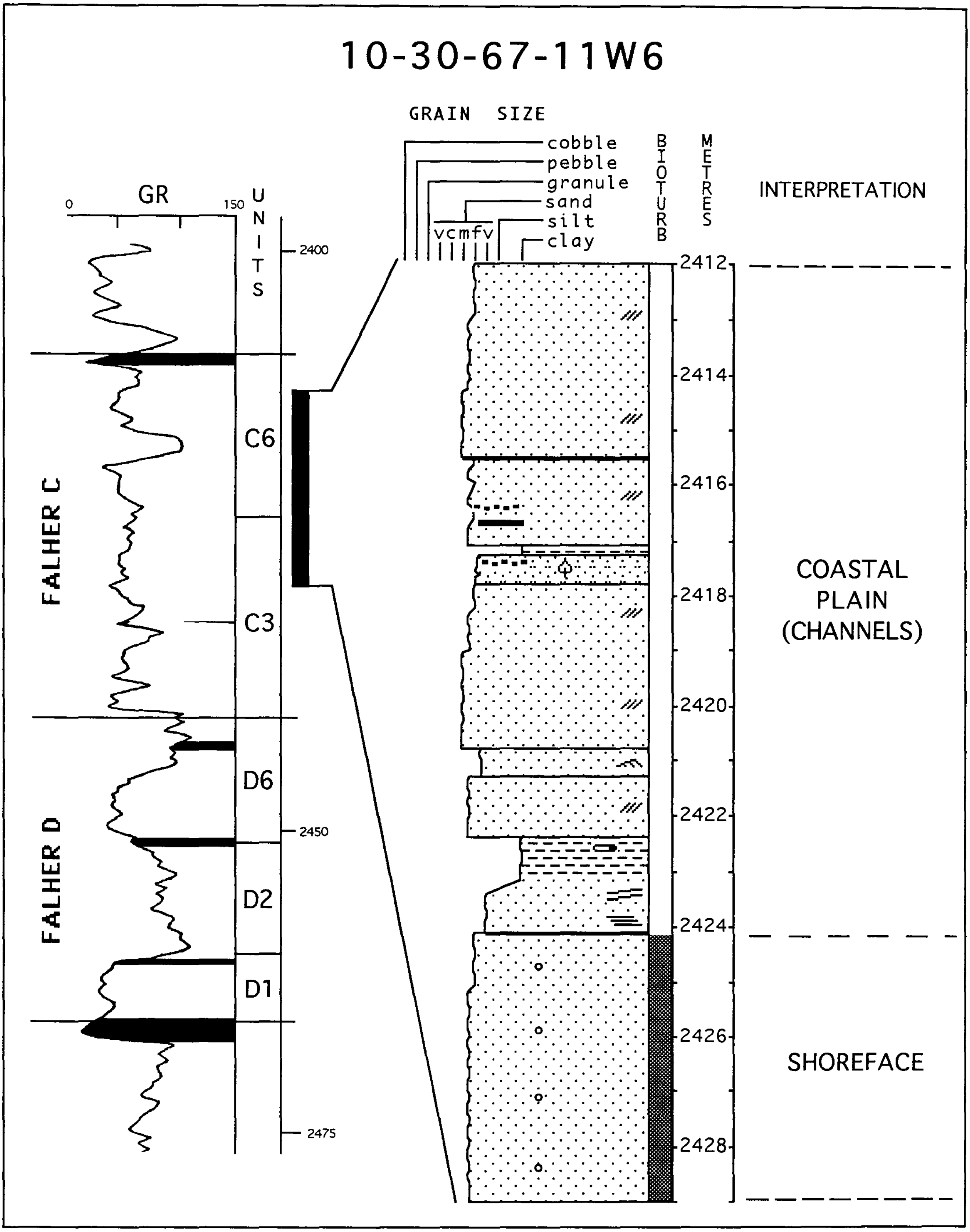

Appendix A11. Detailed sedimentary core log of 10-30-67-11W6. See Appendix A1 for legend and Figure 36 for location.

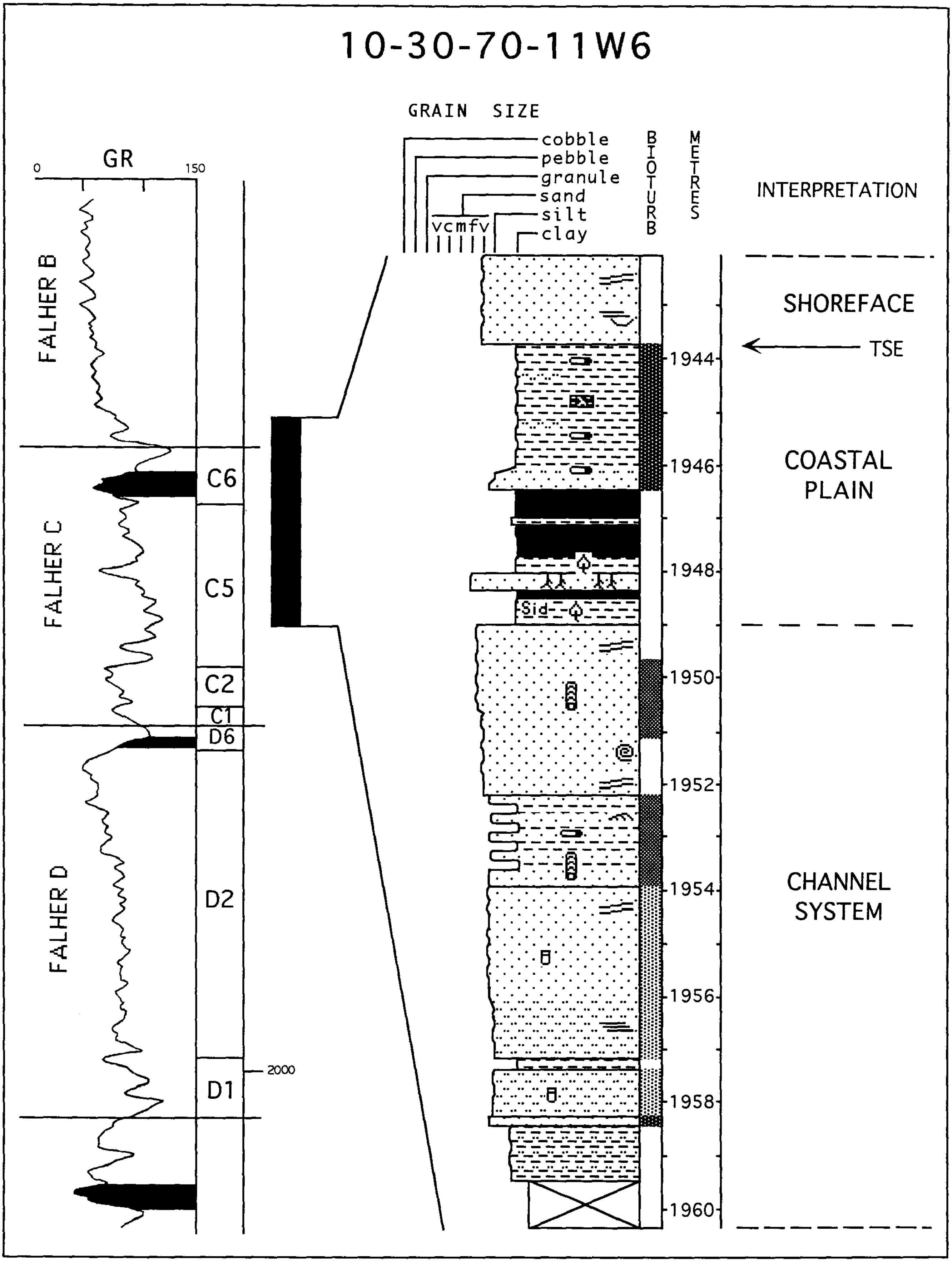

Appendix A12. Detailed sedimentary core log of 10-30-70-11W6. See Appendix A1 for legend and Figure 36 for location.

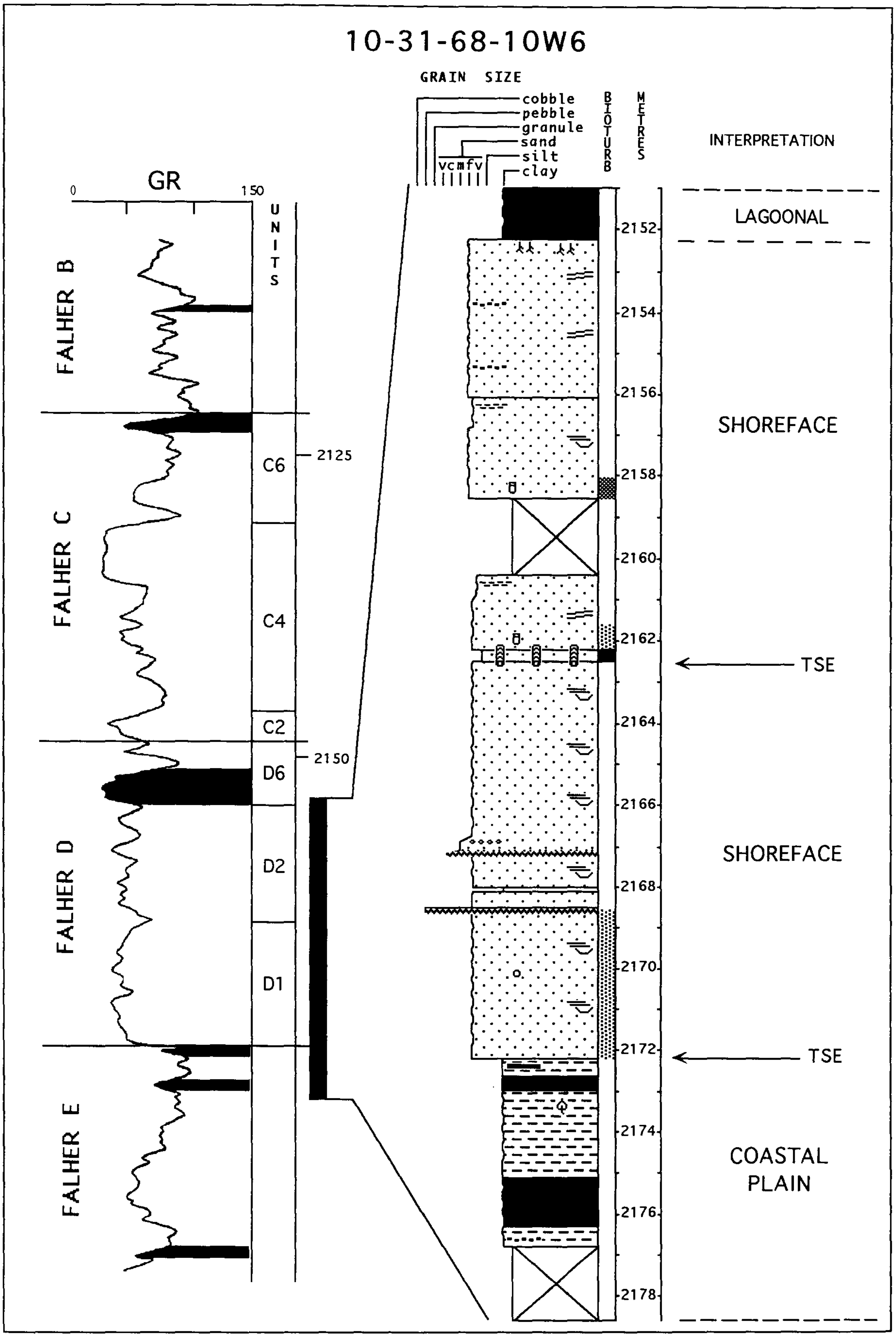

Appendix A13. Detailed sedimentary core log of 10-31-68-10W6. See Appendix A1 for legend and Figure 36 for location.

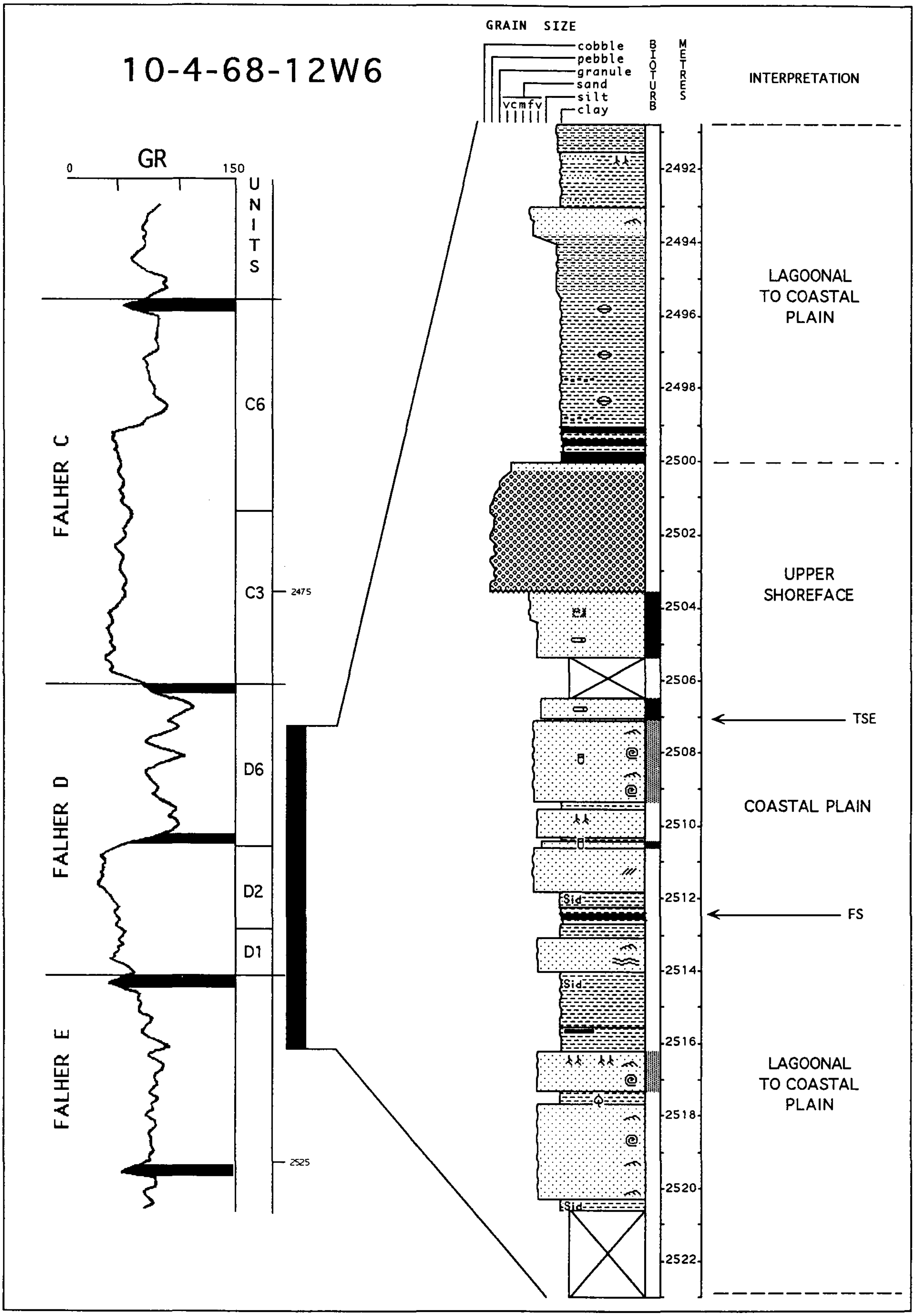

Appendix A14. Detailed sedimentary core log of 10-4-68-12W6. See Appendix A1 for legend and Figure 36 for location.

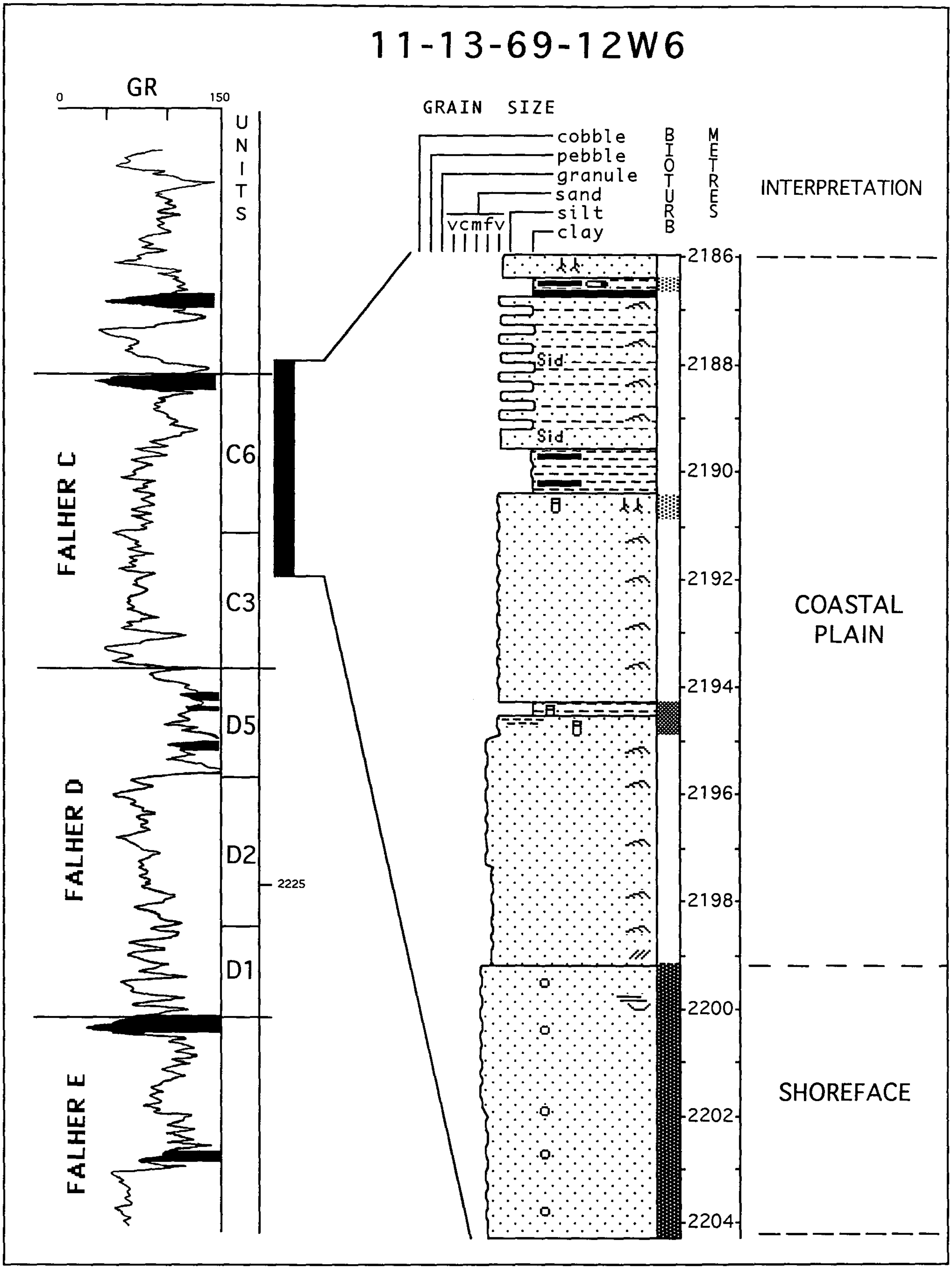

Appendix A15. Detailed sedimentary core log of 11-13-69-12W6. See Appendix A1 for legend and Figure 36 for location.

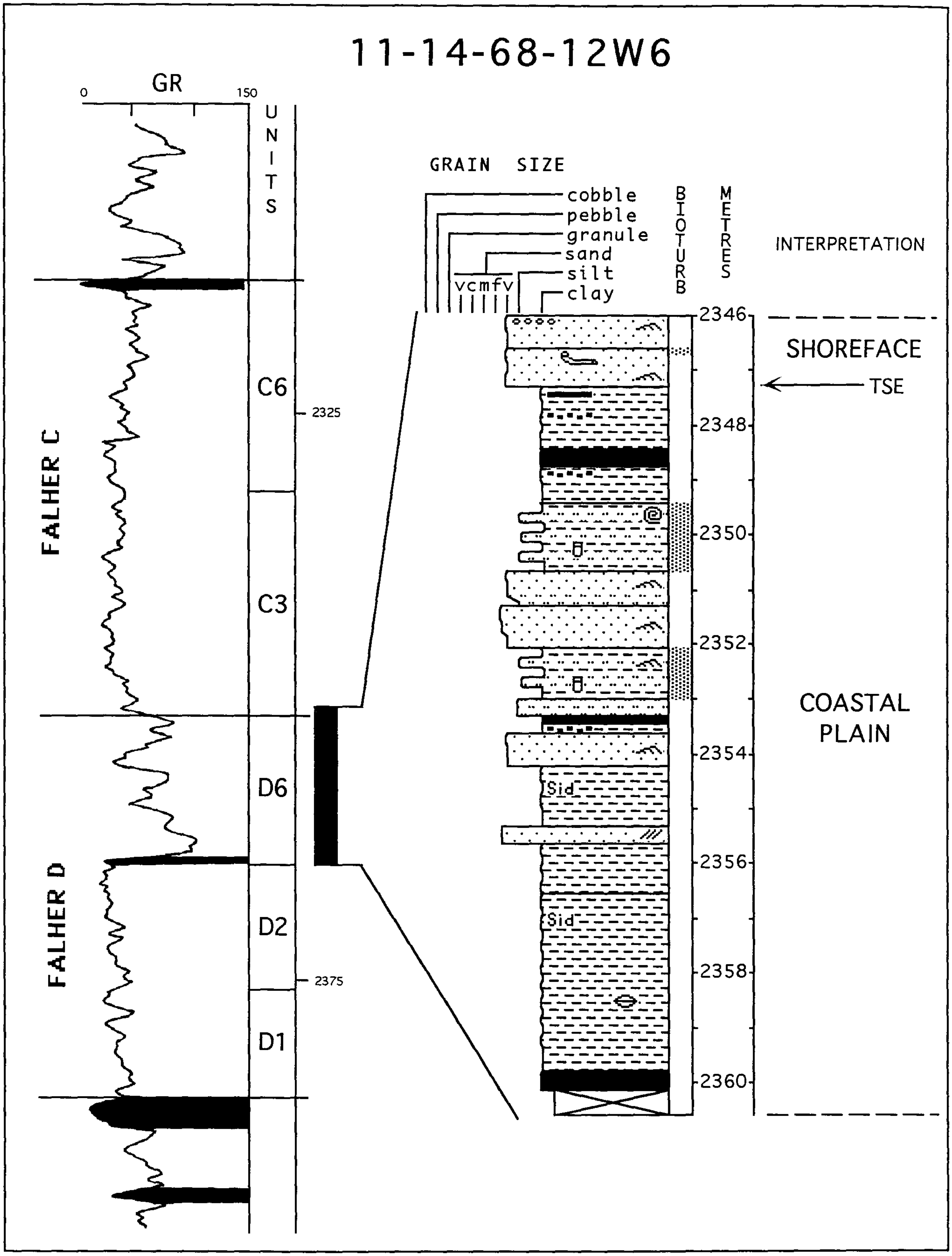

Appendix A16. Detailed sedimentary core log of 11-14-68-12W6. See Appendix A1 for legend and Figure 36 for location.

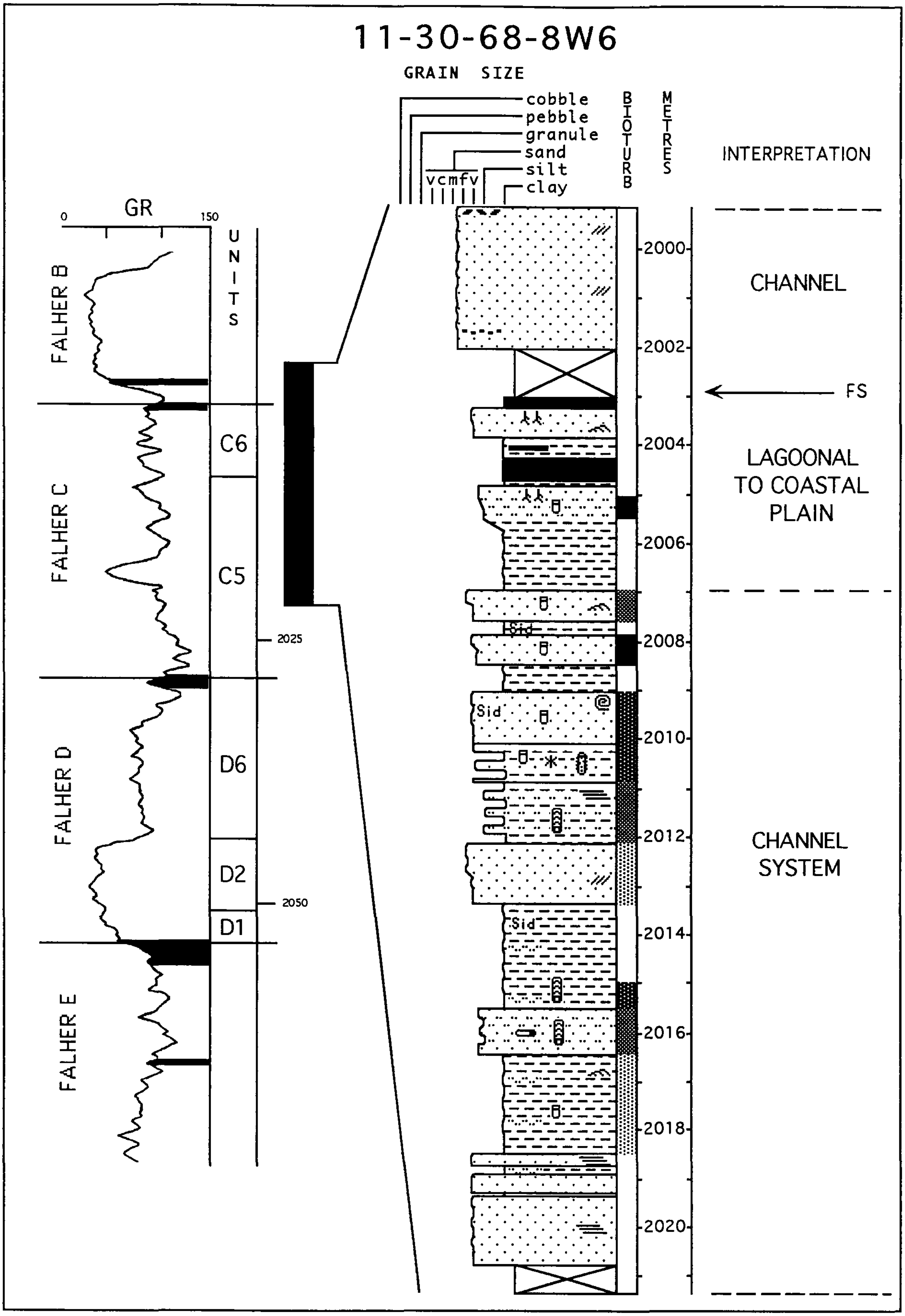

Appendix A17. Detailed sedimentary core log of 11-30-68-8W6. See Appendix A1 for legend and Figure 36 for location.

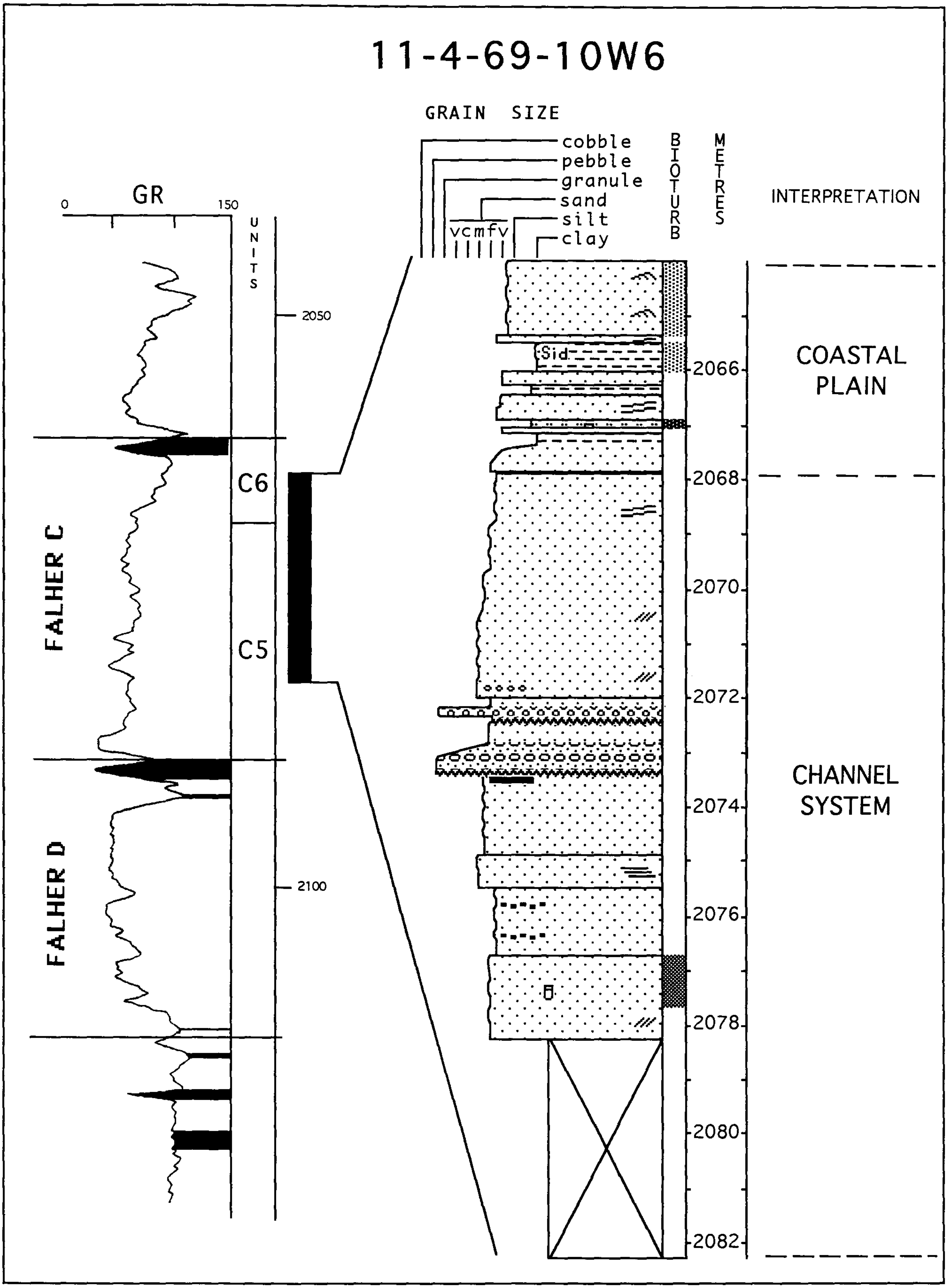

Appendix A18. Detailed sedimentary core log of 11-4-69-10W6. See Appendix A1 for legend and Figure 36 for location.

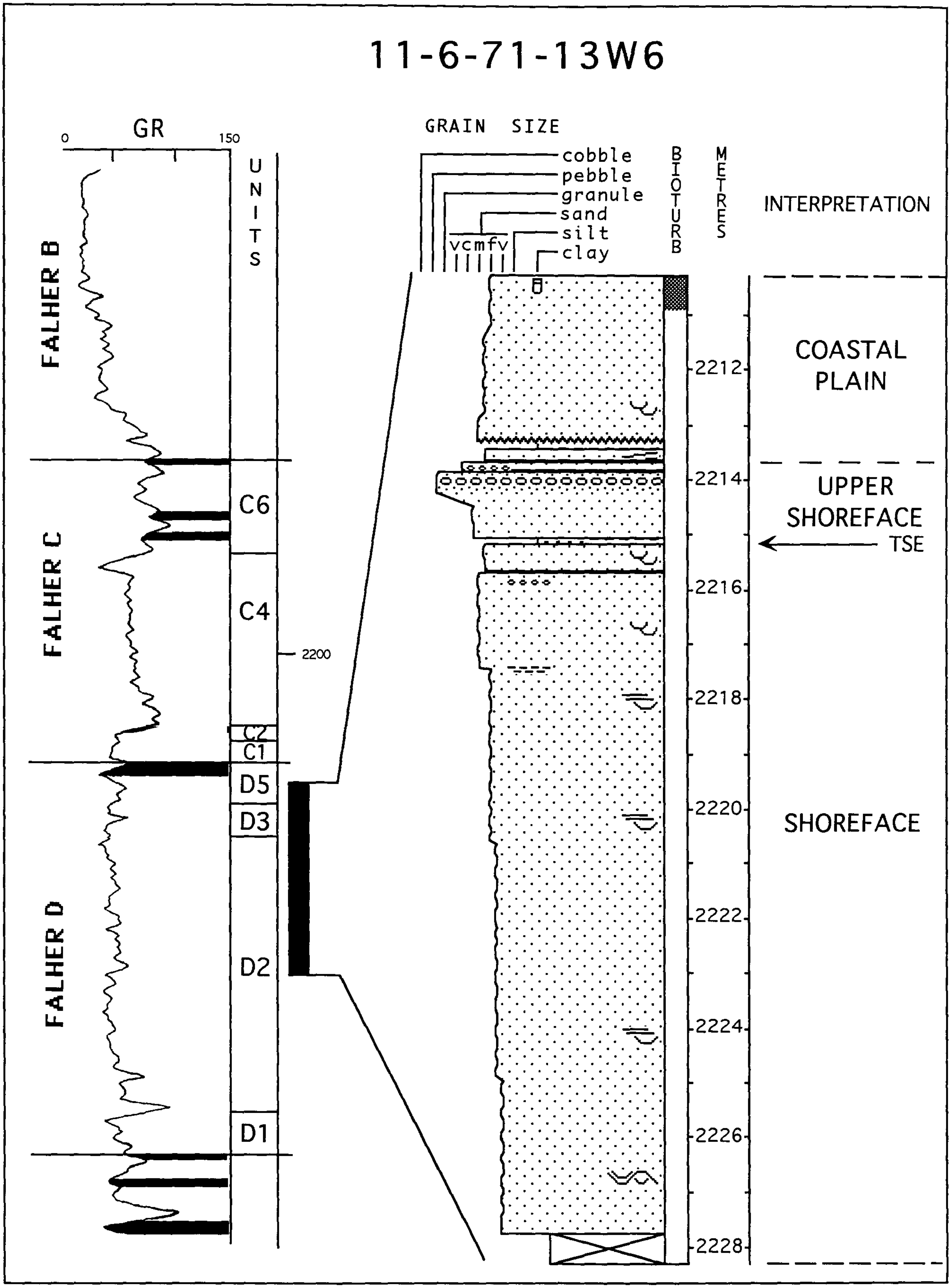

Appendix A19. Detailed sedimentary core log of 11-6-71-13W6. See Appendix A1 for legend and Figure 36 for location.

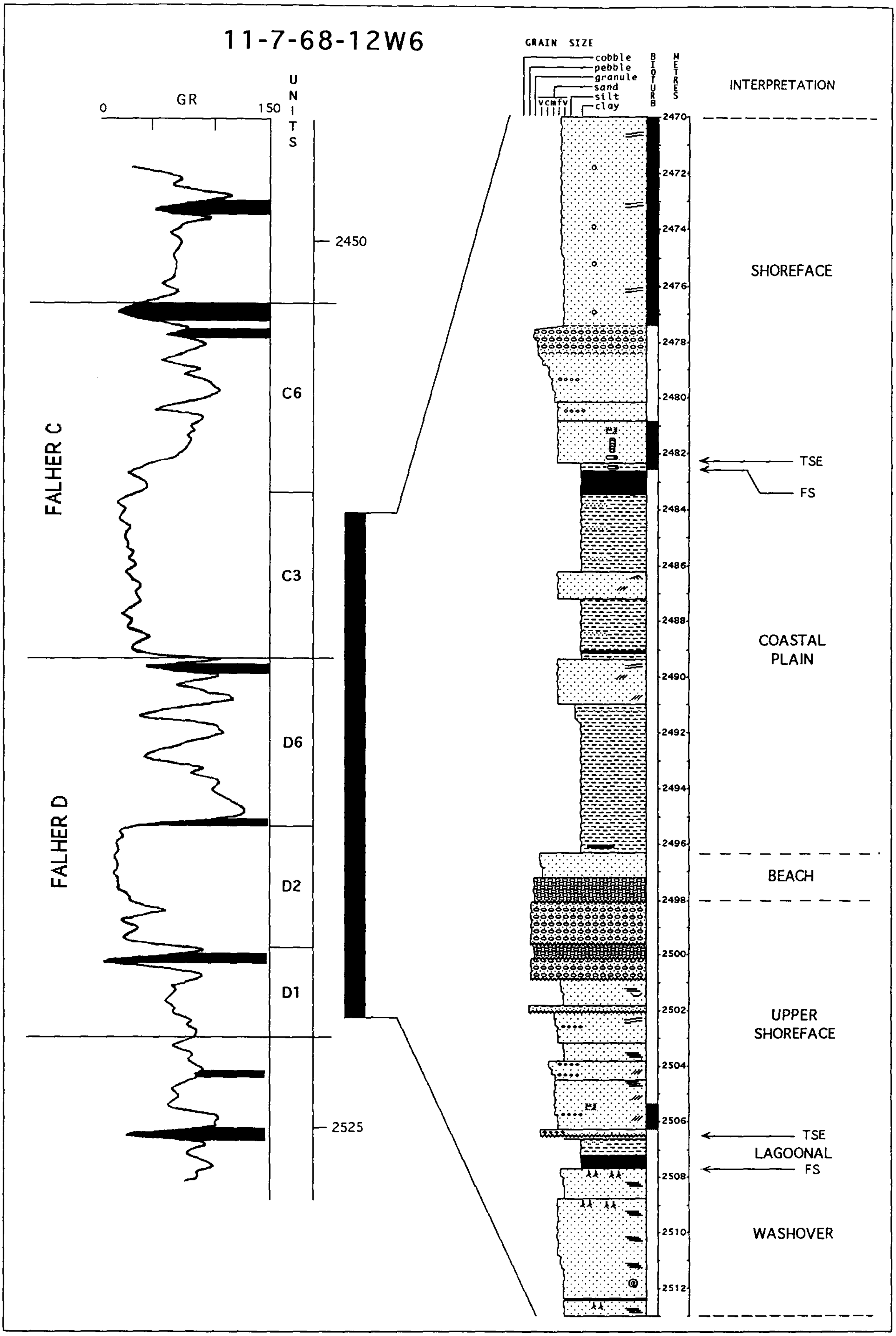

Appendix A20. Detailed sedimentary core log of 11-7-68-12W6.
See Appendix A1 for legend and Figure 36 for location.

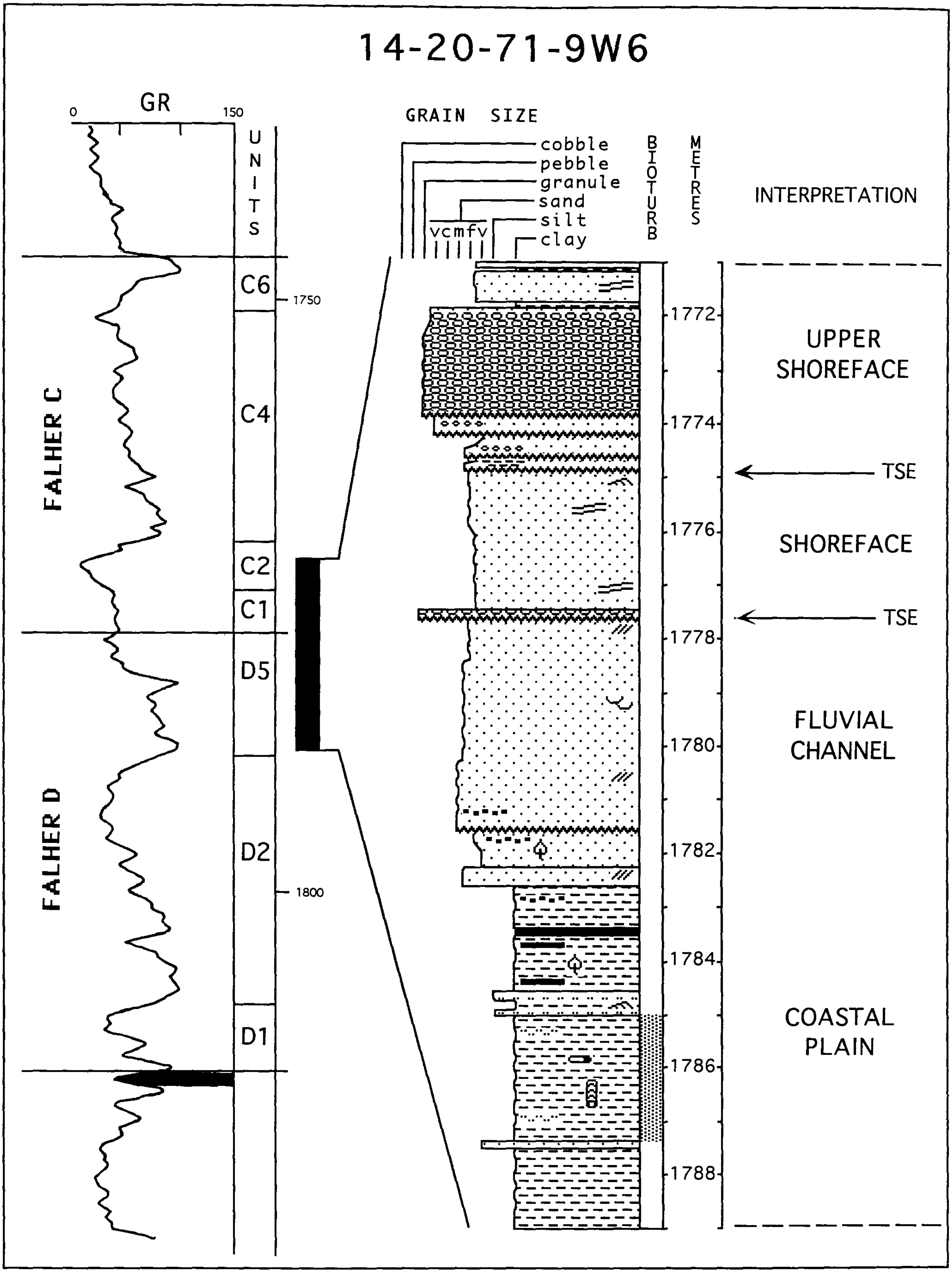

Appendix A21. Detailed sedimentary core log of 14-20-71-9W6. See Appendix A1 for legend and Figure 36 for location.

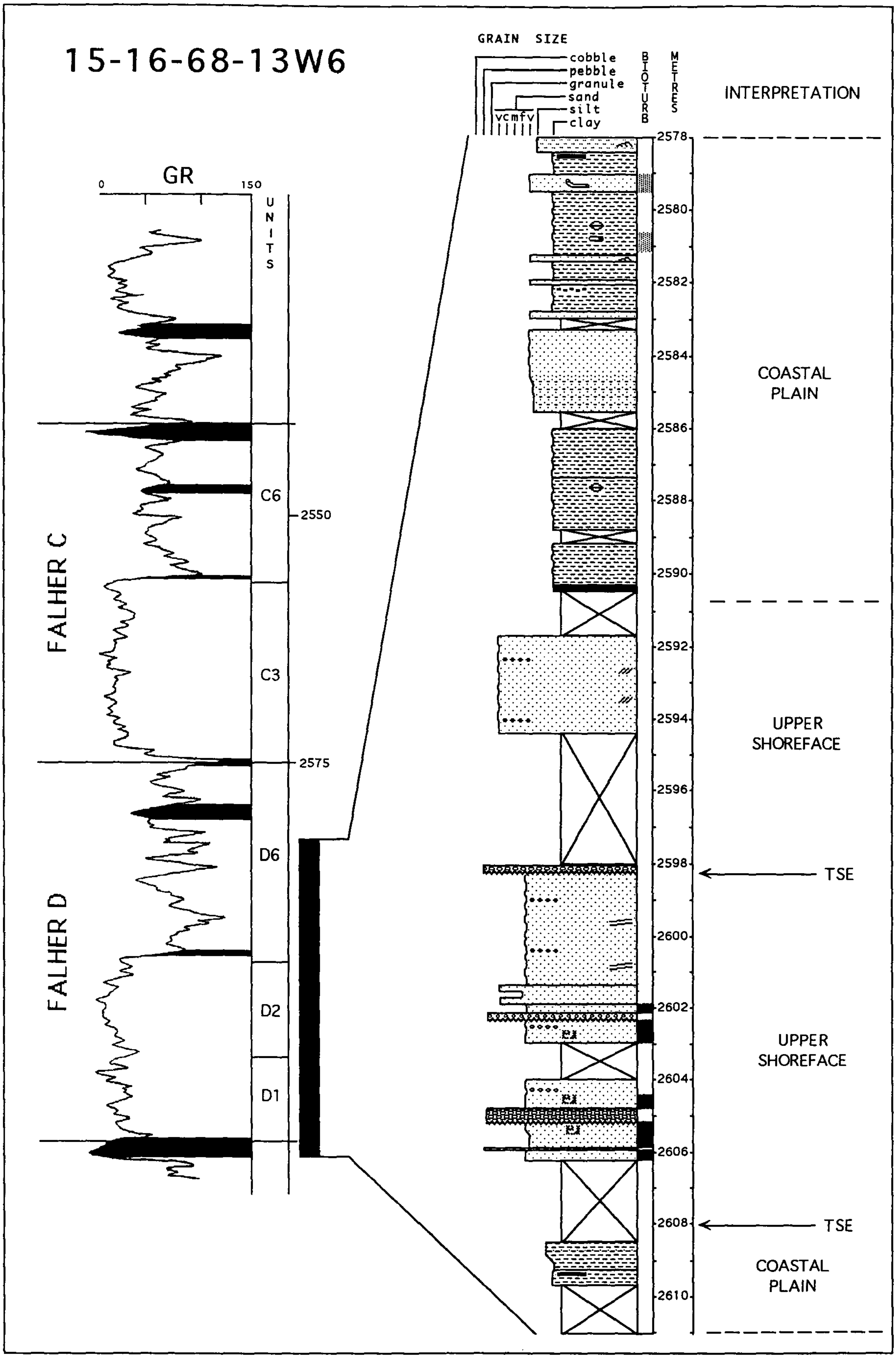

Appendix A22. Detailed sedimentary core log of 15-16-68-13W6. See Appendix A1 for legend and Figure 36 for location.

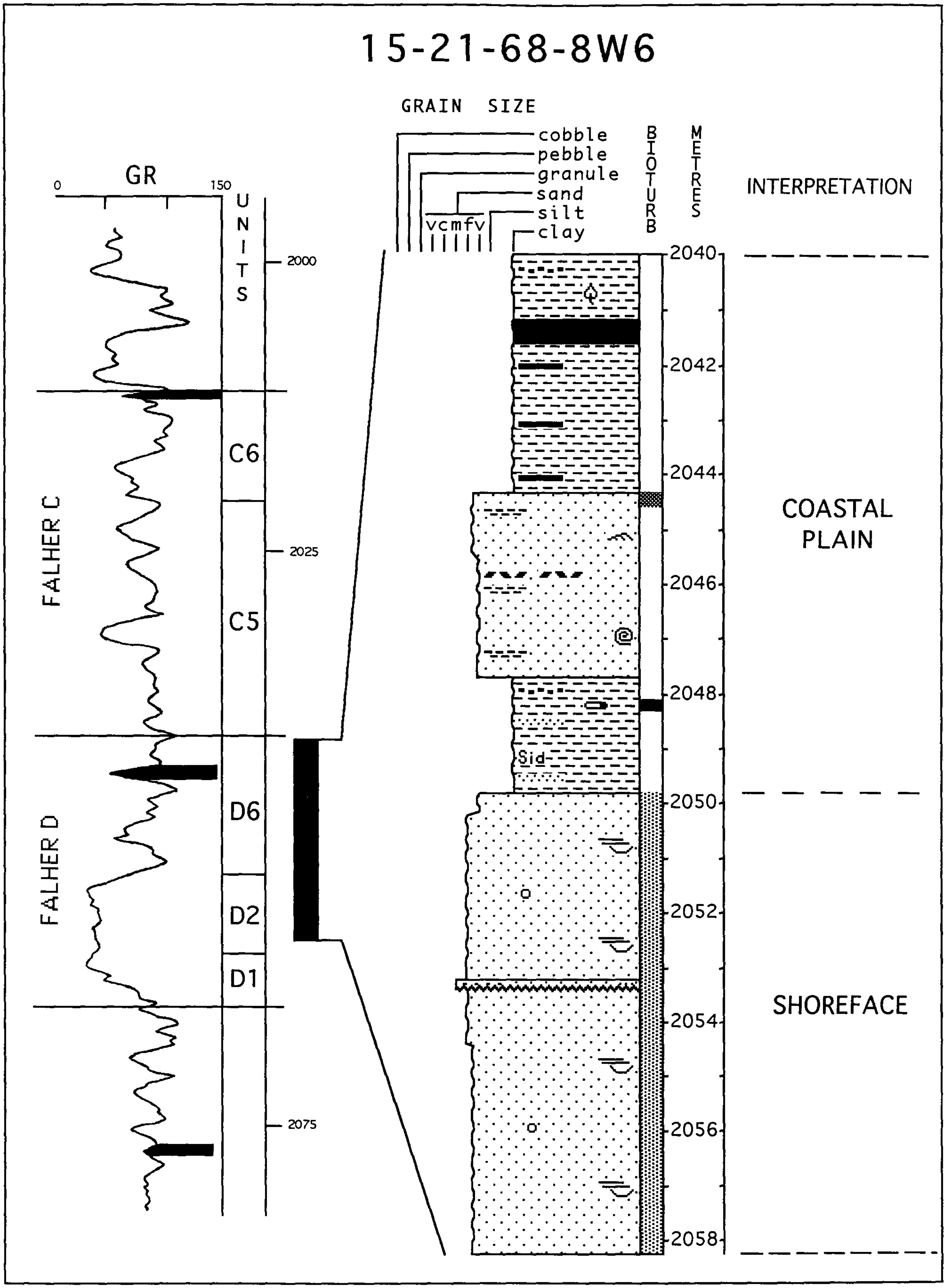

Appendix A23. Detailed sedimentary core log of 15-21-68-8W6. See Appendix A1 for legend and Figure 36 for location.

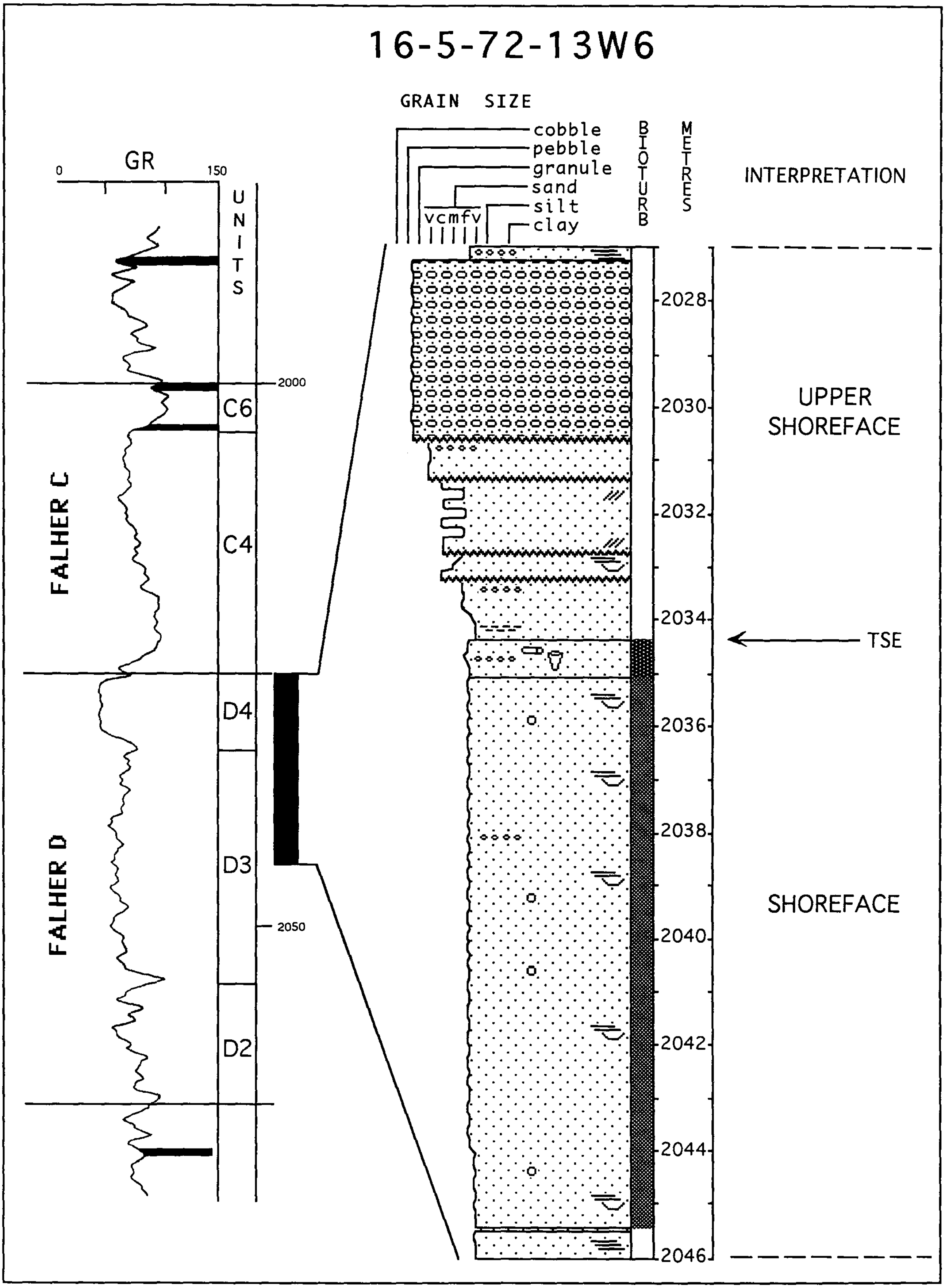

Appendix A24. Detailed sedimentary core log of 16-5-72-13W6. See Appendix A1 for legend and Figure 36 for location.

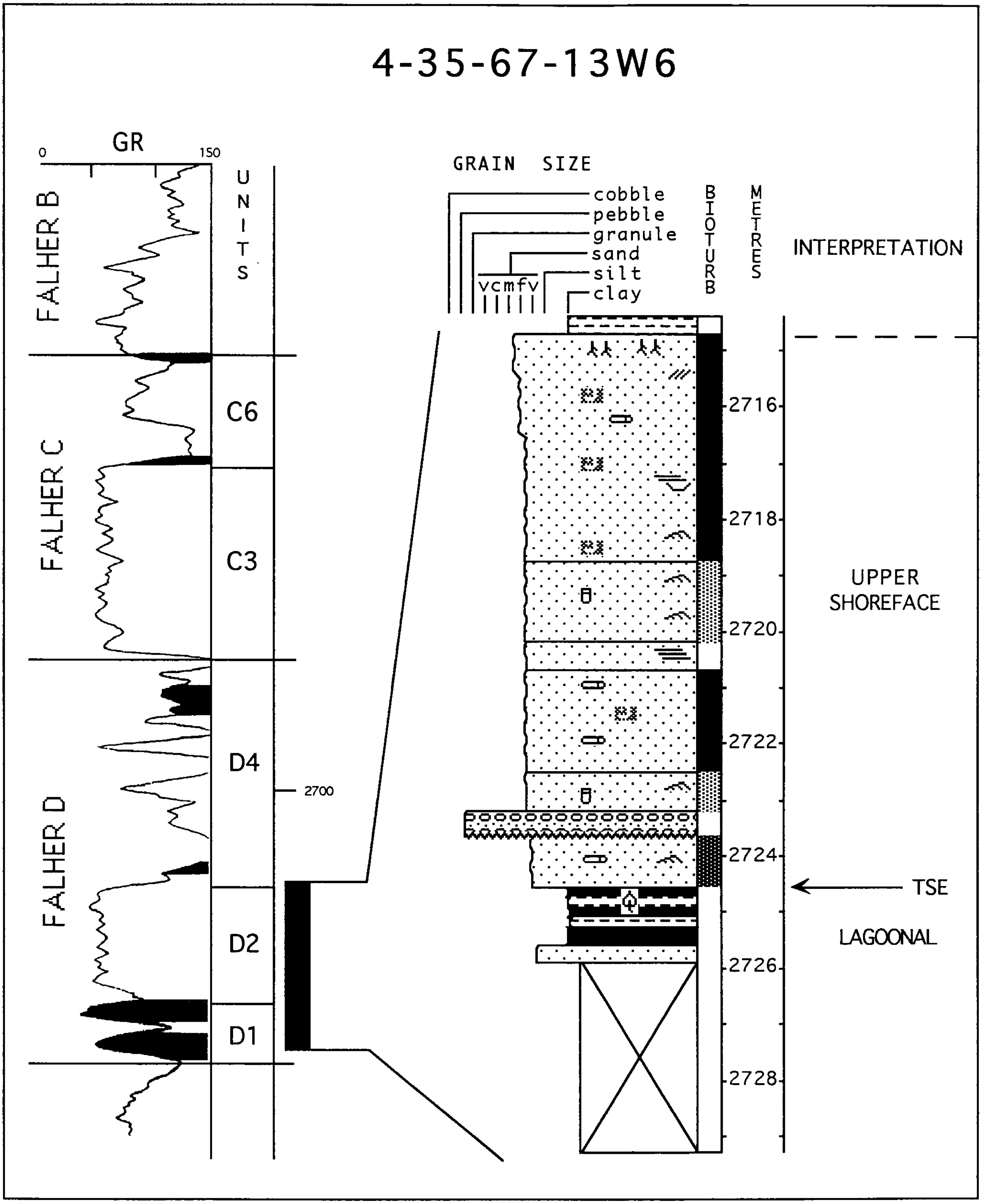

Appendix A25. Detailed sedimentary core log of 4-35-67-13W6. See Appendix A1 for legend and Figure 36 for location.

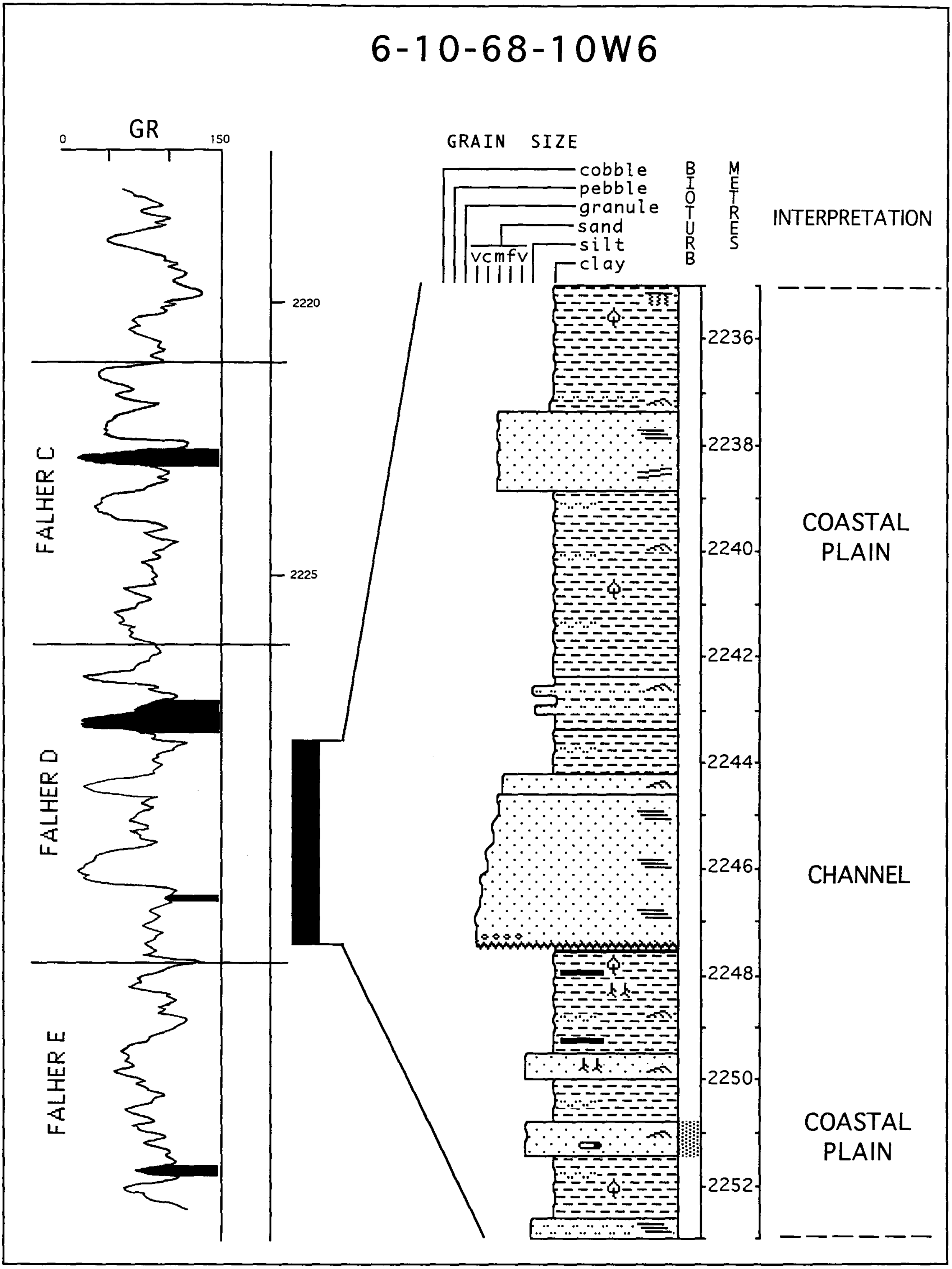

Appendix A26. Detailed sedimentary core log of 6-10-68-10W6. See Appendix A1 for legend and Figure 36 for location.

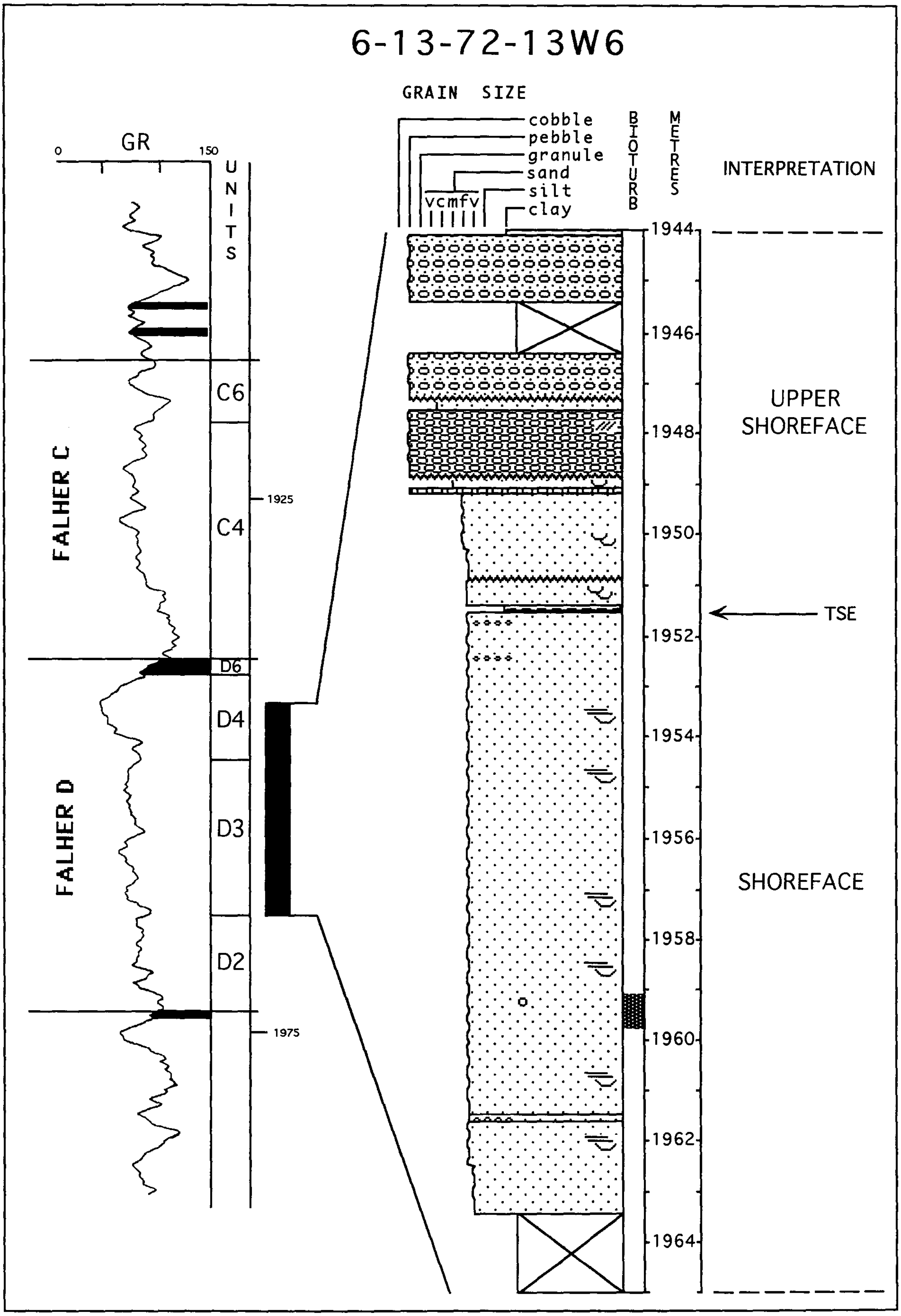

Appendix A27. Detailed sedimentary core log of 6-13-72-13W6. See Appendix A1 for legend and Figure 36 for location.

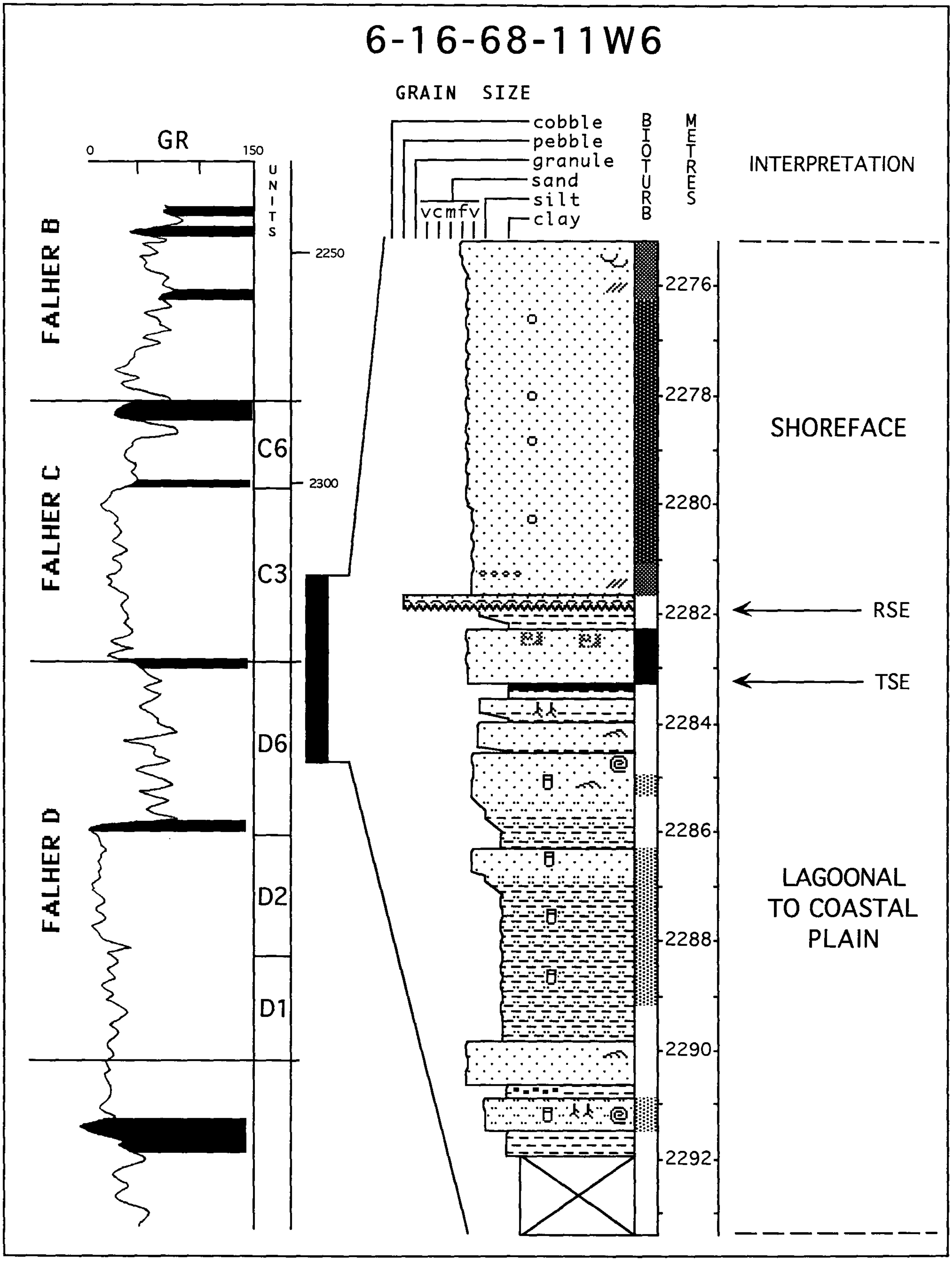

Appendix A28. Detailed sedimentary core log of 6-16-68-11W6. See Appendix A1 for legend and Figure 36 for location.

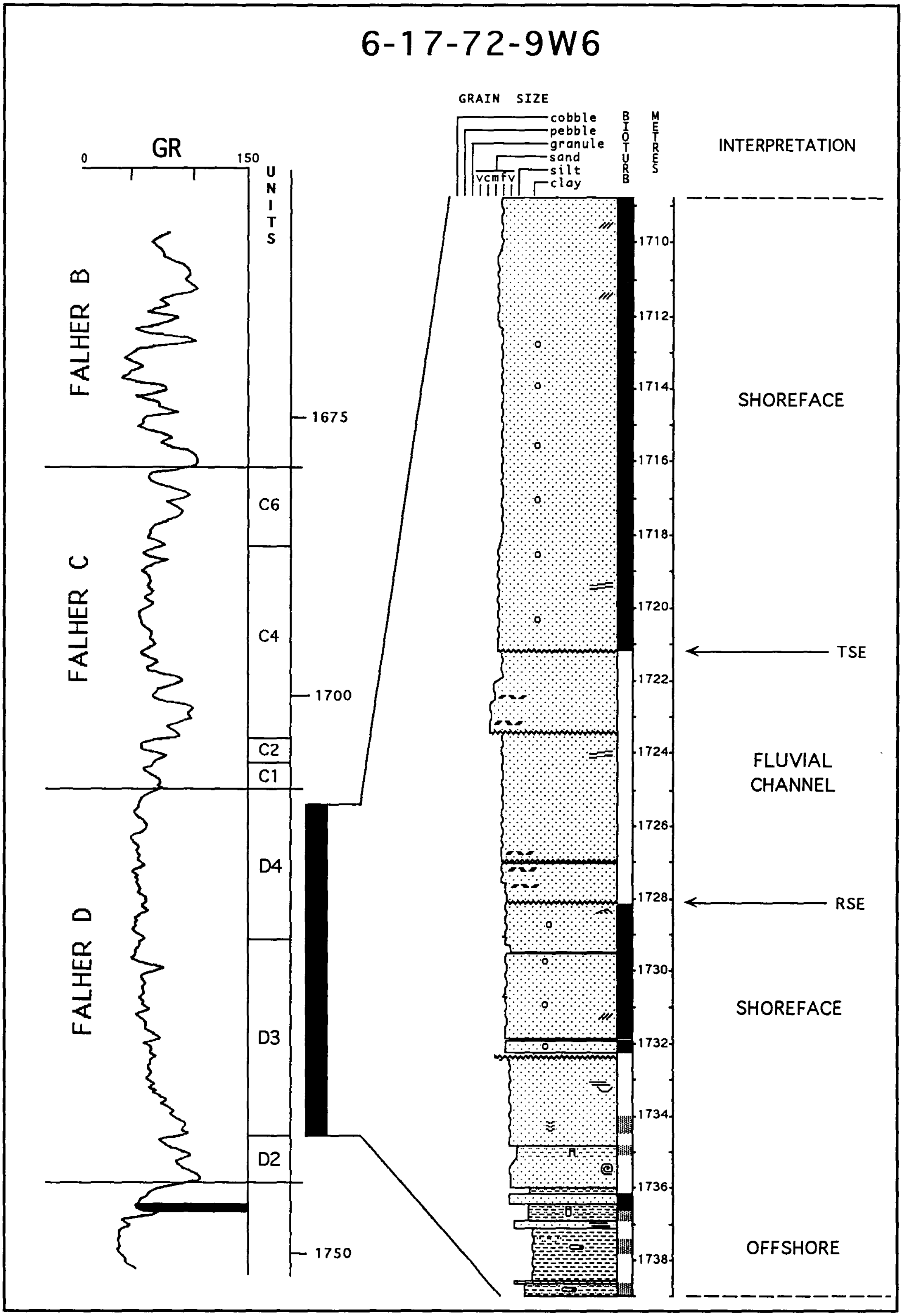

Appendix A29. Detailed sedimentary core log of 6-17-72-9W6. See Appendix A1 for legend and Figure 36 for location.

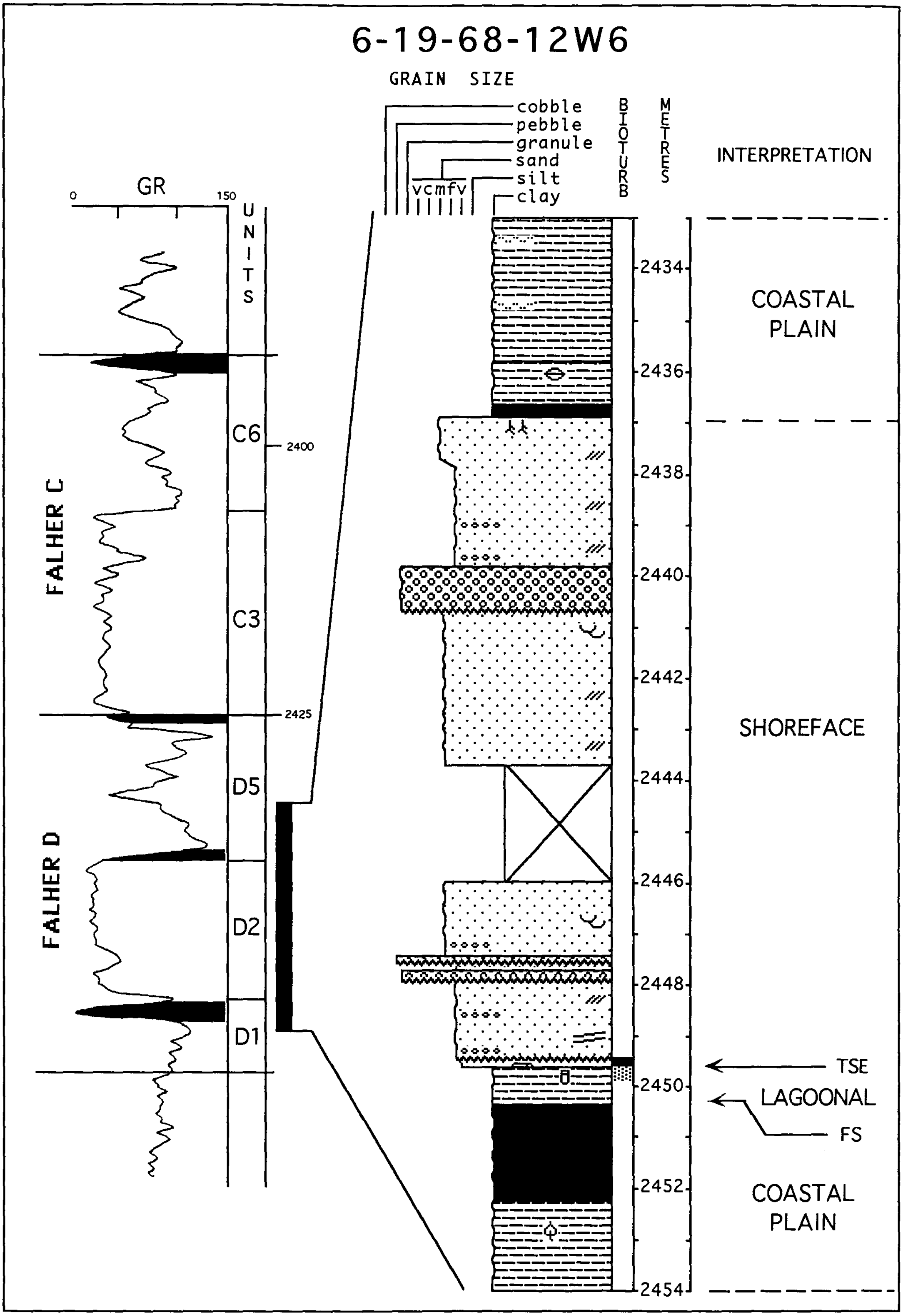

Appendix A30. Detailed sedimentary core log of 6-19-68-12W6.
See Appendix A1 for legend and Figure 36 for location.

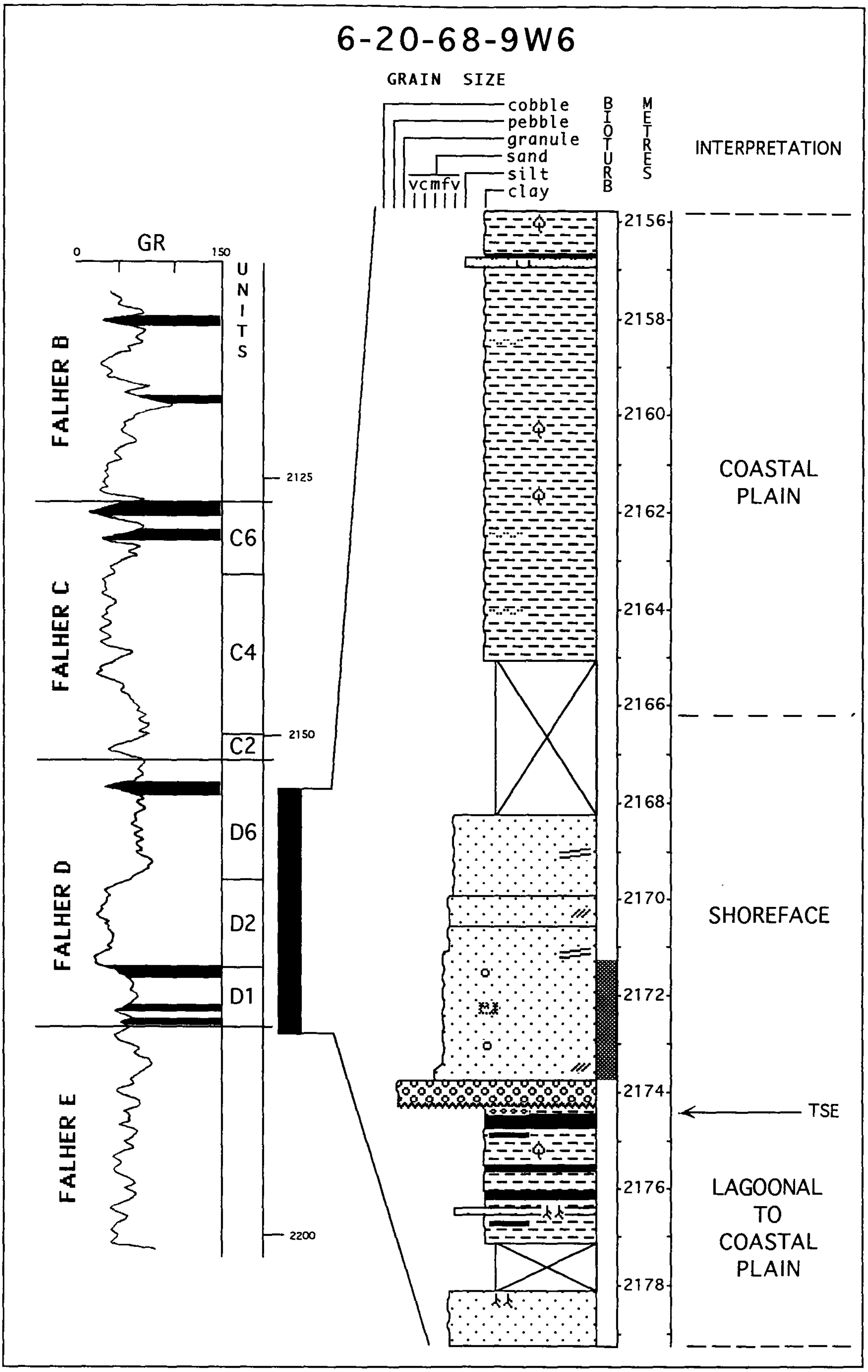

Appendix A31. Detailed sedimentary core log of 6-20-68-9W6. See Appendix A1 for legend and Figure 36 for location.

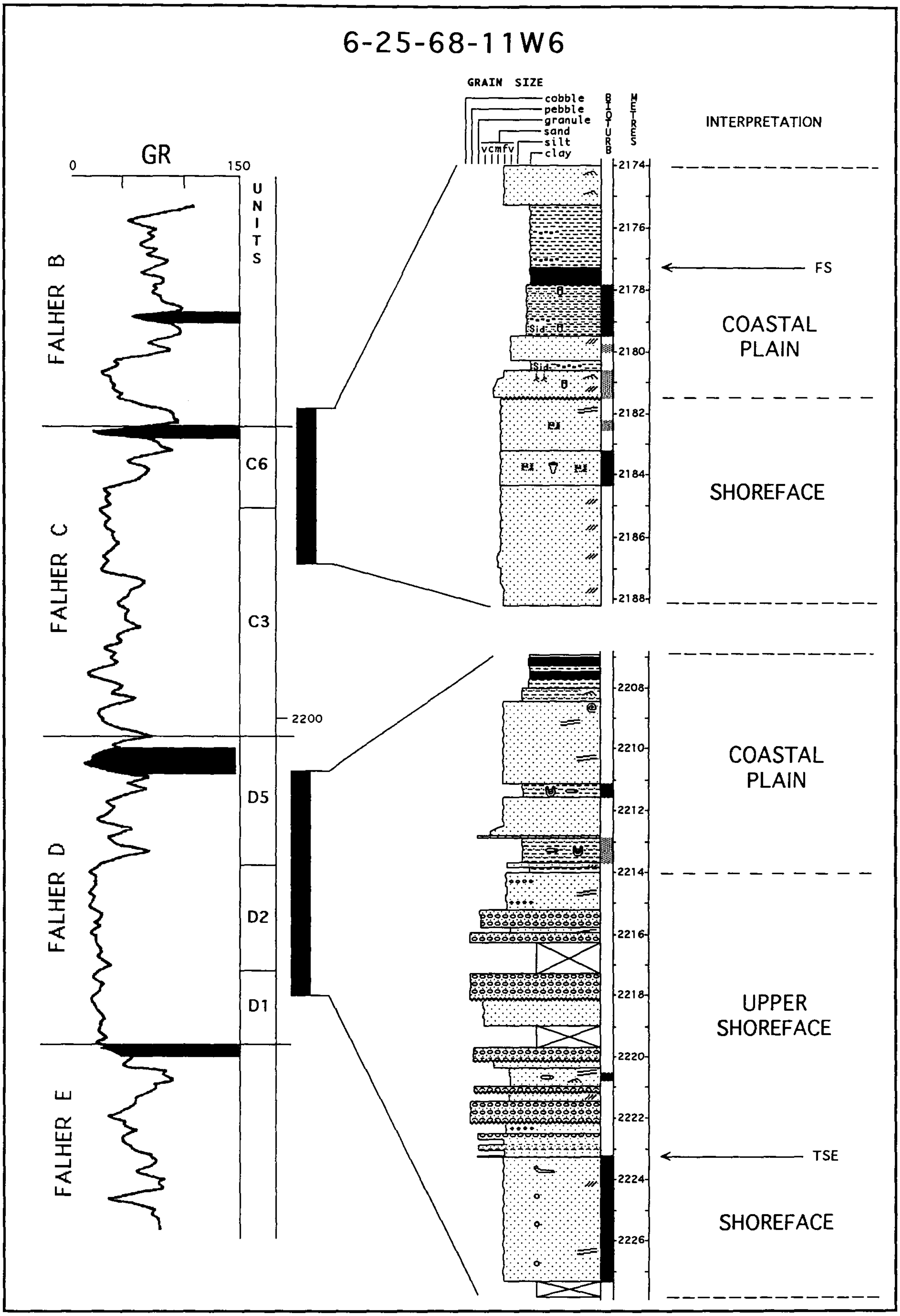

Appendix A32. Detailed sedimentary core log of 6-25-68-11W6.
See Appendix A1 for legend and Figure 36 for location.

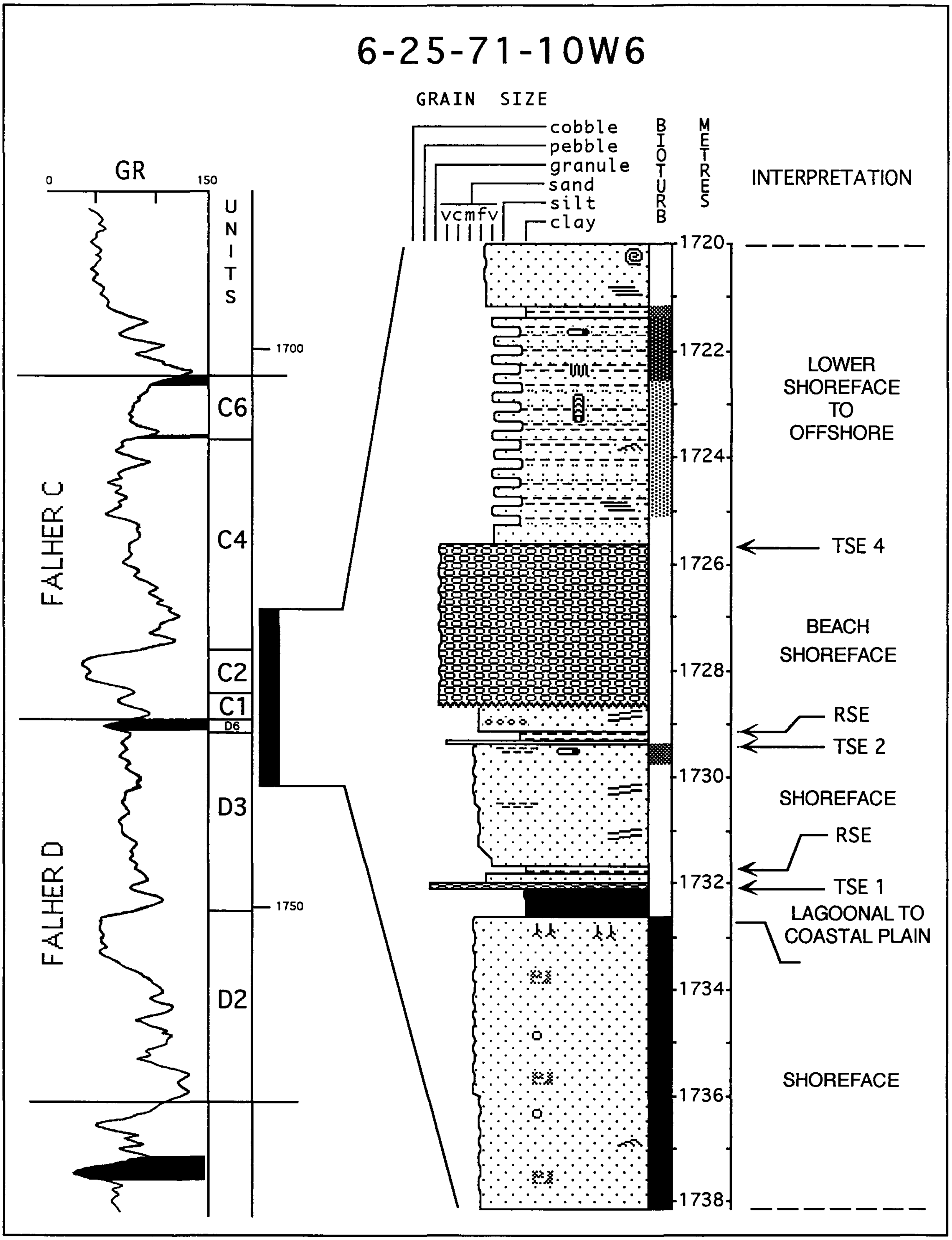

Appendix A33. Detailed sedimentary core log of 6-25-71-10W6. See Appendix A1 for legend and Figure 36 for location.

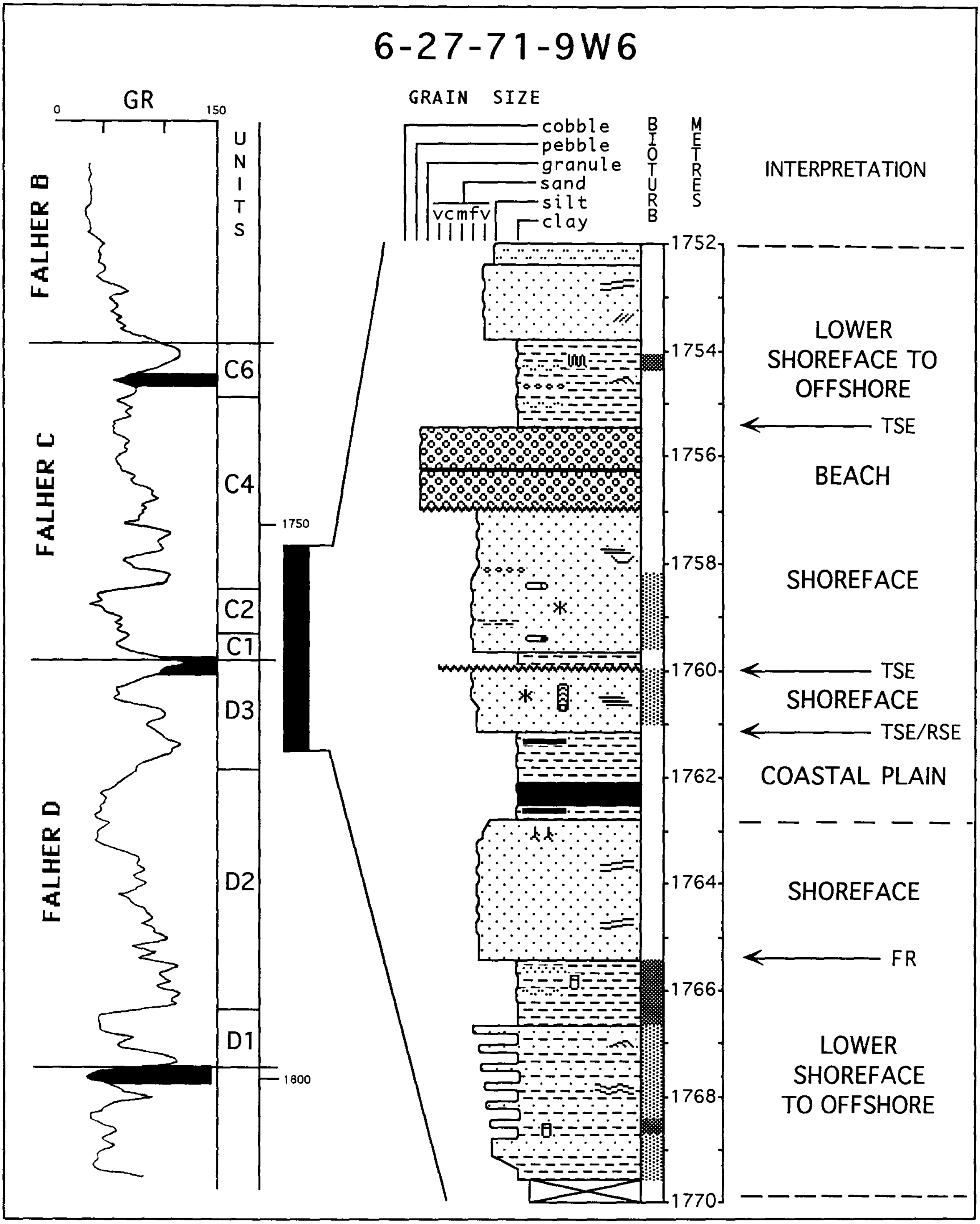

Appendix A34. Detailed sedimentary core log of 6-27-71-9W6. See Appendix A1 for legend and Figure 36 for location.

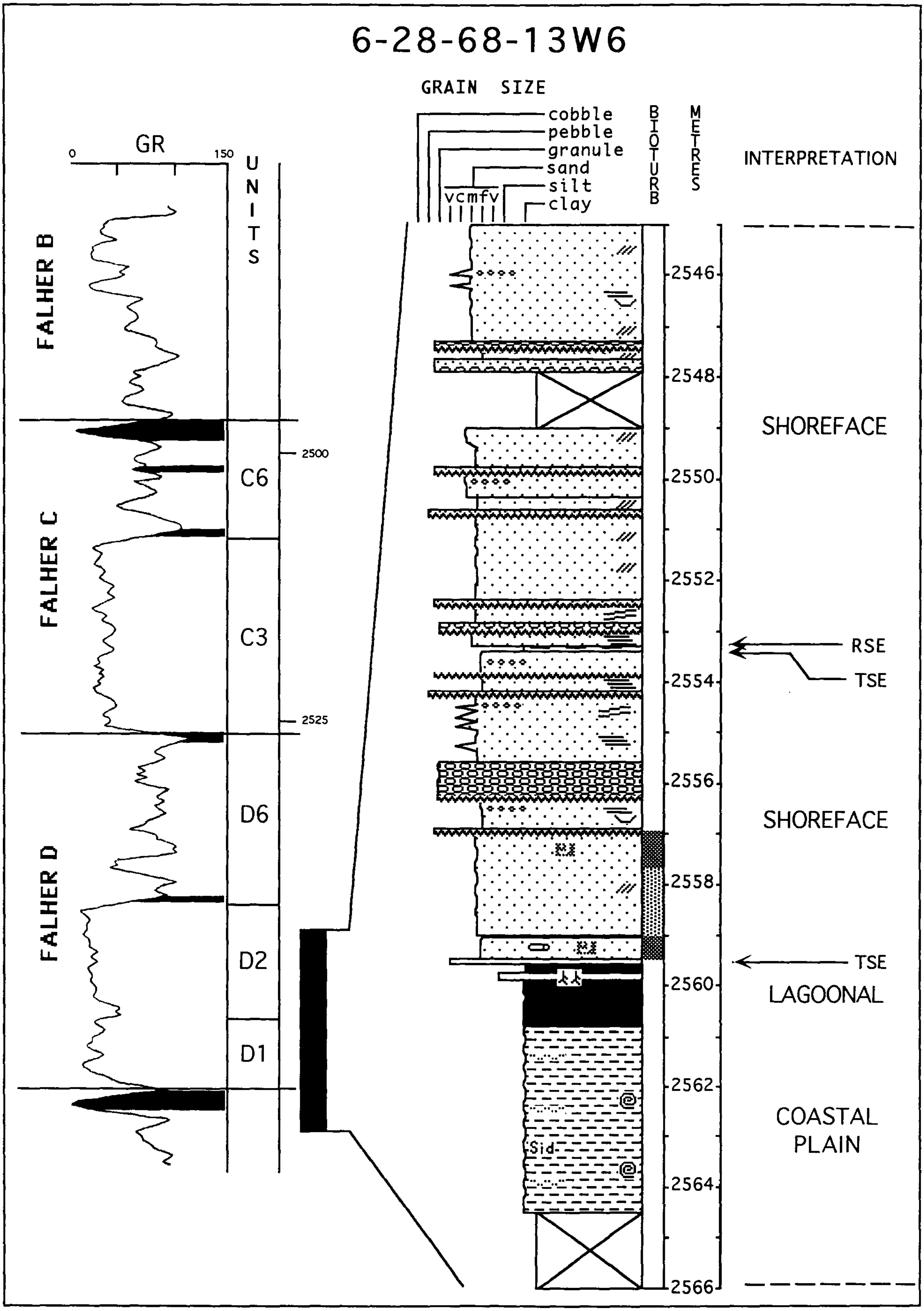

Appendix A35. Detailed sedimentary core log of 6-28-68-13W6. See Appendix A1 for legend and Figure 36 for location.

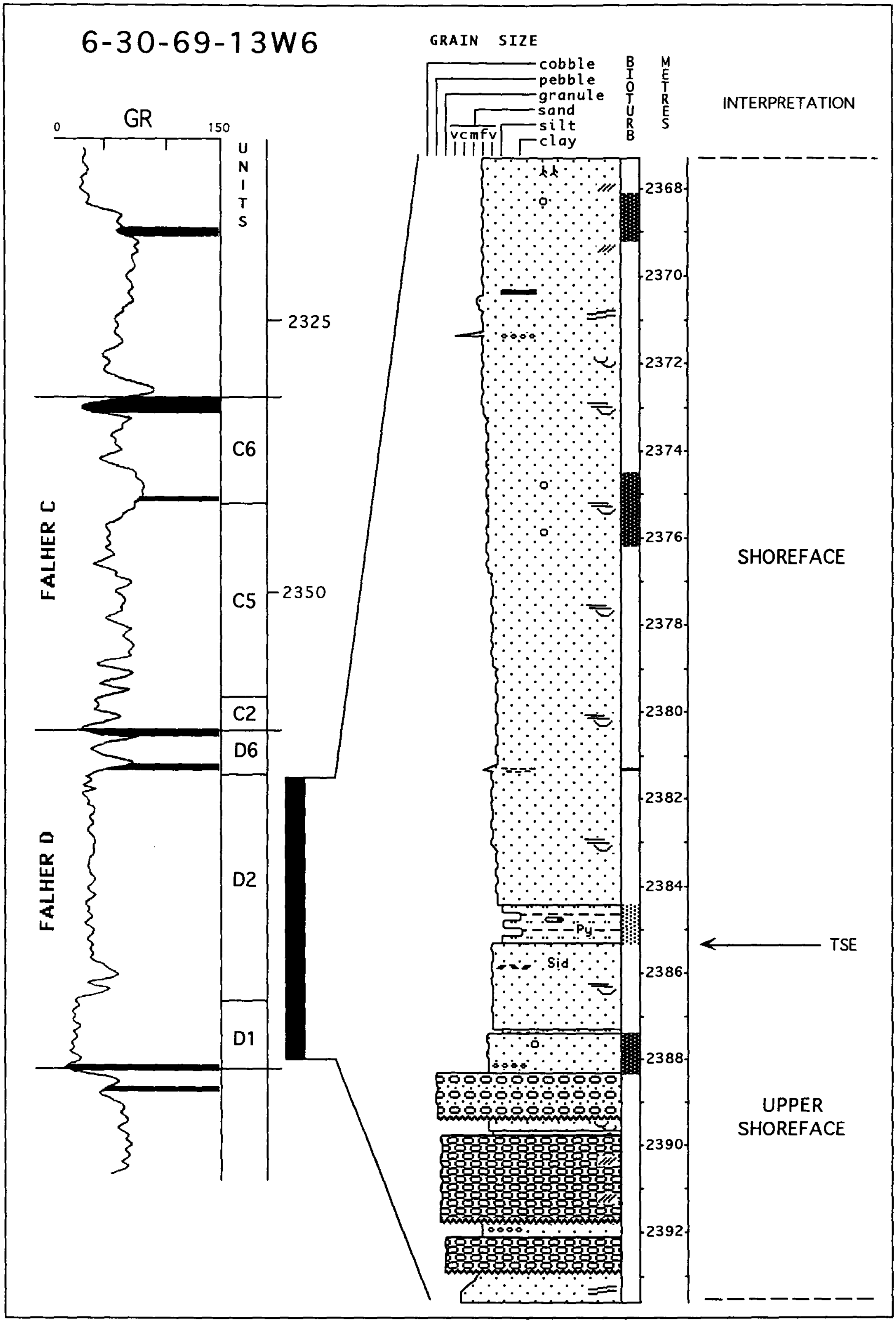

Appendix A36. Detailed sedimentary core log of 6-30-69-13W6. See Appendix A1 for legend and Figure 36 for location.

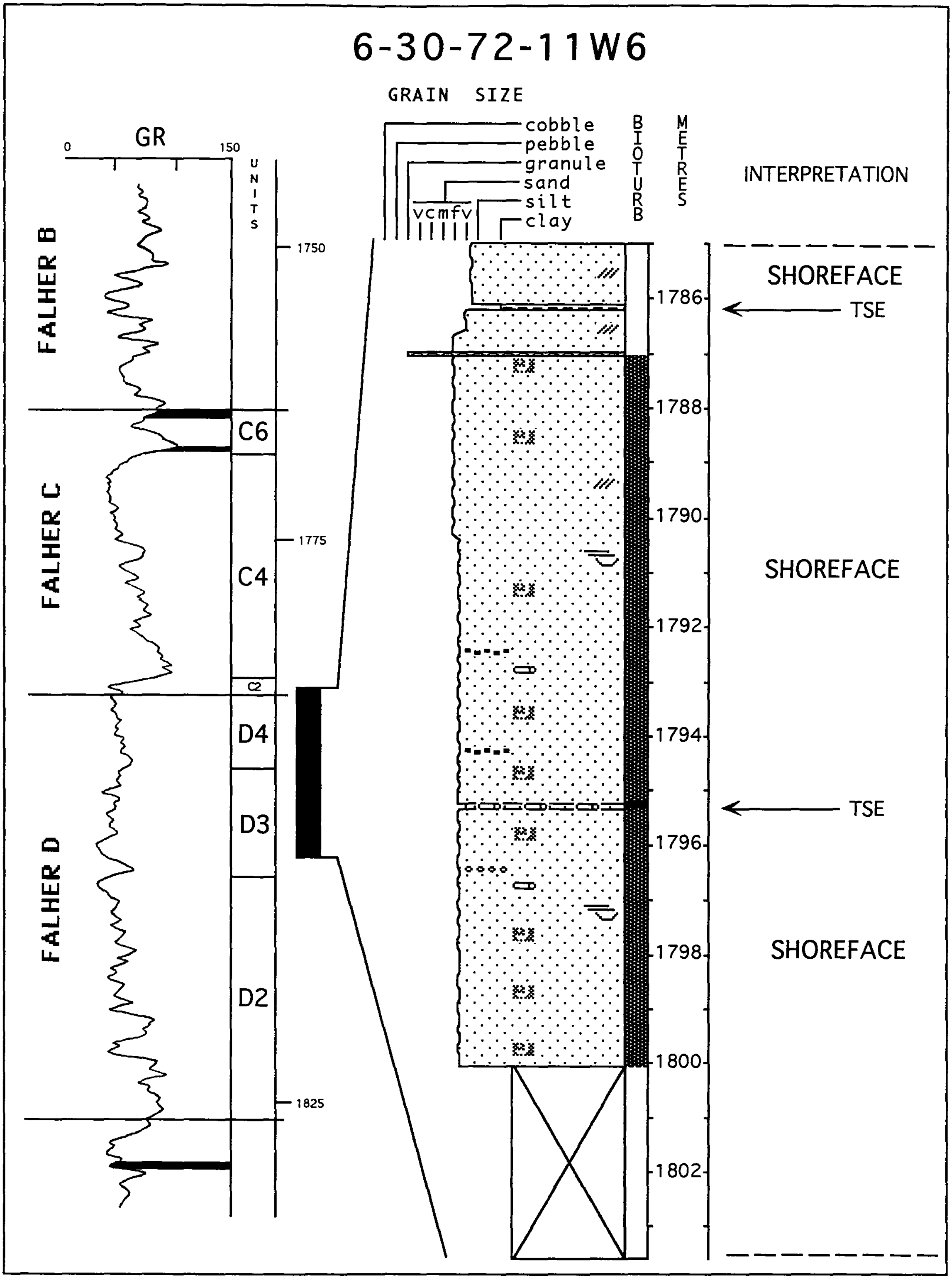

Appendix A37. Detailed sedimentary core log of 6-30-72-11W6. See Appendix A1 for legend and Figure 36 for location.

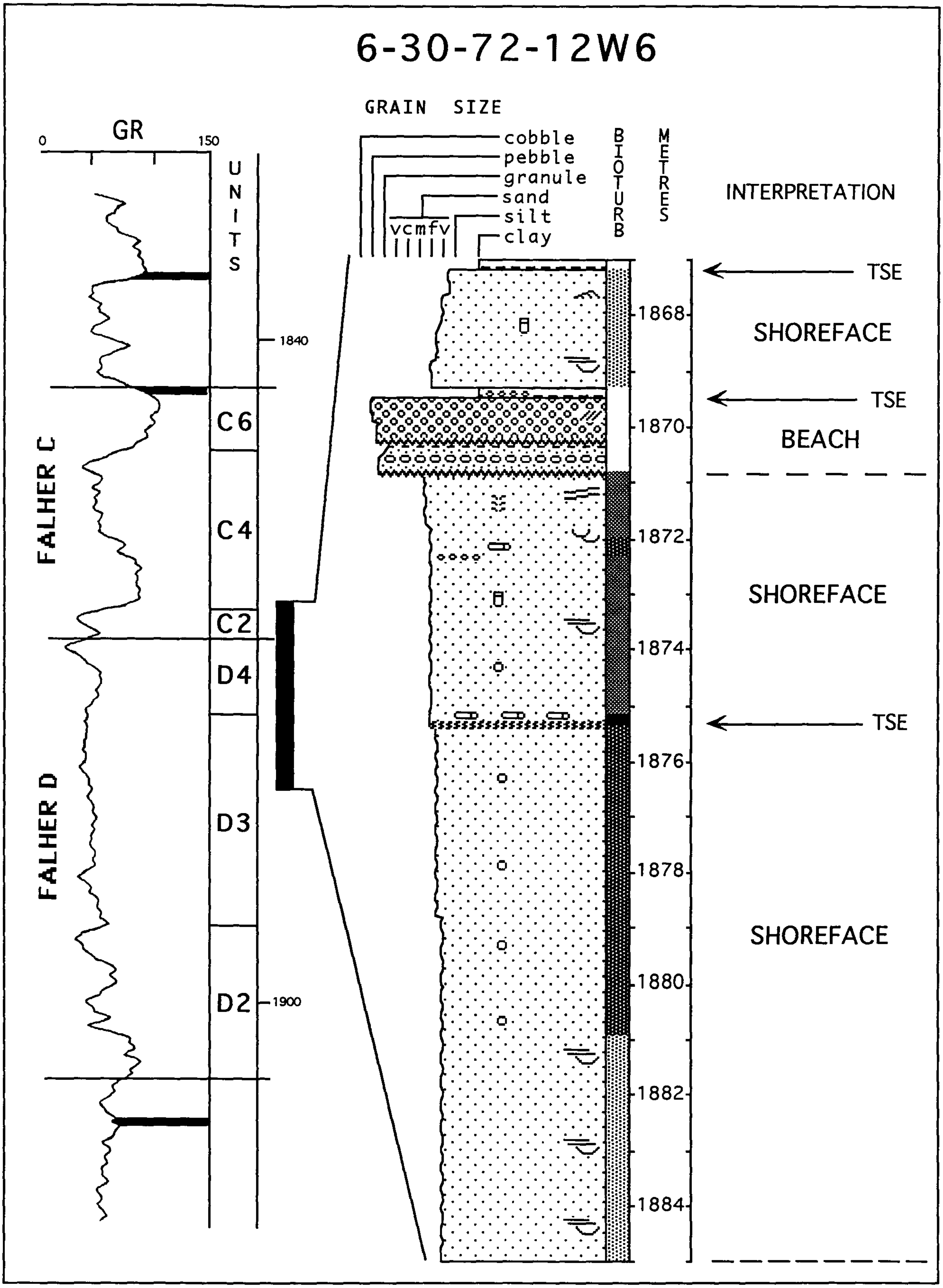

Appendix A38. Detailed sedimentary core log of 6-30-72-12W6. See Appendix A1 for legend and Figure 36 for location.

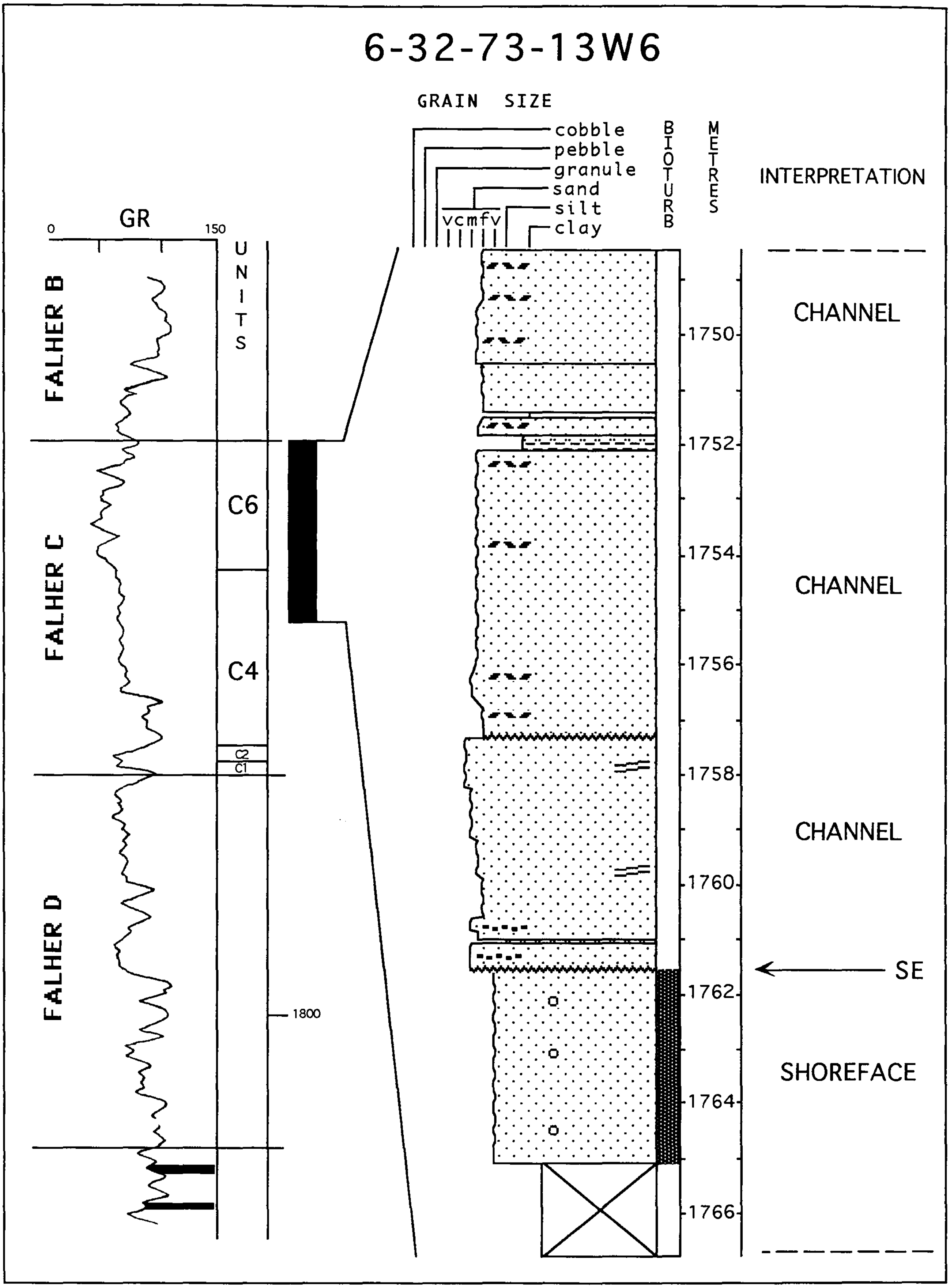

Appendix A39. Detailed sedimentary core log of 6-32-73-13W6. See Appendix A1 for legend and Figure 36 for location.

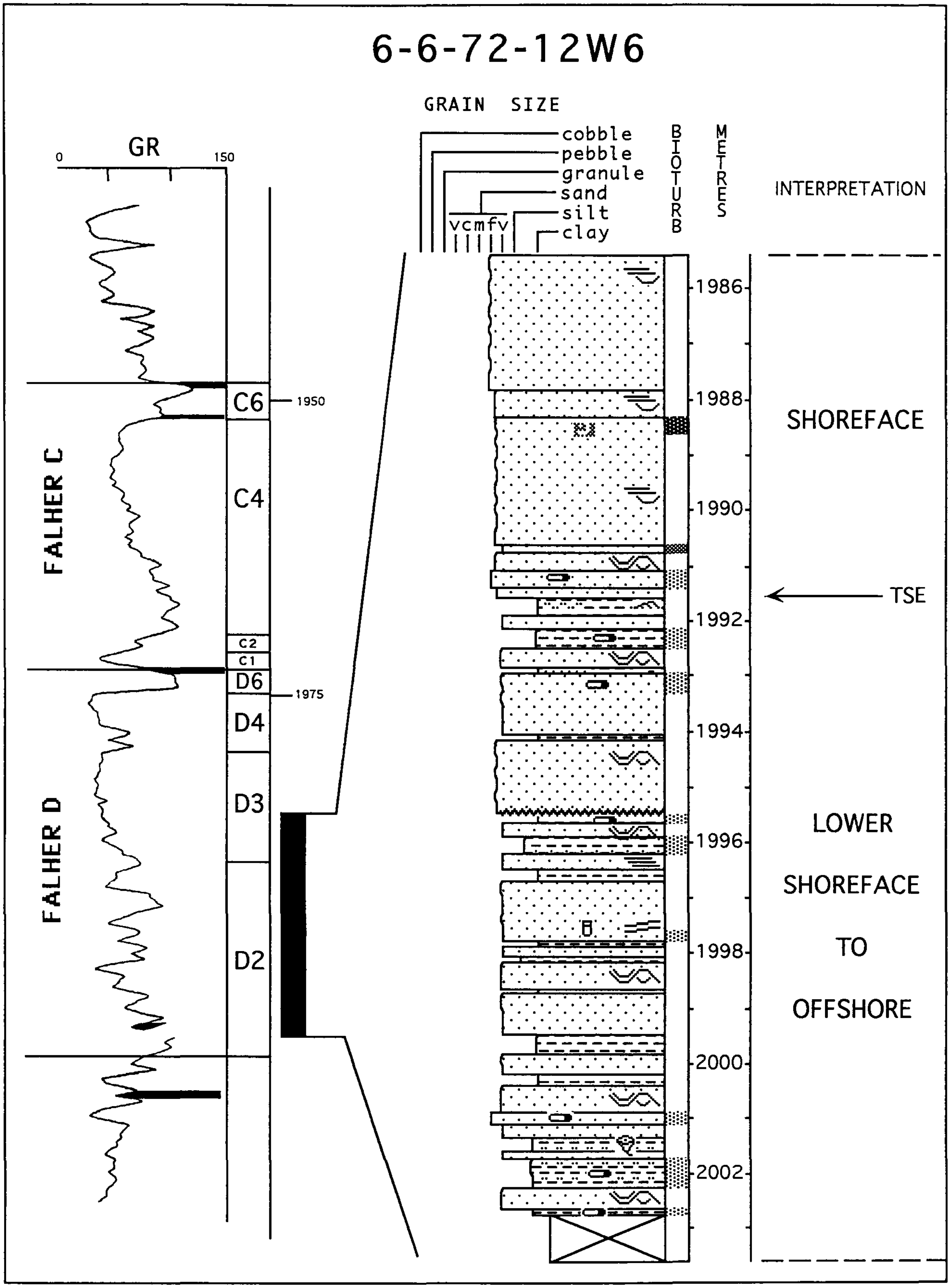

Appendix A40. Detailed sedimentary core log of 6-6-72-12W6. See Appendix A1 for legend and Figure 36 for location.

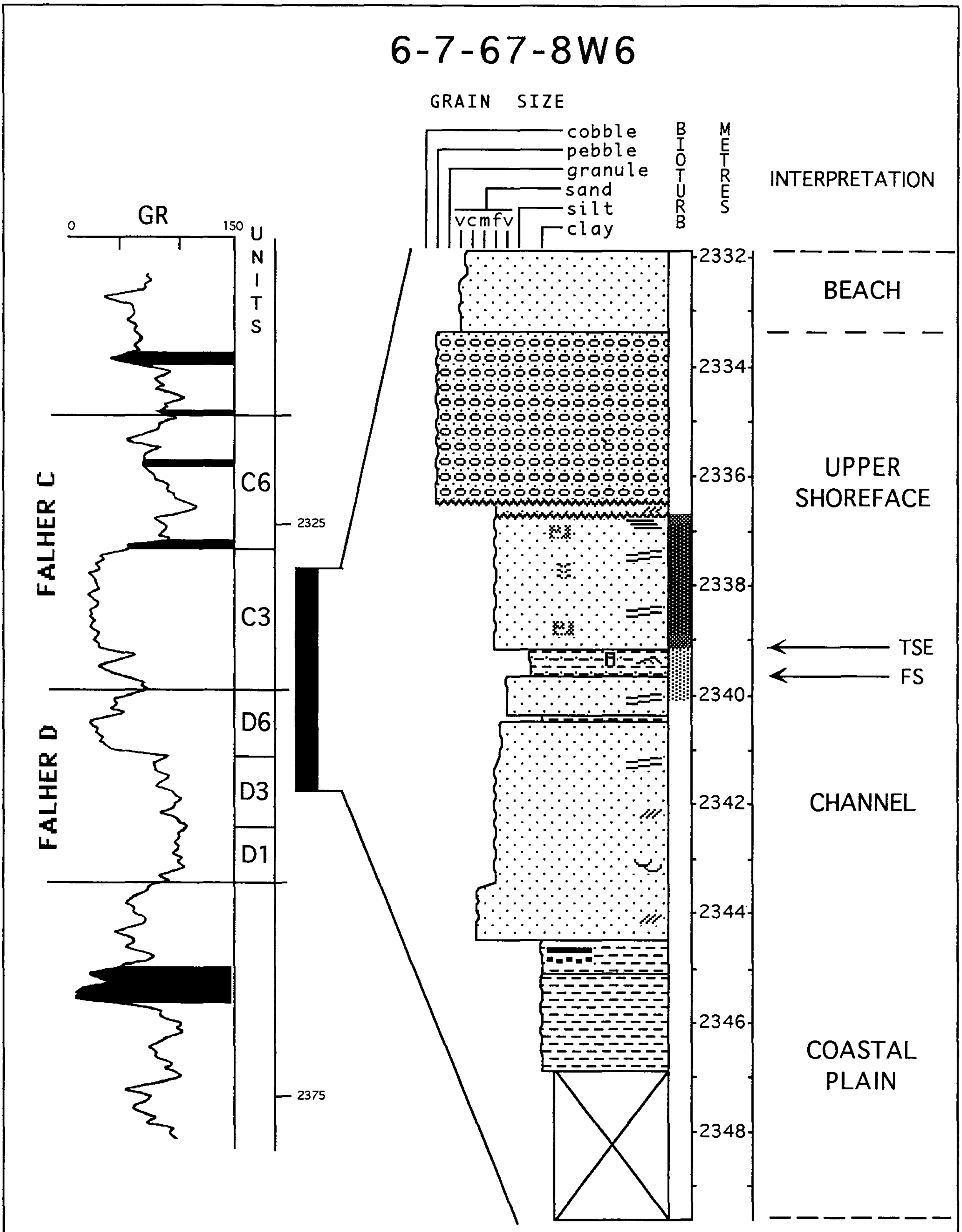

Appendix A41. Detailed sedimentary core log of 6-7-67-8W6. See Appendix A1 for legend and Figure 36 for location.

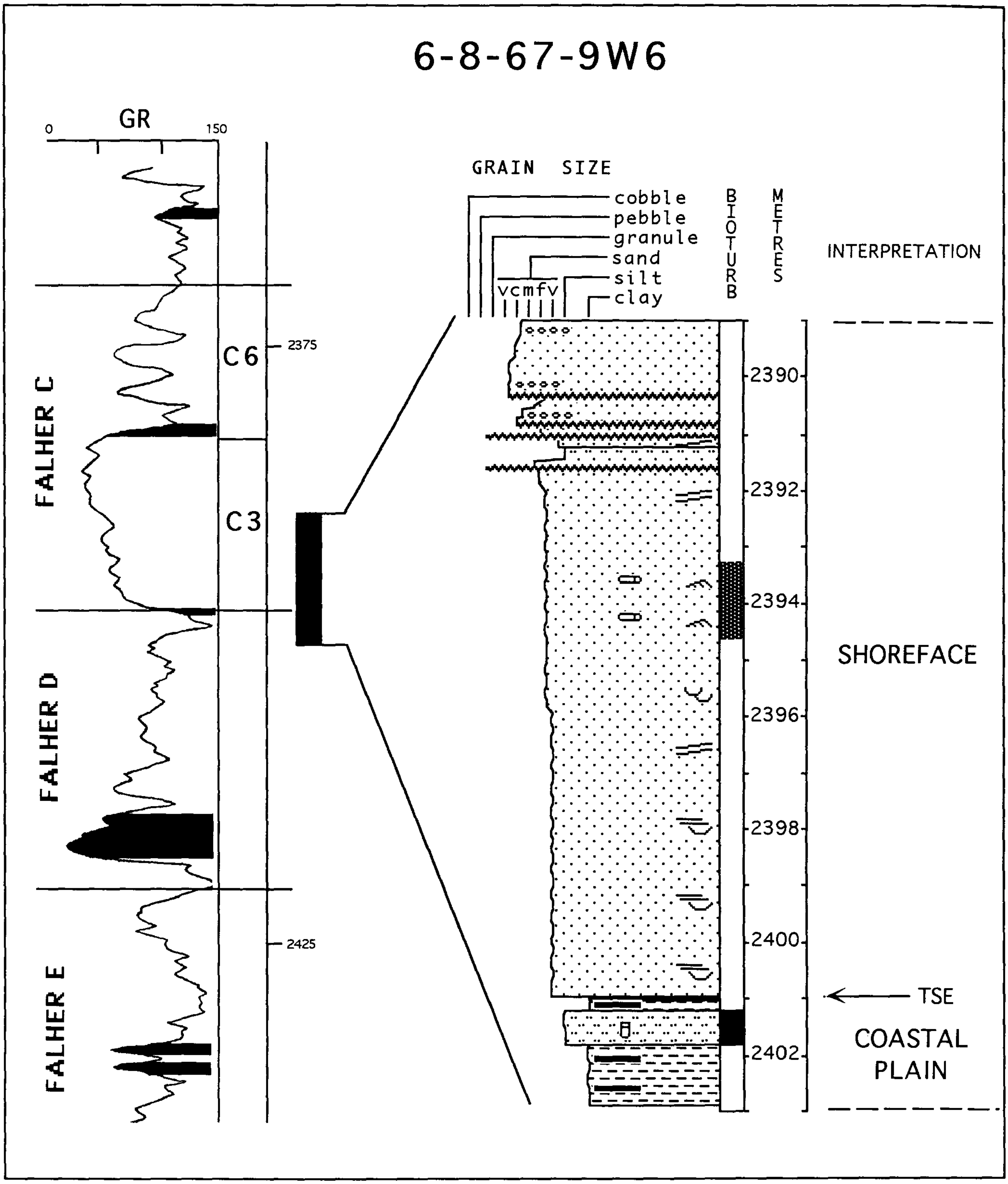

Appendix A42. Detailed sedimentary core log of 6-8-67-9W6. See Appendix A1 for legend and Figure 36 for location.

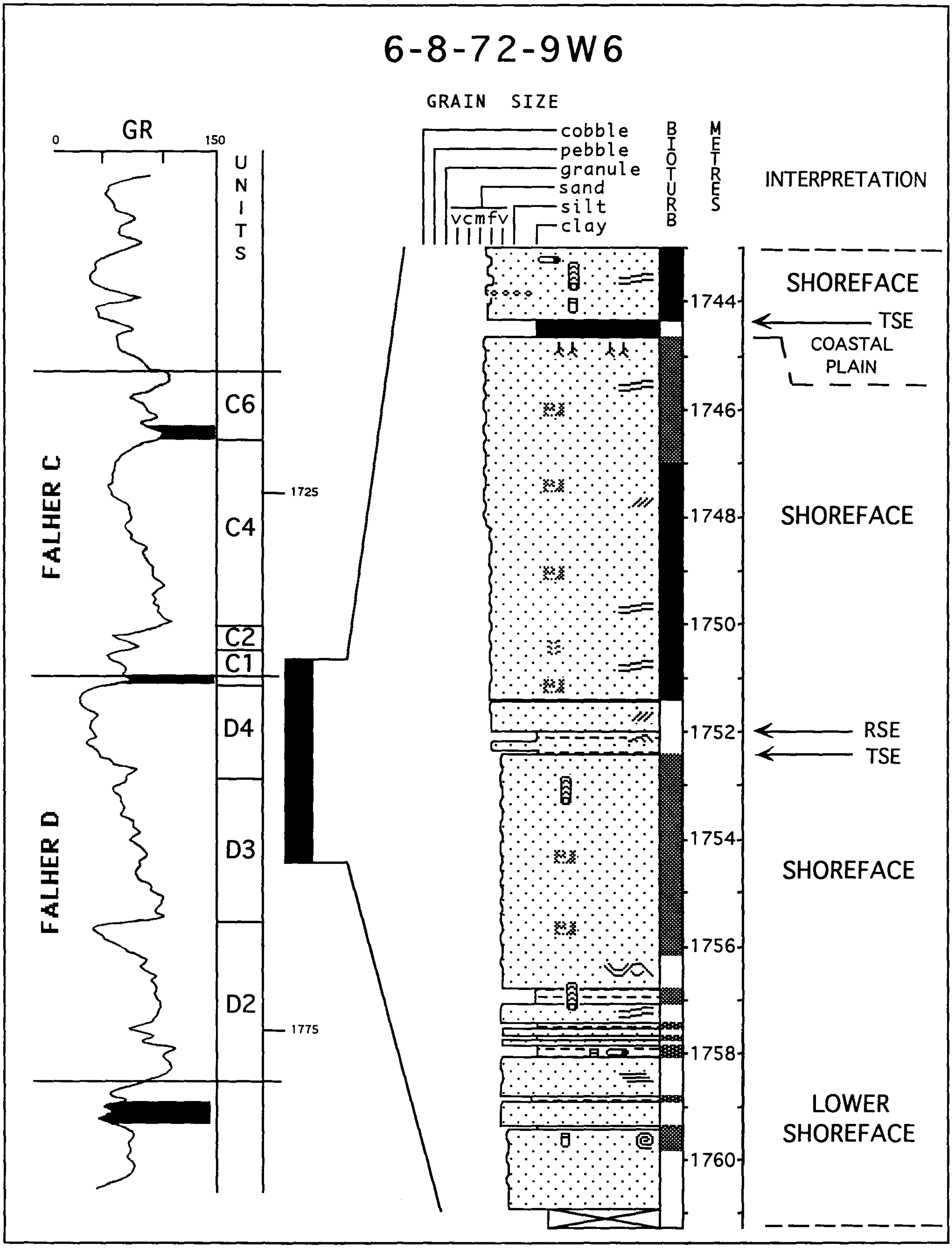

Appendix A43. Detailed sedimentary core log of 6-8-72-9W6. See Appendix A1 for legend and Figure 36 for location.

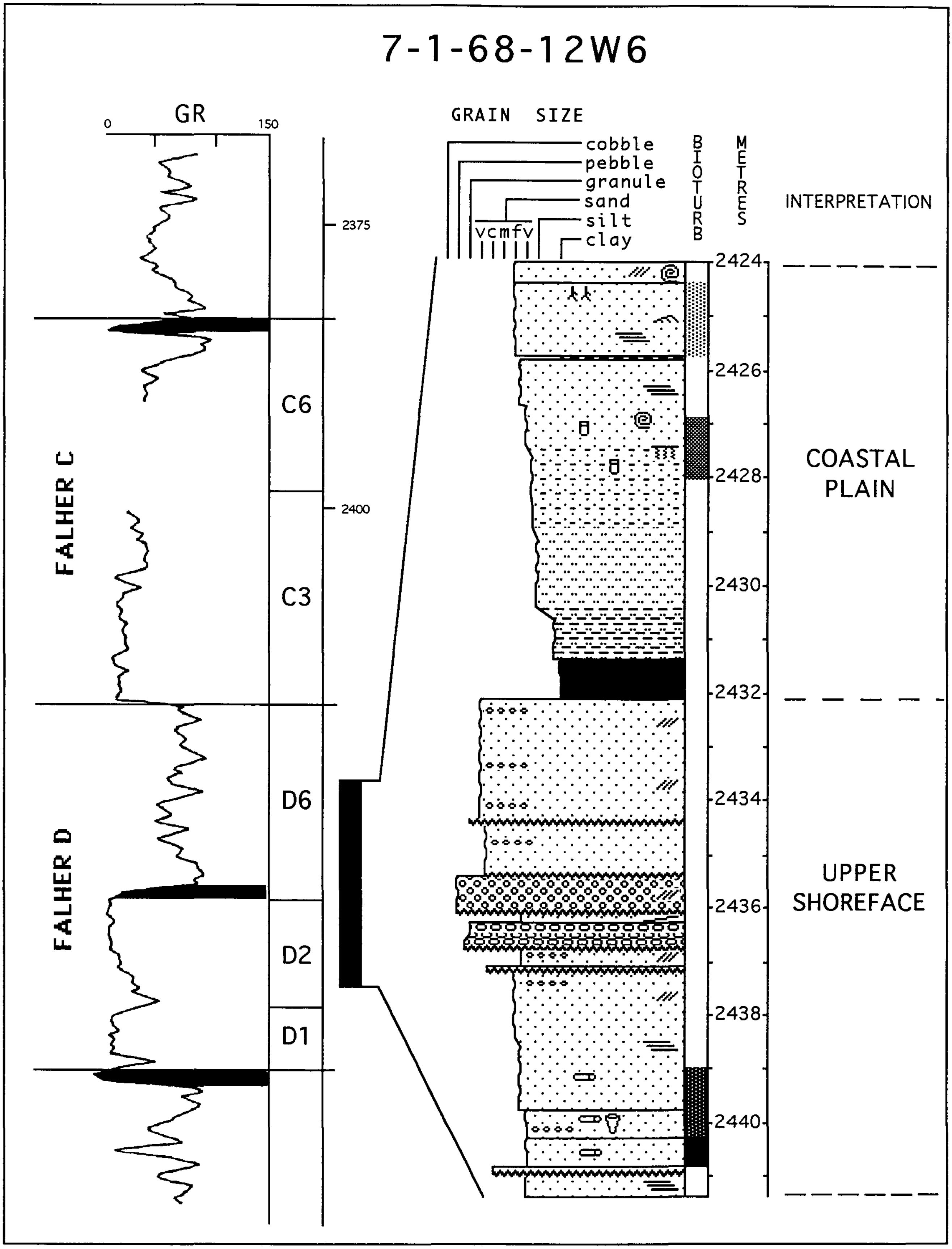

Appendix A44. Detailed sedimentary core log of 7-1-68-12W6. See Appendix A1 for legend and Figure 36 for location.

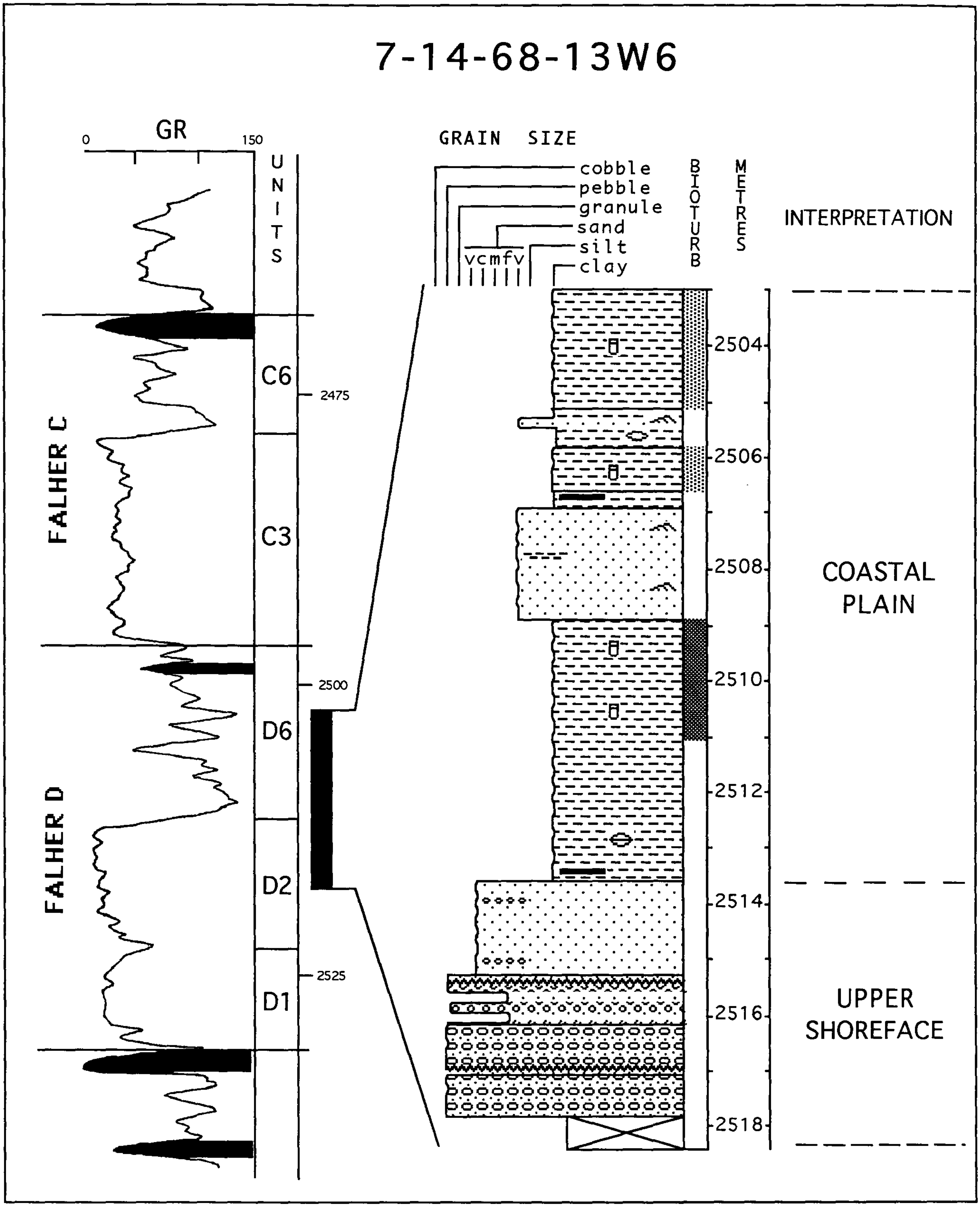

Appendix A45. Detailed sedimentary core log of 7-14-68-13W6. See Appendix A1 for legend and Figure 36 for location.

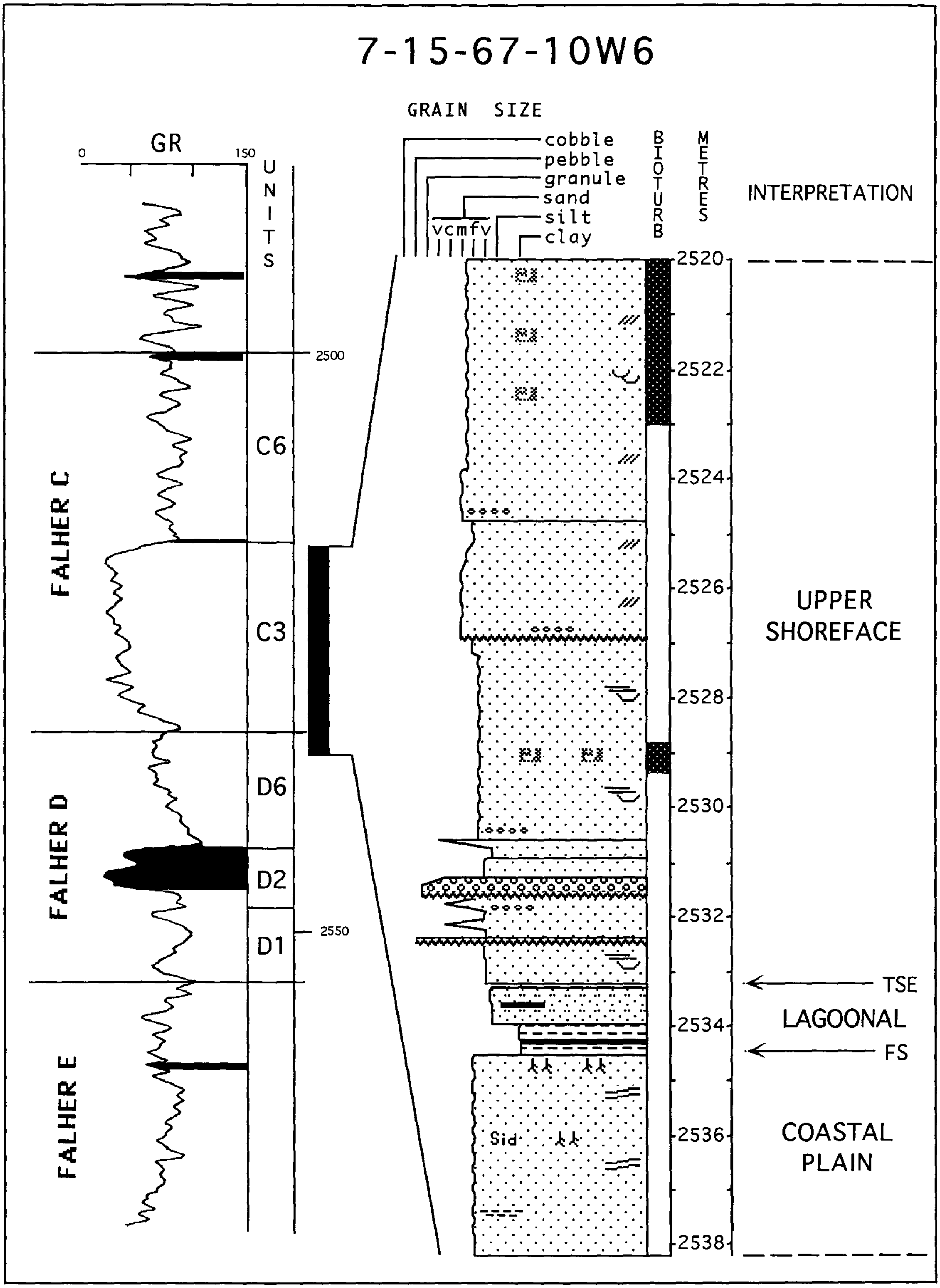

Appendix A46. Detailed sedimentary core log of 7-15-67-10W6. See Appendix A1 for legend and Figure 36 for location.

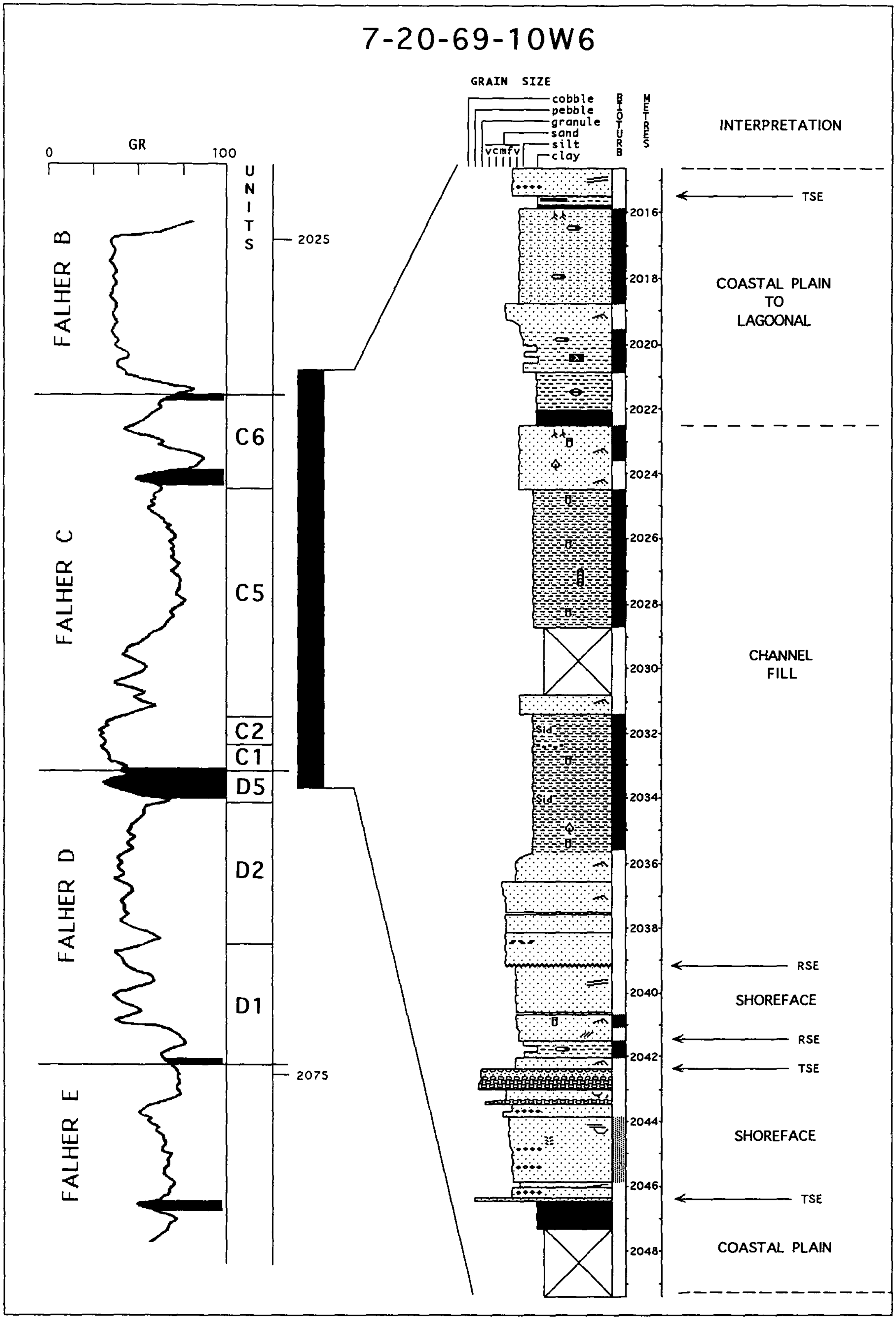

Appendix A47. Detailed sedimentary core log of 7-20-69-10W6. See Appendix A1 for legend and Figure 36 for location.

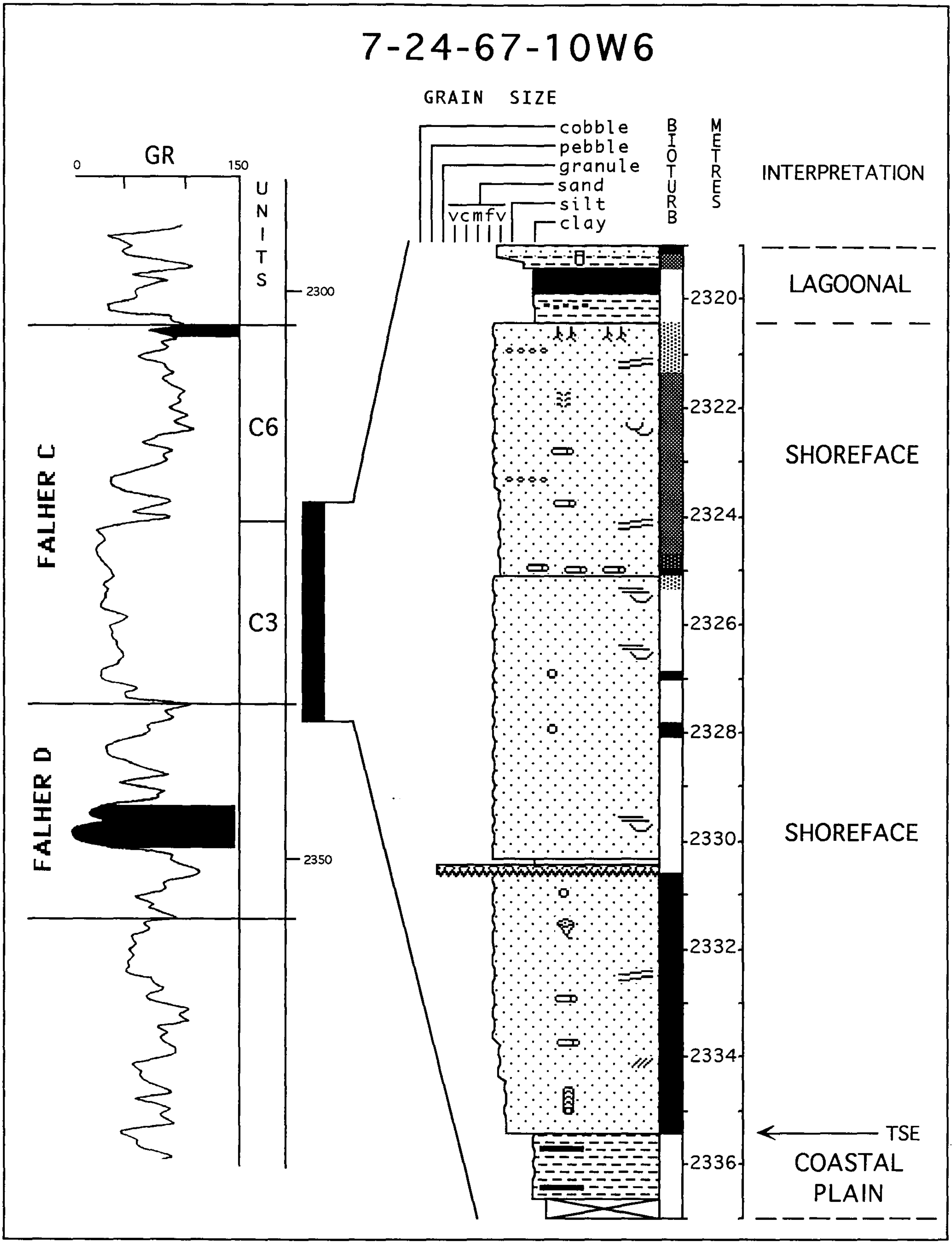

Appendix A48. Detailed sedimentary core log of 7-24-67-10W6. See Appendix A1 for legend and Figure 36 for location.

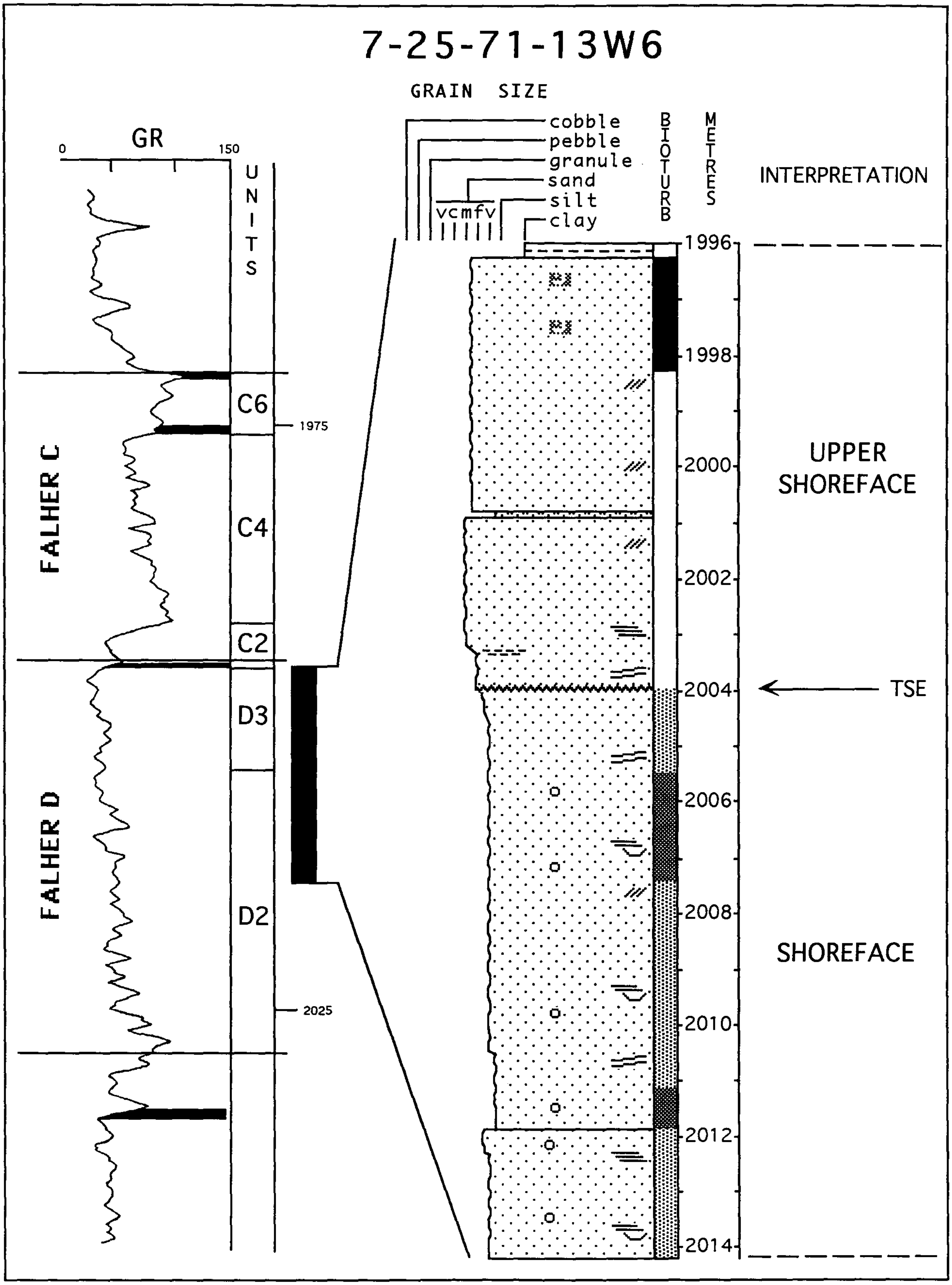

Appendix A49. Detailed sedimentary core log of 7-25-71-13W6. See Appendix A1 for legend and Figure 36 for location.

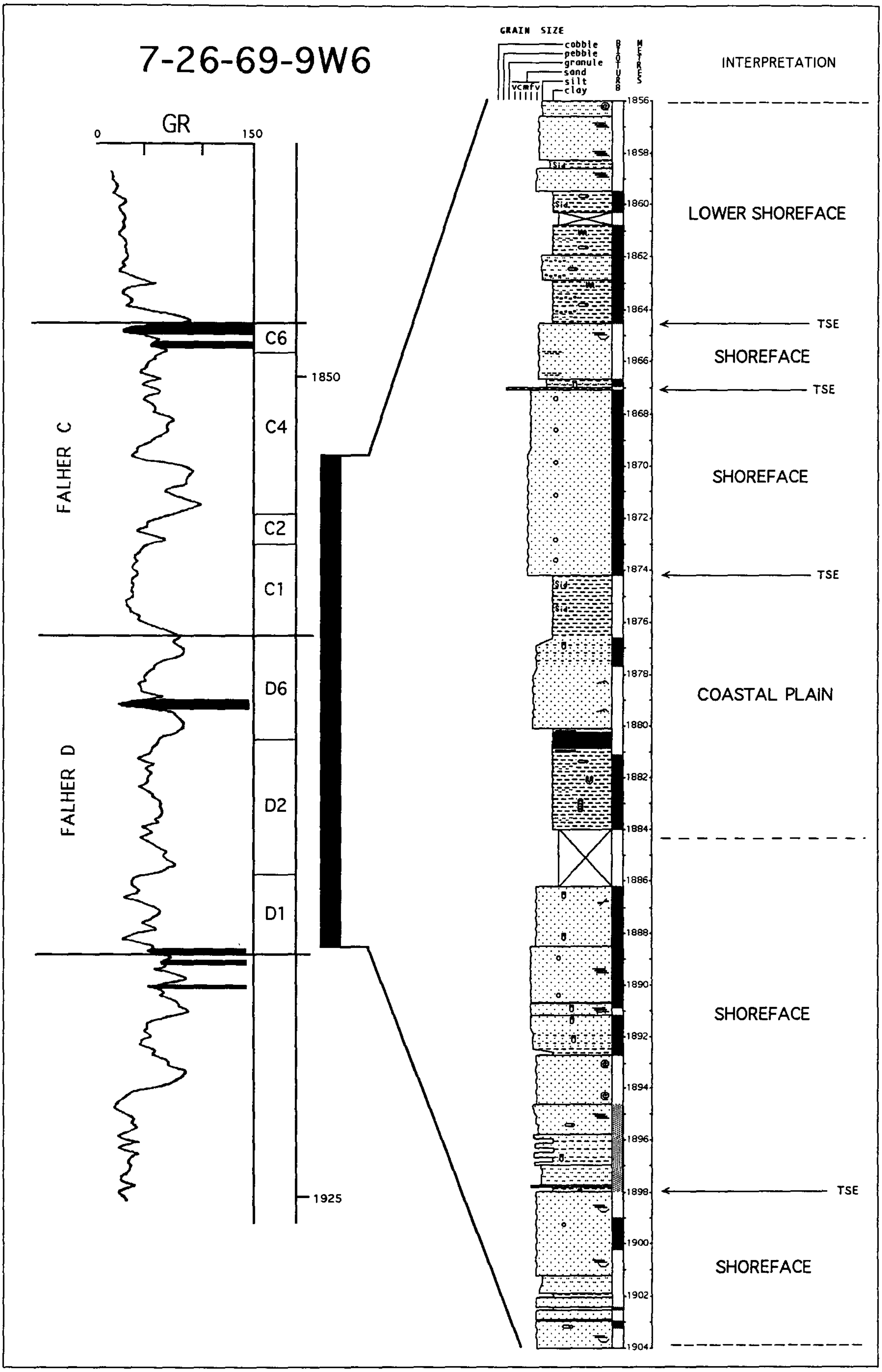

Appendix A50. Detailed sedimentary core log of 7-26-69-9W6. See Appendix A1 for legend and Figure 36 for location.

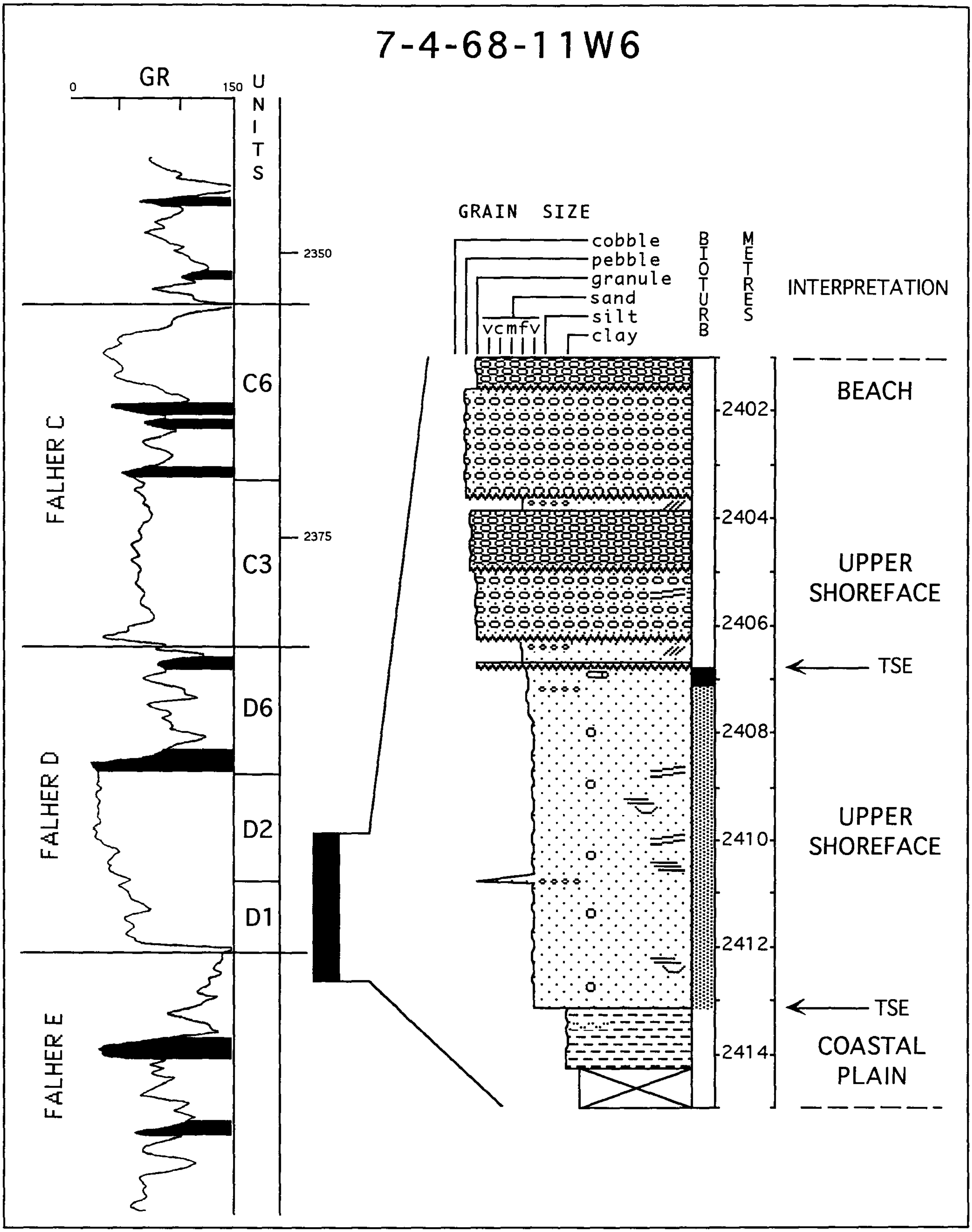

Appendix A51. Detailed sedimentary core log of 7-4-68-11W6.
See Appendix A1 for legend and Figure 36 for location.

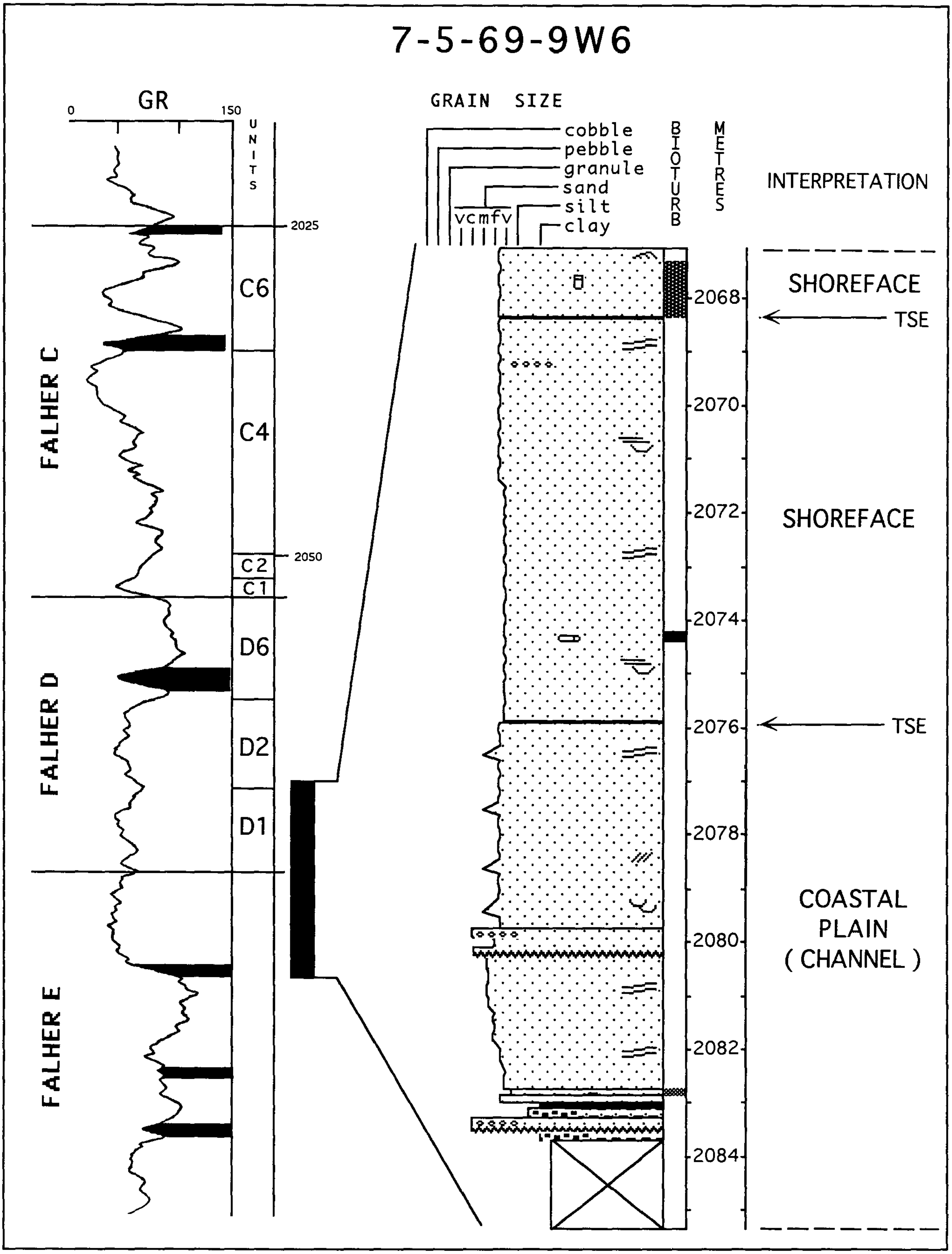

Appendix A52. Detailed sedimentary core log of 7-5-69-9W6. See Appendix A1 for legend and Figure 36 for location.

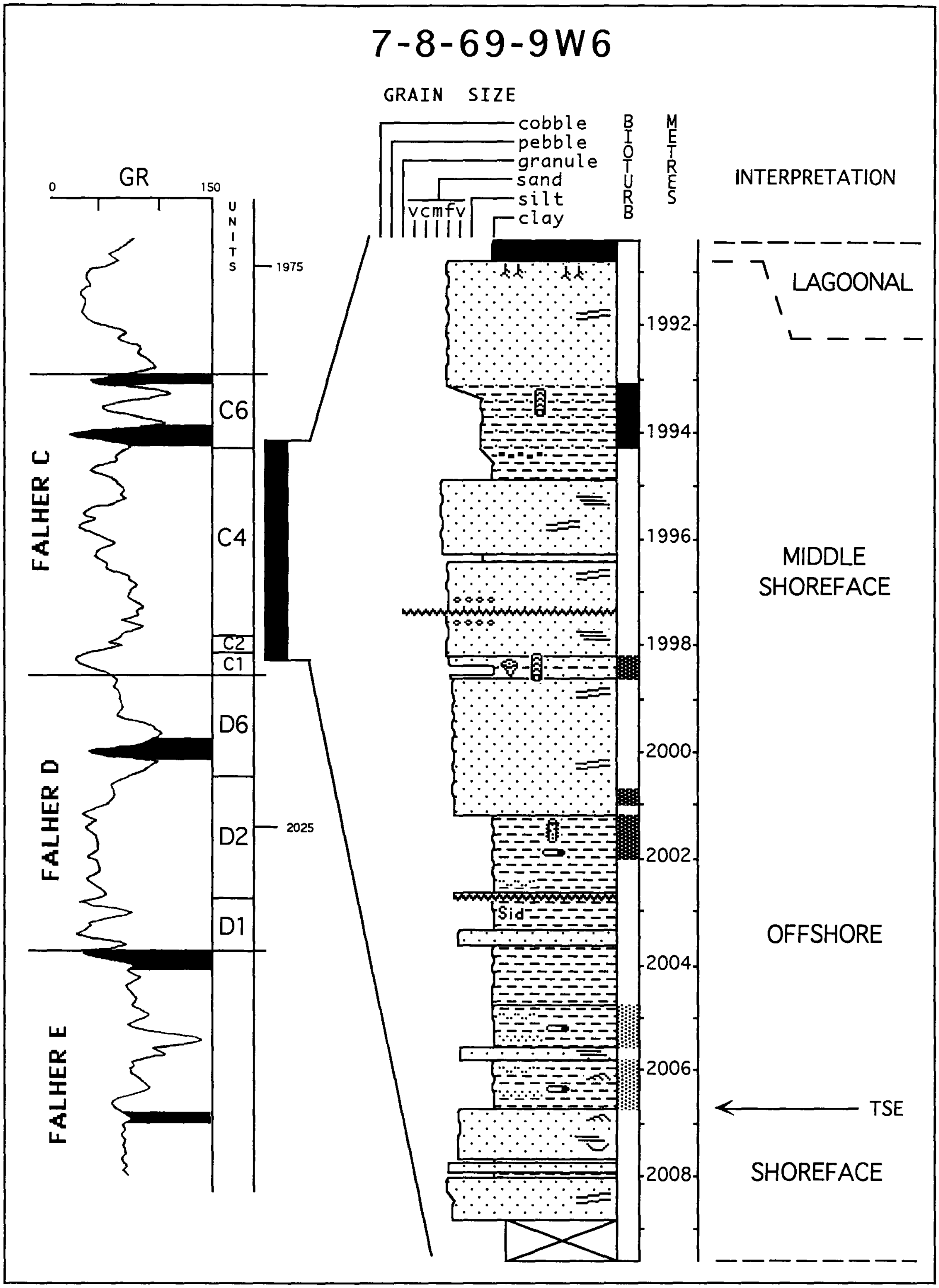

Appendix A53. Detailed sedimentary core log of 7-8-69-9W6. See Appendix A1 for legend and Figure 36 for location.

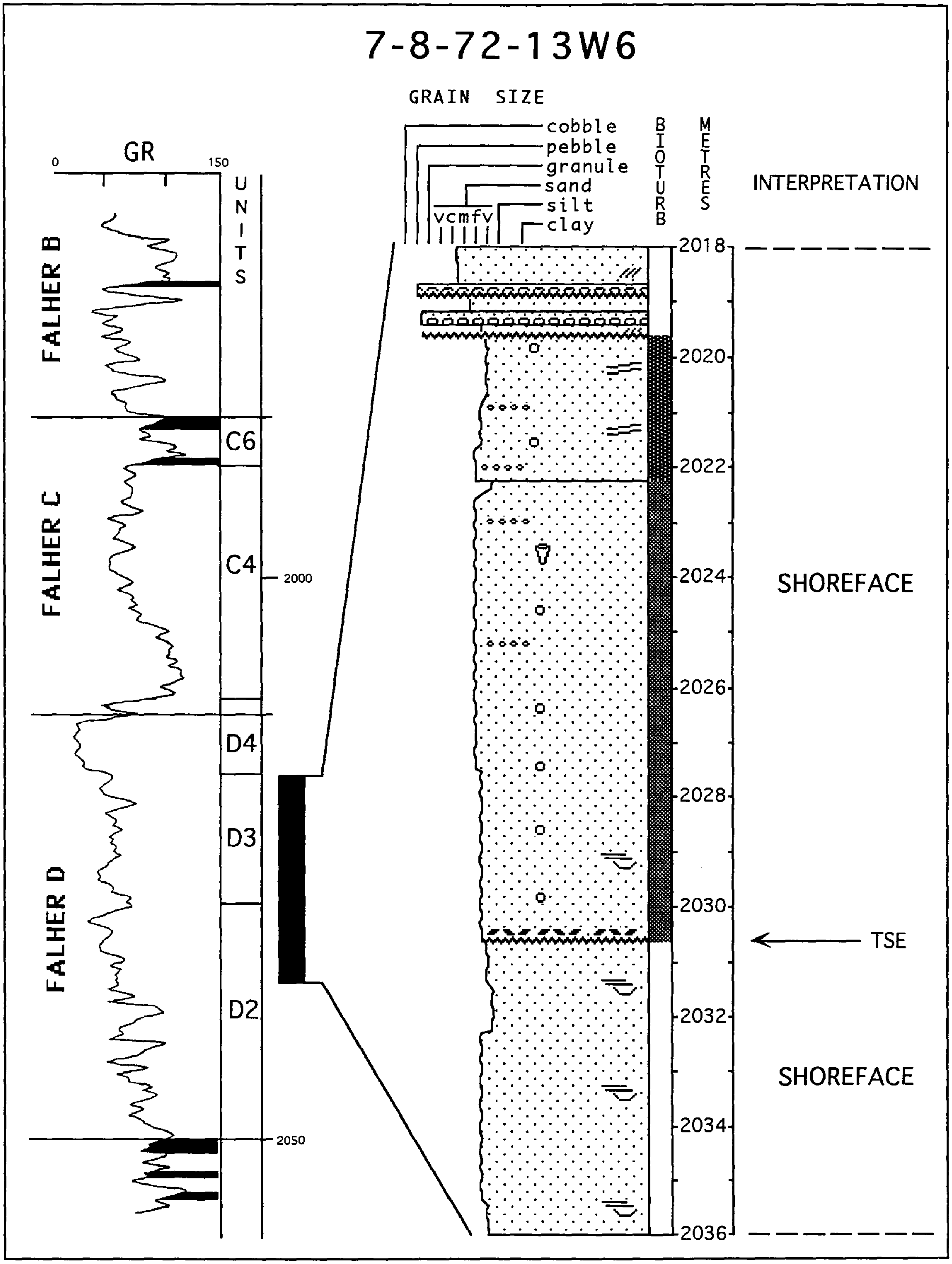

Appendix A54. Detailed sedimentary core log of 7-8-72-13W6. See Appendix A1 for legend and Figure 36 for location.

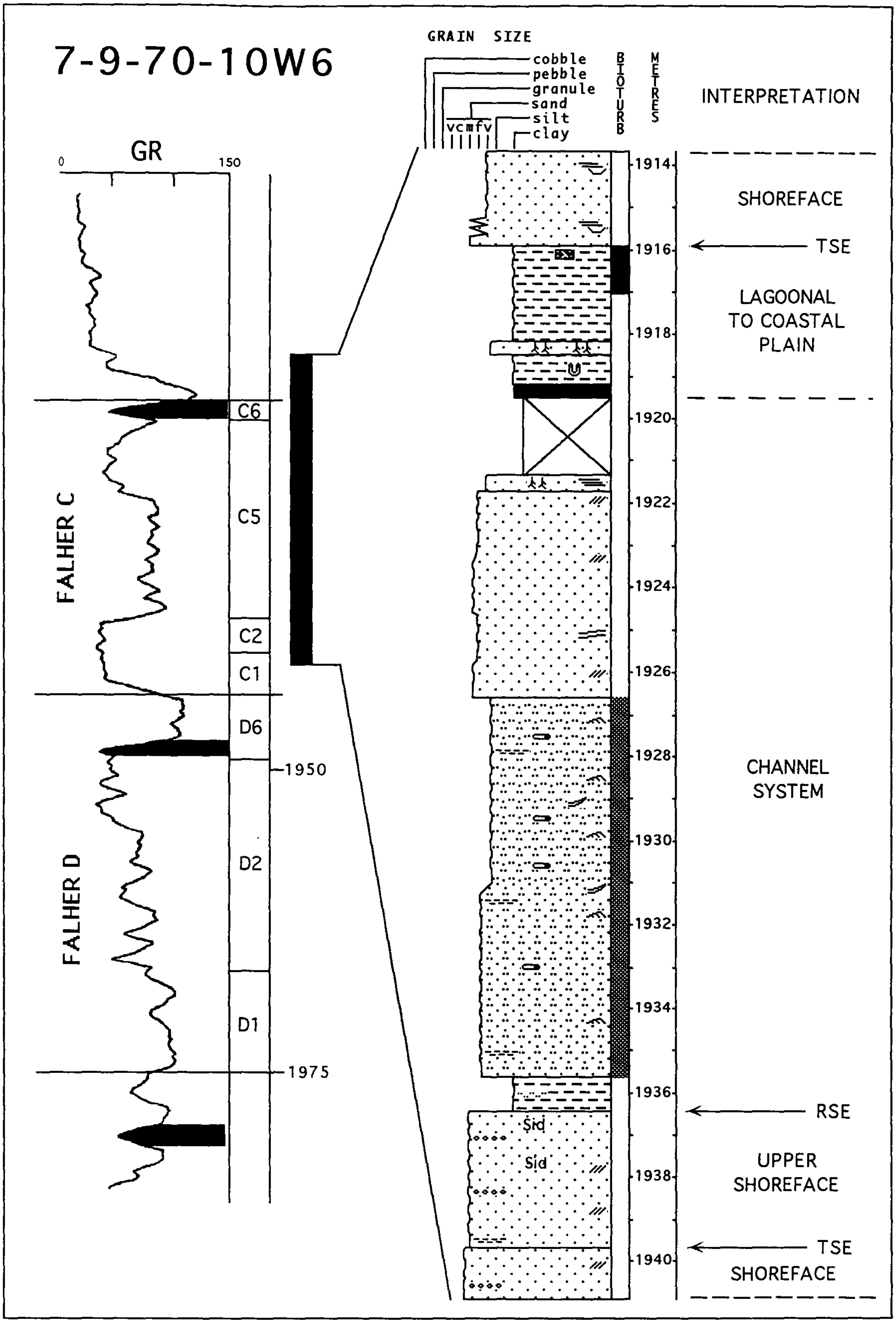

Appendix A55. Detailed sedimentary core log of 7-9-70-10W6. See Appendix A1 for legend and Figure 36 for location.

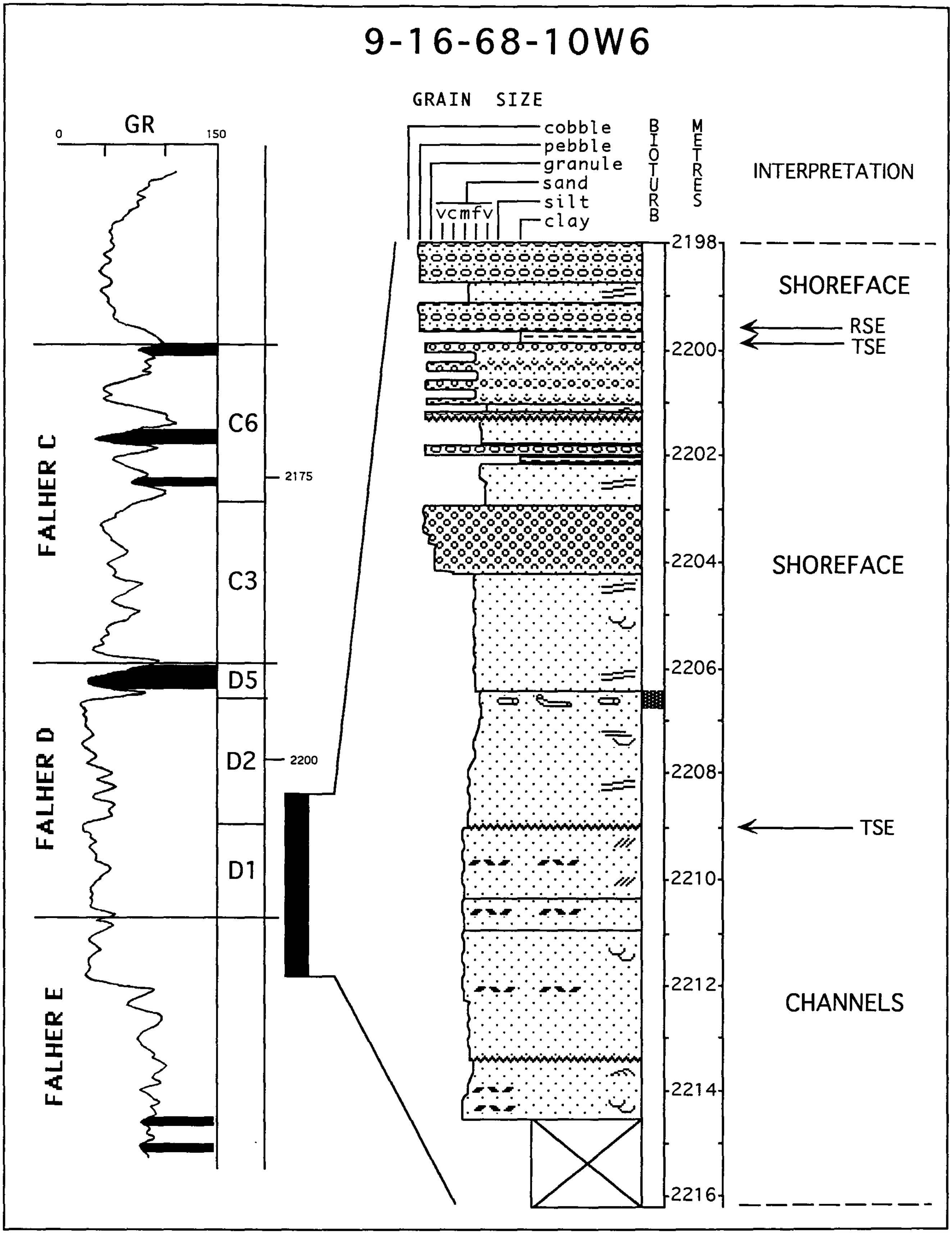

Appendix A56. Detailed sedimentary core log of 9-16-68-10W6. See Appendix A1 for legend and Figure 36 for location.

APPENDIX B

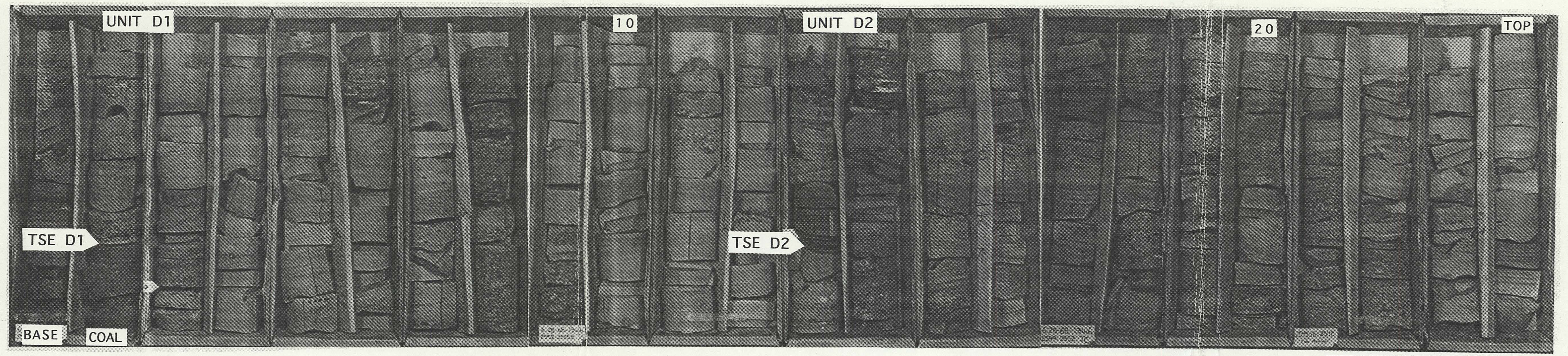

APPENDIX B1
CORE 6-28-68-13W6
3" SLABBED

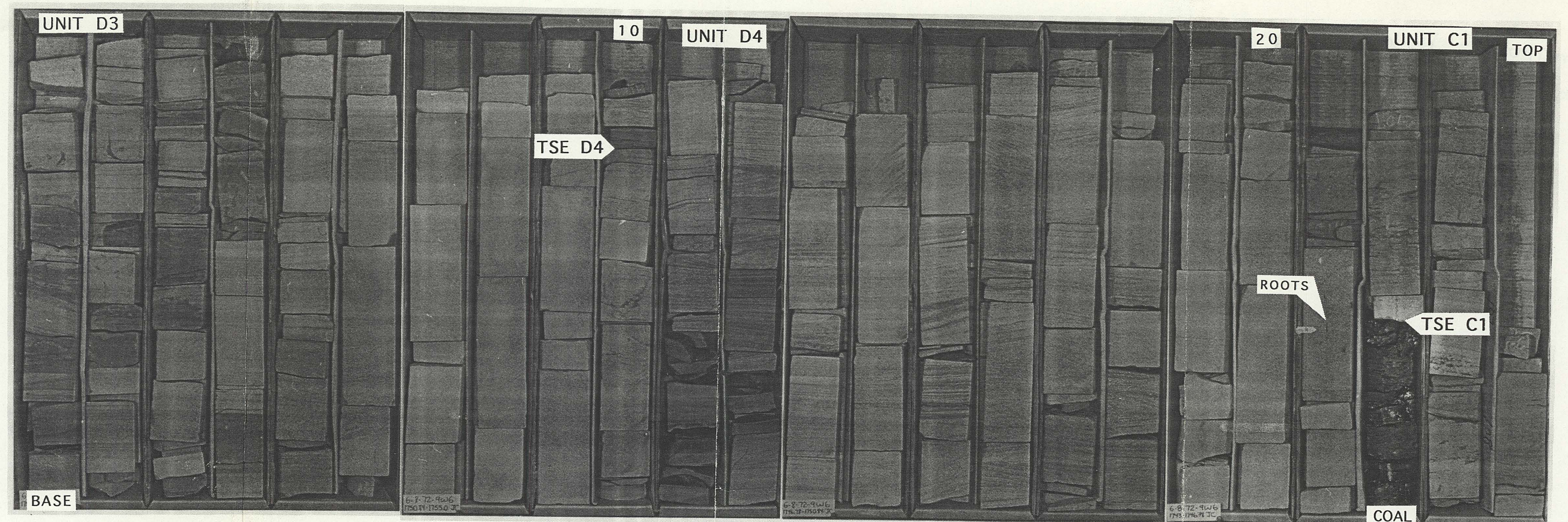

APPENDIX B2
CORE 6-8-72-9W6
3" SLABBED

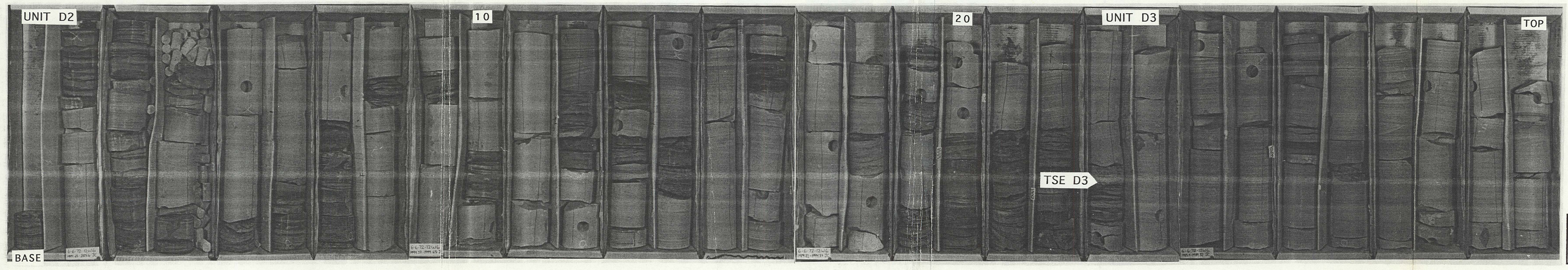

APPENDIX B3
CORE 6-6-72-12W6
4" UNSLABBED

T.S.E. - TRANSGRESSIVE SURFACE OF EROSION
R.S.E. - REGRESSIVE SURFACE OF EROSION
F.S. - FLOODING SURFACE
S.E. - SURFACE OF EROSION

T.S.E. - TRANSGRESSIVE SURFACE OF EROSION
R.S.E. - REGRESSIVE SURFACE OF EROSION
F.S. - FLOODING SURFACE
S.E. - SURFACE OF EROSION

APPENDIX B4
CORE 11-7-68-12W6
4" UNSLABBED

APPENDIX B5
CORE 7-20-69-10W6
4" SLABBED

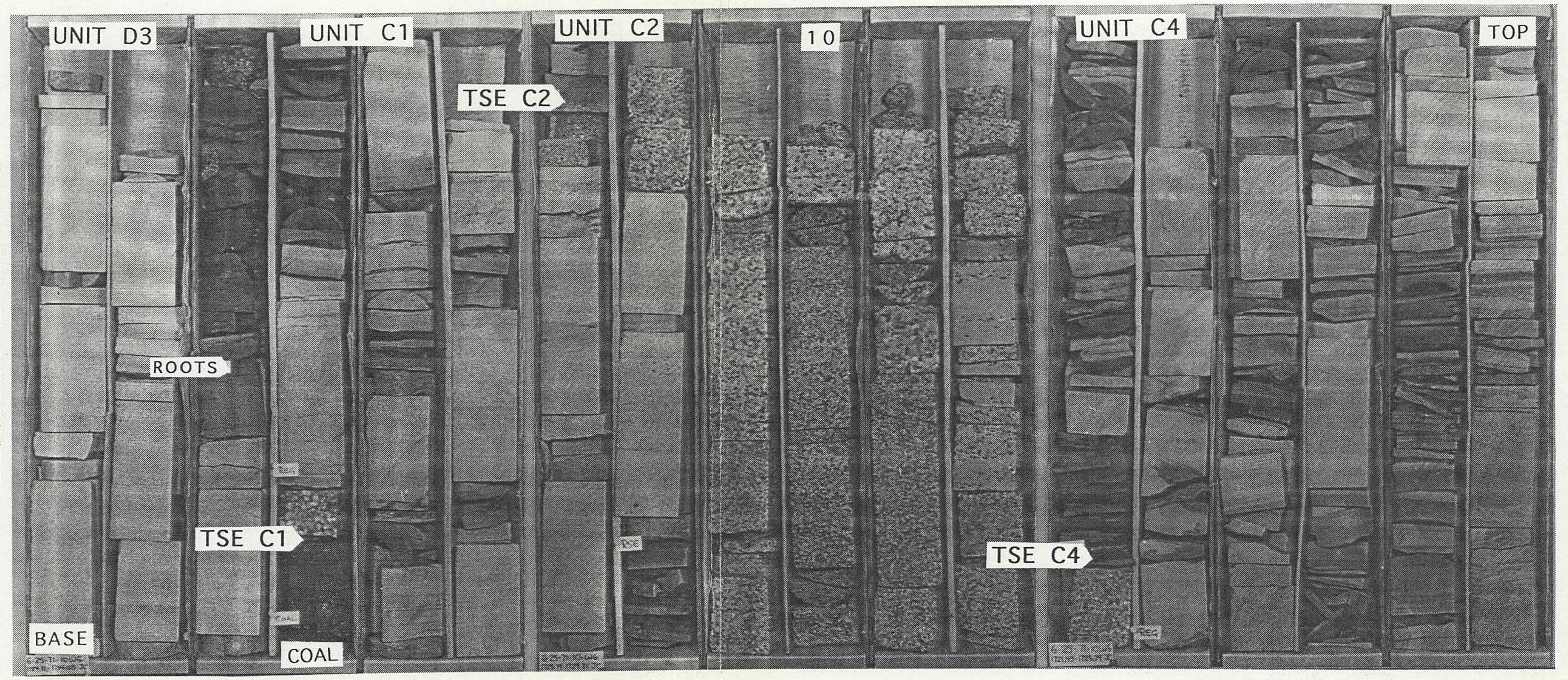

APPENDIX B6
CORE 6-25-71-10W6
3" SLABBED

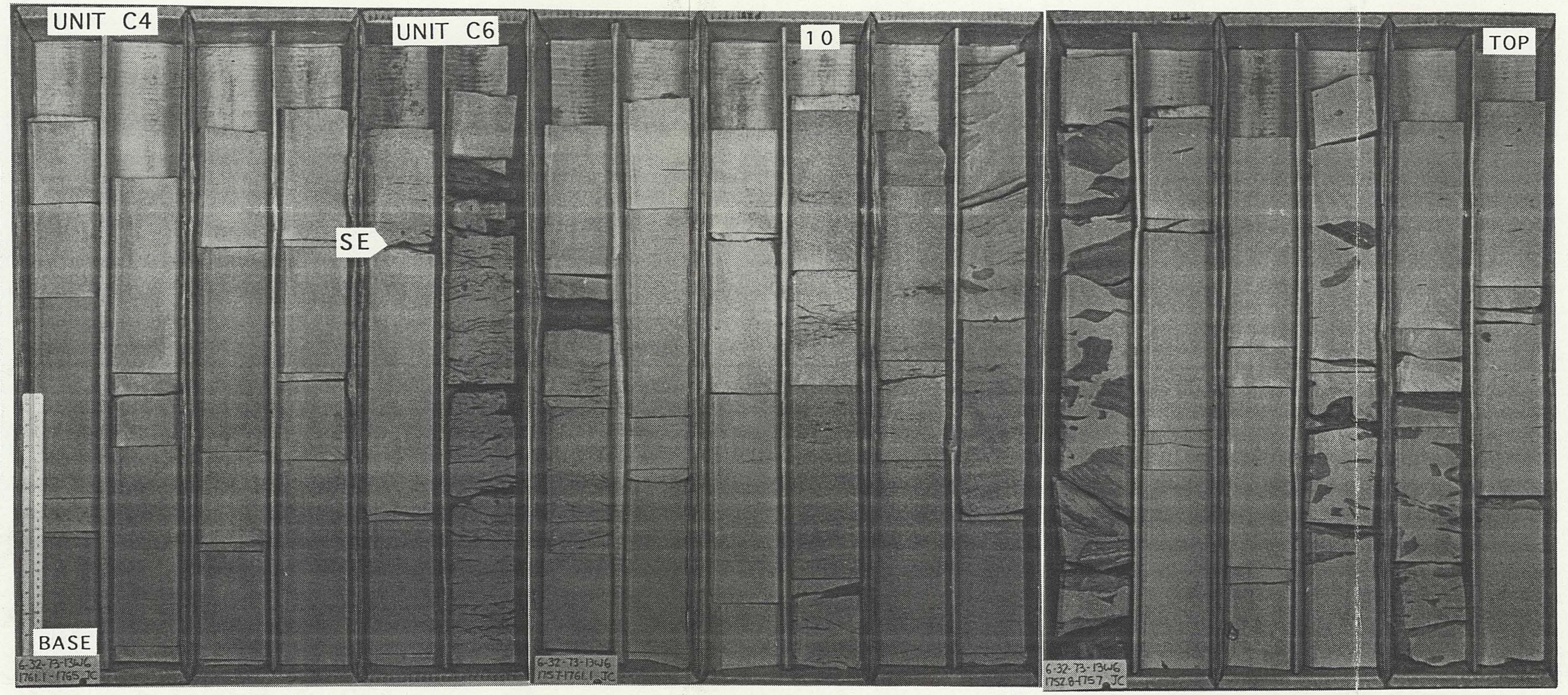

APPENDIX B7
CORE 6-32-73-13W6
3" SLABBED

T.S.E. - TRANSGRESSIVE SURFACE OF EROSION
R.S.E. - REGRESSIVE SURFACE OF EROSION
F.S. - FLOODING SURFACE
S.E. - SURFACE OF EROSION

APPENDIX C

APPENDIX C1

Log Cross-section of Falher D and C

The Datum is a composition of TSE C3 and TSE C4

See Figure 44 for location

The logs are not spaced proportionally to distances between wells

APPENDIX C2

Log Cross-section of Falher D

The Datum is a composition of TSE C3 and TSE C4

See Figure 44 for location

The logs are not spaced proportionally to distances between wells

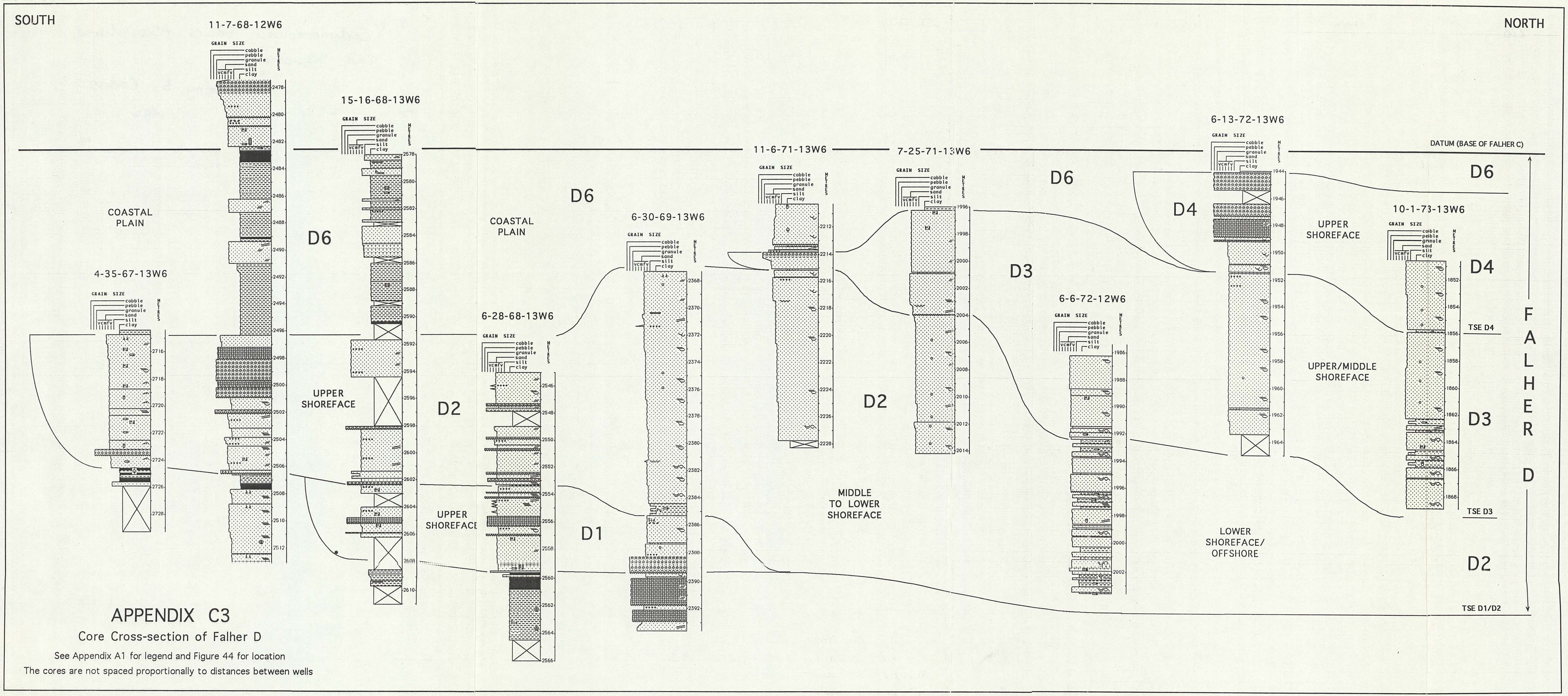

APPENDIX C3

Core Cross-section of Falher D

See Appendix A1 for legend and Figure 44 for location

The cores are not spaced proportionally to distances between wells

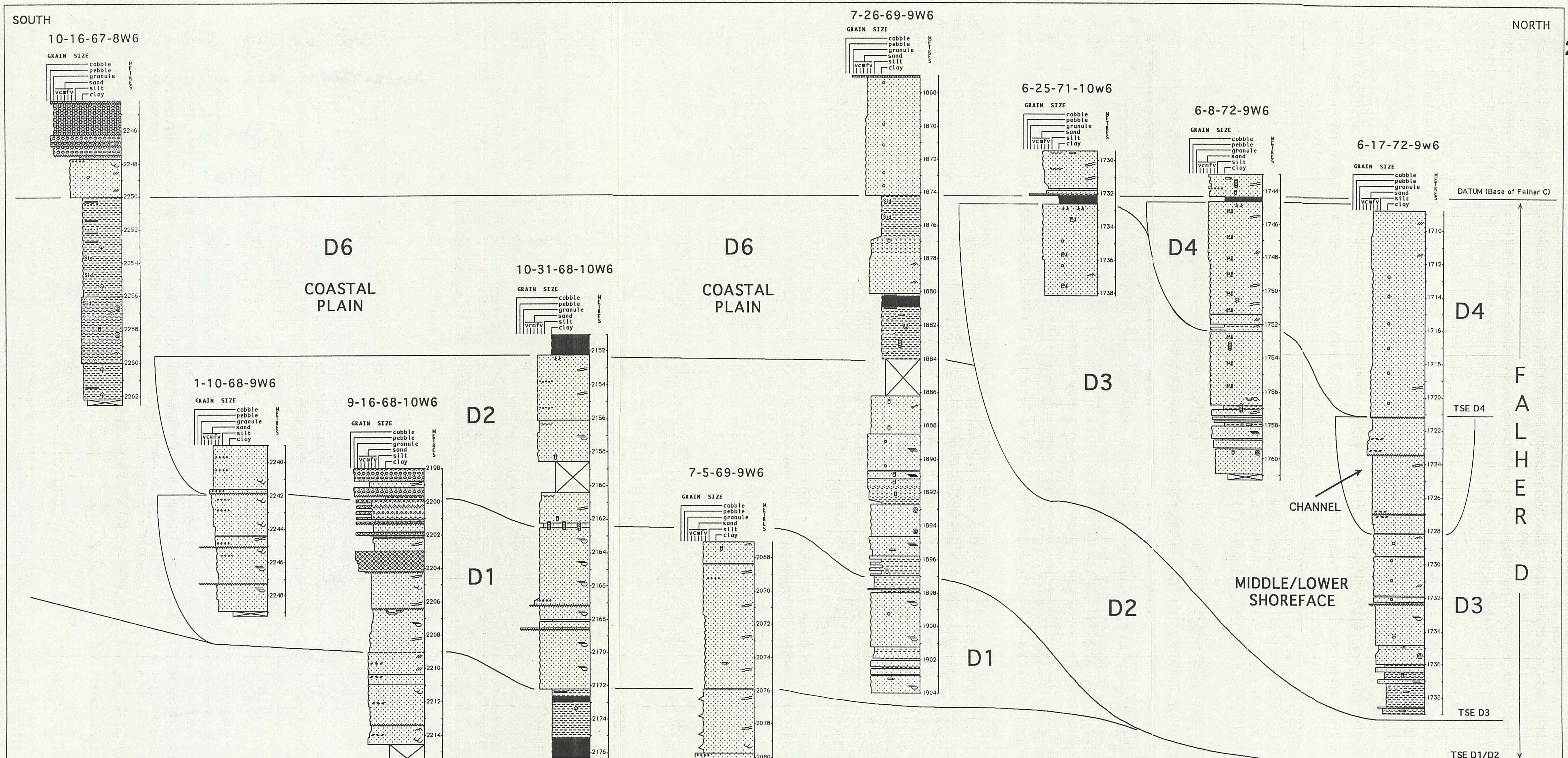

APPENDIX C4

Core Cross-section of Falher D

See Appendix A1 for legend and Figure 44 for location

The cores are not spaced proportionally to distances between wells

APPENDIX C5

Log Cross-section of Falher C

The Datum is a composition of TSE C3 and TSE C4

See Figure 44 for location

The logs are not spaced proportionally to distances between wells

APPENDIX C6

Log Cross-section of Falher C

The Datum is a composition of TSE C3 and TSE C4

See Figure 44 for location

The logs are not spaced proportionally to distances between wells

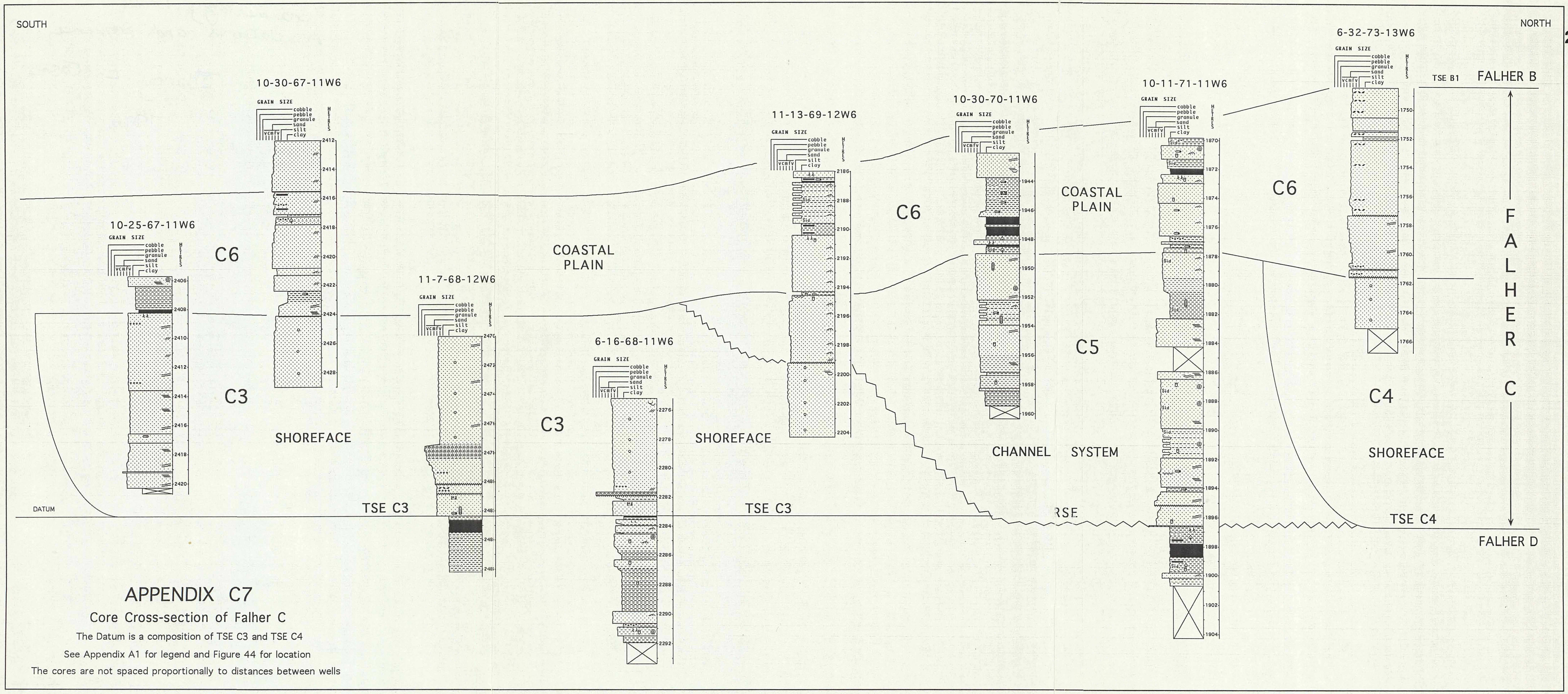

APPENDIX C7

Core Cross-section of Falher C

The Datum is a composition of TSE C3 and TSE C4

See Appendix A1 for legend and Figure 44 for location

The cores are not spaced proportionally to distances between wells

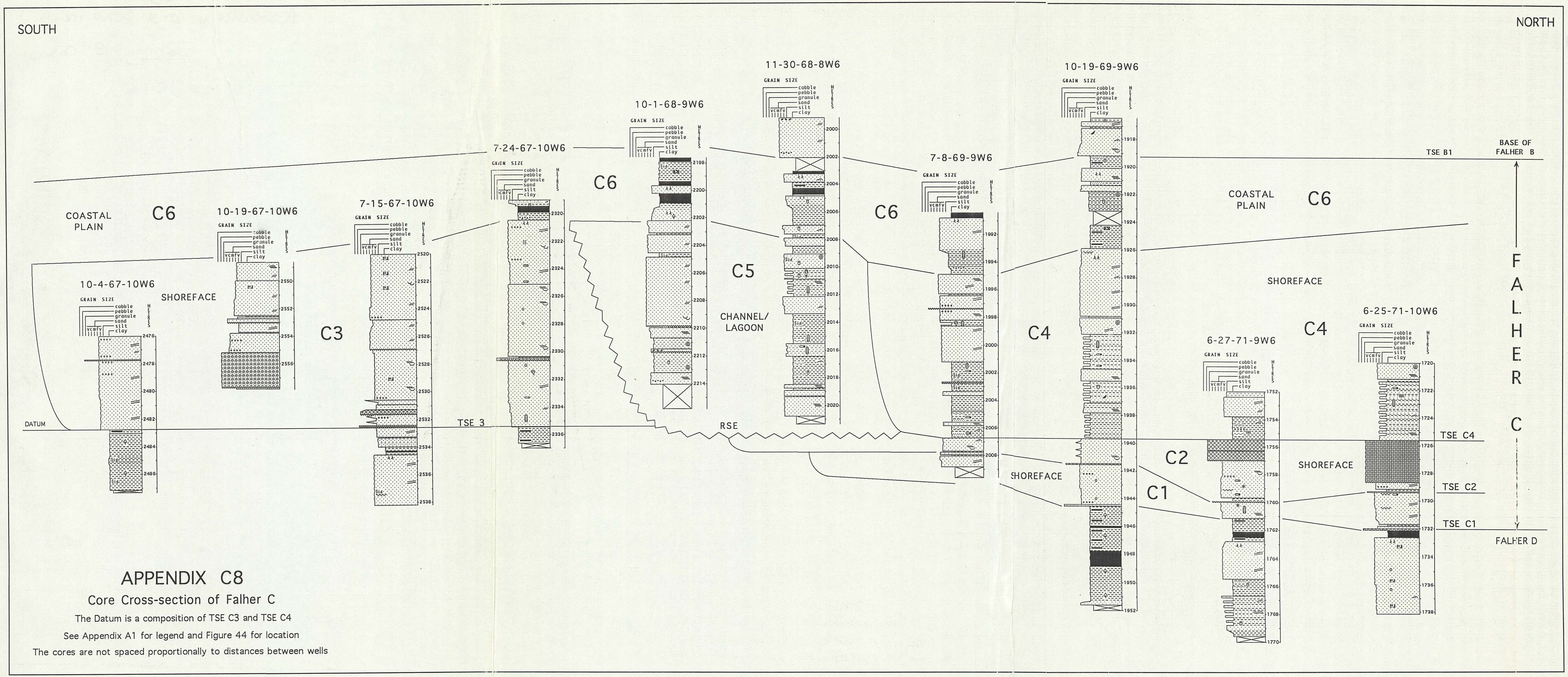

APPENDIX C8

Core Cross-section of Falher C

The Datum is a composition of TSE C3 and TSE C4

See Appendix A1 for legend and Figure 44 for location

The cores are not spaced proportionally to distances between wells